Evaluation of the vegetation along roadways in Edwards Aquifer recharge and contributing zones for storm water management and water quality improvement

Final Report

Submitted May 15, 2023

Revised September 8, 2023

Principal Investigators:

Jeffrey T. Hutchinson, Associate Professor

The University of Texas at San Antonio, College of Sciences, Department of Integrated Biology,

FLN 4.02.56, One UTSA Circle, San Antonio, TX 78249

Phone: 512-618-0272; Email: jeffrey.hutchinson@utsa.edu

Vikram Kapoor, Associate Professor

The University of Texas at San Antonio, College of Engineering, School of Civil & Environmental Engineering, and Construction Management, BSE 1.326, One UTSA Circle, San Antonio, TX 78249

Phone: 210-458-7198; Email: vikram.kapoor@utsa.edu

Samer Dessouky, Professor

The University of Texas at San Antonio, College of Engineering, School of Civil & Environmental Engineering, and Construction Management, BSE 1.322, One UTSA Circle, San Antonio, TX 78249

Phone: 210-458-7072; Email: samer.dessouky@utsa.edu

Prepared for the City of San Antonio, Parks and Recreation Department, Edwards Aquifer Protection Program.

Table of Contents	Page
List of Tables	6
List of Figures	7
Appendices	12
Executive summary	13
Introduction	15
Methods	18
Vegetation and Soils	18
Study sites	18
Field studies	18
Vegetation surveys	18
Vegetation biomass	19
In situ swale plantings	19
Soil samples	20
Preparation of soil samples	20
Bulk density	21
Organic matter	21
Carbon analysis	21
Metal analysis in soils and vegetation samples	22
Oil and grease analysis	22
Greenhouse studies	23
Seed germination	23
Nutrient growth studies	24
Metal uptake in native grasses	25
Statistical analysis	25
Water Quality Monitoring	26
Study Sites	26
Sand filtration systems	26
Swale description	27

Stormwater sampling	27
Water quality analysis	28
Nutrients	28
Carbon, COD, and solids	28
Metal analysis	28
Oil and grease	28
Hydrocarbons	28
Microbial testing for fecal coliform	29
Soil sampling	29
DNA extraction and bacterial 16S rRNA gene sequencing	29
Results	30
Vegetation surveys	30
Mean plant richness, evenness, and diversity	31
Vegetation biomass	32
In swale plantings	32
Greenhouse nutrient study (nitrogen and phosphorous)	33
Greenhouse drought study	34
Ex situ metal uptake in plants	34
Soil analysis	35
Soil type	35
Soil bulk density	35
Soil organic matter	35
Soil organic carbon	35
Soil particle size	35
In situ metal analysis in plants	36
In situ metal analysis in soils	37
Metal concentration by soil depth	37
Seasonal metal concentration in soils	37

Oil and grease analysis in sediment collected from runoff	38
Stormwater Monitoring	38
Bulverde Basin	38
TPC Basin	39
Kyle Basin	39
Fecal coliform results	40
Kyle swale results	40
Plaza swale results	40
Roadrunner way swale results	41
16S rRNA gene sequencing results for soil samples	41
Bulverde Basin	41
TPC and Kyle Basins	42
Discussion	42
Vegetation richness and cover	43
Greenhouse studies	48
Soils	48
Bulk density	48
Organic matter and carbon	49
Particle size	49
Metals	50
Plant uptake	50
Metal concentrations in soils	51
Oil and grease	51
Oil and grease concentrations in soils	51
Sediment particle size collected from roadway runoff	52
Stormwater Monitoring	52
Bulverde basin water quality	52
TPC and Kyle water quality	54

Bacterial communities in detention basins	55
Management Recommendations	56
Acknowledgements	58
Literature Cited	50

List of Tables

Table 1. Total species richness for plant status by LID type and time period72
Table 2. Total coverage (%) for plant status by LID type and time period72
Table 3. Total species richness for plant group type by LID type and time period73
Table 4. Total percent (%) coverage for plant group type by LID type and time period73
Table 5. Total species richness for plant life cycle ¹ by LID type and time period74
Table 6. Total percent (%) coverage for plant life cycle ¹ by LID type and time period75
Table 7. Total species richness for plant growth form by LID type and time period76
Table 8. Total percent coverage for plant growth form by LID type and time period77
Table 9. Total species richness for plant USDA Wetland Classification by LID type and time period
Table 10. Total percent (%) coverage for plant USDA Wetland Classification by LID type and time period
Table 11. List of Polycyclic Aromatic Hydrocarbons in this study80
Table 12. Storm events monitored in Bulverde basin
Table 13. Storm events monitored in the TPC basin
Table 14. Storm events monitored in Kyle basin
Table 15. Storm events monitored in swales84

List of Figures

Figure 1. General location of study sites in the United States and Texas, Bexar County, and primary and secondary sand filtration systems and swales in northern Bexar County85
Figure 2. Non-linear regression analysis of the total percent coverage of each native and non-native species
Figure 3. Regression analysis of native and non-native plant percent coverage and species richness
Figure 4. Comparison of mean species richness, Simpsons' Index of Diversity, evenness, and percent cover for swales and sand filtration systems
Figure 5. Diversity indices for a) Mean species richness, Simpsons' Index of Diversity, evenness and mean percent cover for swales and sand filtration systems by season and year91
Figure 6. Mean coverage (%) for herbs/forbs and graminoids in swales and sand filtration systems with native and non-native species combined for year and season92
Figure 7. Dry weights (g m ²⁻¹) of native and non-native forbs and graminoids in swales and sand filtration systems
Figure 8. Dry weights (g m ²⁻¹) of litter biomass in swales and sand filtration systems during the summers and winters of 2020 and 202194
Figure 9. Mean dry weights (g m ²⁻¹) of native and non-native species in swales and sand filtration systems with greater than 3 g m ²⁻¹ 95
Figure 10. <i>In situ</i> swale planting of six native grass species for survival, dry weight, and root-to-shoot ratios from May 2021 to October 2022
Figure 11. Root dry weights for nitrogen at four increasing concentrations for a) buffalograss, eastern gamagrass, sideoats grama, silver bluestem, switchgrass, and white grown for 3 months under greenhouse conditions
Figure 12. Shoot dry weights of native grasses for nitrogen at four increasing concentrations for buffalograss, eastern gamagrass, sideoats grama, silver bluestem, switchgrass, and white tridens grown for 3 months under greenhouse conditions
Figure 13. Total dry weights (roots + shoots) of native grasses for nitrogen at four increasing concentrations for buffalograss, eastern gamagrass, sideoats grama, silver bluestem, switchgrass, and white tridens grown for 3 months under greenhouse conditions
Figure 14. Root-to-shoot ratios of native grasses for nitrogen at four increasing concentrations for buffalograss, eastern gamagrass, sideoats grama, silver bluestem, switchgrass, and white tridens grown for 3 months under greenhouse conditions
Figure 15. Relative growth rates (RGR; g g ⁻¹ d ⁻¹) of native grasses for nitrogen at four increasing concentrations for buffalograss, eastern gamagrass, sideoats grama, silver bluestem, switchgrass, and white tridens grown for 3 months under greenhouse conditions

Figure 16. Root dry weights for phosphorus at four increasing concentrations for buffalograss, eastern gamagrass, sideoats grama, silver bluestem, switchgrass, and white tridens grown for 3 months under greenhouse conditions
Figure 17. Shoot dry weights for phosphorus at four increasing concentrations for buffalograss, eastern gamagrass, sideoats grama, silver bluestem, switchgrass, and white tridens grown for 3 months under greenhouse conditions
Figure 18. Total dry weights for phosphorus at four increasing concentrations for buffalograss, eastern gamagrass, sideoats grama, silver bluestem, switchgrass, and white tridens grown for 3 months under greenhouse conditions
Figure 19. Root-to-shoot ratios for phosphorus at four increasing concentrations for buffalograss, eastern gamagrass, sideoats grama, silver bluestem, switchgrass, and white tridens grown for 3 months under greenhouse conditions
Figure 20. Relative growth rates (RGR; g g ⁻¹ d ⁻¹) for phosphorus at four increasing concentrations for buffalograss, eastern gamagrass, sideoats grama, silver bluestem, switchgrass, and white tridens grown for 3 months under greenhouse conditions
Figure 21. Root biomass in response to variable watering regimes (1-24 days and rain days) for buffalograss, eastern gamagrass, sideoats grama, silver bluestem, switchgrass, and white tridens grown for 3 months under greenhouse conditions
Figure 22. Shoot biomass in response to variable watering regimes (1-24 days and rain days) for buffalograss, eastern gamagrass, sideoats grama, silver bluestem, switchgrass, and white tridens grown for 3 months under greenhouse conditions
Figure 23. Total biomass (shoots + roots) in response to variable watering regimes (1-24 days and rain days) for buffalograss, eastern gamagrass, sideoats grama, silver bluestem, switchgrass, and white tridens grown for 3 months under greenhouse conditions
Figure 24. Root-to-shoot ratios in response to variable watering regimes (1-24 days and rain days) for buffalograss, eastern gamagrass, sideoats grama, silver bluestem, switchgrass, and white tridens grown for 3 months under greenhouse conditions
Figure 25. Relative growth rates (RGR; g g ⁻¹ d ⁻¹) in response to variable watering regimes (1-24 days and rain days) for buffalograss, eastern gamagrass, sideoats grama, silver bluestem, switchgrass, and white tridens grown for 3 months under greenhouse conditions
Figure 26. <i>Ex situ</i> metal concentrations (ln value) of chromium in roots, shoots, and soils for controls, low and high concentration for buffalograss, eastern gamagrass, silver bluestem, switchgrass, and white tridens
Figure 27. <i>Ex situ</i> metal concentrations (ln value) of copper in roots, shoots, and soils for controls, low and high concentration for buffalograss, eastern gamagrass, silver bluestem, switchgrass, and white

Figure 28. <i>Ex situ</i> metal concentrations (ln value) of lead in roots, shoots, and soils for controls, low and high concentration for buffalograss, eastern gamagrass, silver bluestem, switchgrass, and white tridens
Figure 29. Soil bulk densities taken from soil cores at depths of 0-10, 10-20, and 20-30 cm in swales and sand filtration systems
Figure 30. Soil organic matter (%) taken from soil cores at depths of 0-10, 10-20, and 20-30 cm in swales and sand filtration systems
Figure 31. Soil organic carbon (g kg ⁻¹) taken from soil cores at depths of 0-10, 10-20, and 20-30 cm in swales and sand filtration systems
Figure 32. Percent sediment particle size (μ m) among sieve sizes ranging from < 63 to 2000 μ m form soil core in swales and sand filtration systems
Figure 33. Concentrations of metal uptake in the roots, shoots, and total for magnesium, iron, zinc, lead, copper, chromium, nickel, and cadmium for frog-fruit, Mexican hat, white tridens, and wild petunia
Figure 34. The root-to-shoot ratios of eight metals in frog-fruit, Mexican hat, white tridens, and wild petunia
Figure 35. Mean metal concentration (µg L ⁻¹) in sand filtration systems and swale soils for Fe, Mg, Zn, Pb, Cu, Cr, and Ni
Figure 36. Soil metal concentrations (μ g L ⁻¹) in sand filtration systems and swale at depths of 0-10, 10-20, and 20-30 cm for concentrations > 50 μ g L ⁻¹ and < 50 μ g L ⁻¹ 145
Figure 37. Concentrations ($\mu g \ L^{-1}$) of metals in sand filtration systems and swales by season for concentrations $> 50 \ \mu g \ L^{-1}$ and concentrations $< 50 \ \mu g \ L^{-1}$
Figure 38. Oil and grease concentration (mg kg ⁻¹) collected from runoff sediment for LID type and sample location (inlet, middle, and outlet) within LID type
Figure 39. Mean total sediment weight by particle size collected from precipitation runoff in swales and sand filtration systems for oil and grease analysis, and weight of sediment by particle size collected from precipitation runoff in swales and sand filtration systems for oil and grease analysis
Figure 40. Study sites' location in Bexar County and the Edwards Aquifer zones149
Figure 41. Bulverde Basin A) plan view image of Bulverde site with the inlet channel, filtration area and outlet pipe B) inlet channel C) basin filtration area D) Outlet pipe
Figure 42. TPC Basin plan view image of TPC site with the inlet channel, filtration area and outlet pipe, the view from the inside of the basin, inlet channel, and outlet pipe151
Figure 43. Kyle Basin plan view image of Kyle site with the inlet channel, sedimentation area, filtration area, rock gabion, outlet pipe, sedimentation area and inlet channel, filtration area and rock gabion, and outlet pipe

Figure 44. Kyle Seale swale
Figure 45. The Plaza swale
Figure 46. Roadrunner Way swale
Figure 47. Bulverde Basin soil core locations
Figure 48. TPC basin soil core locations
Figure 49. Kyle basin soil core locations
Figure 50. Bulverde nutrients box plot shows the sample median and range between all samples' first and third quartiles
Figure 51. Bulverde solids, COD, and oil and grease box plot show the sample median and range between all samples' first and third quartiles
Figure 52. Bulverde PAHs and carbon species box plot shows the sample median and range between all samples' first and third quartiles
Figure 53. Bulverde heavy metals species box plot shows the sample median and range between all samples' first and third quartiles
Figure 54. TPC nutrients box plot shows the sample median and range between all samples' first and third quartiles
Figure 55. TPC solids, COD, and oil and grease box plot show the sample median and range between all samples' first and third quartiles
Figure 56. TPC PAHs, carbon species box plot shows the sample median and range between all samples' first and third quartiles
Figure 57. TPC heavy metals species box plot shows the sample median and range between all samples' first and third quartiles
Figure 58. Kyle nutrients box plot shows the sample median and range between all samples' first and third quartiles
Figure 59. Kyle solids, COD, and oil and grease box plots show the sample median and range between all samples' first and third quartiles
Figure 60. Kyle PAHs, carbon species box plot shows the sample median and range between all samples' first and third quartiles
Figure 61. Kyle heavy metals species box plot shows the sample median and range between all samples' first and third quartiles
Figure 62. Fecal coliform box plot for all basins
Figure 63. Kyle swale solids, COD, and Oil and grease box plots162
Figure 64. Kyle swale nutrients box plots

Figure 65. Kyle swale carbon species box plot shows the sample median and range between samples' first and third quartiles	
Figure 66. Kyle swale heavy metals species box plot shows the sample median and range between all samples' first and third quartiles	.164
Figure 67. Plaza swale solids, COD, and oil and grease box plots	.164
Figure 68. Plaza swale nutrients box plots	.165
Figure 69. Plaza carbon species box plots	.165
Figure 70. Heavy metals box plots	.166
Figure 71. Roadrunner way swale solids, COD, and oil and grease box plots	.166
Figure 72. Roadrunner way swale nutrients box plots	.167
Figure 73. Roadrunner way swale carbon species box plots	.167
Figure 74. Heavy metals box plots	.168
Figure 75. Bulverde basin relative abundance of the top 10 bacterial phyla in the different layers and seasons	
Figure 76. Bulverde basin Alpha and Beta diversity of soil samples	.169
Figure 77. TPC basin relative abundance of the top 10 bacterial phyla in the different soil and seasons	•
Figure 78. Kyle basin relative abundance of the top 10 bacterial phyla in the different soil and seasons	•
Figure 79. TPC basin Alpha and Beta diversity of soil samples	.172
Figure 80. Kyle basin Alpha and Beta diversity of soil samples	.173

Appendices

Appendix 1. Low Impact Sites (LID; sand filtration systems and swales), GPS locations, and photos of each site
Appendix 2.1. Photos of the Bulverde Road Basin B sand filtration system175
Appendix 2.2. Photos of the Brandeis High School sand filtration system176
Appendix 2.3. Photos of the TPC Parkway Basin A sand filtration system177
Appendix 2.4. Photos of the Bulverde Road Basin D sand infiltration system178
Appendix 2.5. Photos of the Prue Road sand filtration system
Appendix 2.6. Photos of the TPC Parkway Basin B sand filtration system180
Appendix 2.7. Photos of the Babcock Road swale
Appendix 2.8. Photos of the Brandeis High School swale
Appendix 2.9. Photos of The Plaza swale
Appendix 2.10. Photos of the Roadrunner Way Road swale
Appendix 2.11. Photos of the Savannah Oaks Apartment swale
Appendix 2.12. Photos of The Rim swale
Appendix 3. Common name, taxonomic name, USDA code, status (native or non-native), group (monocot or dicot), duration (annual, perennial, etc.), growth habit (forb/herb, graminoid, shrub, etc.), and wetland status (obligate, facultative wetland, facultative, etc.) of plants observed along line transects in sand filtration systems and swales from 2020-2021
Appendix 4. Native plant species suggested for planting in Low Impact Development Structures in Bexar County

Executive Summary

In this study, we evaluated the vegetation composition in swales and sand retention basins and water from roadway runoff entering these engineered structures. The purpose of the study was to determine if the vegetation in swales and sand filtration systems are effective in controlling and containing roadside runoff and its associated sediment and pollutants. The study was conducted in six swales and six sand filtration systems within the Edwards Aquifer recharge zone except one swale that was located in the contributing zone. The primary objectives of this study are to 1) evaluate the sediment and pollutant composition in sand filtration systems and vegetated swales over multiple stormwater events along three major highways in recharge and contributing zones of northern Bexar County, 2) determine the vegetative composition and soil types at each site, 3) document the vegetation species most efficient at uptake of various nutrients and metals, and 4) make recommendations of xeric species of vegetation most resilient and resistant to extreme environmental conditions and most adaptable for long-term survival in LID structures receiving roadway and impervious structure stormwater runoff.

The vegetation found in swales and infiltration systems experiences multiple disturbances that include mowing, raking, sand replacement, flooding, lengthy droughts, pollutants from runoff, and extreme heat during the summer months. The high species richness documented in this study reflects these disturbances where some species become dominant during droughts, others respond to periods of high precipitation, and other invade gaps created by scouring, raking, mowing, and other disturbances.

Vegetation documented in the swales and sand filtration systems were novel ecosystems containing a mixture of ruderal native and non-native species. The majority of the species documented were primarily upland, facultative upland, and facultative species with limited facultative wetland and obligate wetland species. The wetland plants documented were primarily found in low depressions formed by scouring from high influent volume at the inlet.

Over the duration of the study, we documented 154 plant species represented by 114 native and 40 non-native plant species. A total of 121 plant species (89 native and 26 non-native) were recorded in the swales, and a total of 94 plant species (68 native and 26 non-native) were recorded in sand filtration systems. Based on the results of the most common native plants docuemnted, we recommend 56 native species for planting in Low Impact Development structures (LID) that represent mulitple functional groups and may be most resilient to climate change. These spontaneous occurring plants have adapted to extreme environmental conditions and represent plants suitable for use in LID structures in Bexar County and other areas of Central Texas.

The vegetation found in swales and sand filtration systems is comprised primarily of spontaneous vegatation that established from seeds and rhizomes that were washed or blown into the LID structures. With the exception of the Babcock Swale, no intentional seeding or planting was known from the other swales or sand filtration basins. Vegetation in the swales and sand filtration systems in this study were found to have high native species richness of forbs and graminoids, but five non-native grasses dominated coverage and biomass. Native grasses are recommended for planting in LIDs along with seeding of forbs and herbs to increase diversity.

Greenhouse studies indicated increasing but limited growth of native grasses with increasing concentrations of nitrogen and phosphorus. The greenhouse study indicated that the native grasses analyzed in the greenhouse study will be more affected by competition with non-native grasses rather than nitrogen or phosphorus limitations. Based on watering regimes ranging from 1 to 24 days, it was found that silver bluestem, white tridens, and sideoats grama were the most drought tolerent of the grasses evaluated, while switchgrass and eastern gamagrass were the least drought tolerent.

Based on *in situ* plantings of native grasses in swales monitored over two growing seasons, white tridens, silver bluestem, and sideoats grama had high to moderate survival rates and are recommended as priority species for use in LIDs. Switchgrass also had some surival in small plots and should be consider for additional studies for use in LIDs. Additional studies are needed for native herbs and forbs for use in LIDs. We suggest that perennial plants be used in LIDs because once established, no additional maintenance will be required.

The soils in sand filtration systems and swales were found to have high bulk densities 10 cm below the surface which may inhibit root growth of native graminoids and forbs/herbs in sand filtration systems. Sand infiltration systems appear to be more suitable habitat for annuals and forbs and herbs with shallow root systems. In addition, the high bulk density may slow percolation of water through the soil media. At depths > 10 cm, the soils became highly compacted and obtaining deeper soil samples was difficult. Soils were classified as clay loam with 10-20% limstone in swales, and as sand in the upper 10-15 cm, and a mix of quartz sand and sandy clay loam at depths of 15-30 cm in sand infiltration systems.

Soil organic matter and carbon was significantly greater in swales compared to detention ponds which can be attributed to management that occurs in sand filtration systems. In swales, less sediment was captured in traps placed systematically in the LID compared to sand filtration systems indicating that greater vegetation coverage results in better capture of sediment in swales compared to sand filtration systems.

Four common native roadside plants (frog-fruit, Mexican hat, common wild petunia, and white tridents) in this study were found to be accumulators of metal sequestering greater metal concentrations in their roots and shoots than metal concentrations detected in soils of swales and sand filtration systems.

Oil and grease concentrations in swales and sand filtration systems were high indicating these LIDs are efficient at capturing hydrocarbons. It appears the hydrocarbons are sorbed to the upper layer of the sediment as the water in the LID recedes but become suspended when the LID is flooded. It is unclear how these hydrocarbon break down into other compounds that may percolate through sand media and eneter the outlow into surface waters, but additional studies are needed.

Limited vegetation management is recommended in swales and sand filtration systems during the growing season and preferably at the end of the growing season when plants become dormant. It is suggested that all mowed plant parts be collected and disposed of in a landfill to prevent recycling of nutrients and metals. The creation of berms or a series of berms in the swales and sand filtration systems to hold water for longer periods would result in increased denitirfication

and less nitrate entering the outflow and flowing into surface and groundwaters. Additional recommendations are made at the end of the report.

Introduction

Texas is the second most populous state and San Antonio is the seventh largest city in the United States (U.S. Census Bureau, 2018). San Antonio experienced the highest per capita growth of any major city in 2017 and population is expected to increase. The population of Bexar County is estimated to reach 2.8 million by 2060 representing a 94% increase from 2000 to 2060 (TWDB, 2011). Increased population is characterized by loss of natural habitat, fragmented ecosystems, and impacts on environmental processes and ecosystems services. Development and habitat fragmentation result not only in increased stormwater runoff, but also loss of ecosystem service and declines in biodiversity which can impact water quality (Vitousek 1994, Walsh 2000).

Increased impervious surface is another factor that results from increased population growth and urbanization, and impacts water quality and quantity. As watersheds are cleared of natural vegetation, precipitation events result in high flow pulses from rapid runoff and decreased infiltration of groundwater. In the past 20-30 years, the area of impervious cover in Texas has increased faster than any other state in the United States (Xian et al., 2011). As the population expands into the recharge and contributing zones of Edwards Aquifer in northern Bexar County, more impervious structures will be built to facilitate residential, commercial, and industrial development.

Most environmental problems in the urban environment are created locally with roadways and associated vehicle traffic being major contributors (Bolund and Hunhammar, 1999). Transportation infrastructure such as roadways and parking areas along with rooftops are the primary of impervious surfaces, but highly compacted soils also result in a high volume of stormwater runoff. Paved surfaces alter the hydrological cycle by decreasing rates of infiltration, evaporation, transpiration, and subsurface flow. Surface runoff is expected to increase with the loss of natural habitat and increased urbanization (LaFontaine et al. 2015). Additionally, impervious surfaces reduce groundwater recharge and increase runoff. Moreover, in karst zones such as the Edwards Aquifer Recharge zone, the rapid runoff from impervious structures can result in pollutants rapidly entering the karst aquifer. Roadside runoff results in significant amounts of suspended solids, nutrients, hydrocarbons, and metals that can infiltrate groundwater and aquifers (Muthusamy et al. 2018; Zhao et al. 2018).

Alteration to the natural landscape in Bexar County has been associated with the development of public transportation including interstate and state highways in association with the North American Free Trade Agreement (Yi et al. 2017). From 1976 to 1991, Kreuter et al. (2001) reported rangeland decreased by 65%, urban growth increased by 29%, and ecosystems services losses were greater than \$6.2 million within Bexar County. American Forests (2002) estimated changes in forests and associated ecosystem services in the San Antonio region from 1985 and 2001 and reported a 39% decrease in the woodlands and negative impacts on stormwater management. Yi et al. (2017) reported losses of 73,146 ha forest, 22,075 ha rangeland, and 19,224 ha of agriculture lands in Bexar County from 1984 to 2010. The loss of natural and cultivated habitat in association with increases in impervious surfaces and structures will

continue to impact water quality in Bexar County and has the potential to impact the Edwards Aquifer.

Conventional approaches to stormwater management design typically include only the hydrologic components of precipitation, runoff conveyance and storage capacity within their scopes. Low Impact Development (LID) recognizes the significance of other components of the hydrologic cycle as well, which includes the use of native vegetation. In arid and semi-arid regions such as central Texas, the use of native perennial and evergreen xeric vegetation in stormwater retention basins represents a cost-effective method that may control sediment and pollutants.

LID favors the use of decentralized control systems by keeping precipitation close to the source where it lands allowing the rainwater to percolate through the soil. Linear highway systems are typically decentralized already since the available controllable drainage area is only the right-of-way. Department of Transportation officials do not have the option of changing the road locations, but implementing LID efficient practices that utilize native vegetation to reduce pollutants is a cost-effective option that can improve water quality. Vegetated swales along roadways have been reported to remove 70% of all total suspended solids (Schueler et al. 1992, Li et al. 2008). Vegetation cover greater than 90% along roadways is most effective in removing total suspended solids (Barrett et al. 2004, Li et al. 2008). The removal of pollutants in LID structures can be accomplished by plant uptake, microbial processes, and sorption to organic matter (Barrett et al. 1998, Stagge et al. 2012).

To successfully integrate LID practices into a site, careful consideration must be given to where to introduce vegetation and the most suitable location to pond and infiltrate stormwater. Understanding the vegetation composition and coverage will provide insight into which species are most efficient in trapping sediment and removing pollutants from stormwater runoff along highways.

Based on a review of roadway runoff characteristics from 29 peer-reviewed manuscripts, Kayhanian et al. (2012) suggested that total suspended solids, total dissolved solids, total organic carbon and iron can serve as surrogates for comprehensive monitoring programs for monitoring pollutants from roadway runoff. In addition, sediment < 250 μm was found to contain greater concentrations of metals (Zanders 2005). Controlling and containing roadway sediment within detention basins reduces pollutant runoff into surface waters and shallow aquifers. The use of evergreen and perennial vegetation would provide year-round control of sediment and uptake of pollutants.

Storm-flow events in areas with a high percentage of impervious cover result in rapid runoff of nutrients, pollutants and trash that are directed into surface waters. Moreover, rapid runoff from impervious surfaces can impact groundwater in areas with karst topography such as the Edwards Aquifer recharge and contributing zones. Multiple roadways in northern Bexar County bisect the recharge and contributing zones of the Edwards Aquifer. Highway medians and setback vegetation along these major roadways range in size, but little is known about the effectiveness of vegetation bordering these roadways in Bexar County in uptake and containment of pollutant runoff.

Roadside corridors and associated drainage basins are managed utilizing plants and maintained with mowing to improve visibility for drivers' safety. Phytoremediation techniques utilizing vegetation provide stormwater management and pollutant removal. Vegetated areas intercept precipitation, decrease stormwater discharge volume, and trap sediment. Vegetation removes pollutants from infiltrated stormwater through root zone uptake and accumulating sediment. Vegetation has been shown to slow water velocity in aquatic and terrestrial systems resulting in sediment deposition. Incorporating vegetation into the landscape is a stormwater management technique that utilizes naturally occurring, environmentally beneficial mechanisms and requires minimal maintenance.

Most of the studies that have evaluated stormwater runoff along highways focused on the impacts to surface waters (e.g., rivers, lakes, and reservoirs). However, within the Edwards Aquifer recharge and contributing zones, the impact of pollutants in stormwater runoff from roadways can greatly impact the drinking water of millions of people and potentially result in millions of dollars in remediation costs for cleanup of pollutants contaminating the aquifer. Highway runoff in karst zones is a significant issue since the roadway runoff can flow directly into the aquifer through fissures, cracks, and sinkholes with minimal filtration due to a thin or non-existent soil layer (Stephenson and Beck 1995). As urbanization and development continue to expand into the northern Bexar County, the recharge and contributing zones will be exposed to continuing pollutants from roadways and impervious structures.

In some watersheds, groundwater and aquifer levels can decline due to increases in impervious surfaces as most stormwater runoff is diverted into drainages instead of infiltrating and percolating into the aquifer. Such recurring events have the potential to lower aquifer levels over time as more development occurs. Vegetated landscapes along roadways result in retention of runoff through interception, infiltration, and evapotranspiration. Water quality within vegetative stormwater basins is improved through natural processes that include sedimentation, sorption, plant uptake, and microbial breakdown.

Precipitation events less than 0.2 cm can generate rapid runoff due to soil compaction and impervious structures in urban and developed areas (Li et al. 2008). Low impact development favors the use of decentralized source control systems especially for micro-storm events and can buffer pollutants from entering surface and groundwater. The use of native vegetation for landscapes along roadways preserves some of the natural ecology and restores ecosystem services such as improvement of water quality, reduced erosion, and wildlife habitat. In addition, naturally landscaped roadways provide visual esthetics and habitat for species of invertebrates and birds.

Limited research has evaluated native plants that are effective in intercepting sediment and nutrient uptake from stormwater runoff along highways. Based on a 2010 report, there is no program that tracks the location, design type and maintenance of stormwater basins in the recharge and contributing zones of Bexar County (GEAA, Greater Edwards Aquifer Alliance, 2010). Gaining information on the vegetation within stormwater retention basins can be implemented to improve best management practices and result in reduced costs and improved water quality from stormwater runoff along roadways.

The primary objectives of this study are to 1) evaluate the sediment and pollutant composition in sand filtration systems and vegetated swales over multiple stormwater events along three major

highways in the Edwards Aquifer recharge and contributing zones of northern Bexar County, 2) determine the vegetative composition and soil types at each site, 3) document the vegetation species most efficient at uptake of various nutrients and metals, and 4) make recommendations of xeric species of vegetation most resilient and resistant to extreme environmental conditions and most adaptable for long-term survival in LID structures receiving roadway and impervious structure stormwater runoff.

Methods

Vegetation and Soils

Study Sites

The study sites are managed by the City of San Antonio's Public Works Department. Sand filtration systems (n = 6) and swales (n = 5) were selected along roadways within the Edwards Aquifer Recharge Zone (Figure 1; Appendix 1). One additional swale (Babcock Road site) was located in the Edwards Aquifer Contributing Zone. All 12 sites were sampled for vegetation during the summers and winters of 2020 and 2021. Six of the sites were classed as primary and the other six sites were listed as secondary. Primary sites were only sampled for raodway runoff for water quality variables. Secondary sites were only sampled for vegetation composition and soil characteristics. Sand filtration systems are managed by removing trash, mowing, and removing and replacing the top 5 cm of quartz sand two times per year. The swales are managed by mowing the vegetaton a minimum of two times per year. Vegetation and soil samples were collected from all 12 sites.

Field Studies

Vegetation surveys

At each sand filtration system and swale, three random line transects were placed across the width of the site with a meter tape and temporarily staked. Line transects were variable depending on the width of the site and ranged from 8 to 22 m. All vegetation along each transect was recorded by species to the nearest cm along the line (Canfield 1941). The total distance (cm) of each plant species was divided by the length of the line to determine the percent coverage of each species. The coverage of each species along the lines at each site was combined as a composite sample and the mean and standard error were calculated for each species. Species were classified as native or non-native. Species richness patterns were determined by counting the number of plant species that intersected each transect line. Species evenness patterns were determined using the methods of Williams (1964). Evenness (E) patterns were calculated as

$$E = 1/DS$$

where D is the Simpson's Diversity Index, and n = the total number of each species, and N = the total number of all species

$$\sum (n/N)^2$$

and S is species richness (Williams 1964). The three lines at each site were averaged to obtain the mean species richness and evenness per site.

Plants were classified by functional groups that included status (native or non-native), life cycle (annual, biannual, perennial, annual/biannual, biannual/perennial, annual/biannual/perennial), plant type (monocot or dicot), growth form (fern, graminoid, forb/herb, shrub, and tree), and wetland classification (upland, facultative upland, facultative, facultative wetland, obligate wetland) (USDA, 2022).

Vegetation biomass

Within each transect line, three 0.25 m² plots were randomly selected along the line for analysis of plant dry weight. Plants growing within the plots were identified by species, and all above ground plant parts were cut and placed into paper bags and labeled by species, plot location, site, and date. All dead and partially decomposed organic matter on the soil surface was collected as litter and bagged.

Plant samples were transported from the field to the lab, labeled, bagged, and dried at 60 °C in drying ovens for > 48 hours. Following drying, samples were weighed for biomass to the nearest 0.001 g to estimate plant density by biomass at each site and converted to g m⁻². Plants were grinded into a homogenized powder < 10 μ m using a Wiley Mill grinder. Ground plants samples were poured into labeled plastic bags and stored in a freezer at 4 °C until further analysis for organic matter, total organic carbon, and metals.

In situ swale plantings

Six native grasses were grown from seeds and two amphibious graminoids were propagated from rhizomes for planting in the six swales. Native grasses included switchgrass (*Panicum virgatum*), white tridens (*Tridens albescens*), silver bluestem (*Bothriochloa laguroides*), bushy bluestem (*Andropogon glomeratus*), buffalograss (*Bouteloua dactyloides*), and sideoats grama (*Bouteloua curtipendula*). The two amphibious graminoids selected were knotgrass (*Paspalum distichum*) and beaked spikerush (*Eleocharis rostellata*). Plants were maintained in the UTSA greenhouse for 3 months until planting in swales. No planting occurred in detention ponds since maintenance occurs twice per year in which the upper 5 cm of sediment is removed.

Plantings occurred in May 2021 and plants were harvested in October 2022 to allow the plants to establish over two growing seasons. In each plot, all above ground plant parts were cut at soil level and discarded prior to planting. The soil was excavated with a shovel within each plot to a depth of 20 cm and soil was broken up to homogenize the soil and grubbed to remove existing roots and rhizomes. In each of the six swales, four randomly placed 0.25 m² plots were selected in the lower basin with no plots being placed on the slopes. Native grasses (two of each of the five species) were planted in two plots and amphibious plants (five of each of the two species) were planted in the other two plots within the lower basin of each swale.

Plants were harvested by digging up the plots and extracting the plants and soils. Plants and soil were placed in plastic containers, brought back to the UTSA greenhouse, and soaked in water for 48 hours. Individual plants were then removed and washed with a stream of water to separate roots and shoots. Roots and shoots were placed separately in labeled paper bags and dried at 60 °C in drying ovens for >48 hours. Following drying, samples were weighed for biomass to the nearest 0.001 g to estimate plant biomass at each site.

Soil samples

Prior to the collection of soil samples, all litter and plant matter present on the surface was removed. Three soil cores were taken at each site to a depth of 30 cm at the beginning, middle, and end of each line based on the length and width of the site (Winiarski et. al, 2006) (Table 3). Each soil core sample was separated into three subsamples by depth: top (0-10 cm), middle (10-20 cm), and bottom (20-30 cm) sections. Soil samples were placed in plastic bags, labeled, and transported back to the lab to be immediately dried prior to processing. Because soil in these areas can commonly contain rocks and dense clay, dispensable and cost-efficient steel pipes were used to collect soil samples. Soil volume of the core was estimated using the formula:

$$Volume = (\pi)(r^2)(H)$$

The dimensions of the steel pipe soil cores were 30 cm H x 4.2 cm W (r = 2.1 cm) resulting in a soil core volume of 415 cm³. The dimensions of the three soil core sections were 10 cm H x 4.2 cm W, resulting in section volumes of 138 cm³ of soil.

Preparation of soil samples

Each soil sample was placed in an aluminum pan for drying. Soil samples were identified by a metal tag labeled with the data and site location. The aluminum pans and soils samples were dried at 105 °C for > 48 hr (Kavehei et. al, 2019). Dried soils were pounded with a hammer to break apart clumped soil aggregates, sieved, and separated by particle size (4000, 2000, 500, 250, 125, and 63 μ m), and weighed for particle size distribution. Soil samples were then sieved through a 2-mm mesh, removing small rocks and plant material (Winiarski et. al, 2006; Zeng et. al, 2011). To prepare soil for organic carbon analysis, a small portion of the sieved soil was placed in a clean mortar and pestle and ground completely until it was a fine homogenized powder. Soils that were not used immediately were stored in a freezer at 4°C until carbon analysis.

Bulk density

Soil bulk density was determined using standard methods of a volumetric soil sample from a soil core (Weil & Brady 2019; NRCS 2001). The volume of the core was calculated and the height at which the soil filled the core was recorded to determine the volume of the soil if the core was not filled. The soil wet weight was taken and then placed in an oven for 24 hrs at 105° C until the weight remained constant. The dry weight was recorded and the soil was sieved through 2 mm to remove rocks and particles ≥ 2 mm.

The volume of rocks was determined using methods from NRCS (2001) by using water displacement in a 1/3 filled graduated cylinder of water. The difference is equal to the volume of rocks. Soil bulk density (D_b) was calculated based on the following equation (NRCS, 2001):

Volume of soil = Total volume of soil – volume of rocks

Following the removal of rocks, the bulk density was calculated using the equation from NCRS (2001):

 $D_b = (\text{oven dried weight of soil}) / (\text{volume of soil})$

Organic matter

Soil samples (30 cm cores) were collected from all sites during the summer and winter of 2021 and processed as described above. Following processing, soils were analyzed for organic matter content using the loss-on-ignition method (Wang et al., 2012; Heiri et al., 2001). Three replicate soil samples were weighed to 5 g (+/- 0.001 g), placed in crucibles, and ignited at 550 °C for 4 hours in a muffle furnace. Organic matter was estimated by the formula:

Organic matter (%) =
$$\frac{LOI\ weight}{Dry\ weight} * 100$$

Carbon analysis

Total organic carbon (TOC) analysis for soil samples was analyzed using a Shimadzu TOC-SSM Carbon Analyzer. Soil samples for the sites in this study required an alternative method of TOC analysis due to large amounts of sand present in the samples which resulted in errors with readings being negative due to high inorganic carbon content. To correct for the high amount of sand and obtain correct TOC readings, soil samples were treated with acid to remove the inorganic carbon (IC) from the sample prior to analysis (Bisutti et al. 2004; Shimadzu, 2012). Acid treatment was performed by adding a 1:1 ratio of hydrochloric acid and deionized water to a 2 g subsample of soil. The acid treatment was replicated twice for each soil sample to remove IC from the sample. The first treatment of 3 mL acid was pipetted directly onto the soil, and then after 24 hours a second 3 mL of acid was pipetted onto the soil to ensure all the IC was removed from the soil subsamples (Dhillon et. al, 2015). After the IC finished reacting with the acid solution, the samples were re-dried at 105 °C for > 30 minutes to remove moisture (Dhillon et. al, 2015; Kavehei et. al, 2019). Each dried sample was analyzed for TOC after removal of IC. Three replicates of 100 mg subsamples from the 2 g soil were analyzed for organic carbon.

Metal analysis in soil and vegetation samples

Soils were analyzed at the end of the experiment for metal concentrations that included magnesium (Mg), iron (Fe), zinc (Zn), lead (Pb), copper (Cu), chromium (Cr), nickel (Ni), and cadmium (Cd). Common native plants found in both swales and sand filtration systems were selected for analysis. Plants were collected during the summer when plants were actively growing. No plants were collected during the winter when most plants were dormant. Three forbs/herbs and one grass were selected for metal analysis in roots and shoots and included: frog-

fruit (*Phyla nodiflora*), Mexican hat (*Ratibida columnifera*), white tridens (*Tridens albescens*), and wild petunia (*Ruellia nudiflora*). Plants were harvested from swales and sand filtration systems, separated by roots and shoots, and each part was rinsed with deionized water to remove soil. The lengths of the plant roots and shoots were measured to the nearest 0.1 cm. Plant parts were oven dried at 70 °C for 5 days and weighed to nearest 0.1 gram. Plant parts were then ground to 420 µm with a Wiley-Mill (Thomas Wiley Mini-Mill, Fisher Scientific, Hampton, NH). A subsample of 0.1 mg of plant parts and soils was selected from each sample and digested in 9 mL of HNO³. For soils, an additional 3 mL of hydrofluoric acid was treated for 15 minutes in a MARS 5 microwave (U.S. Environmental Protection Agency, 1995). The acid was centrifuged at 10,000 rpm for 15 minutes to settle any remaining solids. Following centrifuging, a 0.1 mL of the acid solution was diluted into 9.9 mL of deionized water for analysis of metal ppm per 0.1 mg of sample using inductively coupled plasma - optical emission spectrometry (ICP-OES).

Oil and grease analysis

Sediment from roadway runoff following precipitation for oil and grease analysis was captured at each site using a systematic sampling design. Each site contained a 3-by-3 matrix of sample locations with traps spaced. Two sets of traps were placed in the same location to capture sediment to examine particle size and oil and grease concentration. Cylindrical traps (413 cm³, 5.1 cm in height) with four 1.6 mm holes in the bottom and 6.4 mm holes in the top to allow for drainage were used to capture sediment samples for particle size following a precipitation event. Additional cylindrical traps (824 cm³, 10.2 cm in height) were placed 10 cm from the sediment traps at each site to capture sediment samples for oil and grease analysis. The bottom of the traps contained 50 µm mesh to trap the sediment within the cylinder. All sediment traps were buried into the soil with the tops 0.6 cm above soil level for collection of sediment during rain events.

Sediment traps were collected within 24 h following a precipitation event. The sediment was collected from the traps and placed in labeled sealed 1 L plastic bags and taken to the lab for processing. In the lab, the mesh with collected sediment for oil and grease analysis was removed. Sediment was manually removed from each piece of mesh. Samples (n = 3) from the inlet, middle, and end were combined into one composite sample. For oil and grease samples, sediment was placed in sealed glass containers and placed in a 4 °C freezer until the oil and grease analysis was performed. Samples for grain size analysis were poured directly into an aluminum container and placed in a 50 °C oven for a minimum 48 hours to dry. Following drying, these samples were individually bagged and labeled until sieving for particle size analysis (as described above).

Oil and grease samples were measured using a Horiba OCMA-350 Oil Content Analyzer (Horiba Ltd., Kyoto, Japan). Soil analysis using the OCMA-350 was performed with a proprietary solvent extraction and spectroscopic analysis procedure meeting the protocol for measurement of soil samples according to EPA test method 418.1, Total Recoverable Petroleum Hydrocarbons (TPH) (Horiba, 1995, U.S. Environmental Protection Agency, 1983). Calibration and span procedures were performed using a measurement span setting of 200 mg/L, with 1.0 g of soil and 10.0 mL of proprietary solvent (Horiba, 1995). A 1.0 g subsample of each sediment was weighed to the nearest 0.01 g and was placed in a clean 25 mL Erlenmeyer flask. Anhydrous sodium sulfate (Na₂SO₄) was added to dry the soil sample and mixed thoroughly into the soil sample

with a stainless-steel spatula. In each sample flask, 10 mL of proprietary Horiba solvent was added to the solution. Extraction was then performed for oil in soil to oil in solvent. The sample flask was sealed using a stopper and shaken vigorously by hand for two minutes to form a homogenous solution. After shaking, the flask was placed on a flat surface for \geq 10 minutes to allow suspended material to settle.

An 11 cm diameter Whatman filter paper (No. 40) was inserted into a glass funnel and 2.0 g (± 0.01g) of conditioned silica gel (60-to-200 mesh) conditioned to between 1-2% moisture was placed in the filter paper. The solvent mixture in the settled sample was extracted from the flask using a pipette and filtered through the silica gel and filter paper into a clean 25 mL flask. Using a pipette, 8.0 mL of the filtered extract in the flask was transferred into the OCMA-350 measurement cell. The measurement cell was placed into the OCMA-350, followed by a measurement and stability check. Once the reading on the OCMA-350 stabilized, it was recorded as the oil and grease concentration per mg kg⁻¹ of total oil and grease in the sample. The OCMA-350 was recalibrated after every 10 samples.

Sediment samples collected from runoff were dried at 50°C oven for a minimum 48 hours to dry. Particle size of each composite sediment sample was sieved through a series of wire mesh stainless steel Fieldmaster sieves at 4000, 2000, 500, 250, 125, and 63 µm (Forestry Suppliers, Inc., Jackson, MS 39201). Following sorting by particle size, the mass of each collected sample by particle size was recorded to the nearest 0.01 g.

Greenhouse studies

Seed germination

The seeds of six native grasses were collected locally from study site swales and ephemeral streams on UTSA's campus. Species selected for the study were based on native grasses observed in the study swales or ephemeral streams. The native grass species used in this study included silver bluestem (*Bothriochloa laguroides*), switchgrass (*Panicum virgatum*), white tridens (*Tridens albescens*), sideoats grama (*Bouteloua curtipendula*), eastern gamagrass (*Tripsacum dactyloides*), and buffalograss (*Bouteloua dactyloides*).

Seeds (n = 500 to 750) of each species were potted in 5.7 L rectangular plastic containers (34.6 cm L x 21 cm W x 12.4 cm H) filled with a commercial potting soil (Miracle-Gro Premium Potting Mix, 0.21% N, 0.11% P, and 0.16 K). Seeds were watered every two days to maintain saturated soils and promote germination. Once germination occurred, individual seedlings were removed once they reached 6-8 cm in height. Seedlings were potted in round plastic pots (763 cm³) and filled with 740 cm³ of Miracle-Gro Premium Potting Mix. Seedlings were maintained in the UTSA Environmental Science greenhouse in the southeast section of campus for ca. 2-3 months until used in the studies below. Day and night ambient air temperatures in the greenhouse were recorded every 15 minutes using HoboTemp data loggers with mean temperature of 37.2 C (SE = 0.36) from 0700-2100 hours and 27.0 C (SE = 0.09) from 2100-0700 hours. *Drought tolerance*

Six species of native grasses (silver bluestem, switchgrass, white tridens, sideoats grama, eastern gamagrass, and buffalograss) were propagated as described above and watered at varying water

regimes for 3 months from July to September of 2021. There were ten replicates per treatment and plants were watered every 1, 2, 3, 6, 12, 24, and rain days. On watering days, plants were watered to field capacity. The determination of rain day watering was taken by watering the plants in this treatment on the days it rained at UTSA's campus that included 13 days in July, 10 days in August, and 2 days in September. The rain day watering regime was selected to account for the natural variability plants experience in the sub-tropical, sub-humid environment in San Antonio. Plants were harvested at 3 months, separated by roots and shoots, and the soil was washed off the roots. Following harvest, plant parts were bagged and labeled, and placed in a drying oven for 96 hours at 60 °C. Plant shoots and roots were weighed to the nearest 0.1 gram.

Nutrient growth studies (nitrogen and phosphorous)

Six species of native grasses (silver bluestem, switchgrass, white tridens, sideoats grama, eastern gamagrass, and buffalograss) were propagated and then potted as described above. Seedlings were potted in soils with nitrogen concentrations of 1.2, 2.4, 4.8, and 9.6 mg L⁻¹ and phosphorus concentrations of 0.12, 0.24, 0.48, and 0.96 mg L⁻¹. Plants were watered daily to field capacity using a hand nozzle with low flow pattern. There were eight replicates of each species per nutrient treatment. Plants were harvested at 3 months and separated by roots and shoots. Following harvest, plant parts were bagged and labeled, and placed in a drying oven for 96 hours at 60 °C. Plant shoots and roots were weighed to the nearest 0.1 gram.

Metal uptake in native grasses

Five species of native grasses (buffalograss, eastern gamagrass, silver bluestem, switchgrass, and white tridens) were used in the *ex situ* analysis of metal uptake in the roots and shoots. Plants were propagated as described above and seedlings were randomly selected for the study. Three metals [copper (CuCl₂), lead (PbCl₂), and chromium (CrCl₃)] were selected based on preliminary analysis of roadway runoff samples from this study during 2020. Metals were mixed homogenously into the soil at concentrations of 0.101 and 0.504 mg kg⁻¹ for copper, 0.052 and 0.262 mg kg⁻¹ for lead, and 0.021 and 0.106 mg kg⁻¹ for chromium.

Individual plants were grown in a greenhouse for eight weeks in randomized order. Plants were watered every 3-4 days with 236 mL of tap water. Plants were harvested, separated by roots and shoots, had soil shaken off the roots, then both parts were rinsed with deionized water to remove any remaining soil. The length of the plant roots and shoots was measured to the nearest 0.1 cm. Plants were oven dried at 70 °C for 5 days and weighed to nearest gram. Plant parts were then ground to 420 µm using a Wiley Mill (Thomas® Wiley® Mini-Mill, Fisher Scientific, Hampton, NH). A subsample of 0.1 mg was selected from each sample and digested in 9 mL of HNO³. Soil samples were further digested in 3 mL of hydrofluoric acid for 15 minutes in a MARS 5 microwave (U.S. Environmental Protection Agency, 1995). The acid was centrifuged at 10,000 rpm for 15 minutes to settle any remaining particulates. Following centrifuging, a 0.1 mL of the acid solution was diluted into a vial containing 9.9 mL of deionized water for analysis of metal

ppm per 0.1 mg of sample using inductively coupled plasma - optical emission spectrometry (ICP-OES).

Statistical analysis

Data was maintained, organized, and arranged in Excel spreadsheets. Descriptive statistics (means and standard error) were calculated for all varaibles. All data was checked for normality and equality of variance. If data did not meet parametric assumptions, the data was transformed using log or square-root transformations to meet assumptions and parametric statitical tests were used. Following transformations, if data did not meet parametric assumptions, non-parametric statistical analysis tests were used. All statistical tests were analyzed with a P-value of 0.05. Linear and non-linear regression was used to compare native and non-native species richness based on total coverage. Mean species richness, diversity, evenness, and mean cover were analyzed between swales and detention ponds with a Student's t-test. Seasonal differences (summer and winter) by year among swales and detention ponds were analyzed with a one-way ANOVA or Kruskal-Wallis test. The mean coverage, dry weights of herbs/forbs and grasses and leaf litter in swales and detention ponds were analyzed with a one-way ANOVA. Differences in the dry weights of native and non-native plants were analyzed with a one-way ANOVA. *In situ* planting of grasses in swales was analyzed for survival (%), root, shoot, and total biomass, and root to shoot ratio with a one-way ANOVA or Kruskal-Wallis test.

Native grasses grown in the greenhouse at different concentrations of nitrogen and phosphorus were analyzed with a one-way ANOVA or Kruskal-Wallis test for root, shoot, and total biomass, root to shoot ratio, and realtive growth rates. Greenhouse grasses tested for tolerence to water regimes were evaluated for root, shoot, and total biomass, root to shoot ratio, and realtive growth rate with a one-way ANOVA. Uptake of metals by five species of native grasses under greenhouse conditions was evaluted with a Kruskal-Wallis test using Ln transformed data.

Soil bulk density, organic matter, organic carbon, and soil particle size were analyzed with a one-way ANOVA or Kruskal-Wallis test. *In situ* analysis of four common roadside plants' uptake of metals was analyzed with a one-way ANOVA for root, shoot, and total biomass, and root to shoot ratio. *In situ* metal concentrations in soils of swale and detention ponds were compared with a Student's t-test. *In situ* metal concentrations in soils at different depths and seasonal differences were analyzed between swales and sand filtration systems using a Kruskal-Wallis test. Oil and grease concentrations and sediment weight collected from runoff following precipitation were analyzed with a Student's t-test to compare differences between swales and sand filtration systems. Differences in oil and grease concentrations and mean sediment weight were analyzed for differences with a one-way ANOVA or Kruskal-Wallis test. Data was analyzed using SigmaPlot (Version 14.0, Systat Software, Inc., San Jose CA) and PC-ORD (Version 5.10, MjM Software, Glenden Beach, OR).

Water Quality Monitoring

Study Sites

We monitored three basins within the recharge zone of the Edwards Aquifer, which are described in the following section.

<u>Bulverde Basin</u> - The Bulverde basin is located in the recharge zone of the Edwards Aquifer in Bexar County, Texas, USA. The basin is situated in the north side of San Antonio, with the following approximate geographical coordinates: 29°36′24.7″N 98°25′04.9″W. The basin receives runoff from a watershed having 72% impervious surface area including developed area consisting of a 55,980 m² large residential area, 16,586 m² commercial area, and 21,660 m² of roads; and an undeveloped area of 37,304 m² of natural vegetation cover. The basin has a total area of 474 m² and a filtration area of 357 m². The basin consists of a 45 cm deep sand layer on top of filter-fabric underlain by a 45 cm deep gravel layer. The bottom layer of the basin consists of 15 cm perforated pipes that transfer the filtered water approximately 61 m downstream of the basin where the filtered effluent is discharged on the surface.

TPC Basin - TPC basin was located in the north-side of San Antonio on the TPC parkway, which averaged 18,820 vehicles per day on an annual basis. Through one circular channel of 0.9 meters (3 feet) in diameter, runoff was received from a watershed that covered 42,000 m² and 47% impervious surface area, including 2,000 m² and 7,200 m² of undeveloped meadows and brush. In addition, the area contained 8,800 m² of dispersed areas and 7,200 m² of high-density residential areas. Additionally, the area covered by commercial, industrial, transportation, and streets was 240, 12,000, and 4,400 m², respectively. The basin had a total area of 771 m² with 208 m² filtration area and 5.5 m² of baffle blocks. The filtration area consisted of 45 cm sand area on top of filter fabric underlain by 30 cm gravel layer. The bottom layer of the basin consists of 10 cm perforated pipes that are connected to the main 15 cm pipe which transfers the filtered water approximately 20 m downstream of the basin where the filtered effluent is discharged on the surface.

Kyle Seale Parkway Basin - Kyle Seale Parkway basin is located in the north-west of the city of San Antonio on Kyle Seale Parkway. The basin receives runoff from a watershed with a total area of 16,000 m² and 63 percent impervious cover. The channel receives runoff through one 1.12 m (3.5 ft) square reinforced concrete channel. There was a total of 1,818 m² of undeveloped brush, 9,870 m² of high-density residential area, 519 m² of open space, 3,636 m² of streets and transportation land use with an average annual traffic volume of 13127 vehicles per day.

With a total area of 339 m², the basin included 111 m² of filtration area and 39 m² of rock gabion filtration area. After entering the sedimentation area of the basin, the water then passed through the rock gabion and entered the filtration area. Approximately 45 centimeters of sand are laid over a geotextile filter fabric underlain by a 15-centimeter gravel layer as the filtration area. At the base of the basin are 10 cm perforated pipes connected to a 20 cm pipe that carries filtered water approximately 50 meters downstream of the basin, where it is discharged to the surface.

Swale descriptions

Three grassy swales were selected including Kyle Seale Parkway swale (29.5644, -98.64500), Plaza swale (29.579594, -98.586080), and Roadrunner Way swale (29.57401, -98.62857) which receive stormwater runoff from residential areas. Satellite pictures of the three swales are shown in Figures 44, 45, and 46.

Stormwater Sampling

Sand filtration Basins – Sand filtration basins' stormwater sampling for water quality analysis was conducted from January to December 2020 at Bulverde basin and from January 2021 to December 2021 at TPC and Kyle basins. Samples were collected from both the inlet of the basin and at the discharge point outside the basin using programmable autosamplers (ISCO 6712, Teledyne ISCO) powered by deep cycle marine batteries. The samplers were triggered by separate flow modules attached to them (ISCO 730 Bubbler Flow Module, Teledyne ISCO), which measures the water depth. Precipitation data were collected using a 674 Rain Gauge (Teledyne ISCO) installed on-site and connected to the inlet autosampler. During each storm event, the inlet autosampler was triggered when the flow depth reached 1.25 cm, which was the minimum depth allowing the intake tube to be submerged during a storm event. The samples were collected every 15 min in 1 L sterile plastic bottles throughout the storm event or until all sample bottles were filled. The outlet autosampler was triggered 15 minutes after the first flow from the outlet pipe was detected to assure collection of the treated flow, not the old water in the system from the previous event; and then collected every 30 minutes or until all sample bottles were filled. Samples were retrieved within 24 h of storm events and transported to the laboratory at the University of Texas at San Antonio (UTSA) in a cooler filled with ice. The event mean concentration (EMC) for the inflow and outflow samples was calculated based on the flow rate of each sample at the collection time.

<u>Swales</u> - Stormwater sampling for swales were performed using three Thermo Scientific Nalgene Storm Water Samplers (Table 15). The length of the swale was carefully measured. The samplers were placed inside the ground, one at the beginning, one in the middle, and one at the end of the swale based on the measurements. Each sampler was equipped with 1-liter amber glass bottle to capture the stormwater. Swale samples were transferred inside a cooler filled with ice to the lab. Samples were treated and processed the same way as the basin samples.

Water Quality Analysis

Nutrients - In the Bulverde basin and Kyle swale Ammonia (NH₃-N), nitrite (NO₂⁻-N), and nitrate (NO₃⁻-N) concentrations were measured by standard colorimetric methods (Crawford et al., 2002; Rhine et al., 1998; Tor et al., 2000) adapted to microtiter plate, and a Synergy HTX Plate Reader (BioTek Instruments, Winooski, VT, USA). Total phosphorus concentrations were measured based on the Acid Persulfate Digestion Method 8190 (HACH TNT Total Phosphorus low range set) and HACH DR 2800 spectrophotometer. Total phosphorus concentrations were measured based on the Acid Persulfate Digestion Method 8190 (HACH TNT Total Phosphorus low range set) and HACH DR 2800 spectrophotometer.

In the TPC basin, Kyle basin and Plaza swale nitrite (NO_2^--N) , nitrate (NO_3^--N) and phosphate (PO_4^{3-}) concentrations were measured using a high-performance liquid chromatography (HPLC) Shimadzu - Nexera series LC-40 (Shimadzu, Japan). As described in the previous section, Ammonia (NH_3-N) was measured using a standard colorimetric method

<u>Carbon, COD, and Solids</u> - In all basins and swales Total Carbon (TC), Total Organic Carbon (TOC), Dissolved Organic Carbon (DOC), Inorganic Carbon (IC), and Total Dissolved Nitrogen (TDN) were measured using a Total Organic Carbon Analyzer (TOC-L, Shimadzu, Japan). Chemical Oxygen Demand (COD) was measured according to the US EPA reactor digestion

method 19 by method 8000 (HACH, COD Digestion vials, high range) and HACH DR 2800 spectrophotometer. Total Suspended Solids (TSS) and Total Dissolved Solid (TDS) concentrations were determined based on the US Environmental Protection Agency's gravimetric method, methods 2540D and 2540C in the Standard Methods for the Examination of Water and Wastewater.

<u>Metal Analysis</u> - In all basins and swales, Inductively Coupled Plasma – Optical Emission Spectrometry (ICP-OES) OptimaTM 7000 (PerkinElmer, USA) was used for metal analysis including Cu, Fe, Cr, Mg, Ni, Pb, Cd, and Zn. To establish a calibration curve, a set of 9 standards (1, 5, 30, 50, 80, 160, 250, 500, 1000 ug/l) were prepared using Multielement Standard Solution 6 for ICP (100 mg/l) from Millipore Sigma Aldrich.

<u>Oil and Grease</u> - For oil and grease measurements in basins and swales, standards were prepared using a commercially bought heavy oil standard solution. Extraction was performed using HORIBA S-316 solvent. The extract was quantified using HORIBA oil content analyzer.

<u>Hydrocarbons</u> - Basin water samples for the PAHs measurement were subjected to extraction using Heidolph rotary evaporator and Dichloromethane (DCM) organic solvent. The PAH extracts were then subjected to Gas Chromatography/Mass Spectrometry (GC/MS) within 40 days of collection. The extracts which contain 1 mL of solution are transferred to the micro tubes provided by Agilent manufacturer.

<u>Microbial testing for fecal coliform</u> - The analysis performed using IDEXX reagent kits (colilert-18), and Quanti-Tray Sealer. The vessels were incubated at 44.5 °C for 18-22 hours. The appearance of the vessels was then compared to the comparator to determine most probable number (MPN).

Soil sampling

The detention basins were divided into three sections based on the length of the basin and a 30 cm soil core sample was collected in the middle of each section. Each core was divided into three samples corresponding to depths of 0-10 cm (top), 10-20 cm (middle), and 20-30 cm (bottom). After collection, the remaining holes were filled with nearby soil to minimize system alteration. Soil cores were collected about five months apart to represent the summer (June 2020) and winter seasons (November 2020), resulting in a total of 18 soil samples. All soil samples were stored in 50 ml conical tubes in a -80 °C freezer until DNA extraction.

DNA Extraction and Bacterial 16S rRNA gene sequencing

After soil samples were allowed to thaw to room temperature, DNA was extracted from 0.25 g of each soil sample using the DNeasy Powerlyzer Powersoil kit (Qiagen, Hilden, Germany) in combination with automated robot Qiacube Connect (Qiagen, Hilden, Germany) according to the manufacturer's instructions. DNA purity and concentration were measured with the Nanodrop One Spectrophotometer (Thermo Scientific, Wilmington, DE) and DNA extracts were stored at -20 °C until used in sequencing.

Stormwater detention basins serve as vital components in mitigating the adverse effects of urban runoff, and investigating the microbial dynamics within these systems is crucial for enhancing their performance and pollutant removal capabilities. The diversity and composition of bacterial communities in the soil samples was investigated by high-throughput sequencing of 16S rRNA gene libraries as described in our previous study (Phan et al., 2020). 16S rRNA gene libraries were

generated with 16S amplicon primers for the V3 and V4 hypervariable region Bact_341F (5'-CCTACGGGNGGCWGCAG-3') and Bact_785R (5'-GACTACHVGGGTATCTAATCC-3') and sequencing was performed on an Illumina Miseq benchtop sequencer using pair-end 300 bps kit at the UTSA Genomics Core, San Antonio, Texas.

Fastq files were analyzed using Quantitative Insights Into Microbial Ecology 2 (QIIME 2, version 2021.11.0). Barcodes, adapters and primer sequences were removed. Sequence quality control and feature table construction was performed using DADA2 (Callahan et al., 2016) pipeline in QIIME 2 for modeling and correcting Illumina sequenced fastq files including removal of chimeras. Fastq files were processed by the QIIME DADA2 denoise-paired command. Alpha and beta-diversity analyses were performed with the q2-diversity plugin in QIIME2. The alpha diversity indices for samples richness and evenness were determined by Shannon diversity index to measure community richness, Faith's phylogenetic diversity to measure community richness that incorporates phylogenic relationships between the features, and Pielou index to measure community evenness. Principle Coordinate Analysis (PCoA) and cluster analysis were carried out to compare the bacterial diversity between different samples (beta diversity) using unweighted UniFrac distance matrices.

For taxa comparisons, relative abundances were used based on all obtained readings. We used the QIIME2 q2-feature-classifier plugin and the Naïve Bayes classifier that was trained on the Greengenes 13.8 99 % OTUs full-length sequences. Relative abundance of the different nitrifying and denitrifying bacterial genera were considered based on recent studies (Huang et al., 2020b; Rajta et al., 2020; Zuo et al., 2020).

Results

Vegetation surveys

A total of 154 plant species were documented in this study with 114 native and 40 non-native species (Appendix 3). In swales, a total of 121 (89 native and 26 non-native) species were recorded with 94 (68 native and 26 non-native) species recorded in sand filtration systems. The ratio of native to non-native plant species was similar between swales (2.8:1) and sand filtration systems (2.6:1).

Species area curves (Figure 2) and regresson analysis (Figure 3) based on total coverage indicated that non-native species were domiant over native plants. Twelve non-native species had total percent coverage ranging from 101.0 to 1738.7 %, while seven native species had total percent coverage ranging from 121.6 to 267.4 % over the study period. Overall, total plant species richness was higher for native plants compared to non-native plants, but total percent cover was higher for non-native species. Non-native plants exhibited a moderate positive relationship in swales (y = 41.8x + 348.6; $R^2 = 0.51$) and low negative relationship in sand filtration systems (y = -139.9 + 2565.0; $R^2 = 0.23$) based on percent coverage. Native plants exhibited a moderate positive relationship based on percent cover for both swales (y = 9.9x + 74.5; $R^2 = 0.40$) and sand filtration systems (y = 3.9x + 121.9; $R^2 = 0.58$).

Native species richness was higher in the summer months compared to winter but varied depending if the sites had been mowed (Table 1). In addition, many of the native species are deciduous and go dormant in the winter months. Non-native richness was generally similar among sites, season, and year with some exceptions due to maintenance by removing and replenishing the top 5 cm of sand in the detention ponds. Total species richenss was higher for native plants (range 17-49) compared to non-native (range 8-25) in both swales and detention ponds (Table 1). However, the reverse was found for total percent coverage with non-native species coverage having higher percent coverage (range 175-1326) compared to native coverage (166-712) in both swales and detention ponds (Table 2).

Native dicot species richness was higher (range 13-38) compared to native monocots (range 1-12), non-native dicots (range 5-15) and monocots (3-10) (Table 3). Conversely, total percent coverage was higher for non-native monocots (range 76-1256) compared to non-native dicots (range 70-329), native dicots (range 51-323) and monocots (range 1-403) (Table 4).

Native perennial plants had higher richness (range 6-26) than other life cycles (Table 5). Native monocots had higher species richness than all non-native life cycle groups. However, non-native perennials had the highest total percent cover (range 76-1290) with native perennial coverage having the next highest coverage (range 25-481) (Table 6).

Native forbs and herbs species richness was higher (range 10-48) compared to all other plant growth forms (Table 7), but non-native graminoids had the highest total percent coverage (range 0-1256) (Table 8). Forbs and herbs and graminoids were the dominant growth forms in both swales and detention ponds. Ferns, vines, shrubs, and trees were uncommon in swales and detention ponds.

Based on the USDA Wetland Indictor Species (USDA, 2021), native upland (range 8-33) and facultative upland (range 6-22) species had higher species richness (Table 9). As with other plant classification above, the total percent coverage of non-native facultative (range 28-774), facultative upland (range 64-459), and upland (range 10-609) was higher than natives for any class based on wetland status (Table 10). For both species richness and total percent cover, native obligate and facultative wetland species were low but higher than all non-native obligate and facultative wetland species.

Mean plant richness, diversity, evenness, and cover

Mean plant species richness was significantly greater (t = 2.69, df = 11, P = 0.008) in swales compared to sand filtration systems (Figure 4a). Mean plant species richness was 11.0 (SE = 0.33) in sand filtration systems, and 8.6 (SE = 0.34) in swales. There was no significant difference (t = 0.78, df = 11, P = 0.44) in the mean Simpson's Index of Diversity for swales (\bar{x} = 0.64; SE = 0.14) and sand filtration systems (\bar{x} = 0.61; SE = 0.13) (Figure 4b). Mean species evenness was significantly greater (t = -3.03, df = 11, P = 0.003) in sand filtration systems (\bar{x} = 0.47; SE = 0.03) compared to swales (\bar{x} = 0.36; SE = 0.02) (Figure 4c). Mean total percent cover was significantly greater (t = 5.58, df = 11, P < = 0.001) in swales (\bar{x} = 106.0; SE = 4.8) compared to sand filtration systems (\bar{x} = 67.6; SE = 5.0) (Figure 4d).

No trends were observed for species richness, Simpson's Index of Diversity, evenness, and coverage by LID type, season, and year (Figure 5). The highest mean species richness of 15.8 was found in swales during the summer of 2021, and the lowest of 5.2 in sand filtration systems during the winter of 2020. Mean richness was greater (H = 37.72, df = 7, P < 0.001) in swales and sand filtration systems during the summer of 2021 compared to other seasons and years (Figure 5a). Mean Simpson's Index of Diversity was moderate to high in all swales and sand filtration systems during 2020 and 2021 ranging from 0.52 in detention ponds during the winter of 2020 and highest in sand filtration systems during the summer of 2021. The highest diversity (F = 2.95, df = 7, P = 0.007) was found in sand filtration systems during the summer of 2021 but diversity was not different (P < 0.05) in swales (summer 2020, winter 2020, and summer 2021) and sand filtration systems (winter 2021) (Figure 5b). Mean evenness among LID tpye, season, and year was low to moderate and ranged from 0.26 in swales (summer 2021) to 0.56 in sand filtration systems (winter 2020). Mean evenness was higher (F = 3.30, df = 7, P = 0.003) in sand filtration systems (winter 2020) but evenness was not different (P < 0.05) in sand filtration systems (summer 2020 and winter 2021) and swales (summer 2020 and winter 2020) (Figure 5c). Mean coverage was highly variable among LID type, season, and year ranging from 58% cover in sand filtration systems (winter 2020) to 129% coverage in swales (summer 2021). Mean coverage was highest (F = 11.67, df = 7, P < 0.001) in swales (summer 2021) but covearge was not different (P < 0.05) in sand filtration systems (summer 2021) and swales (summer 2020) and winter 2020) (Figure 5d).

Vegetation biomass

Dry weight biomass for native and non-native plants combined was significantly greater (F = 6.71, df = 3, P < 0.001) for graminoids in swales compared to graminoids in sand filtration systems and forbs/herbs in both swales and sand filtration systems (Figure 6). When analyzed by native and non-native species, similar trends were observed but with high variance. Non-native and native graminoids in swales were significantly different from native graminoids and non-native forbs/herbs in sand filtration systems (F = 9.65, df = 7, P < 0.001). However, native graminoid dry weight was not different from native and non-native forbs/herbs in swales, native forbs/herbs and non-native graminoids in sand filtration systems (Figure 7). Dry weights of litter biomass was highest in swales during the winter of 2020 and 2021, but high variance was observed and no significant diffrences (F = 1.60, df = 7, P = 0.215) were detected (Figure 8).

Mean dry weights of dominant native plants exhibited high variance with Texas wintergrass having the greatest dry weight (F = 2.83, df = 9, P = 0.009) but this species was not significantly different from three native graminoids and three native forbs/herbs (Figure 9a). Mean dry weights of dominant non-native plants also exhibited high variance with yellow bluestem having the greatest dry weight (H = 13.4, df = 5, P = 0.02) but this non-native species was not significantly different from four other non-native graminoids (Figure 9b).

In situ swale plantings

White tridens had a significantly greater (F = 6.57, df = 3, P = 0.03) survival compared to the other five native grasses planted in swales after two growing seasons over 16 months (Figure 10a). Survival of white tridens was 87.5%, with survival for silver bluestem and sideoats grama

at 41.7%, and was lowest for switchgrass at 16.7%. Two species (bushy bluestem and buffalograss) had zero survival and were eliminated from analysis. In addition, two native amphibious graminoid species [knotgrass (*Paspulum distichum*) and beaked spikerush (*Eleocharis rostellata*)] were planted in an equal number of separate plots and survival was zero percent at 16 months.

No significant differences were found among root dry weight (H = 2.445, df = 3, P = 0.485; Figure 10b), shoot dry weight (H = 1.528, df = 3, P = 0.676; Figure 10c), total dry weight (H = 1.215, df = 3, P = 0.749; Figure 10d), and root-to-shoot ratio (H = 5.525, df = 3, P = 0.137; Figure 10e) for white tridens, silver bluestem, sideoats grama, and switchgrass plants that survived. All plants that survived allocated greater biomass to shoots than roots.

Greenhouse nutrient study (nitrogen and phosphorus)

All six native grasses except silver bluestem exhibited significant (P < 0.05) increasing biomass for roots (Figure 11), shoots (Figure 12) and total biomass (Figure 13) with increasing concentrations of nitrogen. Total biomass was highest for switchgrass (range 35-46 g) and eastern gamagrass (range 22-30 g). The lowest total biomass was recorded for sideoats grama (range 6 to 8 g). No significant differences (P > 0.05) were found for the root-to-shoot ratios for any species (Figure 14). Buffalograss, eastern gamagrass, and switchgrass exhibited an approximate 1:1 root-to-shoot ratio for all nitrogen concentrations. Sideoats grama, silver bluestem, and white tridens exhibited a pattern of allocating more biomass into shoots than roots with ratios ranging from 0.45:1 to 0.8:1. Similar to biomass allocation, relative growth rates (g g⁻¹ d⁻¹) exhibited significant (P < 0.05) increasing rates with increasing concentrations of nitrogen except for buffalograss and silver bluestem (Figure 15). Overall, switchgrass had the highest relative growth rates (range 0.102 to 0.110 g g⁻¹ d⁻¹) and sideoats grama exhibited the lowest relative growth rates (0.083 to 0.087 g g⁻¹ d⁻¹).

With increasing concentrations of phosphorus, all plants exhibited increasing root biomass with increasing concentrations of phosphorus (Figure 16). However, only side oat grama (Figure 16c), switchgrass (Figure 16e), and white tridens (Figure 16f) were significant (P < 0.05). All plants, except buffalograss, exhibited increases in shoot biomass (P < 0.05) with increasing concentrations of phosphorus (Figure 17). The most significant differences in shoot biomass were observed in eastern gamagrass (Figure 17b), sideoats grama (Figure 17c), silver bluestem (Figure 17d), and white tridens (Figure 17f) at phosphorus concentrations greater than 0.24 mg L^{-1} . For total biomass (roots + shoots), all species, except buffalograss, exhibited increases in total biomass with increasing concentrations of phosphorus (Figure 18). As with shoot biomass, the greatest increase in total biomass was found at phosphorus concentrations greater than 0.24 mg L^{-1} .

The root-to-shoot ratios were significantly different for two of the six plants evaluated (Figure 19). White tridens allocated greater biomass (P < 0.05) to its roots at phosphorus concentrations of 0.12 and 0.24 mg L⁻¹ (Figure 19f). Silver bluestem exhibited variable trends in root-to-shoot ratios with greater allocation of biomass to roots compared to shoots at concentrations of 0.24 mg L⁻¹ but was not significantly different (P < 0.05) from concentrations of 0.12 and 0.96 mg L⁻¹ (Figure 19d). While not significantly different (P > 0.05) among concentrations of phosphorus,

buffalograss (Figure 19a) and eastern gamagrass (Figure 19b) allocated approximately equal amounts of biomass into their roots and shoots. Sideoats grama allocated approximately 50% more biomass into their shoots compared to roots (Figure 19c), while switchgrass allocated 15-20% more biomass into their roots compared to shoots (Figure 19e).

Relative growth rates were significantly greater (P < 0.05) with increasing concentrations of phosphorus for sideoats grama (Figure 20c), silver bluestem (Figure 20d), switchgrass (Figure 20e), and white tridens (Figure 20f). No significant difference (P > 0.05) in relative growth rates were found for buffalograss (Figure 20a) and eastern gamagrass (Figure 20b).

Greenhouse drought study

The allocation of biomass to roots varied among the plants evaluted for watering regime (Figure 21). Buffalograss (Figure 21a), eastern gamagrass (Figure 21b), and switchgrass (Figure 21e) allocated greater biomass (P < 0.05) to roots when watered more frequently. Sideoats grama (Figure 21c) and silver bluestem (Figure 21d) allocated greater biomass (P < 0.05) to their roots when watered less frequently. White tridens exhibited variable trends in the allocation of biomass to their roots (Figure 21f).

Buffalograss (Figure 22a), eastern gamagrass (Figure 22b), and switchgrass (Figure 22e) allocated greater biomass (P < 0.05) to their shoots with more frequent watering days. Sideoats grama (Figure 22c) and silver bluestem (Figure 22d) allocated greater biomass (P < 0.05) to their shoots when watered less frequently. White tridens exhibited variable trends in the allocation of biomass to their shoots (Figure 22f).

As with shoot biomass, buffalograss (Figure 23a), eastern gamagrass (Figure 23b), and switchgrass (Figure 24e) allocated greater total biomass (P < 0.05) with more frequent watering. Sideoats grama (Figure 23c) and silver bluestem (Figure 23d) allocated greater total biomass (P < 0.05) with less frequent watering. White tridens exhibited variable trends in the allocation of total biomass based on watering regime (Figure 23f).

Switchgrass (Figure 24e) and white tridens (Figure 24f) allocated greater root-to-shoot ratios when watered more frequently. With a daily watering regime, switchgrass allocated > 4 parts biomass into its roots for every 1 part biomass allocated into its shoots. White tridens exhibited a 1:1 root-to-shoot ratio with a watering regime of 1 and 2 days, but the root-to-shoot ratio dropped to <0.5:1 when watered every 24 days and during rain days. Eastern gamagrass (Figure 24b), sideoats grama (Figure 24c), and silver bluestem (Figure 24d) root-to-shoot ratios were significant (P < 0.05) based on watering regime but highly variable and no trends were observed. The lowest root-to-shoot ratios (P < 0.05) for silver bluestem was with watering regimes of 3, 24, and rain days. No significant difference (P > 0.05) was observed for the root-to-shoot ratios of buffalograss based on watering regime (Figure 24a).

Relative growth rates were significantly greater (P < 0.05) with more frequent watering for buffalograss (Figure 25a), eastern gamagrass (Figure 25b), and switchgrass (Figure 25e). With less frequent watering, greater relative growth rates (P < 0.05) were observed for sideoats grama

(Figure 25c) and silver bluestem (Figure 25d). White tridens exhibited significant relative growth rates (P < 0.05) with watering regimes but no trends were observed (Figure 25f).

Ex situ metal uptake in plants and soils

Highly variable and inconsistent trends were observed for uptake of chromium (Figures 26 a-e), copper (Figures 27 a-e), and lead (Figures 28 a-e) in the roots and shoots of five native grasses for controls, and plants exposed to low and high concentrations of each metal under controlled greenhouse conditions. No significant differences (P > 0.05) were detected among treatments for plant species or part. Some trace concentrations of each metal were found in both the roots and shoots of each species including control treatments in which no metals were added. The variance in the data was highly variable due to extreme low and high values, and a natural logarithm (ln) transformation of the data only slightly improved the normality and equality of variance.

Soil analysis

Soil type

Soils in the swales were classified as clay loam with 10-20% limestone, while soils in detention ponds were classified as sand in the upper 10-15 cm, and a mix of quartz sand and sandy clay loam at depths of 15-30 cm.

Soil bulk density

Soil bulk density increased significantly from 0-10 to 20-30 cm in both swales and sand filtration systems (F = 52.22, df = 5, P < 0.001) (Figure 29). Soils were more compacted and less porous at deeper depths. Bulk density ranged from 1.44 to 1.62 g cm³⁻¹ in swales, and 1.29 to 1.53 g cm³⁻¹ in sand filtration systems.

Soil organic matter

Organic matter (%) was signifiantly greater (H = 321.58, df = 5, P < 0.001) at all depths (0-10, 10-20, and 20-30 cm) in swales compared to sand filtration systems (Figure 30). Organic matter ranged from 6.1 to 8.0% in swales and 2.1 to 2.9% in sand filtration systems. The highest organic matter content was found in the top 0-10 cm in both swales and sand filtration systems, but was not significantly different (P > 0.05) for organic matter in the lower depths.

Soil organic carbon

Organic carbon exhibited simialar trends to organic matter. Organic carbon was significantly greater (F = 49.62, df = 5, P < 0.001) in the top 0-10 cm of swales compared to lower depths in the swales and all depths in sand filtration systems (Figure 31). Organic carbon at depths of 10-20 and 20-30 cm in swales was significantly different (P < 0.05) than organic carbon at all depths

in sand filtration systems. Organic carbon content ranged from 9.2 to 18.9 g kg^{-1} in swales and 2.7 to 3.5 g kg^{-1} in sand filtration systems.

Soil particle size

Soil particles of 500 μ m were significantly greater (H = 525.9, df = 5, P < 0.001) in swales compared to other particle sizes (Figure 32). In swales, the percent particle size was significantly greater (P < 0.05) for particle sizes of 250 and 125 μ m compared to particle sizes of 2000, 63, and <63 μ m. In contrast, soil particle size was significantly greater (H = 464.8, df = 5, P < 0.001) for particles 500, 250, and 125 μ m in sand filtration systems compared to particle sizes of 2000, 63, and 63 μ m.

In situ metal analysis in plants

Plant uptake of metals from highest to lowest concentrations were Mg > Fe > Zn > Pb > Cu > Cr > Ni > Cd (Figure 33 a-h). No significant differences (P > 0.05) were found in all plants species for roots, shoots, and total (roots + shoots) uptake of metals with the exception of Pb concentrations in the shoots of frog-fruit (F = 4.11, df = 3, P = 0.035) (Figure 33 d). Metal concentrations of Mg, Fe, Zn, Pb, Cu, Cr, Ni, and Cd were detected in all plant species roots and shoots with the exception of Cd which was not detected in the roots or shoots of Mexican hat and white tridens (Figure 33 h).

Of the most toxic metal analyzed, Pb was found in the highest mean concentrations in the roots and shoots of frog-fruit (31.1 and 34.9 μ g L⁻¹, respectively), Mexican hat (25.9 and 24.1 μ g L⁻¹, respectively) and wild petunia (23.0 and 20.1 μ g L⁻¹, respectively) (Figure 33d). The total concentration of Pb found in plants (roots + shoots) ranged from 66.1 μ g L⁻¹ frog-fruit to 20.2 μ g L⁻¹ in white tridens. The total concentration of Cu found in plants (roots + shoots) ranged from 50.3 μ g L⁻¹ in frog-fruit to 4.1 μ g L⁻¹ in white tridens (Figure 33e). Similar trends for the total concentrations were found for Cr with the highest concentrations in frog-fruit (21.4 μ g L⁻¹) and lowest concentration in white tridens (6.8 μ g L⁻¹) (Figure 33f), and Ni with the highest concentrations in frog-fruit (25.0 μ g L⁻¹) and lowest concentration in white tridens (7.1 μ g L⁻¹) (Figure 33g). The total Cd concentrations (roots + shoots) detected were low and similar for frog-fruit (0.8 μ g L⁻¹) and wild petunia (0.9 μ g L⁻¹) (Figure 33h).

No significant difference was found in the allocation of metals between the roots and shoots of frog-fruit (H = 1.897, df = 7, P = 0.965), though high variance was observed for Fe and Mg (Figure 34a). Frog-fruit allocated 2-3 times more Fe and Mg into roots than in shoots while Cd, Ni, Cr, Cu, Pb, and Zn were allocated on a 1 to 1 ratio.

Mexican hat allocated significantly (F = 19.118, df = 6, P < 0.001) more Fe into its roots than shoots for Mg, Cd, and Zn (Figure 34b), but no differences (P < 0.05) were found between Ni, Cr, Cu, Pb. Cadmium was not detected in the shoots or roots of Mexican hat. Mexican hat allocated 2-5 times more Fe into roots than shoots while Ni, Cr, Cu, Pb, and Zn were allocated on a 1 to 1 ratio. Mexican hat allocated 0.4:1 parts Mg into its roots compared to shoots.

White tridens exhibited high variance in the allocation of Mg and Zn between roots and shoots with significant differences (F = 7.576, df = 6, P = 0.002) only found for Cd (Figure 34c) which was not detected in the shoots or roots of white tridens. White tridens allocated 6-7 times more Fe into roots than shoots, while Mg and Zn allocated at a ratio of 2-13 more into roots than shoots. Large variance was found for the samples of Mg and Zn with white tridens. White tridens allocated 1.2 to 1.6 more Ni, Cr, and Cu into their roots compared to shoots, while lead was allocated equally between the roots and shoots of white tridens.

Wild petunia allocated significantly (F = 22.322, df = 6, P < 0.001) more Fe into roots than shoots compared to the other seven metals analyzed (Figure 34d). Wild petunia allocated 2-3 times more Fe into roots than shoots, while Cd, Ni, Cu, and Pb were allocated ca. 1 to 1 into roots and shoots. Cr and Zn were allocated at 1.3 to 1.4 greater concentration in the shoots than roots. Mg was allocated at a lower rate of 0.4 into the roots for every 1 part in the shoots.

In situ metal analysis in soils

Metal in soils from highest to lowest concentrations were Fe > Mg > Zn > Pb > Cu > Cr > Ni, with no Cd being detected in soils (Figure 53 a-g). Soils in swales contained significantly more concentrations of Fe (t = 11.66, df = 106, P < 0.001; Figure 35a), Mg (t = 2.42, df = 106, P = 0.017; Figure 35b), and Cr (t = 5.18, df = 106, P < 0.001; Figure 35f) than sand filtration systems. No significant differences were found for the concentrations of Zn (t = -0.101, df = 106, P = 0.92; Figure 35c), Pb (t = 1.29, df = 106, P = 0.199; Figure 35d), Cu (t = 1.22, df = 106, P = 0.224; Figure 35e), and Ni (t = 1.88, df = 106, P < 0.062; Figure 35g). No cadmium was detected in the soil samples extracted from swales and sand filtration systems. Of the most toxic metals detected in soils, Pb was found at the highest mean concentrations in swales (15.3 μ g L $^{-1}$) and sand filtration systems (9.2 μ g L $^{-1}$). Copper (Cu), Cr, and Ni were detected at mean concentrations of 3.3, 1.3, and 0.24 μ g L $^{-1}$, respectitively, in swales. Copper was detected at a trace mean concentration of 0.07 μ g L $^{-1}$ in sand filtration systems, while Cr and Ni were not detected in soils from sand filtration systems.

Metal concentration by soil depth

For metals detected at concentrations $> 50 \,\mu g \, L^{-1}$, Fe was found at significantly higher concentrations (H = 203.8, df = 17, P < 0.001) at all depths in swales compared to all other metals (Figure 36a). No other significant differences (P > 0.05) were detected for Mg and Zn at at the three depths analyzed in swales and sand filtration systems, but high variance was observed.

For metals detected at concentrations $< 50~\mu g~L^{-1}$, Pb was found at significantly higher concentrations at all depths in swales and sand filtration systems compared to all other metals, except Cu at a depth of 0-10 cm (Figure 36b). However, Cu exhibited high variance and was not significantly different (P > 0.05) from Ni and Cr in swales and sand filtration systems at any depth from 0-30 cm.

Seasonal metal concentrations in soils

Seasonal trends in metal concentrations were comparable to metals detected at different soil depths. Metal concentrations $> 50~\mu g~L^{-1}$ were significantly greater (H = 208.04, df = 11, P < 0.001) for Fe in swales during the winter and summer compared to Mg and Zn in swales and sand filtration systems (Figure 37a). Variable trends were found for Mg and Zn between seasons for swales and sand filtration systems.

For metals detected at concentrations $< 50~\mu g~L^{-1}$, Pb was significantly greater (H = 206.84, df = 11, P < 0.001) during the summer and winter in swales and during the winter in sand filtration systems, but was not significantly different (P < 0.05) from Cu in swales during the winter (Figure 37b). With the exception of Cu in swales during the winter, no other trends for Ni, Cr, and Cu at concentrations $< 50~\mu g~L^{-1}$ were detected (P > 0.05) between swales and sand filtration systems based on season.

Oil and grease analysis in sediment collected from runoff

Oil and grease analysis collected from roadway runoff sediment following rain events ranged from 667 mg kg⁻¹ (SE = 41.9) in swales to 723 mg kg⁻¹ (SE = 41.6) in sand filtration systems, but no significant difference was found (t = 0.945, df = 142, P = 0.34) (Figure 38a). In addition, no significant differences (F = 0.523, df = 5, P = 0.76) were found for oil and grease concentrations from sediment collected at the inlet, middle, and outlet of sand filtration systems and swales (Figure 38b).

While there were no differences in the oil and grease concentrations in sand filtration systems and swales, the total sediment weight and weight by some particle sizes following sieving were significantly different in sand filtration systems compared to swales. The mean sediment weight (g m²⁻¹) captured in oil and grease traps was significantly greater (t = 1.97, df = 142, P < 0.002) in sand filtration systems ($\bar{x} = 6475$; SE = 1193) compared to swales ($\bar{x} = 2443$; SE = 526) (Figure 39a). The mean weight (g m²⁻¹) of particle sizes 500 (3171 g m²⁻¹, SE = 761) and 250 (1849 g m²⁻¹, SE = 348) µm's were significantly greater (H = 586.96, df = 13, P < 0.001) in sand filtration systems compared to other particle sizes except 500 µm (1274 g m²⁻¹, SE = 299) in swales and 125 µm (1074 g m²⁻¹, SE = 158) in swales (Figure 39b).

Stormwater monitoring

<u>Bulverde Basin</u> Average influent and effluent concentrations for all nutrients over the entire study period are shown in Figure 50. The concentration of nitrogen species in the influent and effluent samples showed considerable variation between individual storm events. Inlet and outlet nitrate median EMCs were 0.43 mg/L and 1.63 mg/L, respectively. In most of the sampling events, nitrite had a very low concentration in the inlet samples and was below the quantification limit in the outlet samples. The median ammonia concentration was 0.07 mg/L while the median outlet concentration was 0.02 mg/L. The median inlet and outlet TDN concentrations were 1.07 mg/L and 2.00 mg/L. The median inlet and outlet TP concentrations were 1.02 mg/L and 0.24 mg/L, respectively.

Inlet TSS median value was 106 mg/L while outlet TSS median was 3 mg/L. Inlet and outlet TDS median EMCs were 118 mg/L and 152 mg/L, respectively. The median COD concentration was

103 mg/L while the median outlet concentration was 16 mg/L. The median inlet and outlet oil and grease concentrations were 16.5 mg/L and 5.4 mg/L (Figure 51).

Inlet PAH median value was 1.7 mg/L while outlet PAH median was 0.32 mg/L. Inlet and outlet TC median EMCs were 20 mg/L and 16 mg/L, respectively. The median TOC concentration was 18 mg/L while the median outlet concentration was 12 mg/L. The median inlet and outlet DOC concentrations were 11.1 mg/L and 7.4 mg/L (Figure 52).

In most of the sampling events, Ni and Cr had a very low concentration in the inlet and outlet samples. Inlet and outlet Fe median EMCs were 21.5 μ g/L and 15.8 μ g/L, respectively. Inlet and outlet Pb median EMCs were 5.05 μ g/L and 5.05 μ g/L, respectively. The median inlet Zn concentration was 2.9 μ g/L while the median outlet concentration was 0. The median inlet and outlet Cu concentrations were 4.5 μ g/L and 0.24 μ g/L. Furthermore, Mg had the highest concentrations with in-and outflow medians of 490 and 716 μ g/L, respectively (Figure 53).

<u>TPC Basin</u> - In the TPC site also higher nitrate concentration was observed in the outflow concentrations than inflow with 0.64 mg/L and 0.39 mg/L, respectively. Furthermore, nitrite and ammonia were significantly reduced in the site. TDN in- and outflow concentrations did not change significantly with 1.19 mg/L and 0.92 mg/L respectively. Moreover, phosphate also had a higher outflow concentration than the inflow with 0.27 mg/L and 0.14 mg/L, respectively (Figure 55).

A very high removal was observed in this site for TSS. Furthermore, TDS inflow and outflow median concentrations were 94 mg/L and 139 mg/L. The median COD concentration was 59 mg/L while the median outlet concentration was 26 mg/L. The median inlet and outlet oil and grease concentrations were 63 mg/L and 91 mg/L (Figure 56).

Inlet PAH median value was 0.32 mg/L while outlet PAH median was 0.06 mg/L. Inlet and outlet TC median EMCs were 20 mg/L and 14 mg/L, respectively. The median TOC concentration was 18 mg/L while the median outlet concentration was 13 mg/L. The median inlet and outlet DOC concentrations were 10.7 mg/L and 4.7 mg/L (Figure 57).

In most of the sampling events, Ni and Cr had a very low concentration in the inlet and outlet samples (less than 10 μ g/L). Inlet and outlet Fe median EMCs were 19.9 μ g/L and 9.9 μ g/L, respectively. Inlet and outlet Pb median EMCs were 13.8 μ g/L and 14.2 μ g/L, respectively. The median Zn concentration was 9.7 μ g/L while the median outlet concentration was 5.6 μ g/L. The median inlet and outlet Cu concentrations were 13.8 μ g/L and 4.5 μ g/L. Furthermore, Mg had the highest concentrations with in-and outflow medians of 389 and 859 μ g/L, respectively (Figure 59).

Kyle Basin In the Kyle basin, inflow nitrate median concentration was 0.92 (mg/L) while outflow had 1.62 (mg/L) median concentration. Furthermore, inflow median nitrite and ammonia concentrations were 0.12 (mg/L) and 0.05 (mg/L) respectively and outflow median concentrations were 0.07 (mg/L) and 0.01 (mg/L). TDN median in- and outflow concentrations were 0.88 mg/L and 0.99 mg/L, respectively. Moreover, phosphate in-and outflow median concentrations were 0.05 mg/L and 0.22 mg/L (Figure 60).

TSS concentrations were significantly reduced in this site from 72 mg/L to 13.4 mg/L while TDS in-and outflow concentrations did not change significantly with 146 mg/L and 132 mg/L, respectively. The median COD concentration was 56 mg/L while the median outlet concentration was 31 mg/L. The median inlet and outlet oil and grease concentrations were 17 mg/L and 30 mg/L (Figure 61).

TC and TOC, DOC concentrations did not change significantly between in-and outflow samples. Inlet PAH median value was 0.91 mg/L while outlet PAH median was 0.06 mg/L (Figure 62). In most of the sampling events, Ni and Cr had a very low concentration in the inlet and outlet samples (less than 10 μ g/L). Inlet and outlet Fe median EMCs were 12.9 μ g/L and 13.9 μ g/L, respectively. Inlet and outlet Pb median EMCs were 16 μ g/L. The median Zn concentration was 2.7 μ g/L while the median outlet concentration was 15.9 μ g/L. The median inlet and outlet Cu concentrations did not change significantly. Furthermore, Mg had the highest concentrations with inflow and outflow medians of 339 and 784 μ g/L, respectively (Figure 63).

Fecal Coliform results

There was a median fecal coliform of 9081 MPN in the Bulverde basin inlet and 444 MPN in the outlet (Figure 64). The TPC inlet samples had a median fecal coliform of 14807 MPN and 63 MPN respectively. In the Kyle site, 10918 MPN was recorded in the inlet samples and 8864 MPN in the outlet samples.

Kyle swale results

Results for metals are shown with boxplots in Figure 68. The mean concentration of iron was found to be in the middle as compared to end and beginning. The median concentration of copper was higher in the beginning and end compared to the middle. The range of concentrations detected for zinc in the middle of the swale was lower compared to the beginning and the end of swale.

Magnesium concentrations were significantly higher than other metals, and in some events detected more than 2000 ug/l in the beginning of the swale. The median for the lead was around 4.8 ug/l in the beginning, middle, and end. The mean concentration of lead in the three sections of the swale were close and ranged from 4.4 to 4.6 ug/l. Chromium and nickel were detected in lower concentrations and their medians and means ranged from 0 to 1 ug/l.

Mean concentration of TSS was the highest in the beginning. The median of TSS was around 400 mg/L in the middle and end. The median and mean of TDS in the middle and end of the swale were close and around 110 mg/l. The mean of COD was higher in the beginning followed by the middle and the end. Oil and grease showed lowest range in the middle of the swale. Nitrate (Figure 66) showed highest concentration in the beginning and lowest in the end. Nitrite and ammonia were detected in low amounts (below 1 mg/L). The mean concentration of TP and TN were found to be the lowest at the end of the swale. TC and TOC showed similar trends in terms of mean and median (Figure detected below 10 67). IC was mg/L.

Plaza swale results

In the middle of the swale, TSS showed lower mean concentration, while TDS showed higher (Figure 69). Maximum of COD was detected around 180 mg/L. Oil and grease mean concentration was found to be around 60 mg/L among all three sections. Nitrite, ammonia, and TP were detected below 0.5 mg/L (Figure 70). Maximum concentration of Nitrate was around 3 mg/L at the beginning of the swale. Lower mean concentration was found in the middle for TN. TC and TOC showed similar trend in terms of mean and median (Figure 71). IC was detected in

very low amounts. Higher mean and median of Fe were found in the beginning and lower in the end of the swale (Figure 72). Ni and Cr were detected in very low concentrations. Higher mean concentrations of Pb and Zn were found in the middle. Mean concentration of Cu was found around 10 ug/L among all three sections. Mg was detected in higher concentrations compared to other metals and exceeding 2500 ug/L in the beginning of the swale.

Roadrunner way swale results

The mean and median of TSS were higher in the middle of the swale (Figure 73). For TDS, on the other hand, the median and mean were lower in the middle. The highest concentration of COD was observed in the middle; however, the highest mean and median was found in the end. Oil and grease varied from 0 to 200 mg/L. Nitrite, ammonia, and TDN measurements were mostly below detection limit (Figure 74). TP and TN were detected in very small concentrations. Nitrate was detected up to around 15 mg/L in the beginning, while the mean concentration among all three sections was between 4 to 6 mg/L. TC highest concentration was detected in the beginning (Figure 75). TOC and DOC showed similar results with relatively low variations throughout the swale with the mean and median fluctuating between 5 to 10 mg/L. Cd, Cr, and Ni concentrations were below detection limit (Figure 76). Cu was detected in relatively low amount and only in a few events. Mg concentration was the highest compared to the other metals with concentrations up to around 3500 ug/L. The concentration mean and median of Mg were highest in the middle of the swale. Fe mean concentration varied between 15 to 20 ug/L among the three sections. Highest concentration of Pb was observed in the end. Though Zn was mostly below detection limit, it was detected more frequently in the beginning.

16S rRNA gene sequencing results for soil samples

Bulverde Basin A total of 1,550,436 16S rRNA gene sequencing reads were generated from all the samples. The sequence libraries size ranged from 14,571 to 43,937 reads. Rarefaction curves based on OTUs at 99 % similarity for summer and winter samples were generated based on the different layers and showed that microbial community structure could be well-represented at the sampling depth of 14,000 sequences. The trained Naïve Bayes classifier categorized all the sample OTUs into 47 different bacteria phyla. For both sampling seasons, Actinobacteria, Proteobacteria, Chloroflexi, Acidobacteria, and Planctomycetes, were the most dominant phyla accounting for more than 80 % of relative abundance. The relative abundance of the ten most dominating phyla in the different sampling seasons and layers are shown in Figure 77. In the winter soil samples, the most abundant phylum in all soil layers was Actinobacteria ranging from 24 % to 31 % relative abundance. The other dominating phyla with more than 10 % relative abundance in all layers in winter samples were Proteobacteria and Chloroflexi. In comparison, Proteobacteria was the most abundant phylum in the top and middle layers of the summer soil samples (with an average of 25 % - 28 %) with Actinobacteria and Chloroflexi being the next most abundant phyla.

Species diversity, as assessed by alpha diversity indices, appeared higher in libraries generated from summer samples than from winter samples. Bacterial diversity metrics used in this assessment include Shannon's diversity index, Faith's phylogenetic diversity and Pielou's evenness. Different alpha diversity metrics results are shown in violin plots (Figure 74) for the two sampling seasons. We observed that Shannon (p = 0.17) and faith (p = 0.2) indices (Figure 37) were not significantly different between samples collected in the two different seasons, while

Pielou evenness values (p = 0.030) were significantly different between summer and winter (Figure 78). The bacterial community structure analysis according to the unweighted UniFrac distance matrices and PCoA plots (Figure 78) showed that the top and bottom layer of soil samples were clustered separately. Furthermore, the middle layer samples were clustered either with the top layer or the bottom layer. Moreover, microbial communities did not cluster based on the distance from the inlet.

TPC and Kyle Basins A total of 2,929,056 16S rRNA gene sequencing reads were generated from all samples, with sequence libraries size ranging from 12,400 to 126,000 reads. Rarefaction curves for both sites showed that all samples achieved adequate sequencing depth at 12,000 reads per sample. The trained Naïve Bayes classifier categorized all samples from both sites into 51 different bacterial phyla. Actinobacteria, Proteobacteria, Chloroflexi, Acidobacteria, and Planctomycetes, were the most dominant phyla accounting for more than 80% of relative abundance in most of the samples collected from both sites. The relative abundance of the 10 most dominant phyla detected in the samples during different sampling seasons is shown in Figure 79 and 80.

Proteobacteria and Actinobacteria accounted for nearly 50% (relative abundance) of the total bacterial phyla detected in both sites. In the TPC site, Actinobacteria and Proteobacteria had a relative abundance of 30% and 29%, respectively. On the other hand, in the Kyle site, Actinobacteria and Proteobacteria had a relative abundance of 25% and 26%, respectively. Additionally, Acidobacteria and Chloroflexi were also found to be dominant phyla at both sites. Furthermore, Proteobacteria was found to be the most dominant phylum in summer, whereas Actinobacteria was the more dominant phylum in winter samples at each site. In Kyle's summer samples, on average, Proteobacteria and Actinobacteria accounted for approximately 27% and 23% of total relative abundance, while their relative abundance in winter samples was 25% and 27% respectively. On the other hand, in the TPC site summer samples, Proteobacteria and Actinobacteria had 30% and 27% of relative abundance respectively, and in winter samples, their relative abundance was 27% and 32% respectively.

The alpha diversity metrics (Shannon and Pielou's evenness index) observed in the soil samples collected from Kyle and TPC sites during two sampling seasons are presented in Figure 81 and 82. All samples had a Shannon index of above 7 with no significant difference between sampling seasons in each site. Overall, the Kyle site samples showed a higher alpha diversity index than the TPC site samples. The bacterial community structure analysis according to the unweighted UniFrac distance matrices and PCoA plots showed that the top and bottom layers of soil samples were clustered separately. Furthermore, the middle layer samples were clustered either with the top layer or the bottom layer. Moreover, microbial communities did not cluster based on the distance from the inlet.

Discussion

Studies of roadway runoff and associated pollutants differ significantly by LID structure and size, geographical location, experimental design, and the explanatory variables measured (Boger et al. 2018). Few, if any, studies have evaluated the vegetation in swales and detention ponds, while multiple studies have examined vegetation along roadways (Vasconcelos et al. 2014, Vakhlamova et al. 2016, Auffret and Lindgren 2020). In this study, swales and sand filtration systems differed in their design and features, so comparison of vegetation composition is

difficult. Swales are engineered earthern depressions with vegetation cover that receive runoff, convey the runoff through the swale or series of swales, store the runoff and allow infiltration (Revitt et al. 2004). The side slopes of swales in this study are vegetated at slight angles of 2 to 5 degrees. Sand filtration systems are engineered rectangular structures in earthen depressions, with some re-inforced with concrete walls to 2.5 m in height. The upper soil media in sand filtration systems is composed primarily of quartz sand in which roadway runoff is diverted through a culvert. Sand filtration systems are designed to capture and hold runoff within a defined area until peak flow has passed and then allow water to infiltrate through the soil media. In sand filtration systems, the captured runoff may be directed into an outflow or percolate into groundwater (Revitt et al. 2004).

Differences in plant biomass in this study were influenced by seasonality and management. In swales and sand filtration systems, the majority of the plants became dormant in November or December, and few evergreen plants were documented. The only notable evergreen species documented during the study was the small shrub agarita (*Berberis trifoliata*) which was observed in two swales but not along any line transects. Mowing in swales and detention ponds made identification of many plants difficult as vegetation was mowed at a of height of 8 to 10 cm above soil level. In detention ponds, the upper 5 cm of the surface layer was replaced with a new layer of sand. On one occasion, there were no plants documented when the sand filtration systems was surveyed after the upper layer of sand was replaced. However, the vegetation responded well following sand replacement and was documented at > 50% coverage at 6 months following sand replacement.

Vegetation richness and cover

Disturbed sites in urban areas are often invaded by spontaneous non-native vegetation from propagules (seeds and fragments) adapted to ruderal conditions and frequent anthropogenic disturbances (Cadottee et al. 2017, Del Tredici, 2010). In a study of sand filtration systems, it was found that the dominant species and species coverage were from non-native species, but a large number of sub-dominant species were native (Douthat 2022). Disturbances from management such as sediment replacement and mowing along with variable environemental conditions such as extreme heat, drought, and periods of inudation are likely to result in seasonal and annual changes in plant abundance with the community dynamics being dominated by non-native species.

It is hypothesized that plant communities in swales undergo minimal successional changes, but plant communities in sand filtration systems follow a Gleasonian successional pattern in which plant relative abundance changes with each maintenance procedure, drought, and inundation period (Gleason 1917). Observational evidence from this study indicates the vegetation communities in swales and sand filtration systems are dynamic and in various stages of succession due to management and extreme environmental conditions. Following sand replacement in sand filtration systems, the non-native purple nut sedge was the domiant plant at 3-4 months post management. At 6 months, the sand filtration systems was still dominated by purple nut-sedge but multiple native forbs and herbs, and non-native and native grasses were present. During several days of rainfall, some of the amphibious plants such as sedges, spikerush, and smartweed, become common and formed dense clumps in low depressions. During droughts, the low depressions within the swales and sand filtration systems become dominated by ruderal species such as horseweed, annuals, and non-native grasses. Longer

monitoring periods would be required to determine the true successional patterns in plant communities in sand filtration systems.

Along roadways, LID structures receive stormwater runoff in greater volumes than undisturbed areas that results in new novel vegetative communities (Pyšek et al., 2004). A significantly greater number of native plants were documented in the swales and sand filtration systems compared to non-native plants, but the coverage of 3-4 non-native plants was significantly greater than native plants. Sinclair et al. (2020) documented similar results in stormwater ponds in North-Central Florida in which non-native plant species richness and cover was high in sand filtration systems. In New Jersey sand filtration systems, Douthat (2022) observed that non-native plants were dominant but a large number of native plants were sub-dominant. A greater variation in native plant richness was observed in sand filtration systems compared to swales in this study which is possibly due to more intensive management of sand filtration systems compared to swales.

Based on plant growth form, native forbs and herbs had the highest species richness in sand filtration systems and swales, but total coverage was highest for non-native graminoids in sand filtration systems and swales. Overall, 2-4 non-native graminoids exhibited the highest total coverage being the dominant plant growth type in both swales and sand filtration systems. The dominant plants based on USDA Wetland Classification type documented in swales and sand filtration systems in this study were upland > facultative upland > facultative > facultative wetland > obligate wetland based on species richness and total coverage. It was expected that more facultative wetland and obligate wetland plants would be found in swales and sand filtration systems. The large number of species and greater species coverage of upland and facultative upland plants is most reflective of the short retention time of water in swales (ca. 12-24 hours) and sand filtration systems (ca. 12-48 hours). The few facultative wetland and obligate wetland plants documented in this study is due to the short hydroperiods in both sand filtration systems and swales. Facultative wetland and obligate wetland plants have specific and narrow hydroperiods (Lichvar et al., 2016). Non-native facultative species richness was moderate but overall coverage was highest indicating this group is more tolerant of disturbance and higher nutrient concentrations (Roy et al. 2019). Facultative and obligate wetland plants documented in sand filtration systems and swales in this study were most common in small shallow depressions near the inlet from scouring similar to results of Jean-Philippe et al. (2021).

The mean cover (%) of plants over the entire study was greater in sand filtration systems (\bar{x} = 106 %) compared to swales (\bar{x} = 68 %) but coverage was highly variable seasonally due to maintenance and seasonal temperature differences. For efficient removal of TSS and associated pollutants in swales, plant coverage of > 80% is recommended (Barrett et al., 2004; Li et al., 2008). Maintaining vegetation in the sand filtration systems over the duration of the growing season would result in increased filtration, nutrient, and metal uptake. Vegetation coverage may be less important in sand filtration systems where settling and adsorption through sand are the primarily processes to manage pollutants in stormwater within a confined basin (Wissler et al. 2020; Barrett 2018). However, plants in swales and sand filtration systems are important in the uptake on nutrients (Yuan et al. 2019, Shrestha et al. 2018; Yu et al. 2001), metals (Leroy et al., 2017; Gavrić et al. 2019), and increased soil permeability and infiltration rates of stormwater (Yousef et al., 1987; Henderson et al., 2016; Morbidelli et al., 2016). Moreover, vegetative sites high in plant coverage and deep roots result in 2 to 4 times greater hydraulic conductivity than

bare soil sites (Gonzalez-Merchan et al. 2014) allowing stormwater to percolate through the soil at a faster rate.

Species richness was dominated by a high number of native plants but total coverage was dominated by non-native plants. Mutiple studies have found that non-native plants are the dominant cover in LID structures and along roadways in the urban environment and dominant in the seed banks allowing for continual recolinization both from sexual and asexual reproduction (Lundholm and Marlin, 2006; Vakhlamova et al., 2016; Jean-Philippe et al. 2021). The results of this study are similar to Vasconcelos et al. (2014) where non-native grasses accounted for > 70% coverage and a high number of native species with lower coverage along roadways.

Sand filtration systems were traditionally designed to temporarily capture stormwater flow, reduce total suspended solids, and prevent flooding (Wissler et al., 2020). Maintaining vegetation cover and biodiversity in sand filtration systems will further assist in the uptake of nutrients, metals, and other pollutants. At the end of the growing season in October-November, the vegetation could be cut, harvested, removed from the site, and disposed of in a municipal landfill to prevent the recycling and accumulation of pollutants in the sand filtration systems and possible infiltration into groundwater. Vegetation in LID structures that are not managed was found to be more effective at reducing flow, trapping sediment, and increasing infiltration into the soil (Henderson et. al., 2016). However, in a review article of roadside vegetation management, it was found that species richness was increased with 1 or 2 moving per year along with the removal of mowed plant parts (Jakobsson et al. 2018). In this study, a greater amount of sediment from runoff was captured in sand filtration systems with less vegetation coverage compared to swales with vegetation coverage > 100%. Thus, limiting management that allows uninhibited plant growth, at least through the growing season, is most effective at managing roadway runoff but infrequent mowing will promote plant richness. In another study, mowing increased annual plants but had no impact on perennial species (Young and Claassen 2008). Therefore, mowing the swales and sand filtration systems once at the end of the growing season may promote a mixture of both annuals and perennials during the next growing season.

Maintaining LID structures, including swales and sand filtration systems, with a high diversity of plants will result in some plants becoming dominant during dry periods and long-term droughts, while other plants will become dominant during the rainy season and short periods of inudation. For planting in swales, sand filtration systems, and other LID structures, the selection of a high diversity of plant species with different functional traits will result in increased resilience and resistance to changing environmental conditions such as temperature fluxes, flooding, extended drought, and climate change. Leroy et al. (2017) suggested planting a mixture of forbs and herbs, and graminoids to reduce pollutants from entering groundwater. Moor et al. (2015) model based on climate change scenarios predicted a shift in wetland species that are taller, faster growing, and having greater specific leaf area. Promoting dense buffer zones of vegetaion at the inlet will reduce the amount of total suspended solids and associated pollutants being distributed throughout the LIDs and from entering surface and ground waters. Models indicate that climate change is predicted to result in more intense and flashy precipitation events and increases in peak total suspended solids and associated pollutant loads (Abduljaleel et al. 2023).

The selection of plants with greater above and below ground biomass will result in greater above-ground organic matter as leaves senesce and the absorption of nutrients and metals from roots. Increased organic matter is known to bind metals (Gupta and Sinha 2006) and

hydrocarbon products (Ukalska-Jaruga et al. 2019). Large perennial grasses such as switchgrass, eastern gamagrass, little bluestem, and big bluestem would be ideal but more information is needed on how to properly establish these grasses in various LID structures. Additionally, many forbs and herbs with shallow root systems may be more efficient in the uptake of metals which are primarily found in the upper portion of the topsoil. In contrast, greater plant diversity may not be as important as plants with greater root density and growing depth that promotes percolation and infiltration of stormwater into the soil (Shrestha et al. 2018). Regardless, it is suggested that LIDs contain a high diversity of plants of different functional groups that respond differently to changing environmental conditions and ongoing management.

Of the total 114 native plants documented in this study, we recommend 56 species for planting in LID structures that represent a variety of functional groups (Appendix 4). The selection of native plants found in swales and sand filtration systems have adapted to the urban environment and the extreme environmental conditions in these stormwater management structures. These plants exhibit resilience and resistance to droughts and temporary inudation in sand filtration systems and swales, and are adapted to changing conditions in swales and sand filtration systems. Most of these plant species are easily propagated by seeds, rhizomes, and bare root stock (J. Hutchinson, person. comm.), and appear to have occured spontaneously in swales and sand filtration systems. The only known study site in which native plants were seeded was the Babcock Road swale, and the vegetation community in this swale was a mix of native and nonnative grasses with high species richness of native forbs and herbs, indicating that non-native plant seeds and propagules were coming into the swale with stormwater runoff or present in the soil seed bank.

The three native plants with the greatest biomass (g m²-¹) were perennial grasses that include Texas wintergrass, sideoats gama, and silver bluestem, indicating these native grasses are most suitable for the variable conditions in LID structures. Survival of native grasses planted in swales resulted in a survival of 88% for white tridens, > 40% for silver bluestem and sideoats grama, and 12% for switchgrass but there was no difference in the dry weight biomass among the species. This difference between survival and dry weights among the four grasses may indicate the variable environmental conditions experienced by plants in swales in Central Texas and the need to promote plant species diversity as each plant responds differently to environmental conditions and mowing.

The composition of plants found naturally growing in sand filtration systems and swales may change with global warming. Longer droughts and fewer but more intense precipitation events are expected that would alter plant composition. With longer drought periods, it is expected that pollutants will become concentrated in LID structures (Wijesiri et al., 2020) which may further stress plants. The noval ecosystems found in swales and sand filtration systems develop a feedback repsonse to changing climate conditions and may produce systems that are resilient and resistant to climate change (Suding and Hobbs 2009).

In situ planting of native graminoids in swales was successuful for white tridens with a survival rate of 88%, while sideoats grama and silver bluestem survival rates were moderate at 42%. Switchgrass was found to have low survival rates of 17%. No survival of bushy bluestem, buffalograss, or the two amphbious plants were documented in swales. The survival of the amphbious plants was likely due to a combination of long dry periods and interspecific competetion from non-native grasses. The mean shoot biomass was greater than root biomass

for all the native grasses that survived plantings in swales indicating that competition may have driven above-ground growth for more efficient photosynthesis.

In a 20 year study of infiltration basins planted with native plants, it was found that spontaneous vegetation became dominant and precipitation patterns determined the composition of plant species (Jean-Philippe et al. 2021). This may explain why none of the amphibious plants survived in the swales in this study as Central Texas experience a drought in 2022. Rainfall patterns are highly variable in Central Texas annually. During the two growing seasons of the *in situ* study in swales, rainfall data taken in the general study area recorded 131 cm of rain during 2021 but only 37 cm in 2022 (Jeffrey Hutchinson, unpubl. data). In addition to variable rainfall patterns, competition with established non-native grasses may inhibit the establishment of most native planted in swales and other restoration efforts.

Two factors that impact the survival of plants along roadways and retention basins are soil and hydrological characteristics (Haan et al. 2012, Jean-Philippe et al. 2021). Finer texture soils that promote drainage with lower bulk densities were found to be the detrmining factors to establish plants along severely distrubed soils along roadsides (Haan et al. 2012). Dry conditions in stormwater wetlands were found to favor grassland species (Jean-Philippe et al. 2021). Swales receive large volumes of water following precipitation events, and their hydroperiods are analogous to ephemeral wetlands. The low survival of switchgrass and other grasses in this study may be due to the high bulk density in lower part of the soil column of swales. Bulk density > 1.6 g cm³⁻¹ inhibits root growth deeper in the soil column and results in lower oxygen levels deeper in the soil (Weil & Brady 2019, Mills et al. 2020). In this study, the bulk density at 10-30 cm depth in swales ranged from 1.51 to 1.61 g cm³⁻¹, and ranged from 1.52 to 1.53 g cm³⁻¹ at depths of 20-30 cm in sand filtration systems.

The plants used in this study were propagated from local seed source genotypes collected from ephemeral streams within 10 km of all planting sites. For future plantings in LIDs and restoration efforts along roadways, it will be worth while to evaluate genotypes of native species from other geographical regions in the United States. For example, switchgrass occurs throughout most of the United States with the exception of the west coast (USDA 2022) and switchgrass genotypes prevalent in other areas of the Southwest United States may be more adaptable to climate change. Two plants that need further evaluation for use in LID structures are switchgrass and eastern gamagrass. Both species have high root and shoot biomass and are common in ephemeral streams in Bexar and surrounding counties (Jeffrey Hutchinson, unpubl. data). Ephemeral streams experience similar conditions as LIDs with both being rainfall dependent. Switchgrass was observed in the Babcock swale near the inflow, but was not documented along any transect lines.

Greenhouse studies

All native grasses except silver bluestem exhibited increasing biomass with increasing concentrations of nitrogen but no pattern was found for root to shoot ratios for any grass species. With increasing concentrations of phosphorus, a similar trend was observed. All native grass species except for buffalograss exhibited greater biomass with increasing concentrations of phosphorus. However, only white tridens was found to have decreasing root to shoot ratios with with increasing concentrations of phosphorus. Based on the greenhouse study, the majority of

native grass species evaluated in this study respond postively with biomass to increased concentrations of nitrogen and phosphorus under controlled conditions with no competition. Nitrogen and phosphorus are limiting nutrients under natural conditions. A study that evaluated native grasses for buffers around natural areas in Central Florida found that the addition of fertilizers did not result in greater coverage of native grasses (Jenkins et al. 2004). It is likley that native grasses exhibit a growth response to increasing concentrations of nitrogen and phosphorus in controlled conditions, but under field conditions are in competition with non-native grasses for nutrients and other resources.

Under different watering regimes in the greenhouse, silver bluestem, white tridens, and sideoats grama exhibited the highest total biomass for longer watering periods of 12 or 24 days indicating their tolerence to drought conditions. Switchgrass and eastern gamagrass were found to have the highest total biomass under shorter water periods of 2 or 3 days. Similar patterns were found for root to shoot ratios with silver bluestem and white tridens which put greater growth into their shoots compared to roots under longer watering periods. However, no pattern was observed for sideoats grama that allocated more biomass to its shoots compared to roots regardless of watering regime. Under daily watering, switchgrass allocated two times more biomass into its roots compared to shoots, indicating this species requires soils with longer hydroperiods.

Metal uptake by native grasses in the greenhouse study revealed no trends and high variation. This is likely due to the low concentrations of metals used in the treatments and that contamination from the soil or water used may have impacted the results.

Soils

Bulk density

In both swales and sand filtration systems, soil cores were difficult to obtain to a depth of 30 cm in the soil column. In swales, limestone fragments 1 to 6 cm wide were common throughout the soil. This may be an artificact from fill material that was used in the swales during construction. In sand filtration systems, the soil became highly compacted at depths of 10-15 cm which may be due to smaller particle percolating through the basin over time. In addition, construction and maintenance activities can increase soil bulk density and reduce stormwater infiltration (Ahmed et al. 2015). Soils with high infiltration rates exhibited high removal of metals, nitrogen, and phosphorus (Yousef et al. 1987). In North Carolina, the soil in detention basins was so compacted below 10 cm that only two samples could be taken at depths > 10 cm (Wissler et al. 2020). The efficiency of the infiltration capacity of swales is limited by soil characteristics and increased bulk density (Ekka et al. 2021). However, in this study, the longer retention time of water in sand filtration systems may improve denitrification rates.

Organic matter and carbon

Organic matter and carbon were found to have similar trends with higher percentages of each in swales compared to sand filtration systems. This difference between swales and sand filtration systems is due to different mangement practices. In this study, the upper layer of the soil in sand filtration systems is replaced with quartz sand which results in the removal of any accumulated

organic matter. The swales have vegetation cover throughout the year that results in the accumulation of organic matter. In Virginia, flow was reduced and pollutant loads were less in unmanaged strips than in managed strips (Henderson et al. 2016). The addition of an organic mulch layer improves adsorption of hydrocarbon products (Hunt et al. 2012). The mixing of mulch with sand media in sand filtration systems at $\leq 10\%$ total volume may also improve pollutant capture as stormwater percolates through the soil. However, the use of compost as a media in bioretention basins can result in an export of nitrogen (Shrestha et al. 2018).

Merriman et al. (2017) found that vegetation cover and production was more important than decomposition in the accumulation of carbon in retention ponds. With increasing temperatures due to a changing climate, C₄ photosynthetic plants and especially grasses may be most adaptable to LID structures. C₄ plants are more adapted to warmer temperatures and less rainfall than C₃ plants. Stormwater filtration through sand media is effective for most pollutants except nitrate (Jiang et al. 2015). Denitrification was found to be correlated with organic matter, soil moisture, and microbial biomass (Bettez and Groffman 2012). Negative removal of nitrogen was related to organic matter in roadside ditches due to frequent mowing (Stagge et al. 2012, Yousef et al. 1987). One option for management of swales and ponds is to limit mowing until the end of the growing season and then collect and remove the plant parts from the LID. A study that evaluated different types of LID structures found that LIDs were effective in sequestering carbon (Kavehei et al. 2018). Another study found that LID structures < 10 years old had greater microbial activity that resulted in more efficient carbon and nitorgen cycling than older LIDs but are similar to natural areas (Deeb et al. 2018).

Particle size

The results of this study are similar to those of Niu et al. (2019) in which 71% of roadway runoff particles were in the size class range between 63 to 830 μ m. Andral et al. (1999) found that 53% of the particles in the roadway catchment were between 500 and 1000 μ m. However, soil particles < 250 μ m accounted for 40 to 52% of the pollutants in roadway runoff (Niu et al., 2019). In contast, the majority of suspended particles in roadway runoff are < 63 μ m (Baum et al., 2021). In 179 samples from swales, particle size ranged from 4 to 120 μ m with > 50% of the particles < 6 μ m from swales in Sweden (Bäckström et al. 2006). Kayhanian et al. (2012) found that finer sediment size particles < 75 μ m increased from the inlet to outlet and emphasized the importance of capturing finer particles early and suggested dividing the sand filtration systems into two basins. The limited retention time in swales reduces capture of smaller sediment particles < 63 μ m (Deletic and Fletcher, 2006; Winston and Hunt, 2017). Allowing grasses to grow to heights of 0.5 to > 1.0 m in height and maintaing vegetation cover > 100% will further reduce smaller particles < 63 μ m. In addition, the root systems of grasses promotes increased percolation of water and smaller particles into the LID media.

Metals

Plant uptake

All four of the common native plants analyzed in this study from sand filtration systems and swales exhibited uptake of all metals analyzed with the exception of cadmium. Cadmium was

not detected in the shoots or roots of Mexican hat and white tridens. While no significant differences were found for metal uptake in the roots and shoots, frog-fruit exhibited the highest overall uptake of Pb, Cu, Cr, and Ni. Metal concentrations in the soils were generally much lower than metal concentrations in the plants. Gawryluk et al. (2020) found that Zn, Pb, and Cu concentrations were greater in plant shoots of grasses than in the soil. Based on the total concentration of metals found in the the roots and shoots of plants compared to the concentrations in the soil from this study, frog-fruit and wild petunia are accumulators of Zn and Cu, frog-fruit, Mexican hat, and wild petunia are accumulators of Pb and Cr, and all four study species are accumulators of Ni.

In LID structures, metals accumulate in the top soil layer from continuous roadside runoff and atmostpheric deposition (Bressy 2012). During infiltration, metals adsorb to organic matter limiting their mobility (Gupta and Sinha 2006). However, in this study detention ponds contained mimimal organic matter which may allow metals to percolate through the soil layer in the basin. The results of this study are comparable to other studies that found various plants' uptake of metals was greatest for Zn and Pb along roadways and urban areas (Khalid et al. 2018, Rolli et al. 2016, Pratt and Lottermorser 2007, Aksoy and Dixon 1999).

The root to shoot ratio of metal uptake was generally 1:1 with equal uptake of metals between the roots and shoots. Exceptions were found with Fe (all four species), Mg (frog-fruit and white tridens), and Zn (white tridens) which took in more of these metals in their roots compared to shoots. Metals concentrations in plants were 8 to 11 times greater along roadways to plants at further distances from roadways, but no differences were found for metal concentrations in soils (Khalid et al. 2018). Zhao et al. (2010) found no difference in the metal concentrations with greater distances from roadways. The greater concentration of metals found in plants and soils along roadways is due to automobile emissions and wash off from normal wear of tire, brakes, and other automobile parts (Colvile et al. 2001, Thorpe and Harrison 2008). Rolli et al. (2016) found that metal concentrations were 4 to 63 times higer in soils compared to two plants for Pb, Cu, Zn, Cr, and Ni along roads in India.

In spike mesocosms, a mix of grasses (*Festuca arundinancea*, *F. rubra*, and *Lolium perenne*) was more effective than other plants tested at accumulating Cd and Pb in roots and shoots even though the grass biomass was less than other plants (Leory et al. 2017). Metals concentrated in plants will be recycled or released once perennial plants senesce and annual plants die. It is suggested that mowing occur at the end of the growing season and all cut plant parts be collected and disposed of in a landfill.

Metal concentrations in soils

With the exception of Fe, Mg, and Zn, the concentrations of Pb, Cu, Cr, and Ni were low in the soils of swales and sand filtration systems. Sand-based detention systems and vegetative swales have been proven to be effective in the removal of metals (Gavrić et al. 2019, Søberg et al. 2017). Based on soil core depths in increments of 0-10, 10-20, and 20-30 cm, Fe concentrations were significantly greater in all increments in swales compared to Mg, and Zn. In contrast, Pb was found in equal concentrations at all three soil increments in swales and sand filtration systems with concentrations ranging from 8.5 to 22.6 µg L⁻¹, though high variance was found among samples. Metals in soils are primarily trapped in the topsoil being bound to organic

matter or clay (Li and Davis, 2008; Hortstmeyer et al. 2016) or adsorbed at the soil-water interface (Weiss et al. 2006). In swales, only a small percentage of metals entering swales leach with water into the deeper soil (Kabir et al. 2014).

Oil and Grease

Oil and grease concentrations in soils

The mean concentrations of oil and grease documented in this study for swales and sand filtration systems were similar between sand filtration systems and swales at 723 and 669 mg kg⁻¹, respectively. The 2.6 times greater sediment weight collected in sand filtration systems compared to swales indicates that a greater amount of sediment was trapped in the vegetative swales compared to sand filtration systems. No known studies were found that examined sediment captured from road runoff in sand filtration systems and swales for oil and grease following rain events. Most studies have examined the oil and grease concentrations from water samples collected at the inflow and outflow of LID structures during rain events. Concentrations of oil and grease taken from samples collected from street sweepers along roadways ranged from 34 to 3400 mg kg⁻¹ (Lloyd et al. 2019) indicating that high amounts of oil and grease can buildup on roadways. In the above study, no correlation was found between oil and grease concentrations and average daily traffic or land use patterns (Lloyd et al. 2019). Based on the results taken from soils in the vicinity of a petroleum refinery, the concentration of oil and grease ranged from 100 to 2400 mg kg⁻¹ (Rauckyte et al. 2010).

Several studies have analyzed total petroleum hydrocarbons (TPH) which does not include animal fats and plant derived oils. Khan and Kathi (2014) detected TPH concentrations ranging between 90.7 and 121.8 and 44.9 and 83.4 mg kg⁻¹ in soils collected from roadsides in India adjacent to automobile workshops and agricultural sites, repectively. In contrast, the TPH concentrations ranged from 1179 to 6345 mg kg⁻¹ in agricultural fields in close proximity to a petroleum processing plant in southern China (Li et al. 2012). In soil samples taken from automoble junk yards, the concentrations of TPH ranged from 486 to 4439 and 116 to 433 mg kg⁻¹ at core depths of 0-15 and 15-30 cm, respectively (Chukwujindu et al. 2008).

Oil and grease concentrations provide a general approximation for medium and heavy crude oils present in soils (Efroymson et al. 2004). The high amount of oil and grease documented in this study from roadway runoff in swales and sand filtration systems is concerning since hydrocarbon chemicals including PAHs are major components of oil products (Honda and Suzuki 2020). The accumulation of oil and grease in aquifer water from roadway runoff can alter the physiological processes of invertebrates residing in surface and groundwater (Gossett et al. 2018, Sese et al. 2009). Khan et al. (2007) found that while biodiesel and associated blends were not as toxic to aquatic organisms as diesel, these naturally produced products still significantly impact aquatic species at higher concentrations.

In Austin, Texas, the mean oil and grease concentrations detected from runoff in swales along three highways ranged from 0.5 to 6.5 mg L⁻¹ with the mean annual oil and grease loading ranging from 0.06 to 7.36 kg ha⁻¹ (Barrett et al., 1995). While initial water samples from first flush may have low concentrations of oil and grease, sand filtration systems and swales appear to serve as sinks for oil and grease. Following rain events, oil residue was observed covering the

leaves and clumps of plants in sand filtration systems and swales in this study. It is likely that the oil and grease residue breaks down into other compounds that resuspend in the water column during each rain event. Sand filtration systems and swales with vegetation cover are effective at trapping oils and greases and may serve as sinks for oil and grease and associated petroleum products. Hong et al. (2006) found that a mulch layer removed 80 to 95% of oil and grease products through sorption and filtration with biodegradation occuring within 2 to 8 days.

Sediment particle size collected from roadway runoff

In swales, the mean dry weight of sediment collected from runoff was 2.6 fold less than the mean sediment weight collected in sand filtration systems. The lower amount of sediment collected from runoff in swales agrees with other research on the importance of vegetation in reducing total suspended solids (Lucke et al. 2014, Deletic 2001). In addition, the greater weight of sediment captured in sand filtration systems were found for particles in the 500, 250 125, and 63 μm size classes compared to swales. Sediment particles > 63 μm were found to have higher organic matter than particles < 63 μm which promotes greater adsorbtion of other particles (Karickhoff et al. 1979), but smaller particles have greater surface area and represent a large percentage of the pollutant load (Baum et al. 2021).

Stormwater Monitoring

Bulverde Basin Water quality

The average influent nitrate concentration of 0.7 mg/L observed in this site was comparable to those reported in previous studies, e.g., Morse et al. (2017) reported 0.21 and 0.18 mg/L on average for their inlet nitrate concentrations in wet and dry detention basins, while outlet concentrations were slightly higher. Another study (Zarezadeh et al., 2018) reported an average nitrate inflow concentration of 1.3 mg/L in a sand filter basin located in San Antonio while the effluent concentrations on average were about 0.8 mg/L. Reported nitrate removal in Stormwater Control Measures (SCMs) varies widely (McPhillips et al., 2018; Morse et al., 2017; Payne et al., 2014) with some studies reporting higher nitrate in effluent compared to the inlet. For instance, McPhillips et al. (2018) reported an average inflow concentration for a grassed detention and bioretention basin of 0.33 mg/L and 0.23 mg/L, respectively while the outlet concentrations were considerably higher (on average > 1 mg/L). Net production was also reported in another detention basin study (Birch et al., 2006), with a reported average removal rate of -46 %. In this site, the average outlet EMC nitrate concentration was about 1.4 mg/L, which is consistent with the above studies reporting higher nitrate in the effluent.

The variability in the performance of stormwater basins towards nitrate may be observed due to the differences in nutrient loading, type of vegetation (if any) used in them, soil media type, design as well as the location and natural conditions affecting the basins (Blecken et al., 2017; Søberg et al., 2019). Moreover, maintenance is another important factor affecting the performance of the basins over time, as it has been suggested that maintenance of aged stormwater basins improved their performance significantly and prevented release of polluted sediments in the downstream ecosystems (Blecken et al., 2017). Sandy soils are considered to have low denitrification potential (Hall et al., 2022; Waller et al., 2018). For example, one study (Waller et al., 2018) compared bioretention cells with less than 50 % sands and the ones having more than 80 % sand in the soil

and found lower denitrification potential in the bioretention cells with higher sand content in the soil medium. Although not significant, higher sand content in the detention basin in our study likely attributed to low denitrification observed in our study.

In the present study, considerable differences in the pattern of nitrate removal compared to nitrite and ammonia was observed. Nitrate can be generated in situ in treatment structures from mineralization of organic N and nitrification of NH₄⁺. Moreover, higher concentrations of nitrate can be due to the mineralization and nitrification of soil media (Clivot et al., 2017; Landsman and Davis, 2018). One study (Cho et al., 2009) concluded that nitrate leaching may be caused by nitrification during dry days suggesting that the nitrate removal and leaching of nitrate can be related to the soil texture. Similarly, higher levels of soil moisture due to submerged zone in the soil increase anoxic conditions resulting in an increase in denitrification rates (Søberg et al., 2019). Furthermore, the low ammonia concentration and high concentration of nitrate in the outlet samples in the present study suggest that absorbed ammonia is being nitrified most likely to nitrate (Hatt et al., 2007; Li and Davis, 2014). A recent study (Valenca et al., 2020) reviewed different design and types of the SCMs and suggested that sand filter medias mostly export nitrate irrespective of the local climate or design specifications. Since filter media most often consist of sand, the capacity to remove nitrate by adsorption or biotransformation hence is limited. Oxidation of ammonium to nitrate is another possible reason for nitrate leaching into the filtered stormwater (Landsman and Davis, 2018).

The total phosphorus inlet EMC was about 0.95 mg/L, while the outlet had a mean EMC of about 0.25 mg/L corresponding to an average removal of 65 %. Hence, the Bulverde basin effectively removed TP due to the filtration and the resulting removal of particles and sediments. This is consistent with other studies reporting phosphorus removal, e.g. (Wissler et al., 2020) who studied two dry basins receiving highway runoff and observed that the median removal efficiencies for phosphorus for the two sites were 17 % and 10 %, respectively.

The report from the international stormwater BMP database (Foundation, 2020) indicated that in detention basins the median concentration of TSS inlet in 44 studies was 65 mg/L, while the outlet concentration was 22 mg/L. TSS concentrations were effectively reduced and removed from 106 mg/L to 3 mg/L in the Bulverde site. In contrast, there was no significant change in TDS concentration between the influent and effluent, with medians of 118 mg/L and 152 mg/L, respectively. Additionally, the BMP database report summarized 14 different studies regarding TDS in detention basins, with a median value of 109 mg/L for inlets and 110 mg/L for outlets.

According to the Fundamentals of Urban Runoff report (Shaver et al., 2007) in the US, average COD and Oil EMC concentrations were 52 mg/L and 3 mg/L, respectively. In the Bulverde basin, the average COD and Oil EMC values in the inlet were 125 mg/l and 44 mg/L, respectively. The basin decreased COD concentrations significantly with an average EMC of 32 mg/L, while the Oil EMC values in the effluent were 30 mg/L. The average PAH concentration in stormwater runoff in the U.S. was reported to be 3.5 mg/L according to a summary of EMC data for stormwater runoff (Shaver et al., 2007). In the central and eastern U.S., coal-tar-based sealcoat products are widely used on parking lots, driveways, and even playgrounds. These products contain approximately 200 PAHs, which are one of the sources of pollutants in stormwater (Mahler et al., 2012). In the Bulverde basin, PAH concentrations were reduced from 1.7 mg/L to 0.32 mg/L on a median basis. This confirms previous studies that have suggested that PAH removal is in large part determined by the adsorption process (Mitchell et al., 2023). Further, PAHs are generally associated with suspended solids (Hwang and Foster, 2006), and the lower TSS concentrations in the effluent may be an explanation for the lower PAH concentration in the outlet samples.

In urban stormwater, metal concentrations are often higher than natural background levels due to automobile-related sources such as roads, parking lots, and building materials (e.g., galvanized roofs, gutters, downspouts, and fencing) exposed to rain. Treated wood is also a common source of metals in residential and commercial areas. Depending on the process and management practices of an industrial facility, certain metals may be more prevalent in industrial areas, while landfill leachate, soil erosion, household chemicals, and pesticides may also be other sources of metal pollution (Shaver et al., 2007). Both the inlet and outlet samples contained very low concentrations of Ni and Cr. With more than ten times higher concentrations, the magnesium levels in the measured samples were significantly higher compared to other measured elements in the Bulverde basin.

TPC and Kyle Water quality

In this study, TSS inflow concentrations were higher at Kyle than at TPC. Additionally, TPC site displayed higher removal efficiency for TSS compared to the Kyle site. This may be due to the differences in retention times between the two basins since the filtration area at TPC is almost twice the size of filtration area at Kyle. One of the primary functions of detention basins is the removal of TSS pollutants from stormwater, with 80% TSS reduction as the required target in Texas (Barrett, 2005). It was observed that both TPC and Kyle sites in our study reduced the inflow TSS concentrations significantly with the TPC site exceeding 90 % median removal efficiency. These observed removal percentages agree well with previous studies reporting high TSS removal efficiencies for detention basins (Middleton and Barrett, 2008). In one study, Middleton and Barrett (2008) monitored the performance of a batch-type stormwater detention basin and reported 91 % removal efficiency between inflow and outflow EMC concentrations.

The concentrations of nitrate EMCs in the outflows from both sites were significantly higher than those in the inflows. There are many sources of phosphorus found in urban runoff, such as lawn fertilizers, atmospheric deposition, soil erosion, animal waste, and detergents, which contribute to the pollution of the water (Hsieh et al., 2007). In both sites, phosphorus (PO₄³⁻) exhibited significantly higher concentrations in the outflow samples compared to the inflow samples. Previous studies have also shown that the media of the SCM systems can leach phosphorus into the system. In one study, it has been demonstrated that particulate phosphorus filtered and accumulated in urban stormwater may potentially partition back to the aqueous phase over time (Berretta and Sansalone, 2012). Further, it is possible that dissolved phosphorus could have migrated into the outflow samples due to decomposition of organic matter that may have fallen onto the basin, such as leaves and grass clippings. This would have contributed to higher concentrations measured in the outflow samples due to the presence of dissolved phosphorus (Yang et al., 2021).

According to this study, the TOC median inflow concentrations at Kyle and TPC sites were similar to each other with 18.6 mg/L and 18.4 mg/L, respectively. An earlier study (Aitkenhead-Peterson et al., 2009) investigated the dissolved organic carbon (DOC) concentrations in urban and rural watersheds of south-central Texas, and found that median concentrations ranged from 20 mg/L to 50 mg/L, suggesting that concentrated urban development and open areas had a significant correlation with the concentration of DOC. We observed that TPC inflows were slightly greater in terms of COD concentrations than Kyle. Inlet PAH median values for TPC and Kyle sites were 0.32 mg/L and 0.91 mg/L, respectively, and effluent median values were 0.06 mg/L for both. The Kyle site is located next to a school parking lot, and as mentioned earlier,

parking lots are a source of PAHs. Therefore, higher PAH concentrations can be attributed to the Kyle site than to the TPC.

Both sites showed similar trends for heavy metals, with magnesium concentrations significantly higher than the other elements and higher concentrations at the outlet than at the inlet. In the influent and effluent samples of both sites, Cr and Ni concentrations were less than $10 \,\mu g/L$. Further, while Zn median EMC values were higher in the Kyle site than in the inlet, this trend was reversed in the TPC site, where Zn EMC values were lower in outlet samples compared to inlet samples.

Bacterial communities in detention basins

The bacterial communities in soil samples from two different seasons were studied by highthroughput sequencing of the 16S rRNA genes. The most dominant bacterial phyla observed in the soil samples were Actinobacteria, Proteobacteria, and Chloroflexi, which is consistent with findings in other studies (Wang et al., 2020; Zeng et al., 2016). Actinobacteria was the most abundant phyla in this study. It is one of the most abundant phyla within the earth's biosphere and plays a key role in soil ecology via nitrogen fixation, phosphorus solubilization and mobilization of other nutrients (Stevenson and Hallsworth, 2014); the degradation and mineralization of plant materials in soil and also contribute to carbon cycling (Mafa-Attove et al., 2020). Further, soil depth can play a critical role in the abundance of the microbial community (Upton et al., 2020). In the present study, the relative abundance of Actinobacteria increased with soil depths during both summer and winter which is consistent with findings of other studies (Eilers et al., 2012). Seasonal dynamics and changes in the weather are other factors affecting the microbial soil community (Hullar et al., 2006). In the present study shared microbial communities varied in different seasons and different layers and the Pielou alpha diversity indices differed significantly between summer and winter samples with higher diversity in summer samples. The latter is consistent with findings of Zhang et al. (2020), who also reported higher diversity in summer samples.

Management Recommendations

Most problems associated with pollution in the urban environment are generated locally, and urban ecosystems, whether natural, semi-natural, or engineered structures are an important part of the solution (Boland and Hunhammar 1999). As suggested by Sinclair et al. (2020), urbanization must include mutiple types of natural and engineered LID structures and green infrastructures that include natural areas, public green spaces, green ways, ephemeral pools, swales, detention ponds, constructed wetlands, urban trees, residential lawns, backyard wildlife habitat, rain gardens, and green roofs to buffer and remediate the increased influx of pollutants. In addition to the use of swales and sand filtration systems along roadways, a more comprehensive and cumulative approach will be required to protect the Edwards Aquifer. The promotion and incentives to homeowners, businesses, and industries to protect small tracts of urban land, construct small depressions and rain gardens, create vegetative buffer strips, xeriscape lawns, utilize pervious structures for small parking lots and other paved areas are needed along with larger LID structures on a landscape level. Management in the Edwards Aquifer recharge zone and throughout Bexar County should take a comprehensive landscape approach.

Best management practices for swales and sand filtration systems are listed below:

Vegetation management in swales and sand filtration systems should be limited to the late fall and winter months when plants become dormant. Following mowing, all cut plant parts should be collected and disposed of in a municipal landfill to prevent recycling of nutrients and metals.

Promote plant diversity in LID structures with a focus on deep-rooted and high shoot biomass species such as switchgrass and other native grasses along with forbs and herbs (Appendix 4). The 56 species documented from swales and detention ponds in this study represent a diversity of plant functional groups that may be most resilient to climate change. The use of deep-rooted native grasses promotes runoff infiltration and lower pollutant loading by trapping sediment. The use of annual and perennial plants with shallow root system is also recommended for nutrient and metal removal in the top soil.

The addition of organic matter, compost, etc. is recommended in detention ponds at a 10% to 90% sand v/v media in the upper layer to caputre hydrocarbon products and encourage microbial growth.

Establishing buffer zones of deep-rooted and tall native graminoids such as switchgrass, white tridens, Texas wintergrass, and various species of *Cyperus* spp. 2-4 m from the inflow of LID structures to promote sediment trappings.

Evaluation of native plant genotypes from other areas in the Southwest United States and Northern Mexico that may be more adapable to warmer temperatures, frequent droughts, and more intense rain events predicted from climate change. Surveys in swales and sand filtration systems over time may show changes in plant species and coverage due to climate change.

Seeding LID structures with native grasses and forb/herb seeds is recommended to promote functional diversity and ecosystem services. Seeding should occur in the spring and fall following precipitation events.

Native shrubs and trees are suggested for planting along the top of the slopes of swales and sand filtration systems to capture aerisols and atmospheric particulate matter. As trees mature, they will provide greater aesthetic value and ecosystem services.

Within the Edwards Aquifer recharge zone, require swales and sand filtration systems in series with some cells having longer stormwater detention times for runoff. The construction of earthen berms, check dams, or wiers in swales to promote ponding and extended retention times for stormwater will increase denitrification under anoxic conditions.

In locations where larger tracts of land are available, the construction of larger or a series of swales and sand filtration systems with increase water retention time will result in more efficient nitrogen transformation and mitigation (Mallin et al. 2002, Ekka et al. 2021).

With flashy and more intense precipitation events and inceased sediment loads predicted with climate change, provide incentives (tax breaks, reduced permiting cost, reduced fees, etc.) for developers to construct sand filtration systems, swales, and other LID structures for all new development in the Edwards Aqufier contributing and recharge zones.

The use of pervious pavement should be encouraged and promoted in Bexar County in residential and commercial parking lots. Incentives such as tax breaks, refunds, or streamlined permitting could be provided as incentives to residential homeowners and commercial businesses that use previous pavement.

Require annual inspection for all private and commercial vehicles to reduce vehicle emissions in urban areas and along roadways. A large amount of pollutants are attributed to automobile emissions that impact soil, water and air quality. Reducing vehicle emissions is one step in the process to protect water and air quality.

With increased rainfall and intensity predicted due to climate change, new construction of swales and sand filtration systems should consider larger areas and storage volume due to the expected increases in stormwater volume during storm events (Zhang et al. 2019, Hathaway et al. 2014).

Acknowledgements

The Principal Investigators thank the City of San Antonio and its partners for providing funding for this study under Proposition 1, a voter approved effort to protect the Edwards Aquifer. We thank Karen Bishop for her support, suggestions, and comments throughout the study. We are especially thankful to the staff at the City of San Antonio's Public Works Department for providing support, logistics, and access to all the study sites. These staff members include Martin Hernandez, Les Sabernik, Eric Meyer, and Michael Dicolla. The Department of Integrated Biology and School of Civil & Environmental Engineering, and Construction Management at UTSA provided support throughout the duration of this study. We are especially thankful to multiple graduate and undergraduate students that provided lab, greenhouse, and field support. These students include but are not limited to: Sina Vedadi Moghadam, Arash Jafarzadeh, Jason Kent, Tabyatha Counts, Sherry Lim, Sarah Gorton, Fischer Ridge, David Roberts, Darla Reid, Donjae Galbert, Angela Maroti, Maria Flores, Celicia Garza, Andre Felton, and Angel Chappell.

Literature Cited

Abduljaleel, Y., Salem, A., ul Haq, F., Awad, A., & Amiri, M. (2023). Improving detention ponds for effective stormwater management and water quality enhancement under future climate change: a simulation study using the PCSWMM model. Scientific Reports, 13(1), 5555.

Ahmed, F., Gulliver, J. S., & Nieber, J. L. (2015). Field infiltration measurements in grassed roadside drainage ditches: Spatial and temporal variability. Journal of Hydrology, 530, 604-611.

Aitkenhead-Peterson, J., Steele, M., Nahar, N. & Santhy, K. (2009). Dissolved organic carbon and nitrogen in urban and rural watersheds of south-central Texas: land use and land management influences. Biogeochemistry 96(1), 119-129.

Aksoy, A. H. M. E. T., Hale, W. H., & Dixon, J. M. (1999). Capsella bursa-pastoris (L.) Medic. as a biomonitor of heavy metals. Science of the Total Environment, 226(2-3), 177-186.

American Forests (2002). Urban ecosystem analysis San Antonio, Texas region. Calculating the value of nature. https://www.sierraclub.org/sites/default/files/sce/alamogroup/docs/UEA_San_Antonio-May_2009_small.pdf.

Andral, M. C., Roger, S., Montrejaud-Vignoles, M., & Herremans, L. (1999). Particle size distribution and hydrodynamic characteristics of solid matter carried by runoff from motorways. Water Environment Research, 71(4), 398-407.

Auffret, A. G., & Lindgren, E. (2020). Roadside diversity in relation to age and surrounding source habitat: evidence for long time lags in valuable green infrastructure. Ecological Solutions and Evidence, 1(1), e12005.

Barrett, M.E. (2005). Complying with the Edwards Aquifer Rules: Technical Guidance on Best Management Practices, Texas Commission on Environmental Quality.

Barrett, M. E. (2018). Mitigation of impacts to groundwater quality from highway runoff in a karst terrain. Transportation Research Record, 2672(39), 61-67.

Barrett, M. E., Malina, J. F., Charbeneau, R. J., & Ward, G. H. (1995). Effects of highway construction and operation on water quality and quantity in an ephemeral stream in the Austin, Texas area. Center for Research in Water Resources, University of Texas at Austin. https://repositories.lib.utexas.edu/bitstream/handle/2152/6742/crwr_onlinereport95-10.pdf;sequence=2.

Barrett, M. E., Irish Jr, L. B., Malina Jr, J. F., & Charbeneau, R. J. (1998). Characterization of highway runoff in Austin, Texas, area. Journal of Environmental Engineering, 124(2), 131-137.

Barrett, M. E., Walsh, P. M., Malina Jr, J. F., & Charbeneau, R. J. (1998). Performance of vegetative controls for treating highway runoff. Journal of Environmental Engineering, 124(11), 1121-1128.

- Barrett, M., Lantin, A., & Austrheim-Smith, S. (2004). Storm water pollutant removal in roadside vegetated buffer strips. Transportation Research Record, 1890(1), 129-140.
- Berretta, C. and Sansalone, J. (2012). Fate of phosphorus fractions in an adsorptive-filter subject to intra-and inter-event runoff phenomena. Journal of Environmental Management 103, 83-94.
- Bäckström, M., Viklander, M., & Malmqvist, P. A. (2006). Transport of stormwater pollutants through a roadside grassed swale. Urban Water Journal, 3(2), 55-67.
- Baum, P., Kuch, B., & Dittmer, U. (2021). Adsorption of metals to particles in urban stormwater runoff—Does size really matter? Water, 13(3), 309. https://doi.org/10.3390/w13030309.
- Bettez, N. D., & Groffman, P. M. (2012). Denitrification potential in stormwater control structures and natural riparian zones in an urban landscape. Environmental Science & Technology, 46(20), 10909-10917.
- Birch, G., Matthai, C. and Fazeli, M. (2006). Efficiency of a retention/detention basin to removecontaminants from urban stormwater. Urban Water Journal 3(2), 69-77.
- Bisutti, I., Hilke, I., & Raessler, M. (2004). Determination of total organic carbon—an overview of current methods. TrAC Trends in Analytical Chemistry, 23(10-11), 716-726.
- Blecken, G.-T., Hunt III, W.F., Al-Rubaei, A.M., Viklander, M. and Lord, W.G. (2017). Stormwater control measure (SCM) maintenance considerations to ensure designed functionality. Urban Water Journal 14(3), 278-290.
- Boger, A. R., Ahiablame, L., Mosase, E., & Beck, D. (2018). Effectiveness of roadside vegetated filter strips and swales at treating roadway runoff: a tutorial review. Environmental Science: Water Research & Technology, 4(4), 478-486.
- Bolund, P., & Hunhammar, S. (1999). Ecosystem services in urban areas. Ecological Economics, 29(2), 293-301.
- Bressy, A., Gromaire, M. C., Lorgeoux, C., Saad, M., Leroy, F., & Chebbo, G. (2012). Towards the determination of an optimal scale for stormwater quality management: Micropollutants in a small residential catchment. Water Research, 46(20), 6799-6810.
- Cadotte, M. W., Yasui, S. L. E., Livingstone, S., & MacIvor, J. S. (2017). Are urban systems beneficial, detrimental, or indifferent for biological invasion? Biological Invasions, 19, 3489-3503.
- Canfield, R. H. (1941). Application of the line interception method in sampling range vegetation. Journal of forestry, 39(4), 388-394.
- Cho, K.W., Song, K.G., Cho, J.W., Kim, T.G. and Ahn, K.H. (2009). Removal of nitrogen by a layered soil infiltration system during intermittent storm events. Chemosphere 76(5), 690-696.

- Chukwujindu, M.A.I., Williams, E.S., & Nwajei, G.E. (2008). Characteristic levels of total petroleum hydrocarbon in soil profiles of automobile mechanic waste dumps. International Journal of Soil Science, 3(1), 48-51.
- Clivot, H., Mary, B., Valé, M., Cohan, J.P., Champolivier, L., Piraux, F., Laurent, F. and Justes, E. (2017). Quantifying in situ and modeling net nitrogen mineralization from soil organic matter in arable cropping systems. Soil Biology and Biochemistry 111, 44-59.
- Colvile, R. N., Hutchinson, E. J., Mindell, J. S., & Warren, R. F. (2001). The transport sector as a source of air pollution. Atmospheric Environment, 35(9), 1537-1565.
- Deeb, M., Groffman, P. M., Joyner, J. L., Lozefski, G., Paltseva, A., Lin, B., ... & Cheng, Z. (2018). Soil and microbial properties of green infrastructure stormwater management systems. Ecological Engineering, 125, 68-75.
- Deletic, A. (2001). Modelling of water and sediment transport over grassed areas. Journal of Hydrology, 248(1-4), 168-182.
- Dhillon, G. S., Amichev, B. Y., De Freitas, R., & Van Rees, K. (2015). Accurate and precise measurement of organic carbon content in carbonate-rich soils. Communications in Soil Science and Plant Analysis, 46(21), 2707-2720.
- Douthat, K. D. (2022). Vascular Plant Community Assembly in Stormwater Detention Basins (Doctoral dissertation, Rutgers The State University of New Jersey, School of Graduate Studies).
- Del Tredici, P. (2010). Spontaneous urban vegetation: reflections of change in a globalized world. Nature and Culture, 5(3), 299-315.
- Deletic, A., & Fletcher, T. D. (2006). Performance of grass filters used for stormwater treatment—a field and modelling study. Journal of hydrology, 317(3-4), 261-275.
- Efroymson, R. A., Sample, B. E., & Peterson, M. J. (2004). Ecotoxicity test data for total petroleum hydrocarbons in soil: Plants and soil-dwelling invertebrates. Human and Ecological Risk Assessment, 10(2), 207-231.
- Eilers, K.G., Debenport, S., Anderson, S. and Fierer, N. (2012). Digging deeper to find unique microbial communities: the strong effect of depth on the structure of bacterial and archaeal communities in soil. Soil Biology and Biochemistry 50, 58-65.
- Ekka, S. A., Rujner, H., Leonhardt, G., Blecken, G. T., Viklander, M., & Hunt, W. F. (2021). Next generation swale design for stormwater runoff treatment: A comprehensive approach. Journal of Environmental Management, 279, 111756.
- Foundation, W.R. 2020 International stormwater BMP database.
- Gavrić, S., Larm, T., Österlund, H., Marsalek, J., Wahlsten, A., & Viklander, M. (2019). Measurement and conceptual modelling of retention of metals (Cu, Pb, Zn) in soils of three grass swales. Journal of Hydrology, 574, 1053-1061.

- Gawryluk, A., Wyłupek, T., & Wolański, P. (2020). Assessment of Cu, Pb and Zn content in selected species of grasses and in the soil of the roadside embankment. Ecology and Evolution, 10(18), 9841-9852.
- Gonzalez-Merchan, C., Barraud, S., & Bedell, J. P. (2014). Influence of spontaneous vegetation in stormwater infiltration system clogging. Environmental Science and Pollution Research, 21, 5419-5426.
- Gleason, H. A. (1917). The structure and development of the plant association. Bulletin of the Torrey Botanical Club, 44(10), 463-481.
- Gosset, A., Wigh, A., Bony, S., Devaux, A., Bayard, R., Durrieu, C., ... & Bazin, C. (2018). Assessment of long term ecotoxicity of urban stormwaters using a multigenerational bioassay on Ceriodaphnia dubia: A preliminary study. Journal of Environmental Science and Health, Part A, 53(3), 244-252.
- GEAA Greater Edwards Aquifer Alliance. (2010). Permanent stormwater and pollution prevention systems within the Edwards Aquifer recharge zone in Bexar County, Texas An overview and assessment of current regulatory agency processes. Greater Edwards Aquifer Alliance. Available at:
- http://www.hillcountryalliance.org/uploads/HCA/GEAA_BMP_Final.pdf. Accessed: June 5, 2023.
- Gupta, A. K., & Sinha, S. (2006). Chemical fractionation and heavy metal accumulation in the plant of *Sesamum indicum* (L.) var. T55 grown on soil amended with tannery sludge: Selection of single extractants. Chemosphere, 64(1), 161-173.
- Haan, N. L., Hunter, M. R., & Hunter, M. D. (2012). Investigating predictors of plant establishment during roadside restoration. Restoration Ecology, 20(3), 315-321.
- Hall, N.C., Sikaroodi, M., Hogan, D., Jones, R.C. and Gillevet, P.M. (2022). The presence of denitrifiers in bacterial communities of urban stormwater best management practices (BMPs). Environmental Management 69(1), 89-110.
- Hathaway, J. M., Brown, R. A., Fu, J. S., & Hunt, W. F. (2014). Bioretention function under climate change scenarios in North Carolina, USA. Journal of Hydrology, 519, 503-511.
- Hatt, B.E., Fletcher, T.D. and Deletic, A. (2007). Hydraulic and pollutant removal performance of stormwater filters under variable wetting and drying regimes. Water Science and Technology 56(12), 11-19.
- Heiri, O., Lotter, A. F., & Lemcke, G. (2001). Loss on ignition as a method for estimating organic and carbonate content in sediments: reproducibility and comparability of results. Journal of paleolimnology, 25, 101-110. https://doi.org/10.1016/0009-2541(93)90140-E.

- Henderson, D., Smith, J. A., & Fitch, G. M. (2016). Impact of vegetation management on vegetated roadsides and their performance as a low-impact development practice for linear transportation infrastructure. Transportation Research Record, 2588(1), 172-180.
- Honda, M., & Suzuki, N. (2020). Toxicities of polycyclic aromatic hydrocarbons for aquatic animals. International Journal of Environmental Research and Public Health, 17(4), 1363.
- Hong, E., Seagren, E. A., & Davis, A. P. (2006). Sustainable oil and grease removal from synthetic stormwater runoff using bench-scale bioretention studies. Water Environment Research, 78(2), 141-155.
- Horstmeyer, N., Huber, M., Drewes, J. E., & Helmreich, B. (2016). Evaluation of site-specific factors influencing heavy metal contents in the topsoil of vegetated infiltration swales. Science of the Total Environment, 560, 19-28.
- Hsieh, C.h., Davis, A.P. and Needelman, B.A. (2007). Bioretention column studies of phosphorus removal from urban stormwater runoff. Water Environment Research 79(2), 177-184.
- Hullar, M.A.J., Kaplan, L.A. and Stahl, D.A. (2006). Recurring seasonal dynamics of microbial communities in stream habitats. Applied and Environmental Microbiology 72(1), 713-722.
- Hunt, W. F., Davis, A. P., & Traver, R. G. (2012). Meeting hydrologic and water quality goals through targeted bioretention design. Journal of Environmental Engineering, 138(6), 698-707.
- Hwang, H.-M. and Foster, G.D. (2006). Characterization of polycyclic aromatic hydrocarbons in urban stormwater runoff flowing into the tidal Anacostia River, Washington, DC, USA. Environmental Pollution 140(3), 416-426.
- Jakobsson, S., Bernes, C., Bullock, J. M., Verheyen, K., & Lindborg, R. (2018). How does roadside vegetation management affect the diversity of vascular plants and invertebrates? A systematic review. Environmental Evidence, 7, 1-14.
- Jean-Philippe, B., Marie, H., Muriel, S., & Laurent, L. (2021). Are acts of selective planting and maintenance drivers for vegetation change in stormwater systems? A case study of two infiltration basins. Ecological Engineering, 172, 106400.
- Jenkins, A. M., Gordon, D. R., & Renda, M. T. (2004). Native Alternatives for Non-Native Turfgrasses in Central Florida: Germination and Responses to Cultural Treatments. Restoration Ecology, 12(2), 190-199.
- Jiang, Y., Yuan, Y., & Piza, H. (2015). A review of applicability and effectiveness of low impact development/green infrastructure practices in arid/semi-arid United States. Environments, 2(2), 221-249.
- Kabir, M. I., Daly, E., & Maggi, F. (2014). A review of ion and metal pollutants in urban green water infrastructures. Science of the Total Environment, 470, 695-706.

- Karickhoff, S. W., Brown, D. S., & Scott, T. A. (1979). Sorption of hydrophobic pollutants on natural sediments. Water Research, 13(3), 241-248.
- Kavehei, E., Jenkins, G. A., Adame, M. F., & Lemckert, C. (2018). Carbon sequestration potential for mitigating the carbon footprint of green stormwater infrastructure. Renewable and Sustainable Energy Reviews, 94, 1179-1191.
- Kavehei, E., Jenkins, G. A., Lemckert, C., & Adame, M. F. (2019). Carbon stocks and sequestration of stormwater bioretention/biofiltration basins. Ecological Engineering, 138, 227-236.
- Kayhanian, M., McKenzie, E. R., Leatherbarrow, J. E., & Young, T. M. (2012). Characteristics of road sediment fractionated particles captured from paved surfaces, surface run-off and detention basins. Science of the Total Environment, 439, 172-186.
- Kayhanian, M., Fruchtman, B. D., Gulliver, J. S., Montanaro, C., Ranieri, E., & Wuertz, S. (2012). Review of highway runoff characteristics: Comparative analysis and universal implications. Water Research, 46(20), 6609-6624.
- Khalid, N., Hussain, M., Young, H. S., Boyce, B., Aqeel, M., & Noman, A. (2018). Effects of road proximity on heavy metal concentrations in soils and common roadside plants in Southern California. Environmental Science and Pollution Research, 25, 35257-35265.
- Khan, A. B., & Kathi, S. (2014). Evaluation of heavy metal and total petroleum hydrocarbon contamination of roadside surface soil. International Journal of Environmental Science and Technology, 11, 2259-2270.
- Kreuter, U. P., Harris, H. G., Matlock, M. D., & Lacey, R. E. (2001). Change in ecosystem service values in the San Antonio area, Texas. Ecological Economics, 39(3), 333-346.
- LaFontaine, J. H., Hay, L. E., Viger, R. J., Regan, R. S., & Markstrom, S. L. (2015). Effects of climate and land cover on hydrology in the Southeastern US: Potential impacts on watershed planning. Journal of the American Water Resources Association, 51(5), 1235-1261.
- Landsman, M.R. and Davis, A.P. (2018). Evaluation of nutrients and suspended solids removal by stormwater control measures using high-flow media. Journal of Environmental Engineering 144(10), 04018106.
- Leroy, M. C., Portet-Koltalo, F., Legras, M., Lederf, F., Moncond'Huy, V., Polaert, I., & Marcotte, S. (2016). Performance of vegetated swales for improving road runoff quality in a moderate traffic urban area. Science of the Total Environment, 566, 113-121.
- Leroy, M. C., Marcotte, S., Legras, M., Moncond'Huy, V., Le Derf, F., & Portet-Koltalo, F. (2017). Influence of the vegetative cover on the fate of trace metals in retention systems simulating roadside infiltration swales. Science of the Total Environment, 580, 482-490.
- Li, H., & Davis, A. P. (2008). Heavy metal capture and accumulation in bioretention media. Environmental Science & Technology, 42(14), 5247-5253.

- Li, L. and Davis, A.P. (2014). Urban stormwater runoff nitrogen composition and fate in bioretention systems. Environmental Science and Technology 48(6), 3403-3410.
- Li, J., Zhang, J., Lu, Y., Chen, Y., Dong, S., & Shim, H. (2012). Determination of total petroleum hydrocarbons (TPH) in agricultural soils near a petrochemical complex in Guangzhou, China. Environmental monitoring and assessment, 184, 281-287.
- Li, M. H., Barrett, M. E., Rammohan, P., Olivera, F., & Landphair, H. C. (2008). Documenting stormwater quality on Texas highways and adjacent vegetated roadsides. Journal of Environmental Engineering, 134(1), 48-59.
- Lichvar, R. W., Banks, D. L., Kirchner, W. N., & Melvin, N. C. (2016). The national wetland plant list: 2016 wetland ratings. Phytoneuron, 30, 1-17.
- Lloyd, L. N., Fitch, G. M., Singh, T. S., & Smith, J. A. (2019). Characterization of environmental pollutants in sediment collected during street sweeping operations to evaluate its potential for reuse. Journal of Environmental Engineering, 145(2), 04018141.
- Lucke, T., Kachchu Mohamed, M. A., & Tindale, N. (2014). Pollutant removal and hydraulic reduction performance of field grassed swales during runoff simulation experiments. Water, 6(7), 1887-1904.
- Lundholm, J. T., & Marlin, A. (2006). Habitat origins and microhabitat preferences of urban plant species. Urban Ecosystems, 9, 139-159.
- Mafa-Attoye, T.G., Baskerville, M.A., Ofosu, E., Oelbermann, M., Thevathasan, N.V. and Dunfield, K.E. (2020). Riparian land-use systems impact soil microbial communities and nitrous oxide emissions in an agro-ecosystem. Science of the Total Environment 724, 138148.
- Mahler, B.J., Metre, P.C.V., Crane, J.L., Watts, A.W., Scoggins, M. and Williams, E.S. (2012). Coal-tar-based pavement sealcoat and PAHs: implications for the environment, human health, and stormwater management, ACS Publications.
- Mallin, M. A., Ensign, S. H., Wheeler, T. L., & Mayes, D. B. (2002). Pollutant removal efficacy of three wet detention ponds. Journal of Environmental Quality, 31(2), 654-660.
- McPhillips, L., Goodale, C. and Walter, M.T. (2018). Nutrient leaching and greenhouse gas emissions in grassed detention and bioretention stormwater basins. Journal of Sustainable Water in the Built Environment 4(1), 04017014.
- Merriman, L. S., Moore, T. L. C., Wang, J. W., Osmond, D. L., Al-Rubaei, A. M., Smolek, A. P., ... & Hunt, W. F. (2017). Evaluation of factors affecting soil carbon sequestration services of stormwater wet retention ponds in varying climate zones. Science of the Total Environment, 583, 133-141.
- Middleton, J.R. and Barrett, M.E. (2008). Water quality performance of a batch-type stormwater detention basin. Water Environment Research 80(2), 172-178.

- Mills, S. D., Mamo, M., Schacht, W. H., Abagandura, G. O., & Blanco-Canqui, H. (2020). Soil properties affected vegetation establishment and persistence on roadsides. Water, Air, & Soil Pollution, 231, 1-20.
- Mitchell, C.J., Jayakaran, A.D. and McIntyre, J.K. (2023). Biochar and fungi as bioretention amendments for bacteria and PAH removal from stormwater. Journal of Environmental Management 327, 116915.
- Moor, H., Hylander, K., & Norberg, J. (2015). Predicting climate change effects on wetland ecosystem services using species distribution modeling and plant functional traits. Ambio, 44, 113-126.
- Morbidelli, R., Saltalippi, C., Flammini, A., Cifrodelli, M., Picciafuoco, T., Corradini, C., & Govindaraju, R. S. (2016). Laboratory investigation on the role of slope on infiltration over grassy soils. Journal of Hydrology, 543, 542-547.
- Morse, N.R., McPhillips, L.E., Shapleigh, J.P. and Walter, M.T. (2017). The role of denitrification in stormwater detention basin treatment of nitrogen. Environmental Science & Technology 51(14), 7928-7935.
- Muthusamy, M., Tait, S., Schellart, A., Beg, M. N. A., Carvalho, R. F., & de Lima, J. L. (2018). Improving understanding of the underlying physical process of sediment wash-off from urban road surfaces. Journal of Hydrology, 557, 426-433.
- Niu, S., Chen, Y., Yu, J., Rao, Z., & Zhan, N. (2019). Characteristics of particle size distribution and related contaminants of highway-deposited sediment, Maanshan City, China. Environmental Geochemistry and Health, 41, 2697-2708.
- NRCS (2001) Soil quality test kit guide. Soil Quality Institute: Natural Resources Conservation Service. Retrieved from: https://www.nrcs.usda.gov/Internet/FSE_DOCUMENTS/nrcs142p2 050956.pdf.
- Payne, E.G., Fletcher, T.D., Cook, P.L., Deletic, A. and Hatt, B.E. (2014). Processes and drivers of nitrogen removal in stormwater biofiltration. Critical Reviews in Environmental Science and Technology 44(7), 796-846.
- Pratt, C., & Lottermoser, B. G. (2007). Mobilisation of traffic-derived trace metals from road corridors into coastal stream and estuarine sediments, Cairns, northern Australia. Environmental Geology, 52, 437-448.
- Pyšek, P., Chocholousková, Z., Pyšek, A., Jarošík, V., Chytrý, M., & Tichý, L. (2004). Trends in species diversity and composition of urban vegetation over three decades. Journal of Vegetation Science, 15(6), 781-788.
- Rauckyte, T., Żak, S., Pawlak, Z., & Oloyede, A. (2010). Determination of oil and grease, total petroleum hydrocarbons and volatile aromatic compounds in soil and sediment samples. Journal of Environmental Engineering and Landscape Management, 18(3), 163-169.

- Revitt, D. M., Shutes, R. B. E., Jones, R. H., Forshaw, M., & Winter, B. (2004). The performances of vegetative treatment systems for highway runoff during dry and wet conditions. Science of the Total Environment, 334, 261-270.
- Rolli, N. M., Gadi, S. B., & Giraddi, T. P. (2016). Bioindicators: Study on uptake and accumulation of heavy metals in plant leaves of state highway road, Bagalkot, India. Journal of Agriculture and Ecology Research International, 6(1), 1-8.
- Roy, M. C., Azeria, E. T., Locky, D., & Gibson, J. J. (2019). Plant functional traits as indicator of the ecological condition of wetlands in the grassland and parkland of Alberta, Canada. Ecological Indicators, 98, 483-491.
- Schueler, T.R., P.A. Kumble, and M.A. Heraty (1992). A current assessment of urban best management practices: techniques for reducing nonpoint source pollution in the coastal zone. Metropolitan Washington Council of Governments, Washington, D.C.
- Sese, B. T., Grant, A., & Reid, B. J. (2009). Toxicity of polycyclic aromatic hydrocarbons to the nematode *Caenorhabditis elegans*. Journal of Toxicology and Environmental Health, Part A, 72(19), 1168-1180.
- Shaver, E., Horner, R.R., Skupien, J., May, C. and Ridley, G. (2007). Fundamentals of urban runoff management: Technical and institutional issues, North American Lake Management Society.
- Shimadzu Scientific Instruments (2014) Shimadzu total organic carbon analyzer TOC-LCPH/CPN: User's manual. Columbia, MD: Shimadzu Corporation.
- Søberg, L.C., Viklander, M., Blecken, G.-T. and Hedström, A. (2019). Reduction of Escherichia coli, Enterococcus faecalis and Pseudomonas aeruginosa in stormwater bioretention: effect of drying, temperature and submerged zone. Journal of Hydrology X 3, 100025.
- Shrestha, P., Hurley, S. E., & Wemple, B. C. (2018). Effects of different soil media, vegetation, and hydrologic treatments on nutrient and sediment removal in roadside bioretention systems. Ecological Engineering, 112, 116-131.
- Søberg, L. C., Viklander, M., & Blecken, G. T. (2017). Do salt and low temperature impair metal treatment in stormwater bioretention cells with or without a submerged zone? Science of the Total Environment, 579, 1588-1599.
- Stagge, J. H., Davis, A. P., Jamil, E., & Kim, H. (2012). Performance of grass swales for improving water quality from highway runoff. Water Research, 46(20), 6731-6742.
- Stephenson, J. B., & Beck, B. F. (1995). Management of the discharge quality of highway runoff in karst areas to control impacts to ground water-A review of relevant literature. Karst Geohazards, 297-321.

Stevenson, A. and Hallsworth, J.E. (2014). Water and temperature relations of soil A ctinobacteria. Environmental Microbiology Reports 6(6), 744-755.

Suding, K. N., & Hobbs, R. J. (2009). Threshold models in restoration and conservation: a developing framework. Trends in Ecology & Evolution, 24(5), 271–279. https://doi.org/10.1016/j.tree.2008.11.012.

Thorpe, A., & Harrison, R. M. (2008). Sources and properties of non-exhaust particulate matter from road traffic: a review. Science of the Total Environment, 400(1-3), 270-282.

TWDB (2011). Texas Water Development Board - 2011 South Central Texas Regional Water Plan. South Central Texas Regional Water Planning Group.

Ukalska-Jaruga, A., Smreczak, B., & Klimkowicz-Pawlas, A. (2019). Soil organic matter composition as a factor affecting the accumulation of polycyclic aromatic hydrocarbons. Journal of Soils and Sediments, 19, 1890-1900.

Upton, R.N., Checinska Sielaff, A., Hofmockel, K.S., Xu, X., Polley, H.W. and Wilsey, B.J. (2020). Soil depth and grassland origin cooperatively shape microbial community co-occurrence and function. Ecosphere 11(1), e02973.

U.S. Census Bureau (2018). U.S. and World Population Clock. https://www.census.gov/popclock/.

USDA, NRCS. 2022. The PLANTS Database (http://plants.usda.gov). National Plant Data Team, Greensboro, NC USA.

Vakhlamova, T., Rusterholz, H. P., Kanibolotskaya, Y., & Baur, B. (2016). Effects of road type and urbanization on the diversity and abundance of alien species in roadside verges in Western Siberia. Plant Ecology, 217, 241-252.

Valenca, R., Le, H., Zu, Y., Dittrich, T., Tsang, D.C.W., Dutta, R., Sarkar, D. and Mohanty, S.K. (2020). Nitrate removal uncertainty in stormwater control measures: Is the design or climate a culprit? Water Research, 116781.

Vasconcelos, P. B., Araújo, G. M., & Bruna, E. M. (2014). The role of roadsides in conserving Cerrado plant diversity. Biodiversity and Conservation, 23, 3035-3050.

Vitousek, P. M. (1994). Beyond global warming: ecology and global change. Ecology, 75(7), 1861-1876.

Waller, L.J., Evanylo, G.K., Krometis, L.-A.H., Strickland, M.S., Wynn-Thompson, T. and Badgley, B.D. (2018). Engineered and environmental controls of microbial denitrification in established bioretention cells. Environmental Science & Technology 52(9), 5358-5366.

Walsh, C. J. (2000). Urban impacts on the ecology of receiving waters: a framework for assessment, conservation and restoration. Hydrobiologia, 431(2-3), 107-114.

- Wang X., Wang J., Zhang J. (2012). Comparisons of three methods for organic and inorganic carbon in calcareous soils of Northwestern China. PLoS ONE, 7(8), E44334.
- Wang, Y., Osman, J.R. and DuBow, M.S. (2020). Bacterial communities on the surface of the mineral sandy soil from the Desert of Maine (USA). Current Microbiology 77(8), 1429-1437.
- Weil, R.R., & Brady, N.C. (2019). Elements of the Nature and Properties of Soils.4th edition. NY, NY, Pearson.
- Weiss, J. D., Hondzo, M., & Semmens, M. (2006). Storm water detention ponds: Modeling heavy metal removal by plant species and sediments. Journal of Environmental Engineering, 132(9), 1034-1042.
- Williams, C.B. (1964). Patterns in the Balance of Nature. Academic Press, London, U.K.
- Winiarski, T., Bedell, J. P., Delolme, C., & Perrodin, Y. (2006). The impact of stormwater on a soil profile in an infiltration basin. Hydrogeology Journal, 14, 1244-1251.
- Winston, R. J., & Hunt, W. F. (2017). Characterizing runoff from roads: Particle size distributions, nutrients, and gross solids. Journal of Environmental Engineering, 143(1), 04016074.
- Wijesiri, B., Liu, A., & Goonetilleke, A. (2020). Impact of global warming on urban stormwater quality: From the perspective of an alternative water resource. Journal of Cleaner Production, 262, 121330. https://doi.org/10.1016/j.jclepro.2020.121330.
- Wissler, A. D., Hunt, W. F., & McLaughlin, R. A. (2020). Water Quality and Hydrologic Performance of Two Dry Detention Basins Receiving Highway Stormwater Runoff in the Piedmont Region of North Carolina. Journal of Sustainable Water in the Built Environment, 6(2), 05020002.
- Xian, G., Homer, C., Demitz, J., Fry, J., Hossain, N., & Wickham, J. (2011). Change of impervious surface area between 2001 and 2006 in the conterminous United States. Photogrammetric Engineering and Remote Sensing, 77(8), 758-762.
- Yang, Y.-Y., Asal, S. and Toor, G.S. (2021). Residential catchments to coastal waters: Forms, fluxes, and mechanisms of phosphorus transport. Science of the Total Environment 765, 142767.
- Yi, H., Güneralp, B., Filippi, A. M., Kreuter, U. P., & Güneralp, İ. (2017). Impacts of land change on ecosystem services in the San Antonio River Basin, Texas, from 1984 to 2010. Ecological Economics, 135, 125-135.
- Young, S. L., & Claassen, V. P. (2008). Release of roadside native perennial grasses following removal of yellow starthistle. Ecological Restoration, 26(4), 357-364.
- Yousef, Y. A., Hvitved-Jacobsen, T., Wanielista, M. P., & Harper, H. H. (1987). Removal of contaminants in highway runoff flowing through swales. Science of the Total Environment, 59, 391-399.

- Yu, S. L., Kuo, J. T., Fassman, E. A., & Pan, H. (2001). Field test of grassed-swale performance in removing runoff pollution. Journal of Water Resources Planning and Management, 127(3), 168-171.
- Yuan, D., An, Y., Wang, J., Chu, S., Lim, B., Chen, B., ... & Li, J. (2019). Dissolved organic matter characteristics of urban stormwater runoff from different functional regions during grassy swale treatment. Ecological Indicators, 107, 105667.
- Zanders, J. M. (2005). Road sediment: characterization and implications for the performance of vegetated strips for treating road run-off. Science of the Total Environment, 339(1-3), 41-47.
- Zarezadeh, V., Lung, T., Dorman, T., Shipley, H.J. and Giacomoni, M. (2018). Assessing the performance of sand filter basins in treating urban stormwater runoff. Environmental Monitoring and Assessment 190(12), 1-15.
- Zeng, F., Ali, S., Zhang, H., Ouyang, Y., Qiu, B., Wu, F., & Zhang, G. (2011). The influence of pH and organic matter content in paddy soil on heavy metal availability and their uptake by rice plants. Environmental Pollution, 159(1), 84-91.
- Zeng, Q., Dong, Y. and An, S. (2016). Bacterial community responses to soils along a latitudinal and vegetation gradient on the Loess Plateau, China. PLoS One 11(4), e0152894.
- Zhang, K., Manuelpillai, D., Raut, B., Deletic, A., & Bach, P. M. (2019). Evaluating the reliability of stormwater treatment systems under various future climate conditions. Journal of Hydrology, 568, 57-66.
- Zhang, K., Delgado-Baquerizo, M., Zhu, Y.-G. and Chu, H. (2020). Space is more important than season when shaping soil microbial communities at a large spatial scale. Msystems 5(3), e00783-00719.
- Zhao, H., Cui, B., & Zhang, K. (2010). The distribution of heavy metal in surface soils and their uptake by plants along roadside slopes in longitudinal range gorge region, China. Environmental Earth Sciences, 61, 1013-1023.
- Zhao, H., Li, X., Wang, X., & Tian, D. (2010). Grain size distribution of road-deposited sediment and its contribution to heavy metal pollution in urban runoff in Beijing, China. Journal of Hazardous Materials, 183(1-3), 203-210.

Table 1. Total species richness for plant status by LID type and time period.

LID	Time	Total Species Richness					
Type	Period ¹	Native	Non-Native				
C 1	SUM-20	44	13				
Sand Filtration	WIN-20	17	11				
Systems	SUM-21	35	14				
Systems	WIN-21	19	14				
	SUM-20	49	13				
Swales	WIN-20	40	25				
Swales	SUM-21	44	14				
	WIN-21	18	8				

 $[\]overline{^{1}}$ - SUM = summer, WIN = winter; 20 = 2021, 21 = 2021

Table 2. Total coverage (%) for plant status by LID type and time period.

LID	Time -	Total Coverage (%)					
Type	Period ¹	Native	Non-Native				
C 1	SUM-20	323	1187				
Sand Filtration	WIN-20	230	886 756				
Systems	SUM-21	215					
Systems	WIN-21	166	175				
	SUM-20	486	1326				
Swales	WIN-20	712	1323				
Swales	SUM-21	388	776				
	WIN-21	201	480				

 $[\]frac{1}{1}$ - SUM = summer, WIN = winter; 20 = 2021, 21 = 2021

Table 3. Total species richness for plant group type by LID type and time period.

		Total Species Richness							
		Na	tive	Non-	-native				
LID Type	Time Period ¹	Dicot	Monocot	Dicot	Monocot				
	SUM-20	38	6	7	6				
Sand Filtration	SUM-20	37	12	6	7				
Systems	WIN-20	16	1	5	6				
	WIN-20	31	9	15	10				
	SUM-21	31	4	7	7				
Swales	SUM-21	33	11	7	7				
Swales	WIN-21	16	3	7	7				
	WIN-21	13	5	5	3				

 $[\]overline{^{1}}$ - SUM = summer, WIN = winter; 20 = 2021, 21 = 2021

Table 4. Total percent (%) coverage for plant group type by LID type and time period.

			Total Coverage (%)							
		Na	ative	Non-	native					
LID Type	Time Period ¹			Dicot	Monocot					
	SUM-20	289	34	97	1090					
Sand Filtration	SUM-20	323	163	70	1256					
Systems	WIN-20	229	1	225	660					
	WIN-20	309	403	329	994					
	SUM-21	194	21	163	593					
Swales	SUM-21	265	123	87	689					
Swales	WIN-21	157	8	99	76					
	WIN-21	51	150	120	360					

 $[\]overline{}^{1}$ - SUM = summer, WIN = winter; 20 = 2021, 21 = 2021

Table 5. Total species richness for plant life cycle¹ by LID type and time period.

			Species Richness										
			Native						Non-native				
LID Type	Time Period ²	An/Bi/Pr	Ann/Bie	Ann/Per	Annual	Biennial	Perennial	An/Bi/Pr	Ann/Bie	Ann/Per	Annual	Biennial	Perennial
G 1	SUM-20	2	3	7	9	2	21	1	0	2	3	0	7
Sand	WIN-20	1	2	4	4	0	6	0	0	3	2	0	5
Filtration	SUM-21	4	2	9	5	0	15	1	1	1	4	0	7
Systems	WIN-21	1	2	0	7	0	9	1	2	0	2	1	6
	SUM-20	2	1	6	12	1	26	2	0	1	3	0	7
Swales	WIN-20	1	2	4	11	1	21	1	2	3	10	0	9
	SUM-21	2	1	3	17	1	18	1	1	2	2	0	8
	WIN-21	1	2	2	3	0	10	1	1	0	2	0	4

¹ - An/Ann (annual) = complete life cycle in one growing season; Pr (Perennial) = persist for many growing seasons; Bi (biennial) = require two growing seasons to complete life cycle; An/Bi/Pr, Ann/Bie, or Ann/Per = may require one or multipe years to complete life cycle depending on local climate conditions.

 $^{^{2}}$ - SUM = summer, WIN = winter; 20 = 2021, 21 = 2021

Table 6. Total percent (%) coverage for plant life cycle¹ by LID type and time period.

			Total Coverage (%)												
			Native							Non-Native					
LID Type	Time Period ²	An/Bi/Pr	Ann/Bie	Ann/Per	Annual	Biennial	Perennial	An/Bi/Pr	Ann/Bie	Ann/Per	Annual	Biennial	Perennial		
	SUM-20	1	9	24	100	3	186	2	0	4	40	0	1141		
Sand	WIN-20	3	45	61	40	0	82	0	0	175	9	0	701		
Filtration	SUM-21	33	26	41	32	0	82	37	6	26	18	0	694		
Systems	WIN-21	5	115	0	20	0	25	83	5	0	7	< 1	76		
	SUM-20	22	3	77	22	25	333	4	0	1	31	0	1290		
Swales	WIN-20	5	44	33	146	4	481	33	21	283	98	0	889		
	SUM-21	7	1	37	73	2	247	2	6	6	9	0	754		
	WIN-21	< 1	4	1	14	0	182	61	30	0	28	0	360		

¹ - An/Ann (annual) = complete life cycle in one growing season; Pr (Perennial) = persist for many growing seasons; Bi (biennial) = require two growing seasons to complete life cycle; An/Bi/Pr, Ann/Bie, or Ann/Per = may require one or multipe years to complete life cycle depending on local climate conditions

 $^{^{2}}$ - SUM = summer, WIN = winter; 20 = 2021, 21 = 2021

Table 7. Total species richness for plant growth form by LID type and time period.

			Total Species Richness										
	•		Native						Non-native				
LID Type	Time Period ¹	Forb/herb	Vine	Graminoid	Fern	Shrub	Tree	Forb/herb	Vine	Graminoid	Fern	Shrub	Tree
C 1	SUM-20	48	1	6	0	0	0	7	0	6	0	0	0
Sand Filtration	WIN-20	18	0	0	0	0	0	5	6	0	0	0	0
Systems	SUM-21	31	1	2	0	0	1	7	0	7	0	0	0
Systems	WIN-21	17	0	2	0	0	0	7	0	7	0	0	0
	SUM-20	33	2	11	0	1	1	6	0	7	0	0	0
C1	WIN-20	27	2	7	0	3	1	15	0	10	0	0	0
Swales	SUM-21	31	1	10	0	2	0	7	0	7	0	0	0
	WIN-21	10	0	4	0	1	2	5	0	3	0	0	0

 $[\]overline{}^{1}$ - SUM = summer, WIN = winter; 20 = 2021, 21 = 2021

Table 8. Total percent coverage for plant growth form by LID type and time period.

			Total Coverage (%)										
	_		Native						Non-Native				
LID Type	Time Period ¹	Forb/herb	Vine	Graminoid	Fern	Shrub	Tree	Forb/herb	Vine	Graminoid	Fern	Shrub	Tree
	SUM-20	280	10	34	0	0	0	97	0	1090	0	0	0
Sand Filtration	WIN-20	230	0	0	0	0	0	225	660	0	0	0	0
Systems	SUM-21	195	9	10	0	0	< 1	163	0	593	0	0	0
Systems	WIN-21	158	0	8	0	0	0	99	0	76	0	0	0
	SUM-20	309	< 1	163	0	6	8	70	0	1256	0	0	0
Swales	WIN-20	305	4	398	0	5	1	329	0	994	0	0	0
Swales	SUM-21	234	20	123	0	11	0	87	0	689	0	0	0
	WIN-21	42	0	150	0	5	4	120	0	360	0	0	0

 $^{^{1}}$ - SUM = summer, WIN = winter; 20 = 2021, 21 = 2021

Table 9. Total species richness for plant USDA Wetland Classification by LID type and time period (USDA, 2022).

		Total Species Richness										
			Native					Non-Native				
LID Type	Time Period ²	Obligate	FACW	FAC	FACU	Upland	Obligate	FACW	FAC	FACU	Upland	
	SUM-20	1	4	8	15	16	0	0	5	4	4	
Sand	WIN-20	0	0	3	6	8	0	0	3	6	2	
Filtration	SUM-21	3	1	3	17	11	0	0	6	6	2	
Systems	WIN-21	0	0	3	8	8	0	0	5	5	4	
	SUM-20	2	4	7	19	17	0	0	4	4	5	
	WIN-20	2	0	12	22	33	0	1	6	9	9	
Swales	SUM-21	1	3	8	18	14	0	0	3	5	6	
	WIN-21	0	1	2	6	9	0	0	3	2	3	

¹ - Obligate = almost always occur in wetlands; FACW (facultative wetland) = usually occur in wetlands but may occur in non-wetlands; FAC (facultative) = occur equally in wetlands and non-wetlands; FACU (facultative upland) = usually occur in non-wetlands but may occur in wetlands; Upland = almost never occur in wetlands.

 $^{^{2}}$ - SUM = summer, WIN = winter; 20 = 2021, 21 = 2021

Table 10. Total percent (%) coverage for plant USDA Wetland Classification by LID type and time period (USDA, 2022).

	_		Total Coverage (%)										
	-			Native				Non-Native					
LID Type	Time Period ¹	Obligate	FACW	FAC	FACU	Upland	Obligate	FACW	FAC	FACU	Upland		
L and	SUM-20	5	30	40	40	209	0	0	774	261	152		
Sand Filtration	WIN-20	0	0	32	65	133	0	0	532	151	203		
Systems	SUM-21	2	2	23	97	85	0	0	434	216	105		
Systems	WIN-21	0	0	14	96	56	0	0	28	138	10		
	SUM-20	2	8	38	167	272	0	0	280	436	609		
Cyvolog	WIN-20	1	0	273	486	454	0	1	286	459	577		
Swales	SUM-21	1	13	79	171	125	0	0	142	75	559		
	WIN-21	0	1	5	129	67	0	0	107	64	309		

¹ - Obligate = almost always occur in wetlands; FACW (facultative wetland) = usually occur in wetlands but may occur in non-wetlands; FAC (facultative) = occur equally in wetlands and non-wetlands; FACU (facultative upland) = usually occur in non-wetlands, but may occur in wetlands; Upland = almost never occur in wetlands.

 $^{^{2}}$ - SUM = summer, WIN = winter; 20 = 2021, 21 = 2021

Table 11. List of Polycyclic Aromatic Hydrocarbons in this study.

1. Naphthalene	2. Benz[a]anthracene
3. Acenaphthylene	4. Chrysene
5. Acenaphthene	6. Benzo[a]pyrene
7. Fluorene	8. Benzo[b]fluoranthene
9. Anthracene	10. Benzo[k]fluoranthene
11. Phenanthrene	12. Benzo[g, h, i]perylene
13. Fluoranthene	14. Dibenzo[a, j]pyrene
15. Pyrene	16. Indeno[1,2,3-cd]pyrene

Table 12. Storm events monitored in Bulverde basin.

Storm no.	Date/Time		Precipit	tation			Peak flow (l/s)	
	Beginning	End	Depth (mm)	Duration	Max. intensity (mm/h)	Antecedent dry days	Inlet	Outlet
1	3/4/20, 6:05	3/4/20, 6:55	11.43	50 mins	11.43	13 Days and 5 Hours	122 7.1	12.5
2	3/19/20, 3:40	3/19/2 0, 4:00	0.76	20 mins	0.76	1 Day and 9 Hours	188. 3	8.4
3	5/15/20, 22:40	5/16/2 0, 2:05	28.19	3hr 25 mins	18.80	1 Day and 17 Hours	256 2.2	11.7
4	5/24/20, 20:35	5/25/2 0, 1:00	48.77	4 hr 25 mins	36.22	8 Days and 18 Hours	321 7.3	11.3
5	6/23/20, 8:15	6/23/2 0, 9:05	5.33	50 mins	5.33	6 Days and 14 Hours	873. 5	10.4
6	7/26/20, 5:55	7/26/2 0, 6:55	2.79	1 hr	2.79	29 Days and 16 Hours	559. 4	3.0
7	9/3/20, 17:30	9/3/20, 19:55	21.08	2hr 25 mins	11.43	4 Days	224 4.6	1.6
8	9/8/20, 17:15	9/8/20, 17:40	4.06	25 mins	4.06	1 Day and 8 Hour	593. 1	1.4
9	9/21/20, 10:45	9/21/2 0, 11:55	3.81	1hr 10 mins	3.3	3 Days and 19 Hours	510. 6	8.4
10	11/27/20, 11:50	11/27/ 20, 13:20	1.78	1hr 30 mins	1.52	2 Days and 16 Hours	419. 5	6.7

Table 13. Storm events monitored in the TPC basin.

Storm no.	Date/Time		Precipit	ation			Peak flow (1/s)	
	Beginning	End	Depth (mm)	Duration	Max. intensity (mm/h)	Antecedent dry days	Inlet	Outlet
1	2/11/21, 10:05	2/11/21 , 15:35	22.6	5hr 30 mins	8.3	17 Days and 17 Hours	192 5	11.5
2	3/23/21, 1:25	3/23/21 , 2:10	5.3	45 mins	5.3	8 Days and 16 Hours	622	6.1
3	4/23/21, 8:40	4/23/21 , 14:00	12.2	6hr 20 mins	5.1	6 Days and 20 Hours	167 0	6.9
4	5/11/21, 19:00	5/11/21 , 20:25	12.7	1hr 25 mins	11.2	10 Days and 2 Hours	118 9	6.2
5	6/1/21, 0:15	6/1/21, 4:55	6.6	4hrs and 40 mins	3.8	2 Days and 15 Hours	340	2.1
6	6/27/21, 13:40	6/27/21 , 15:35	5.1	1hr and 55 mins	4.0	21 Days and 22 Hours	622	5.2
7	7/9/21, 3:10	7/9/21, 16:40	32.0	13hrs and 30 mins	12.7	1 Day and 12 Hours	198 2	12.7
8	8/5/21, 9:20	8/5/21, 10:30	5.6	1hr and 10 mins	5.6	2 Days and 20 Hours	538	4.9
9	9/13/21, 12:15	9/13/21 , 13:10	2.5	55 mins	2.5	6 Days and 14 Hours	424	3.4
10	9/28/21, 22:00	9/28/21 , 23:55	25.1	1 hr and 55 mins	22.8	15 Days and 8 Hours	962	7.2
11	10/27/21, 5:05	10/27/2 1, 6:20	22.3	1 hr and 15 mins	21.6	11 Days and 12 Hours	201	7.9
12	11/3/21, 11:05	11/3/21 , 12:20	10.4	1 hr and 15 mins	9.1	8 Days and 2 Hours	116 0	5.1

Table 14. Storm events monitored in Kyle basin.

Storm no.	Date/Time		Precipita	ation			Peak flow (1/s)	
	Beginning	End	Depth (mm)	Duration	Max. intensity (mm/h)	Antecedent dry days	Inlet	Outlet
1	2/11/21, 9:40	2/11/21 , 14:20	15.2	4hr 40 mins	7.1	6 Days and 19 Hours	707	19.8
2	4/23/21, 11:30	4/23/21 , 12:25	5.1	55 mins	5.1	6 Days and 20 Hours	467	2.8
3	5/11/21, 17:30	5/11/21 , 19:05	8.1	1hr 35 mins	8.1	9 Days and 21 Hours	670	11.3
4	6/1/21, 0:05	6/1/21, 1:25	4.6	1hr and 20 mins	4.6	1 Days and 8 Hours	113	2.4
5	6/27/21, 9:05	6/27/21 , 10:20	3.8	1hr and 15 mins	3.8	11 Days and 14 Hours	120	4.1
6	9/28/21, 20:20	9/28/21 , 23:05	35.8	2hrs and 45 mins	19.3	22 Days	254 8	25.4
7	10/13/21, 20:10	10/14/2 1, 1:55	50.8	5hrs and 45 mins	20.8	2 Day and 15 Hours	362 4	28.4
8	10/27/21, 4:10	10/27/2 1, 5:35	14.5	1hr and 15 mins	14.0	12 Days and 23 Hours	226 5	22.6
9	11/3/21, 18:25	11/3/21 , 19:45	7.9	1hr and 20 mins	7.9	7 Days and 4 Hours	566	14.1
10	11/25/21, 4:50	11/25/2 1, 6:45	5.6	1 hr and 55 mins	3.5	21 Days and 12 Hours	424	12.7

Table 15. Storm events monitored in swales.

Kyle Seale	Dates	Plaza	Dates	Roadrunner way	Dates
Event 1	1/17/2020	Event 1	9/29/2021	Event 1	9/4/2022
Event 2	3/3/2020	Event 2	10/14/2021	Event 2	10/18/2022
Event 3	5/21/2020	Event 3	11/4/2021	Event 3	10/31/2022
Event 4	6/22/2020	Event 4	11/29/2021	Event 4	11/19/2022
Event 5	7/24/2020	Event 5	12/20/2021	Event 5	11/22/2022
Event 6	9/3/2020	Event 6	2/8/2022	Event 6	12/19/2022
Event 7	9/8/2020	Event 7	4/11/2022	Event 7	1/24/2023
Event 8	11/26/2020	Event 8	5/25/2022	Event 8	3/17/2023
Event 9	4/28/2021	Event 9	8/15/2022	Event 9	3/22/2023
Event 10	5/21/2021	Event 10	8/25/2022	Event 10	4/6/2023

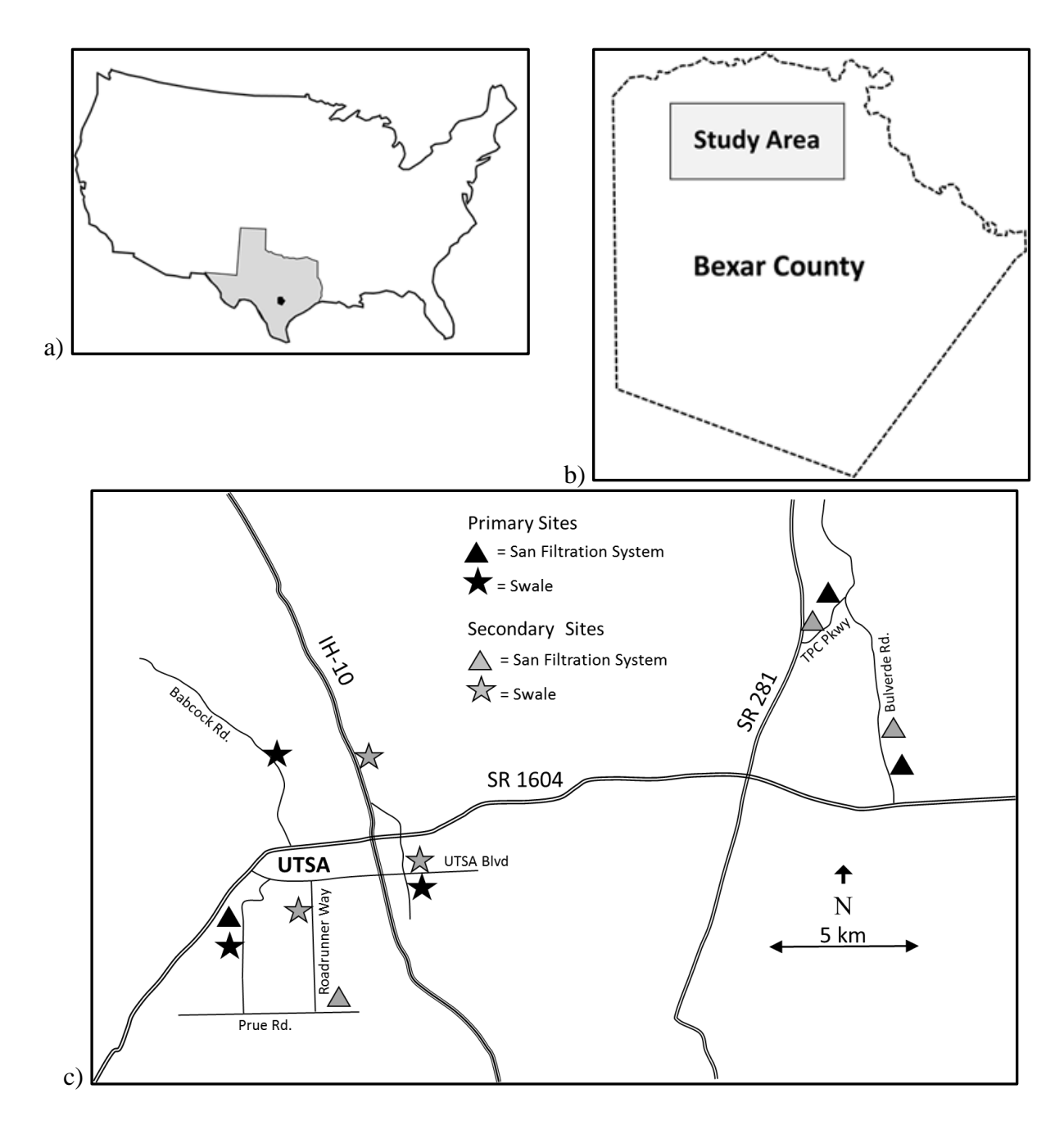


Figure 1. General location of study sites in a) the United States and Texas, b) Bexar County (gray rectangle), and c) primary and secondary sand filtration systems and swales in northern Bexar County.

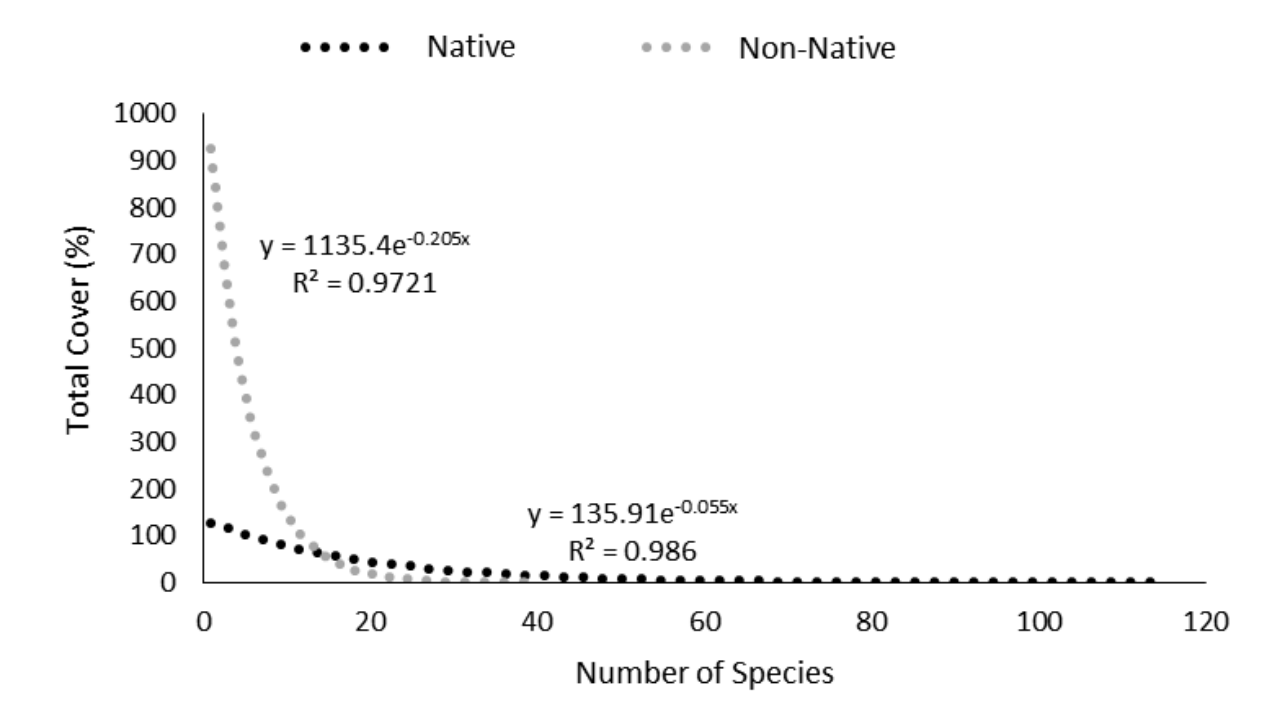


Figure 2. Non-linear regression analysis of the total percent coverage of each native and non-native species. Total plant coverage was combined for individual species in swales and sand filtration systems as one composite sample.

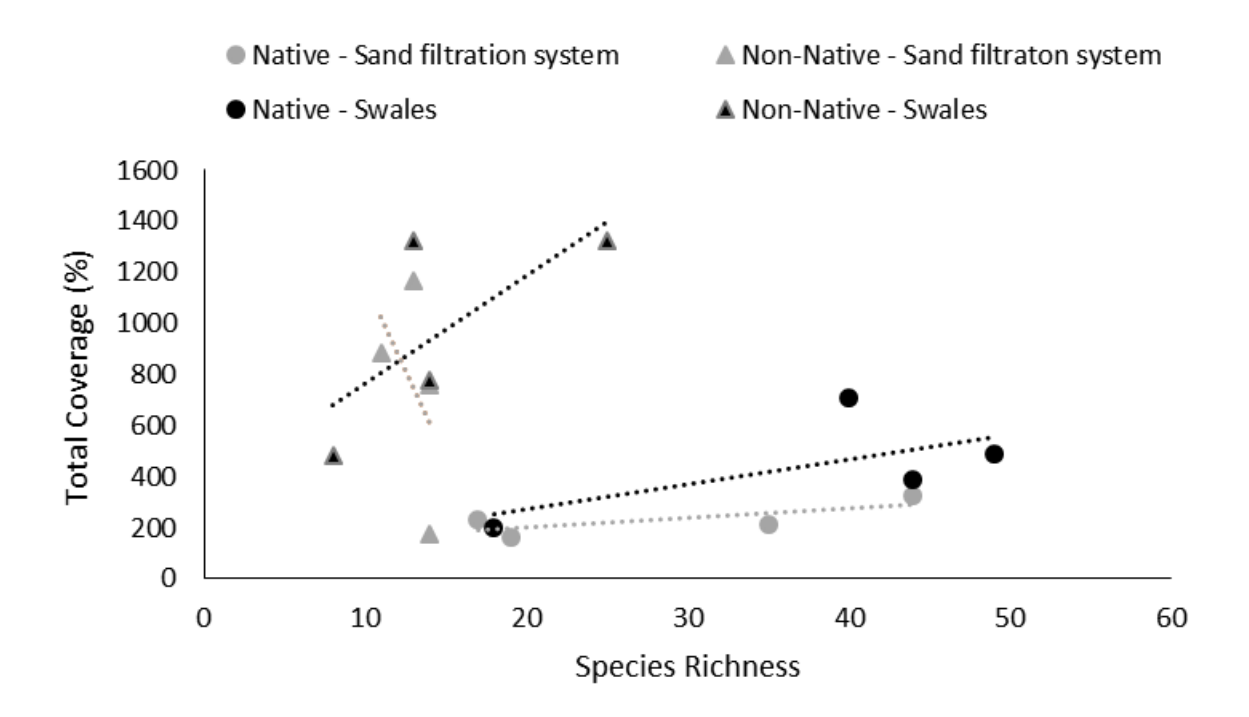
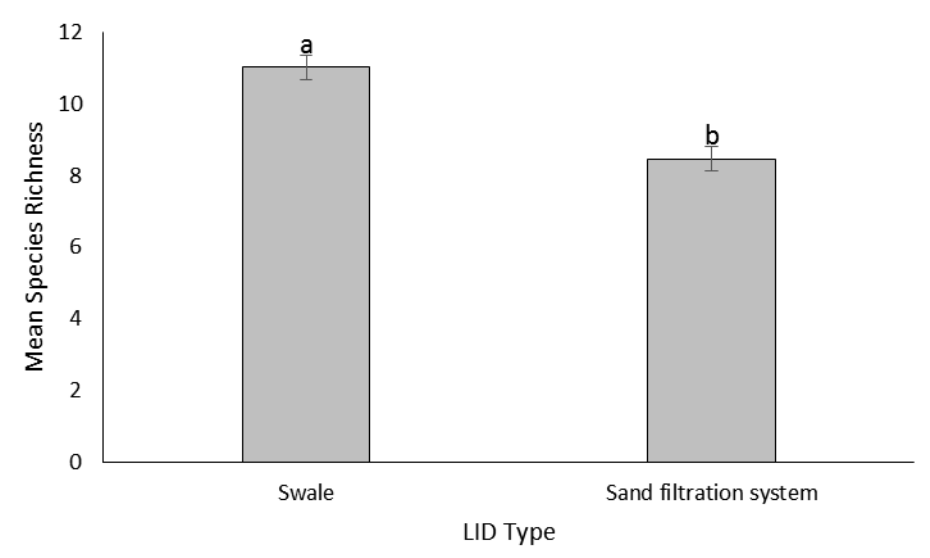
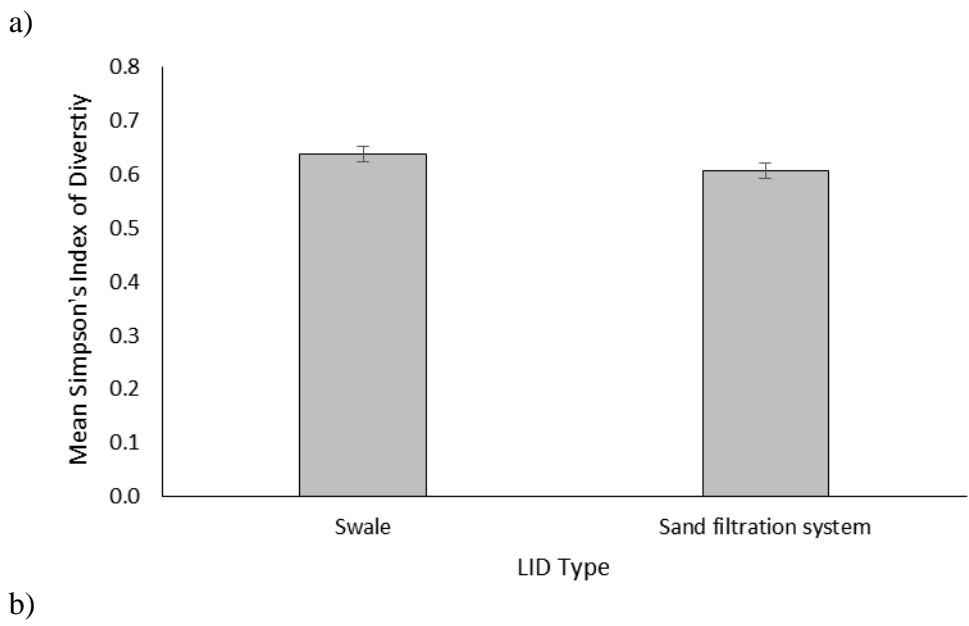
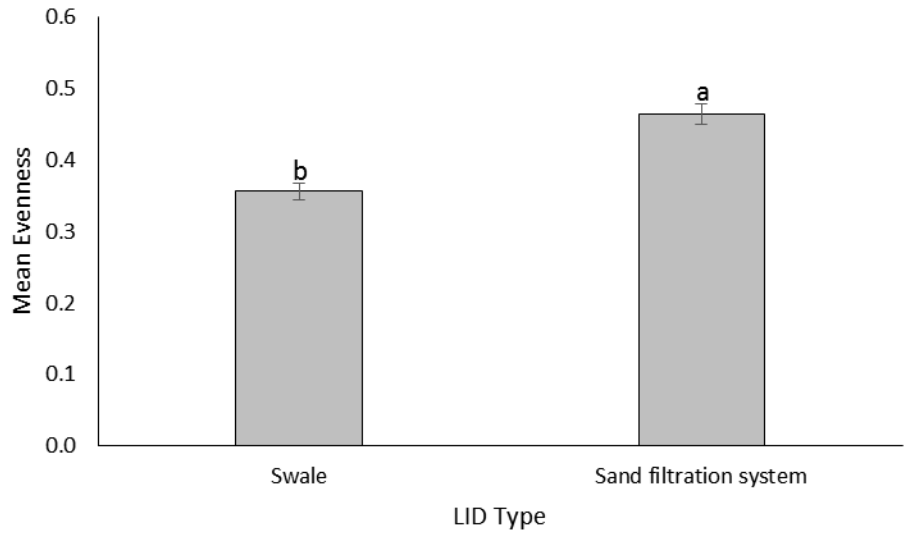


Figure 3. Regression analysis of native and non-native plant percent coverage and species richness. Native plants exhibited a moderate positive relationship in both sand filtration systems (y = 3.9 x + 121.9; $R^2 = 0.58$) and swales (y = 9.9 x + 74.5; $R^2 = 0.40$). Non-native plants exhibited moderate a positive relationship in swales (y = 41.8 x + 348.6; $R^2 = 0.51$) but a weak negative relationship in sand filtration systems (y = -139.9 x + 2565; $R^2 = 0.23$).







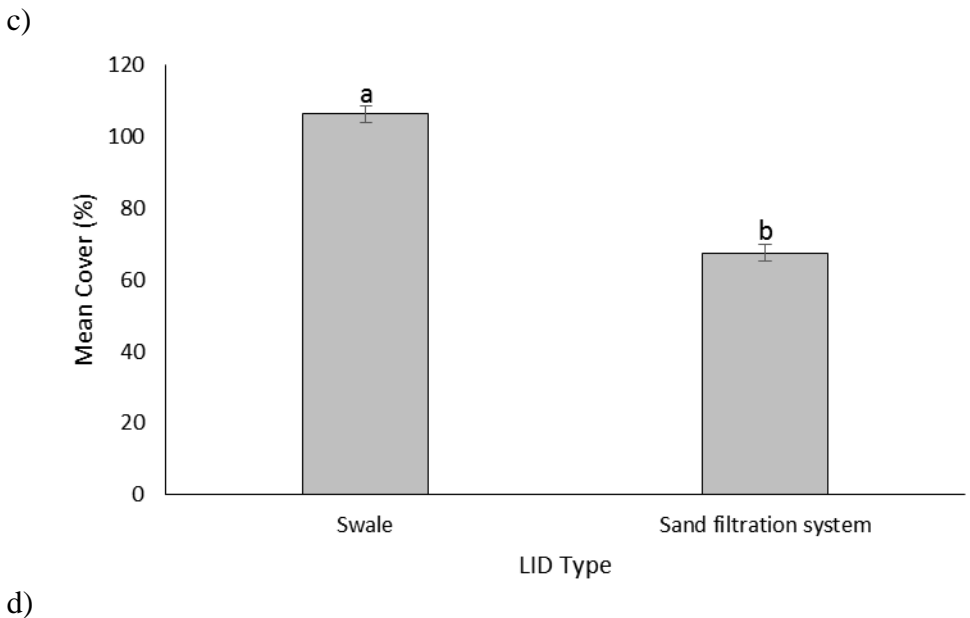
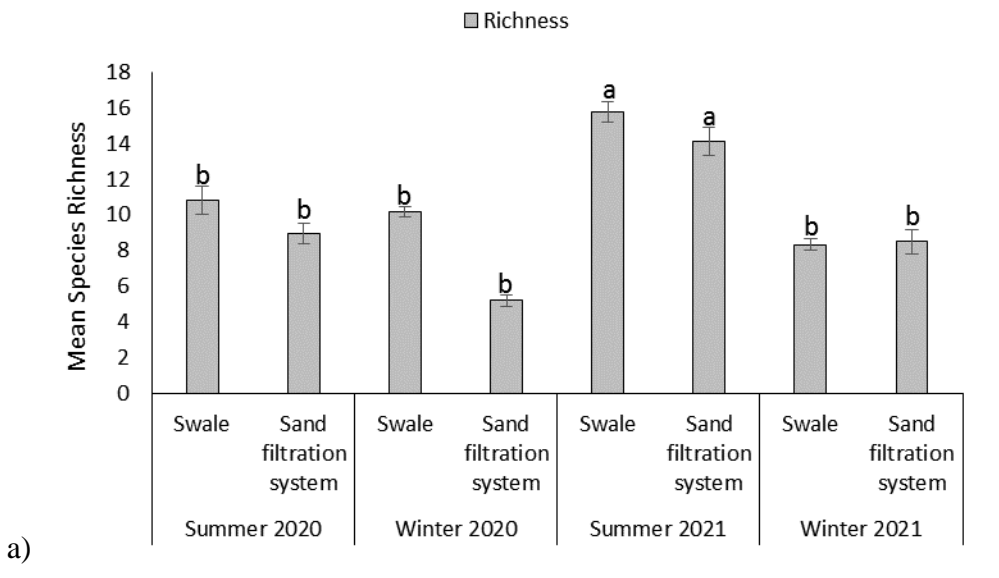


Figure 4. Comparison of a) mean species richness (t = 2.69, df = 111, P = 0.008), b) Simpsons' Index of Diversity (t = 0.779, df = 111, P = 0.438), c) evenness (t = -3.03, df = 111, P = 0.003), and d) percent cover (t = 5.58, df = 111, P < 0.001) for swales and sand filtration systems. Different letters indicate significant differences at P < 0.05). Values are calculated from line transects and bars represent standard error.



■ Diversity 1.0 Mean Simpson's Index of Diversity 8.0 ab ab ab ab b 0.6 ab b 0.4 0.2 0.0 Swale Sand Swale Sand Swale Sand Swale Sand filtration filtration filtration filtration system system system system

Winter 2020

Summer 2020

b)

Summer 2021

Winter 2021

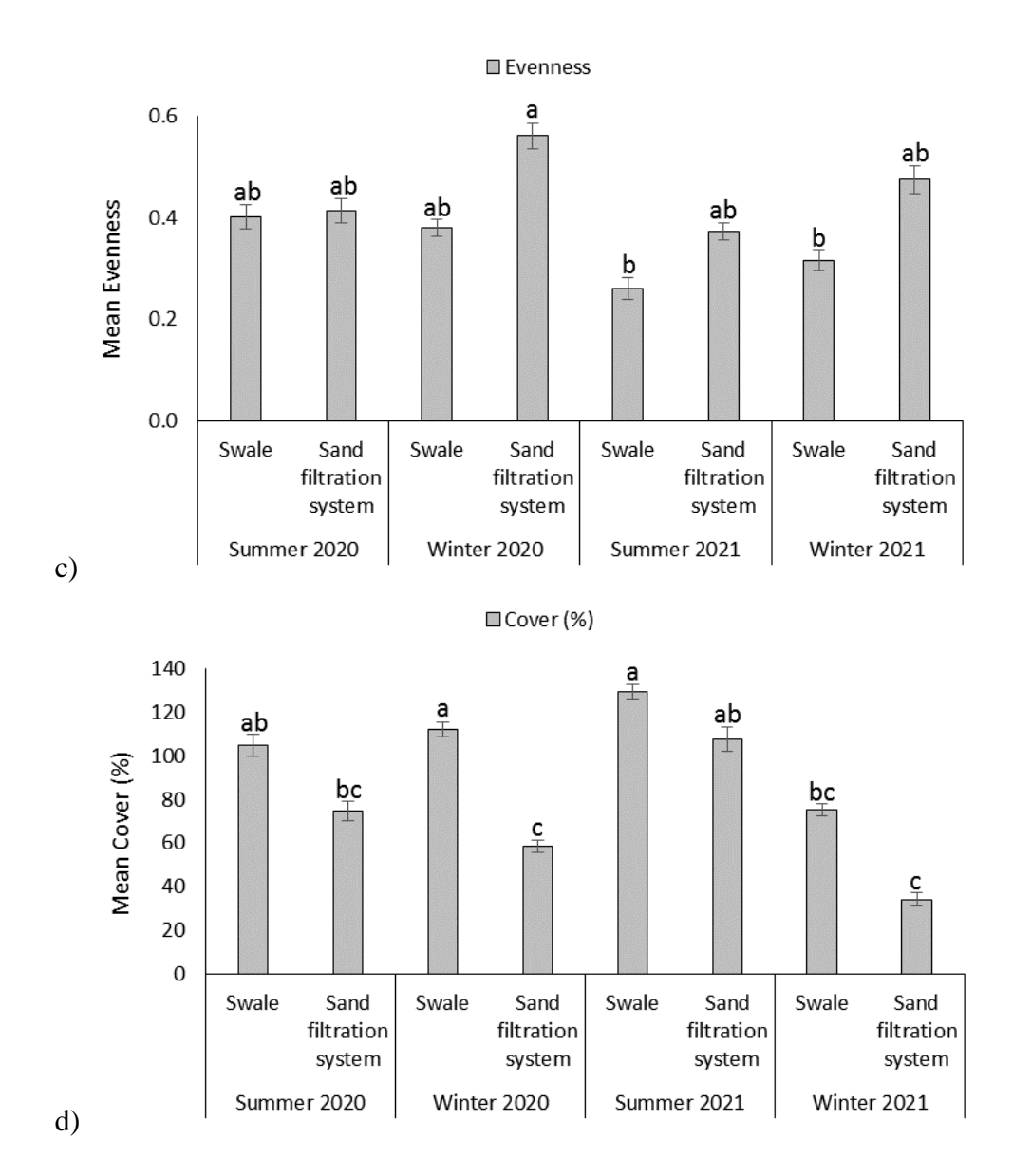


Figure 5. Diversity indices for a) Mean species richness (H = 37.72, df = 7, P < 0.001), b) Simpsons' Index of Diversity (F = 2.95, df = 7, P = 0.007), c) evenness (F = 3.30, df = 7, P = 0.003), and d) mean percent cover (F = 11.67, df = 7, P < 0.001) for swales and sand filtration systems by season and year. Different letters indicate significant differences at P < 0.05 based on Tukey's or Dunn's mean separation test. Values are calculated from line transects and bars represent standard error.

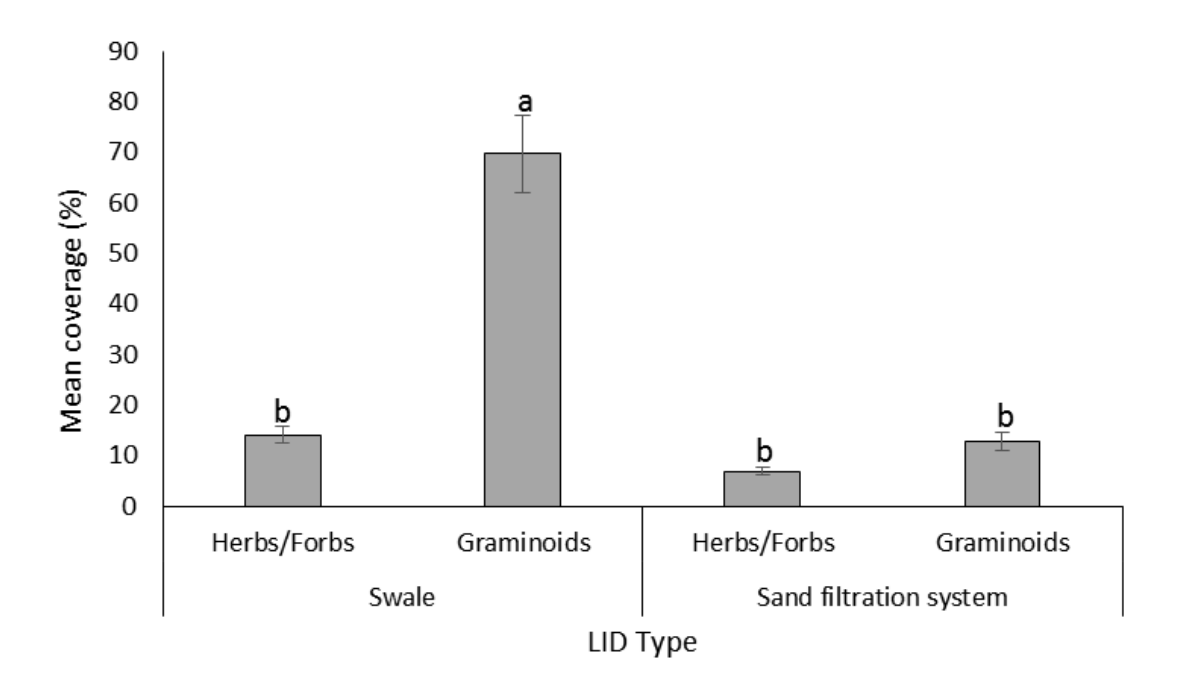


Figure 6. Mean coverage (%) for herbs/forbs and graminoids in swales and sand filtration systems with native and non-native species combined for year and season. Different letters indicate significant differences with an ANOVA (F = 6.71, df = 3, P < 0.001) and Tukey's mean separation test (P < 0.05). Lines indicate standard error.

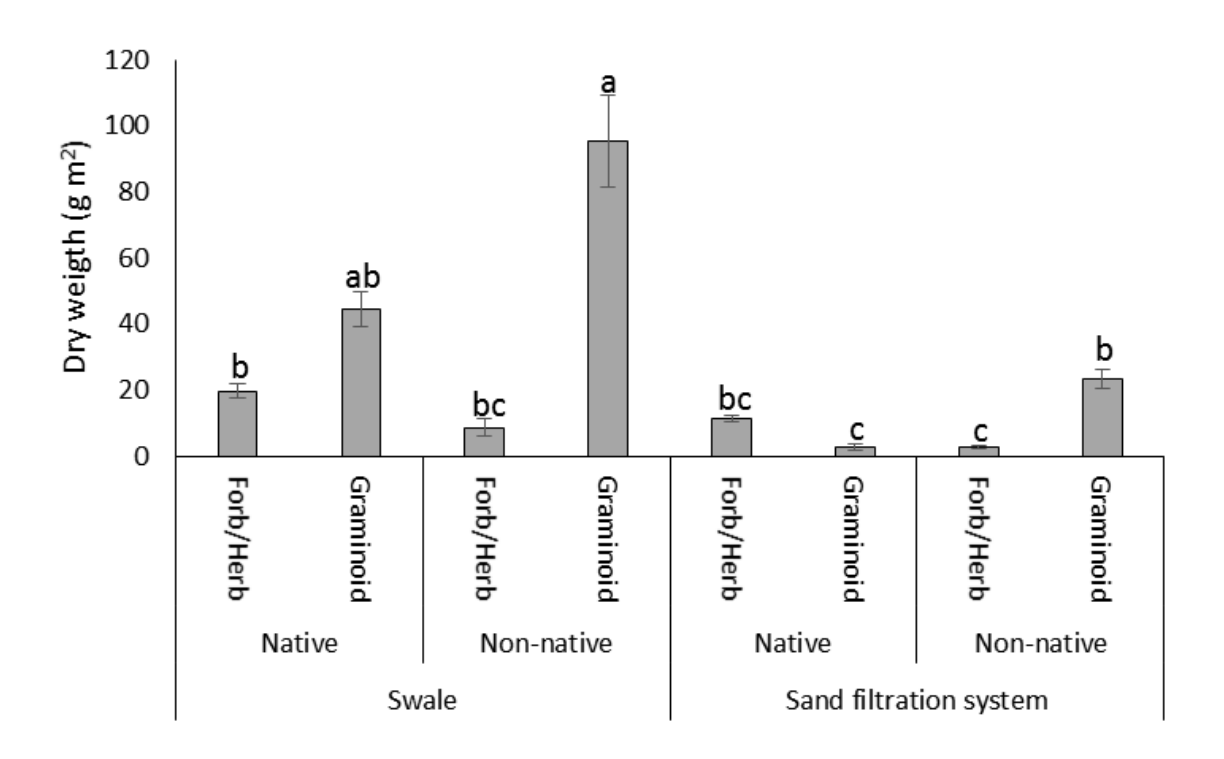


Figure 7. Dry weights (g m $^{2-1}$) of native and non-native forbs and graminoids in swales and sand filtration systems. Different letters indicate significant differences with an ANOVA (F = 9.651, df = 7, P < 0.001) and Tukey's mean separation test (P < 0.05). Lines indicate standard error.

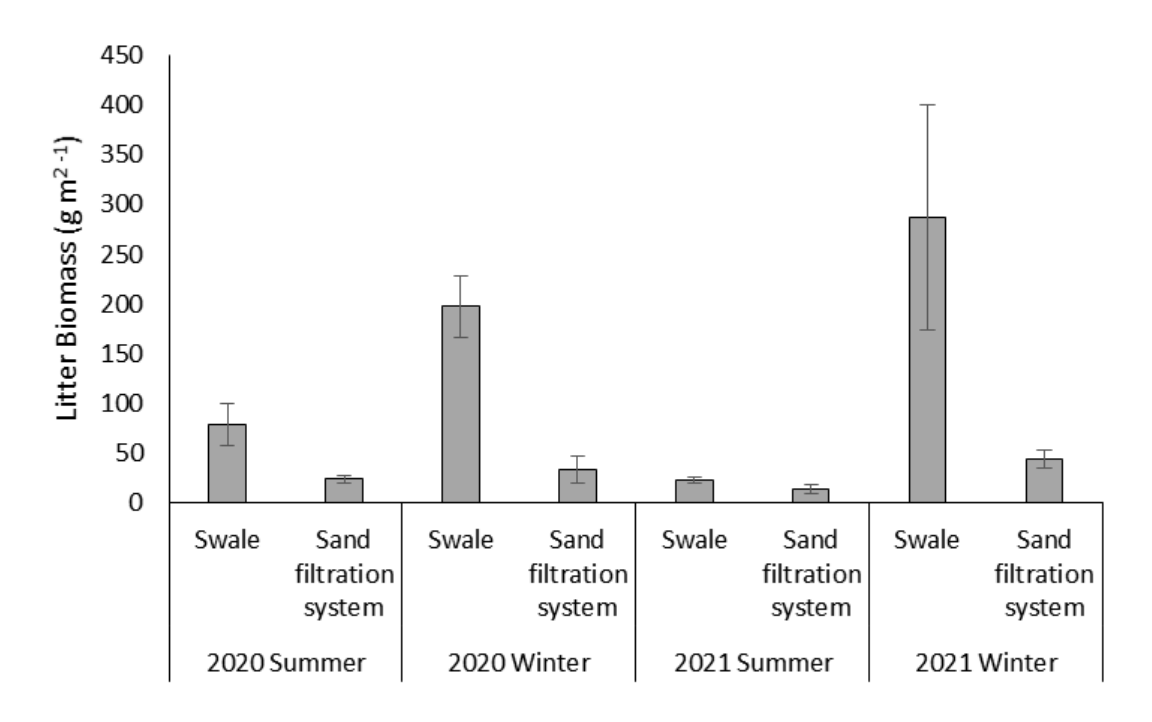


Figure 8. Dry weights (g m^{2-1}) of litter biomass (F = 1.596, df = 7, P = 0.215) in swales and sand filtration systems during the summers and winters of 2020 and 2021. Lines indicate standard error.

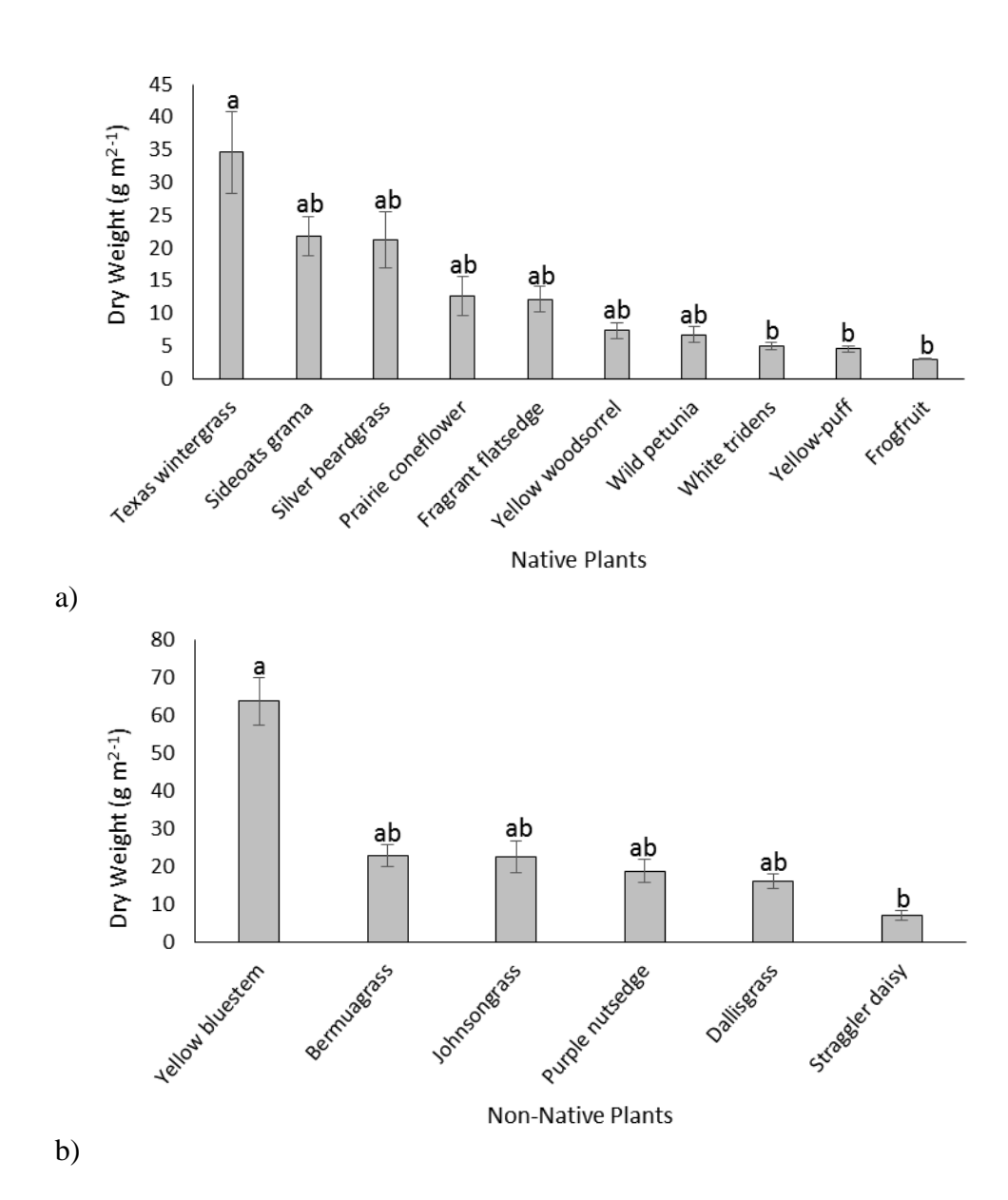
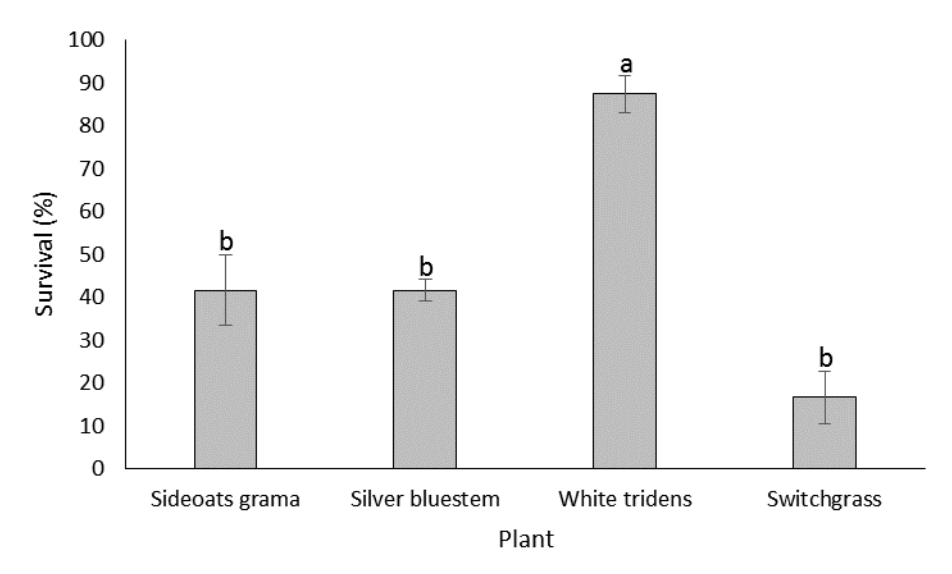
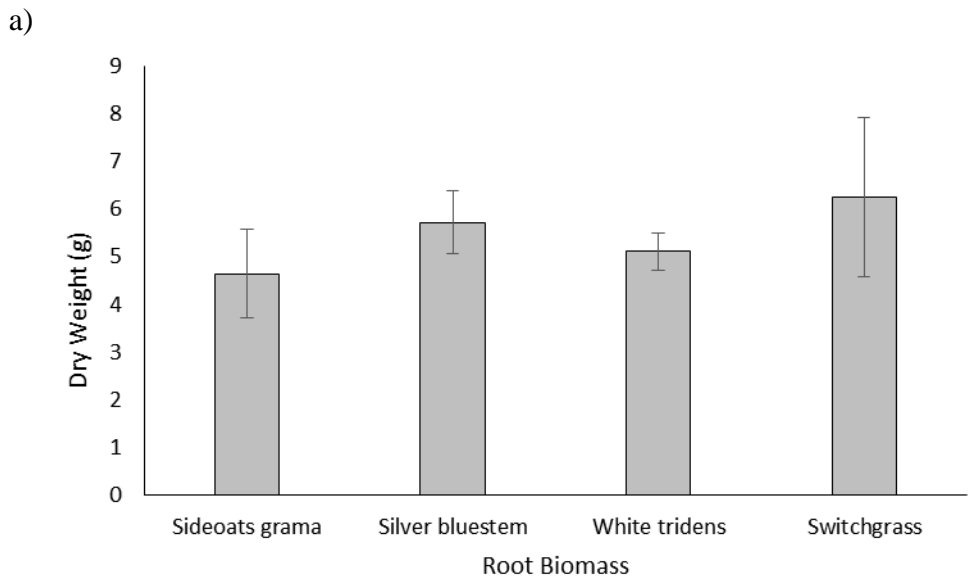


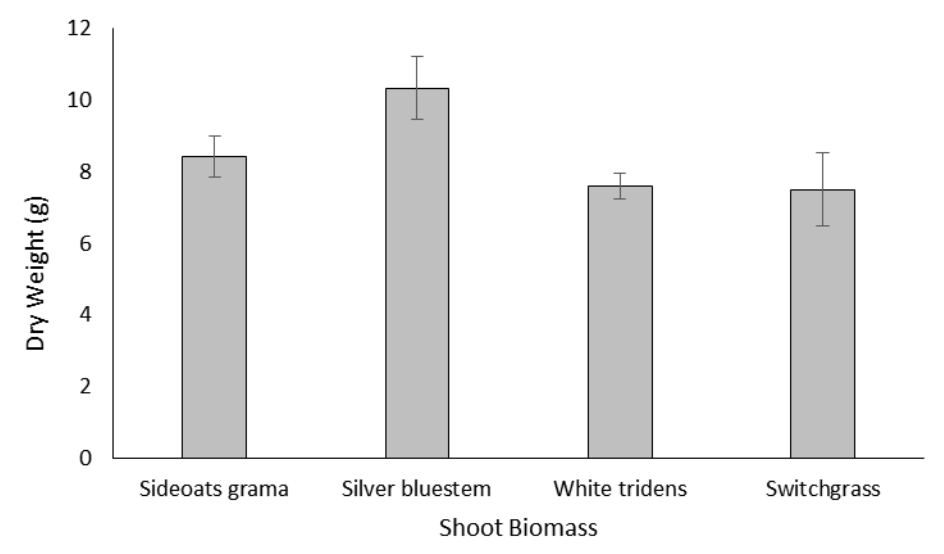
Figure 9. Mean dry weights (g m $^{2-1}$) of native and non-native species in swales and sand filtration systems with greater than 3 g m $^{2-1}$. Different letters indicate significant differences for native plants (F = 2.83, df = 9, P = 0.009) and non-native plants (H = 13.40, df = 5, P = 0.02), and Tukey's mean separation test (P < 0.05). Lines indicate standard error.

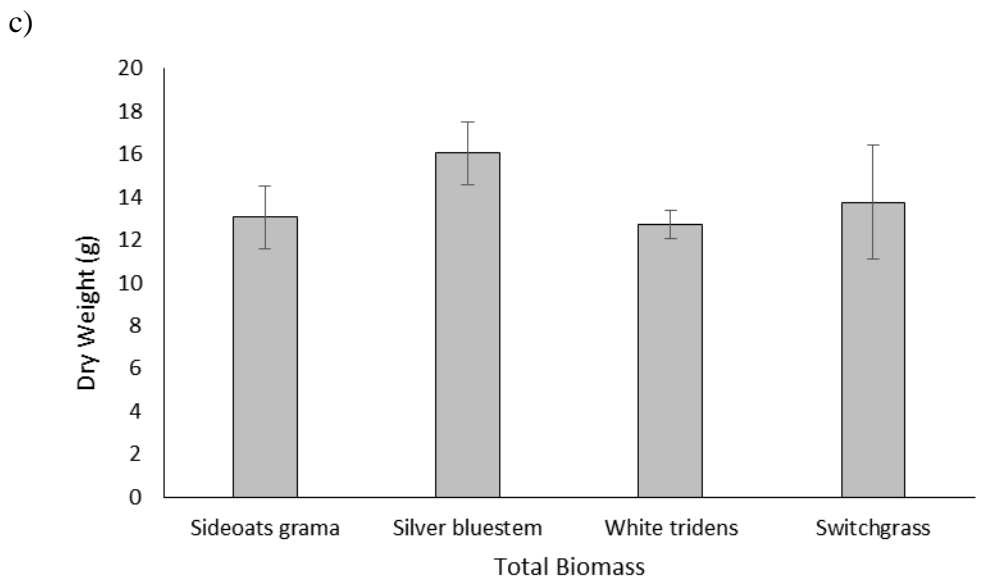




b)

93





d)

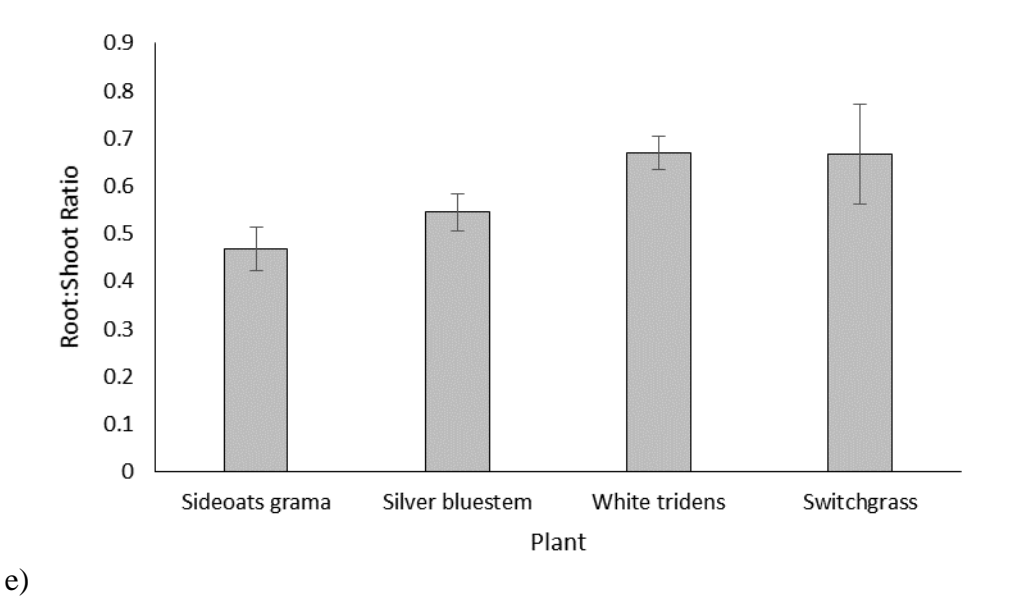
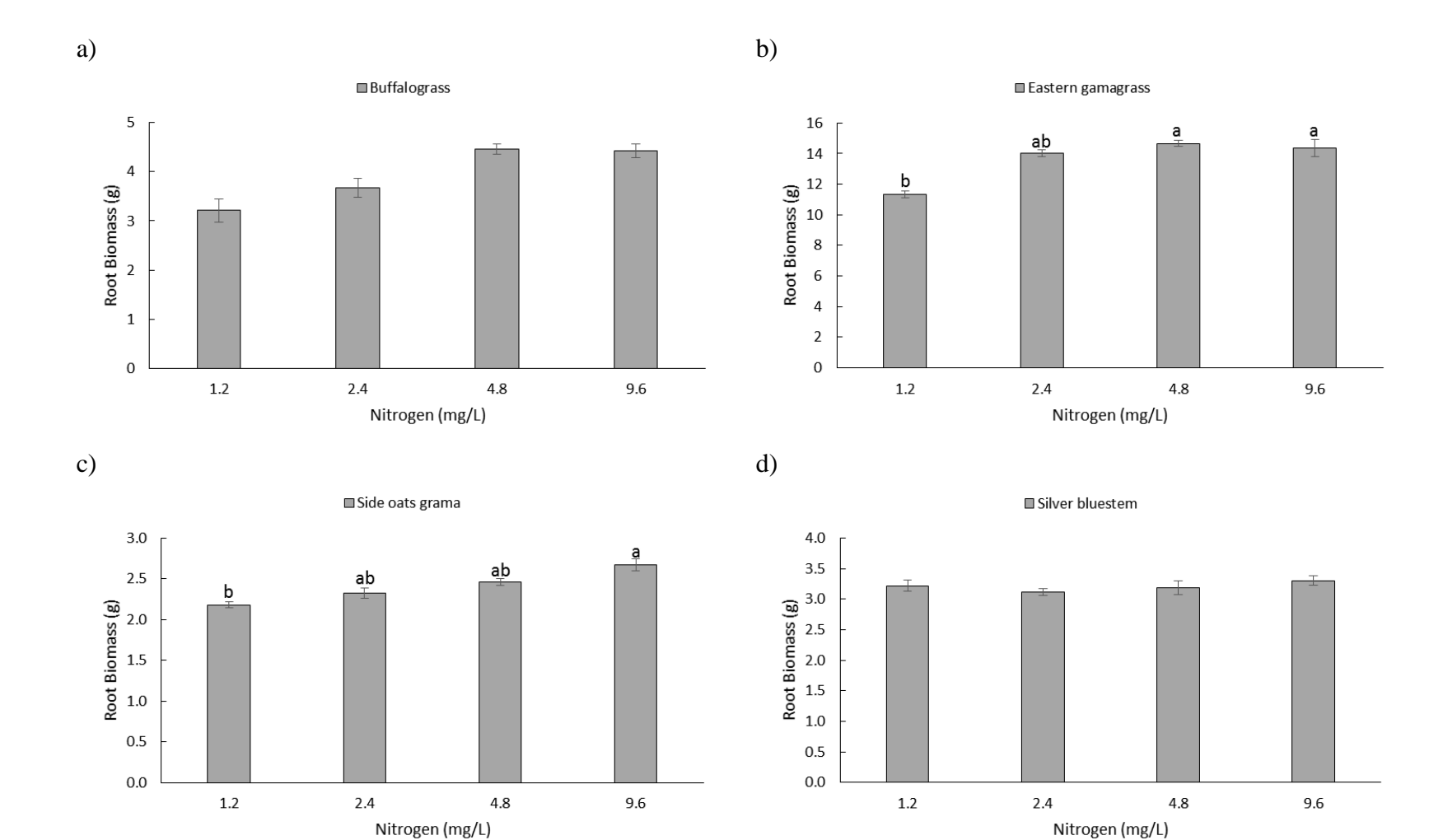


Figure 10. *In situ* swale planting of six native grass species for a) survival (%) (F = 6.57, df = 3, P = 0.003), b) root dry weight (H = 2.445, df = 3, P = 0.485), c) shoot dry weight (H = 1.528, df = 3, P = 0.676), d) total dry weight (H = 1.215, df = 3, P = 0.749), and e) root-to-shoot ratios (H = 5.525, df = 3, P = 0.137) from May 2021 to October 2022. Different letters indicated significant differences (P < 0.05) based on Tukey's mean separation test. Bars represent standard error. Survival of buffalograss and bushy bluestem was 0% and were eliminated from further analysis.



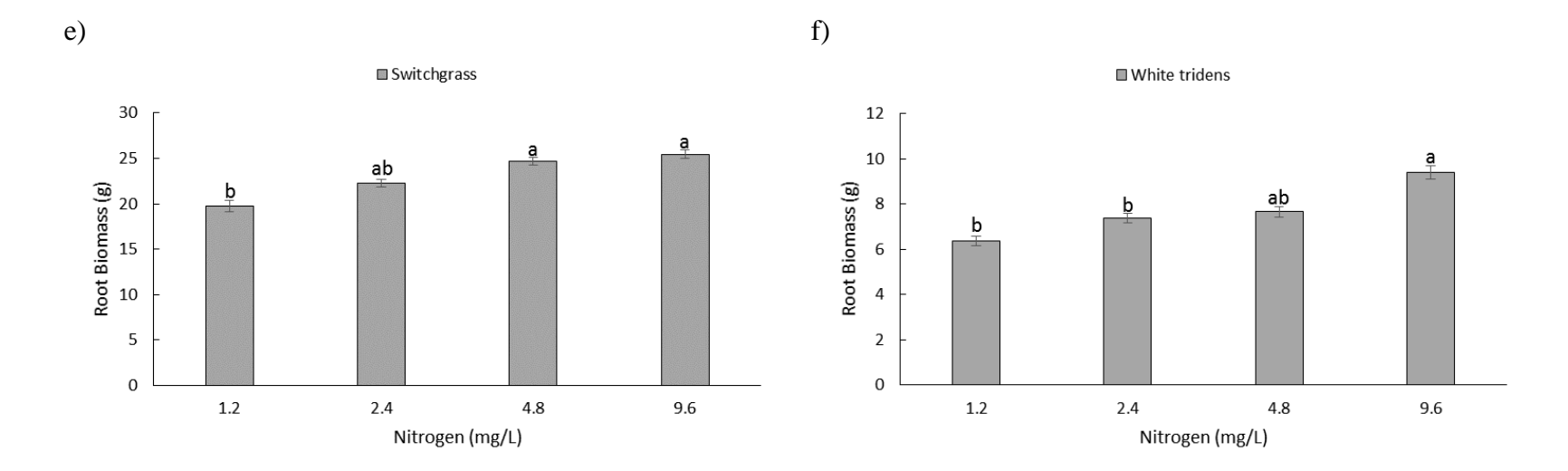
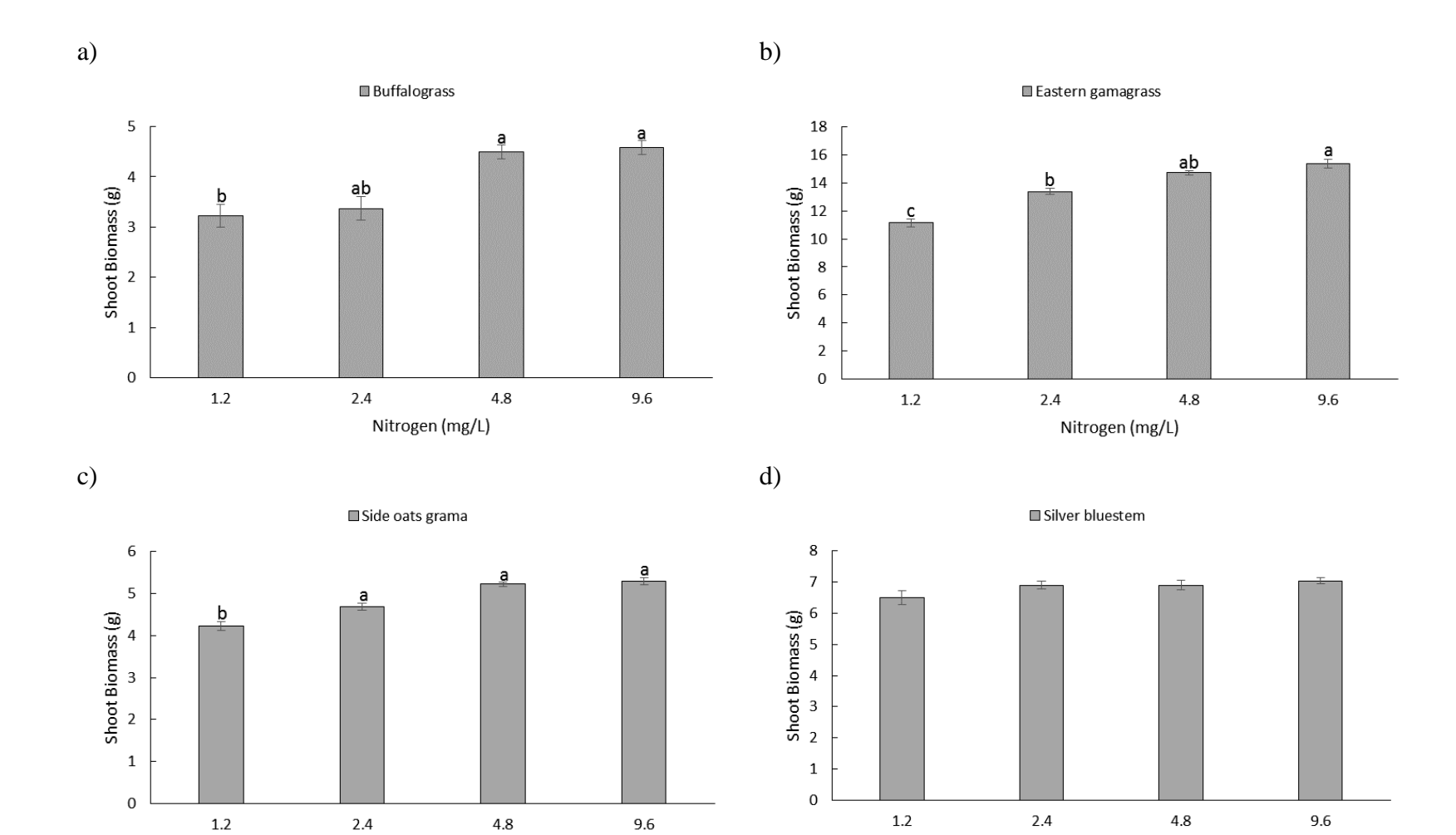


Figure 11. Root dry weights for nitrogen at four increasing concentrations for a) buffalograss (F = 2.7, df = 3, P = 0.073), b) eastern gamagrass (F = 5.05, df = 3, P = 0.009), c) sideoats grama (F = 3.55, df = 3, P = 0.033), d) silver bluestem (F = 0.212, df = 3, P = 0.887), e) switchgrass (F = 6.583, df = 3, P = 0.003), and f) white tridens (F = 6.337, df = 3, P = 0.003) grown for 3 months under greenhouse conditions. Different letters indicate significant differences (P < 0.05) based on Tukey's mean separation test. Bars represent standard error.



Nitrogen (mg/L)

Nitrogen (mg/L)

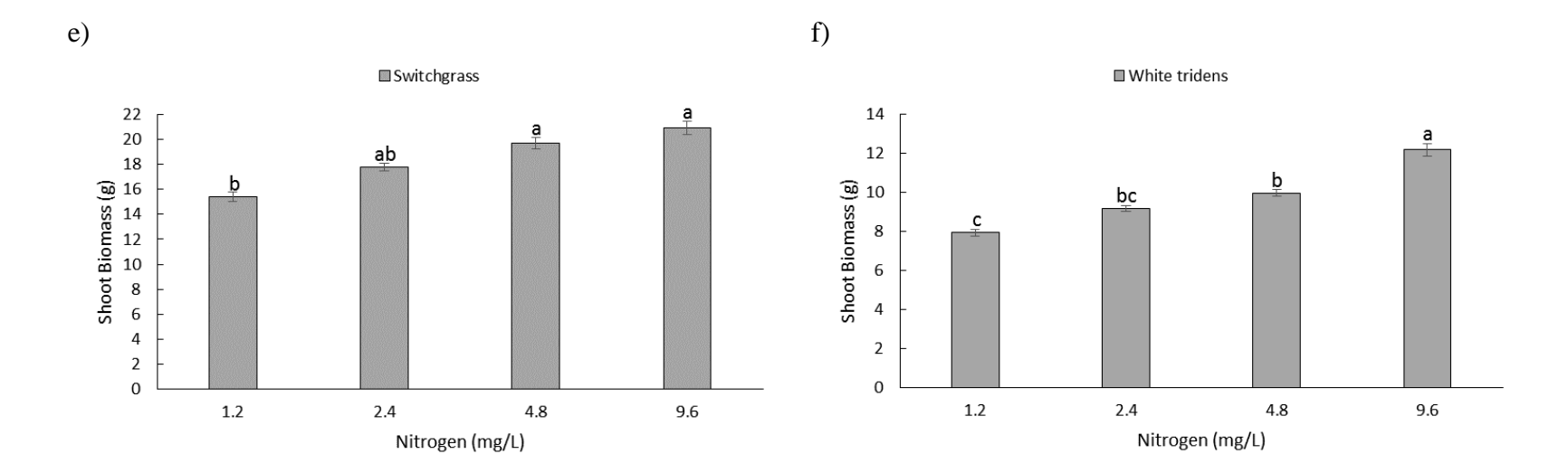
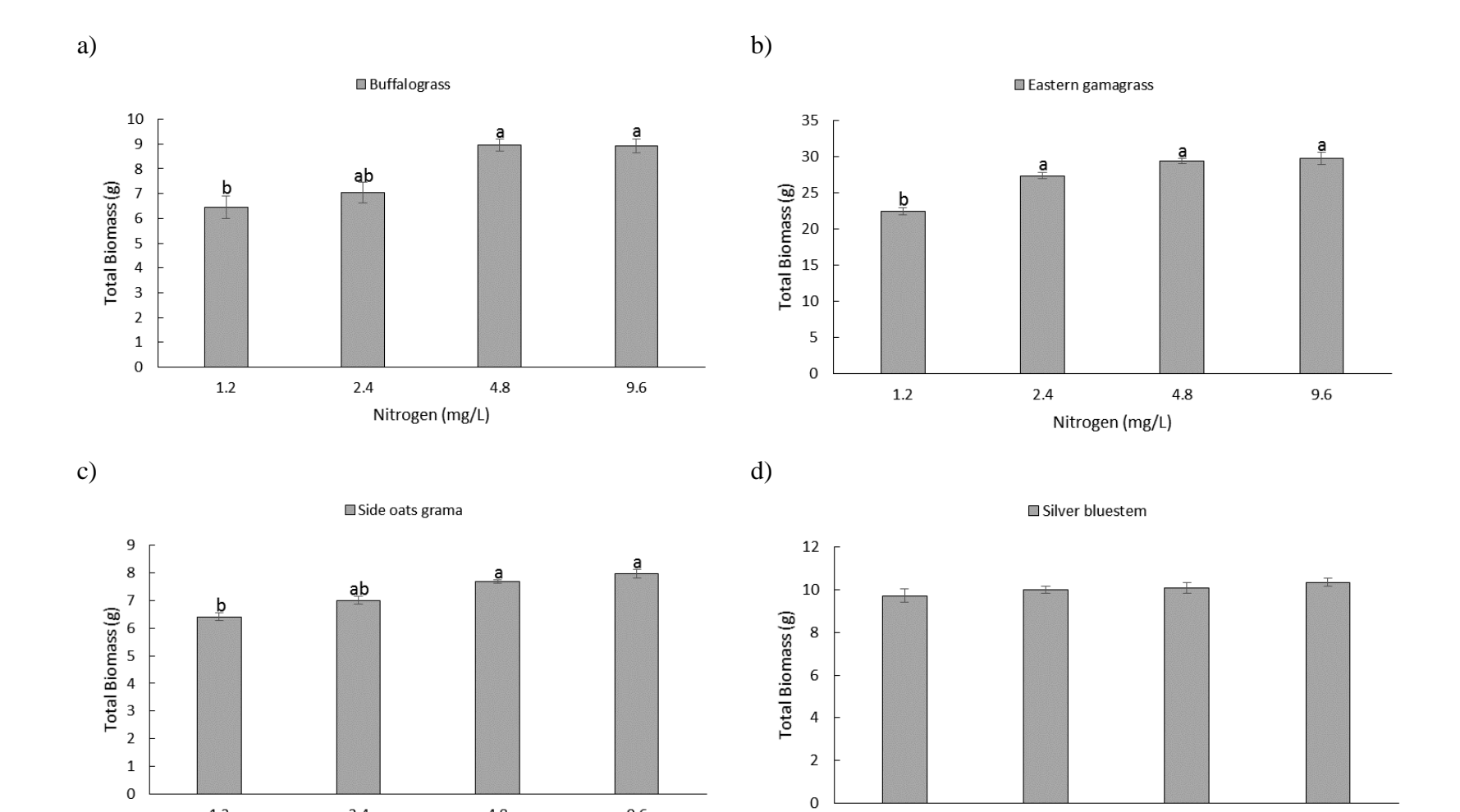


Figure 12. Shoot dry weights of native grasses for nitrogen at four increasing concentrations for a) buffalograss (F = 3.62, df = 3, P = 0.031), b) eastern gamagrass (F = 14.72, df = 3, P < 0.001), c) sideoats grama (F = 9.00, df = 3, P < 0.001), d) silver bluestem (F = 0.55, df = 3, P = 0.657), e) switchgrass (F = 7.60, df = 3, P = 0.001), and f) white tridens (F = 16.59, df = 3, P < 0.001) grown for 3 months under greenhouse conditions. Different letters indicate significant differences (P < 0.05) based on Tukey's mean separation test. Bars represent standard error.



1.2

2.4

Nitrogen (mg/L)

4.8

9.6

1.2

4.8

9.6

2.4

Nitrogen (mg/L)

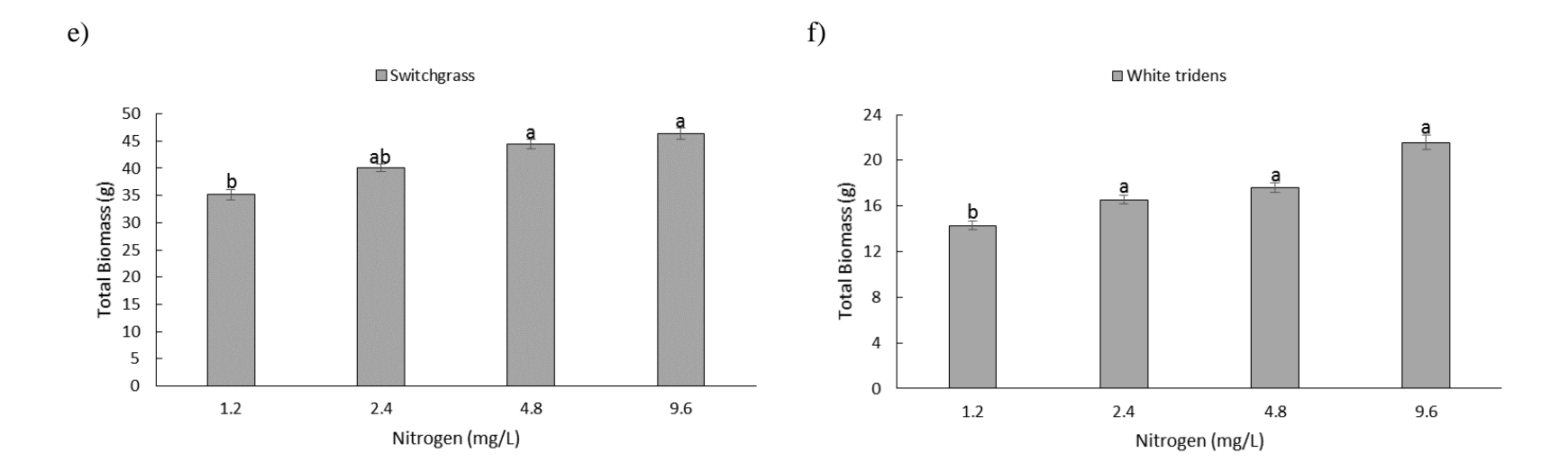
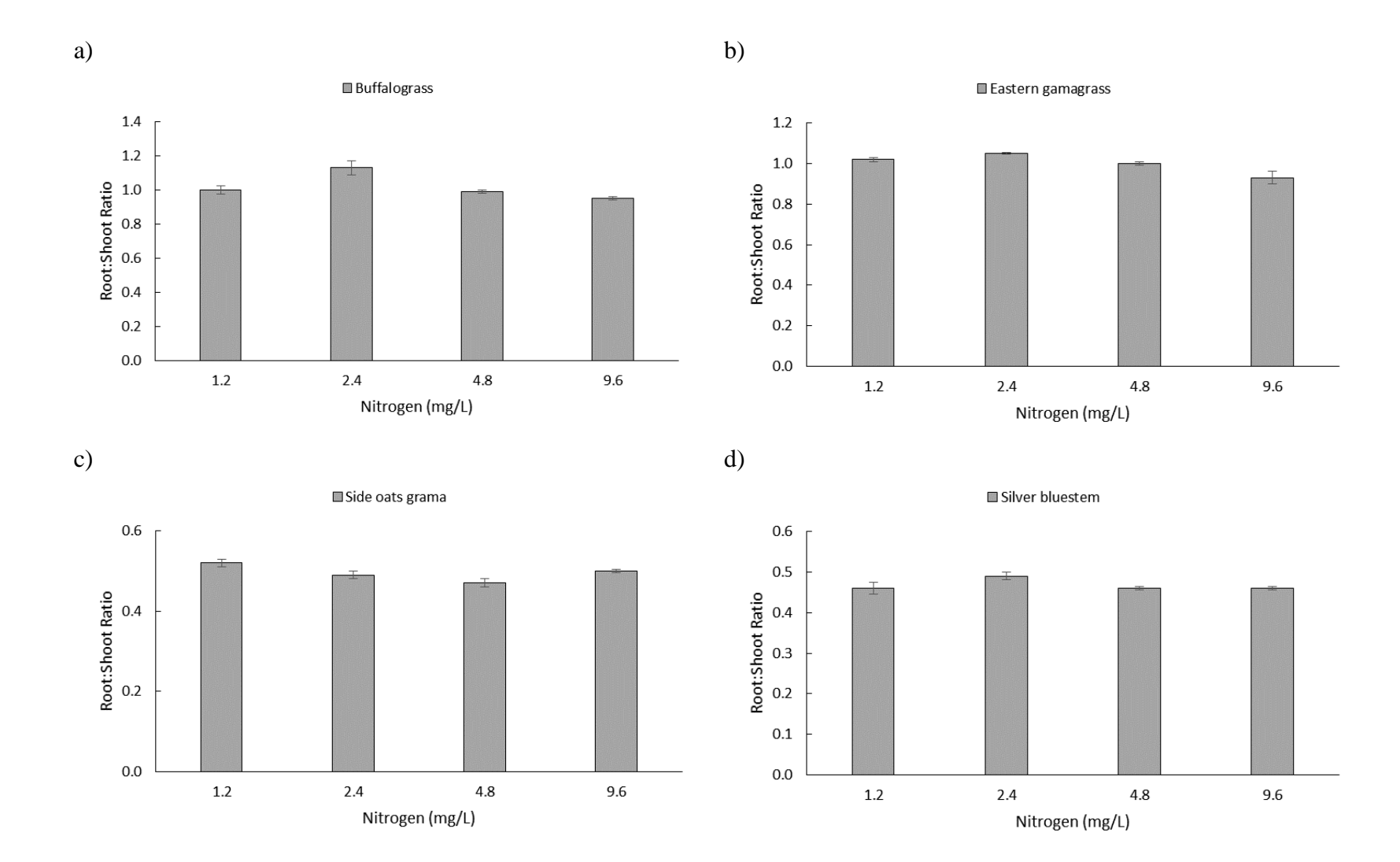


Figure 13. Total dry weights (roots + shoots) of native grasses for nitrogen at four increasing concentrations for a) buffalograss (F = 3.193, df = 3, P = 0.04), b) eastern gamagrass (F = 9.378, df = 3, P < 0.001), c) sideoats grama (F = 7.482, df = 3, P = 0.002), d) silver bluestem (F = 0.31, df = 3, P = 0.818), e) switchgrass (F = 7.8665, df = 3, P = 0.001), and f) white tridens (F = 11.125, df = 3, P < 0.001) grown for 3 months under greenhouse conditions. Different letters indicate significant differences (P < 0.05) based on Tukey's mean separation test. Bars represent standard error.



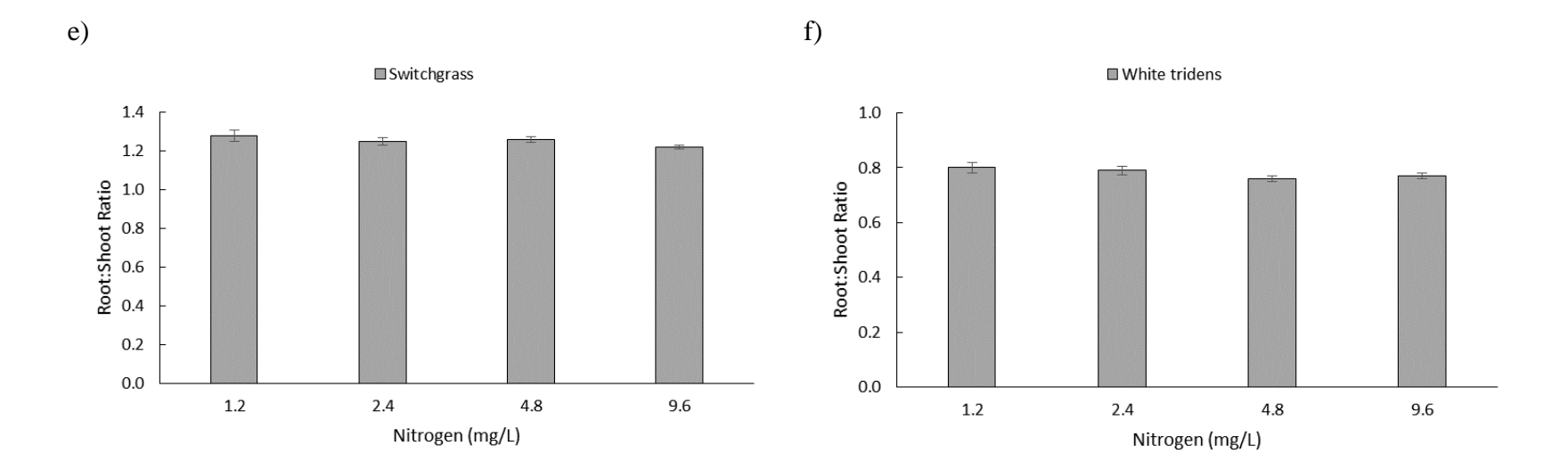
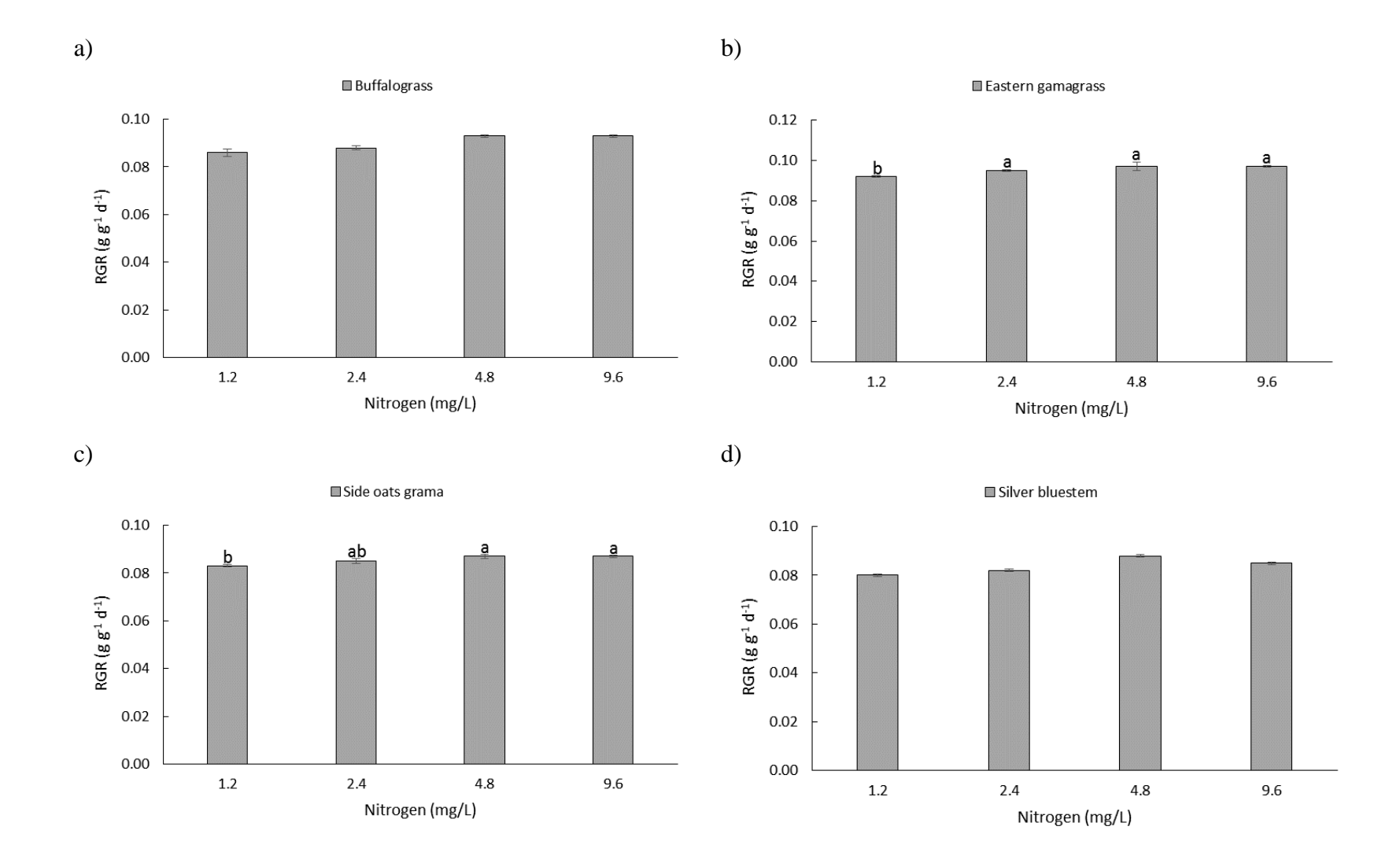


Figure 14. Root-to-shoot ratios of native grasses for nitrogen at four increasing concentrations for a) buffalograss (F = 2.677, df = 3, P = 0.075), b) eastern gamagrass (F = 2.599, df = 3, P = 0.081), c) sideoats grama (F = 1.24, df = 3, P = 0.322), d) silver bluestem (F = 1.685, df = 3, P = 0.202), e) switchgrass (F = 0.436, df = 3, P = 0.73), and f) white tridens (F = 0.481, df = 3, P = 0.699) grown for 3 months under greenhouse conditions. Different letters indicate significant differences (F = 0.081) based on Tukey's mean separation test. Bars represent standard error.



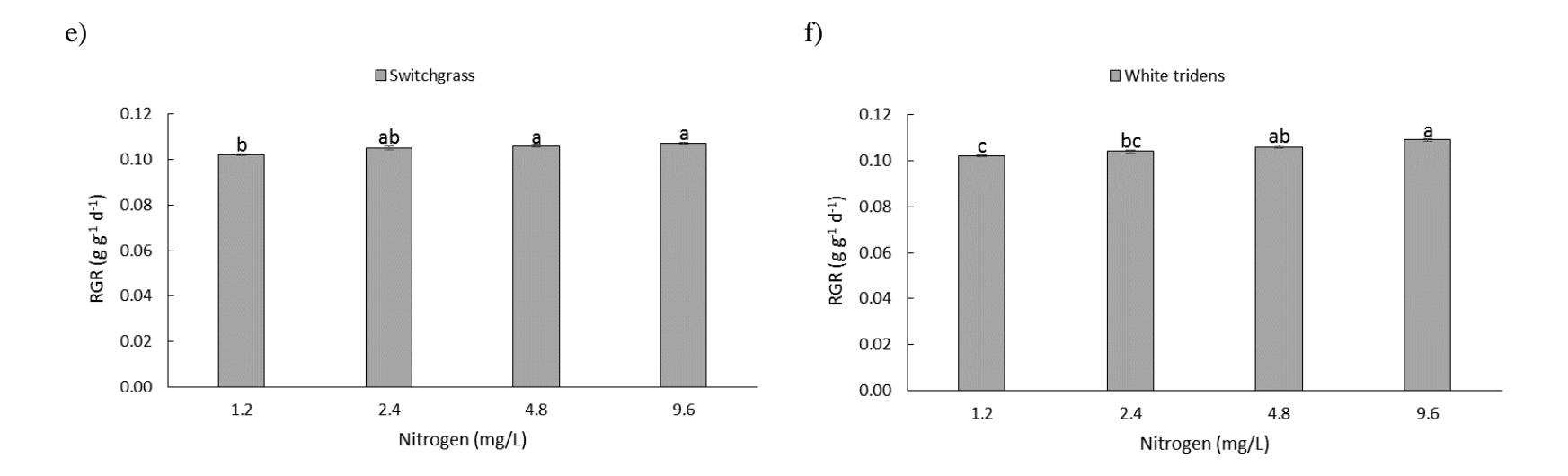
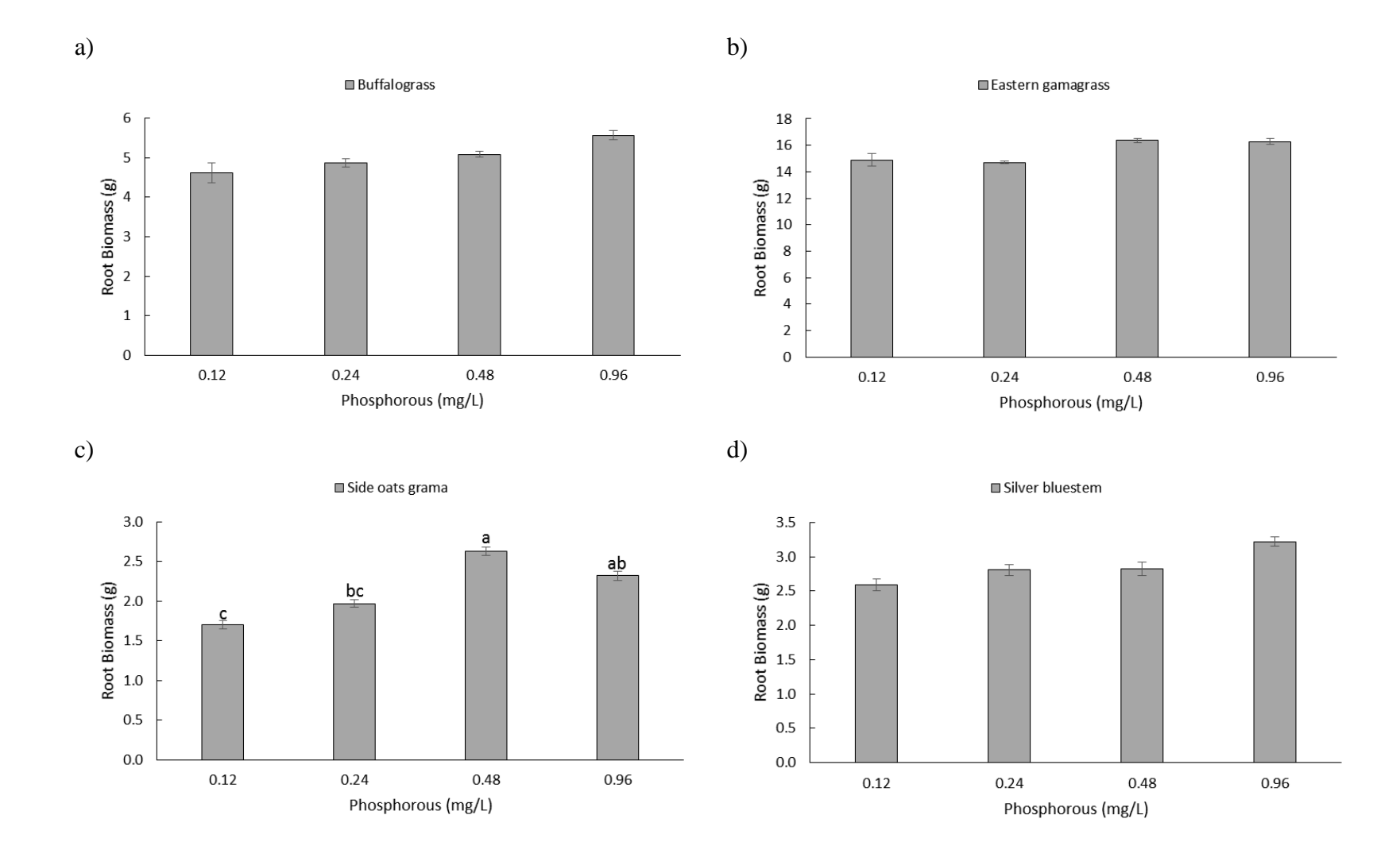


Figure 15. Relative growth rates (RGR; g g⁻¹ d⁻¹) of native grasses for nitrogen at four increasing concentrations for a) buffalograss (F = 3.23, df = 3, P = 0.054), b) eastern gamagrass (F = 9.56, df = 3, P < 0.001), c) sideoats grama (F = 7.49, df = 3, P = 0.001), d) silver bluestem (F = 0.34, df = 3, P = 0.08), e) switchgrass (F = 7.88, df = 3, P = 0.001), and f) white tridens (F = 10.76, df = 3, P < 0.001) grown for 3 months under greenhouse conditions. Different letters indicate significant differences (P < 0.05) based on Tukey's mean separation test. Bars represent standard error.



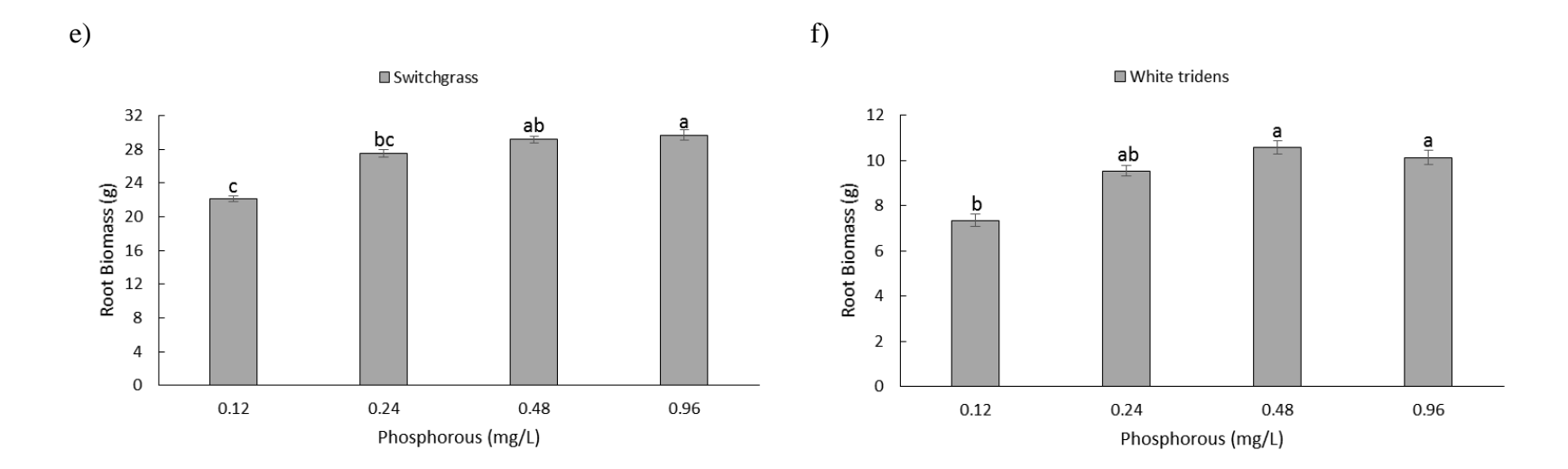
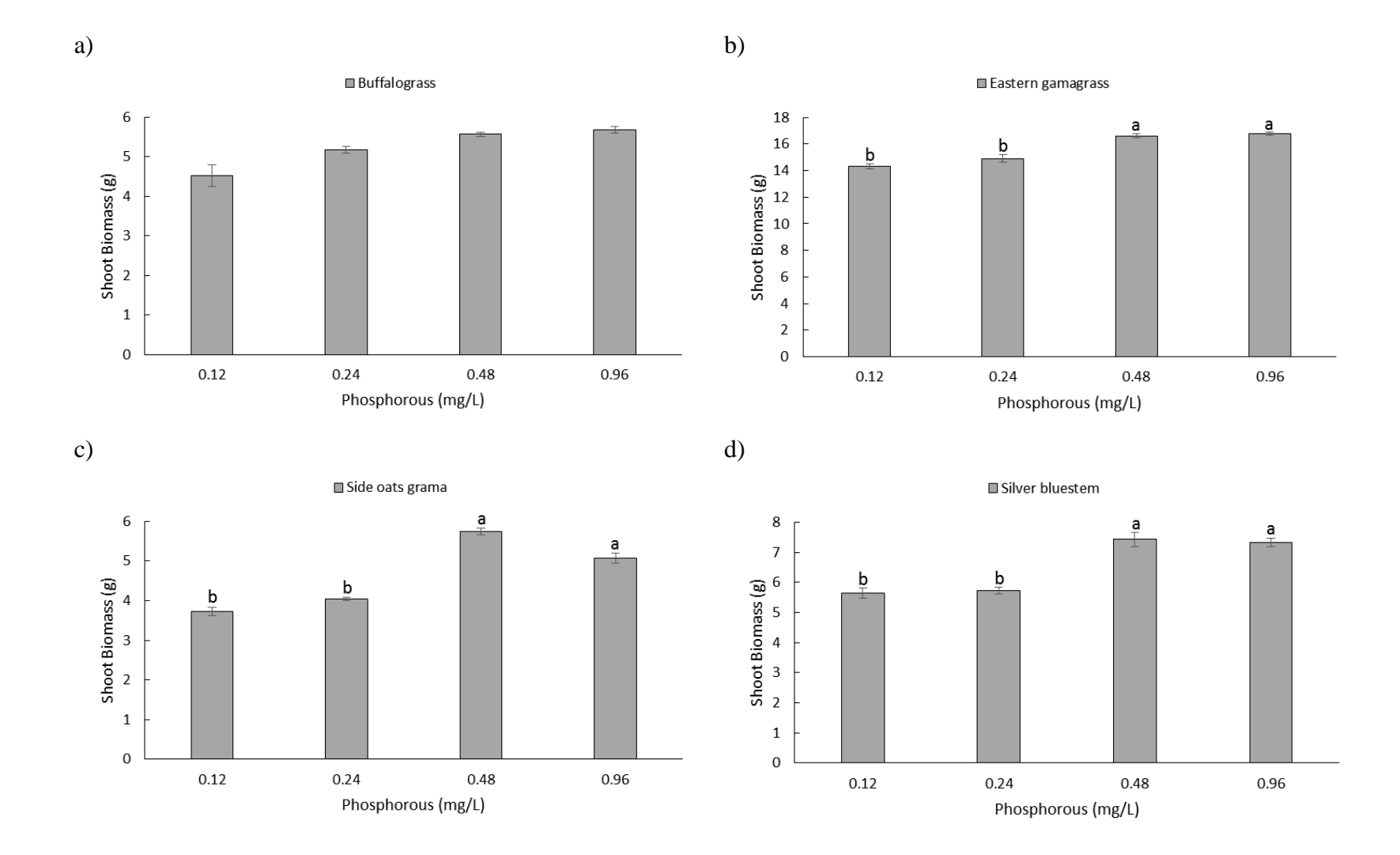


Figure 16. Root dry weights for phosphorus at four increasing concentrations for a) buffalograss (F = 1.835, df = 3, P = 0.173), b) eastern gamagrass (H = 9.396, df = 3, P = 0.05), c) sideoats grama (F = 13.896, df = 3, P < 0.001), d) silver bluestem (F = 2.449, df = 3, P = 0.093), e) switchgrass (F = 14.868, df = 3, P < 0.001), and f) white tridens (F = 6.38, df = 3, P = 0.003) grown for 3 months under greenhouse conditions. Different letters indicate significant differences (P < 0.05) based on Tukey's mean separation test. Bars represent standard error.



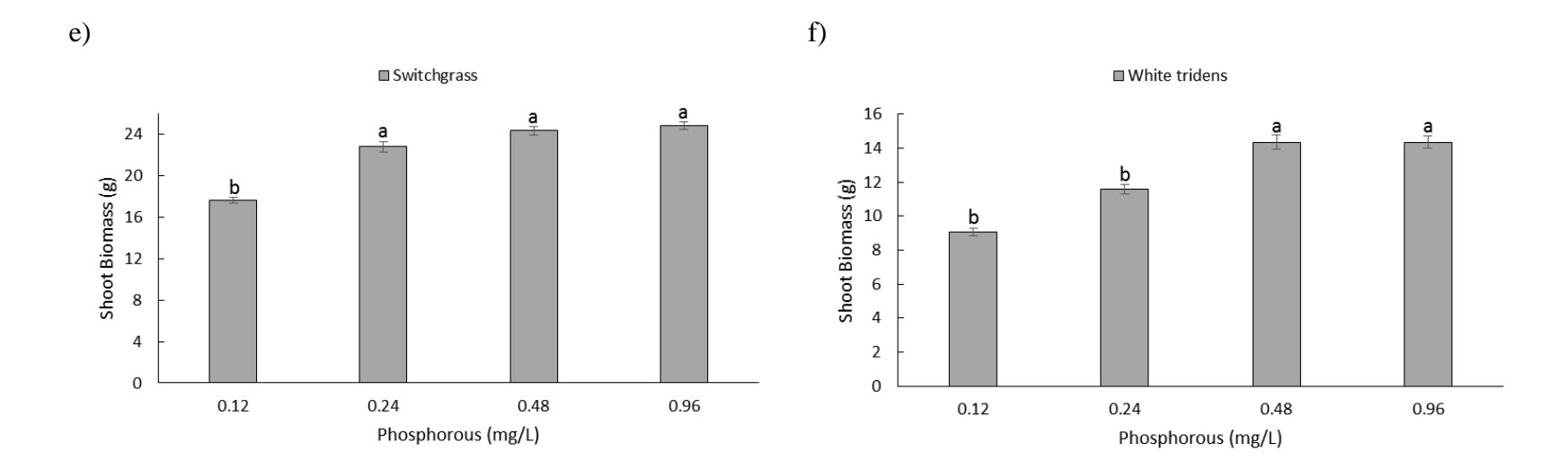
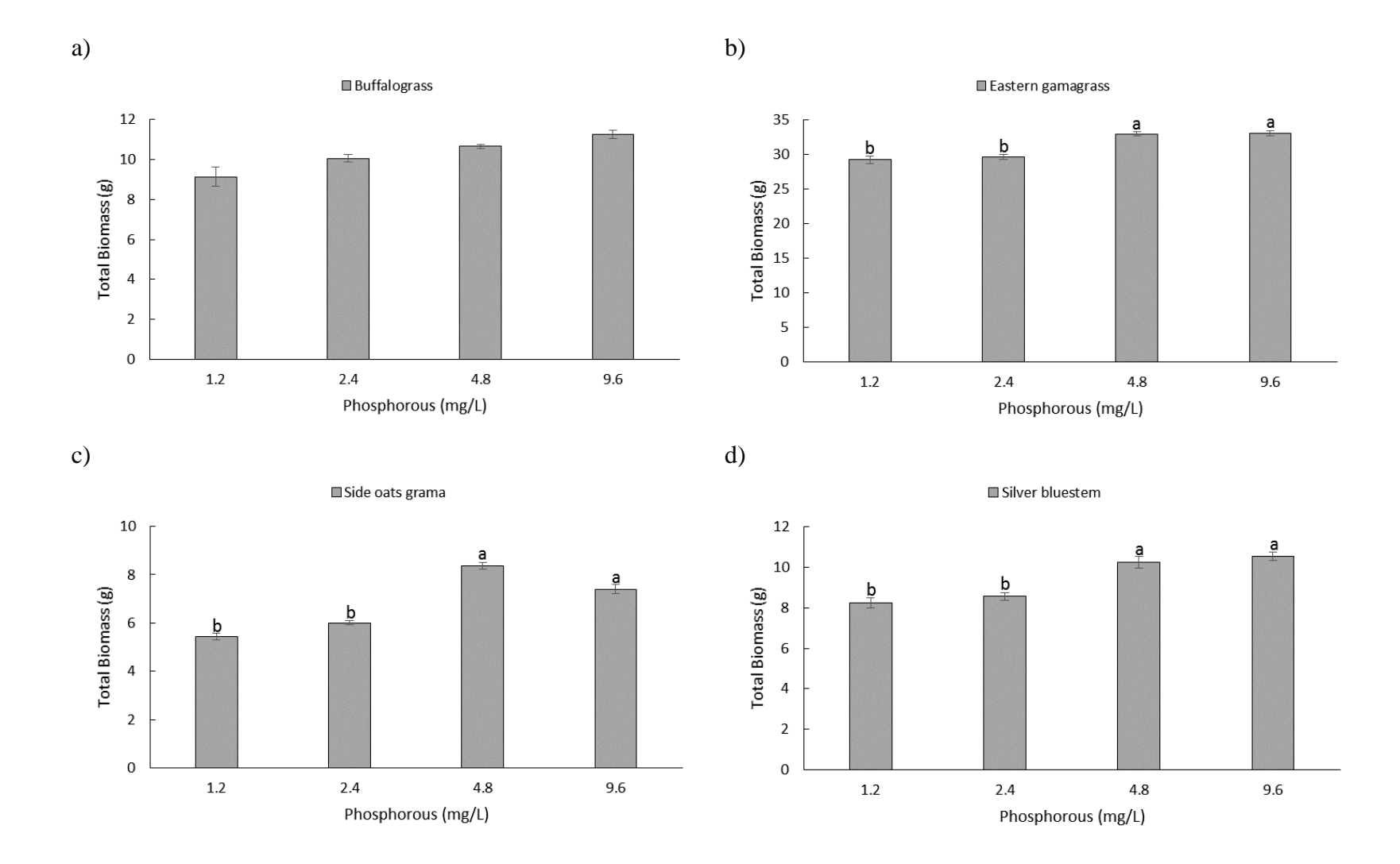


Figure 17. Shoot dry weights for phosphorus at four increasing concentrations for a) buffalograss (H = 6.188, df = 3, P = 0.103), b) eastern gamagrass (F = 10.104, df = 3, P < 0.001), c) sideoats grama (F = 21.566, df = 3, P < 0.001), d) silver bluestem (F = 8.123, df = 3, P < 0.001), e) switchgrass (F = 16.745, df = 3, P < 0.001), and f) white tridens (F = 14.363, df = 3, P < 0.001) grown for 3 months under greenhouse conditions. Different letters indicate significant differences (P < 0.05) based on Tukey's mean separation test. Bars represent standard error.



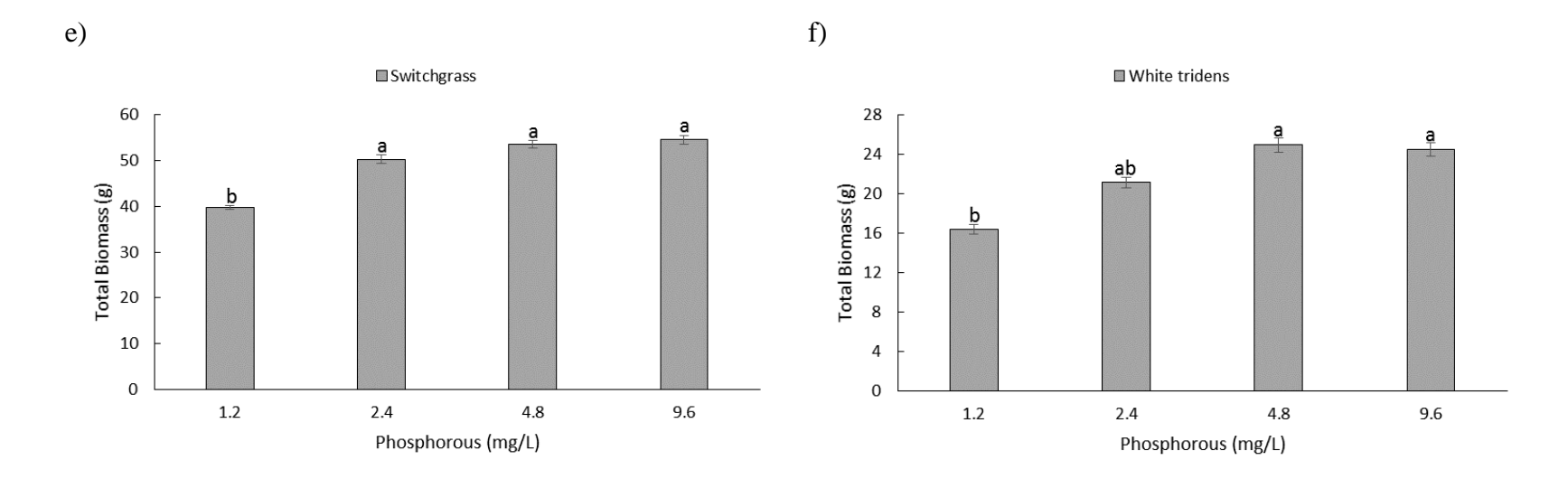
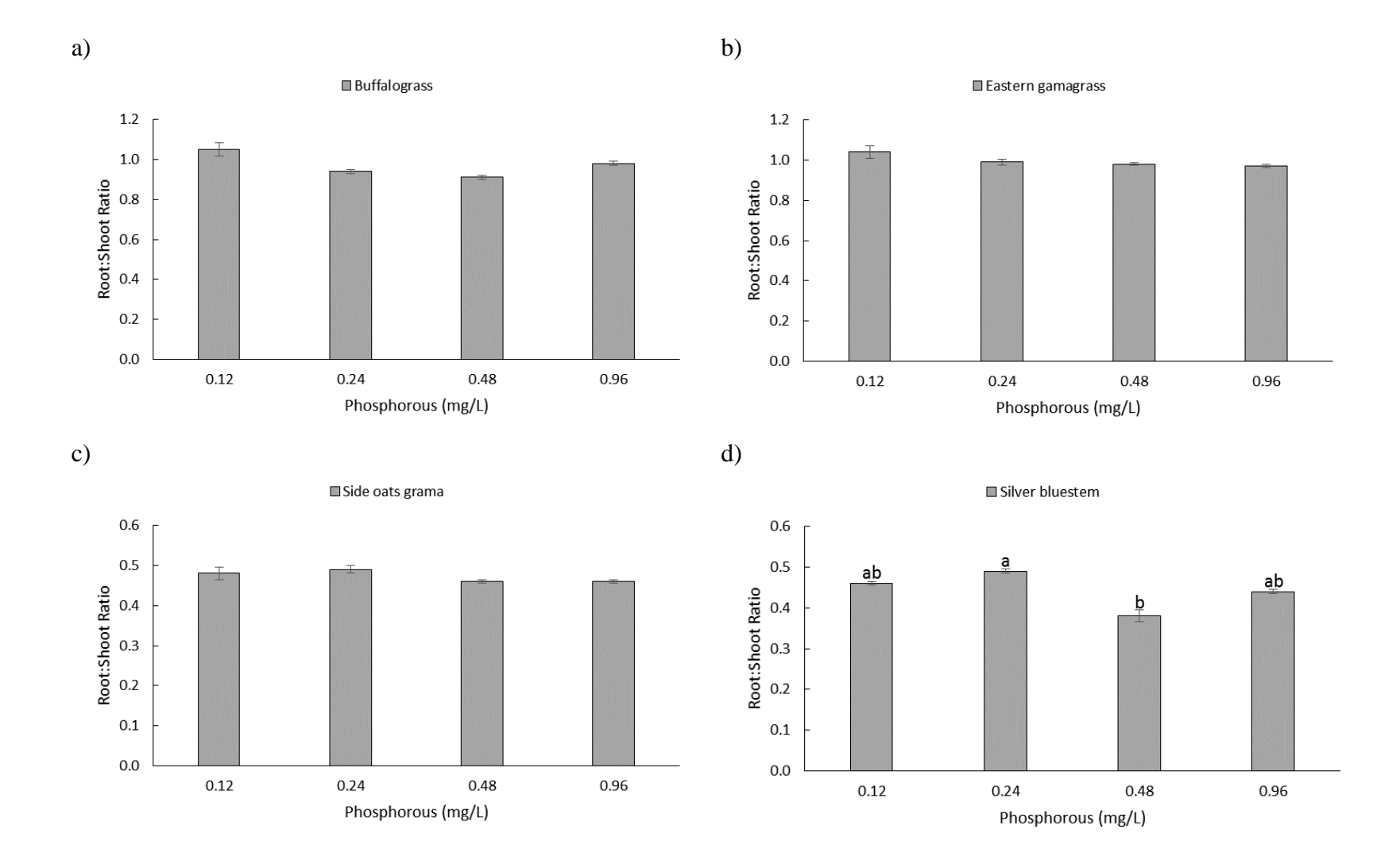


Figure 18. Total dry weights for phosphorus at four increasing concentrations for a) buffalograss (H = 6.127, df = 3, P = 0.106), b) eastern gamagrass (F = 6.652, df = 3, P = 0.003), c) sideoats grama (F = 21.65, df = 3, P < 0.001), d) silver bluestem (F = 6.246, df = 3, P = 0.004), e) switchgrass (F = 17.739, df = 3, P < 0.001), and f) white tridens (F = 10.572, df = 3, P < 0.001) grown for 3 months under greenhouse conditions. Different letters indicate significant differences (P < 0.05) based on Tukey's mean separation test. Bars represent standard error.



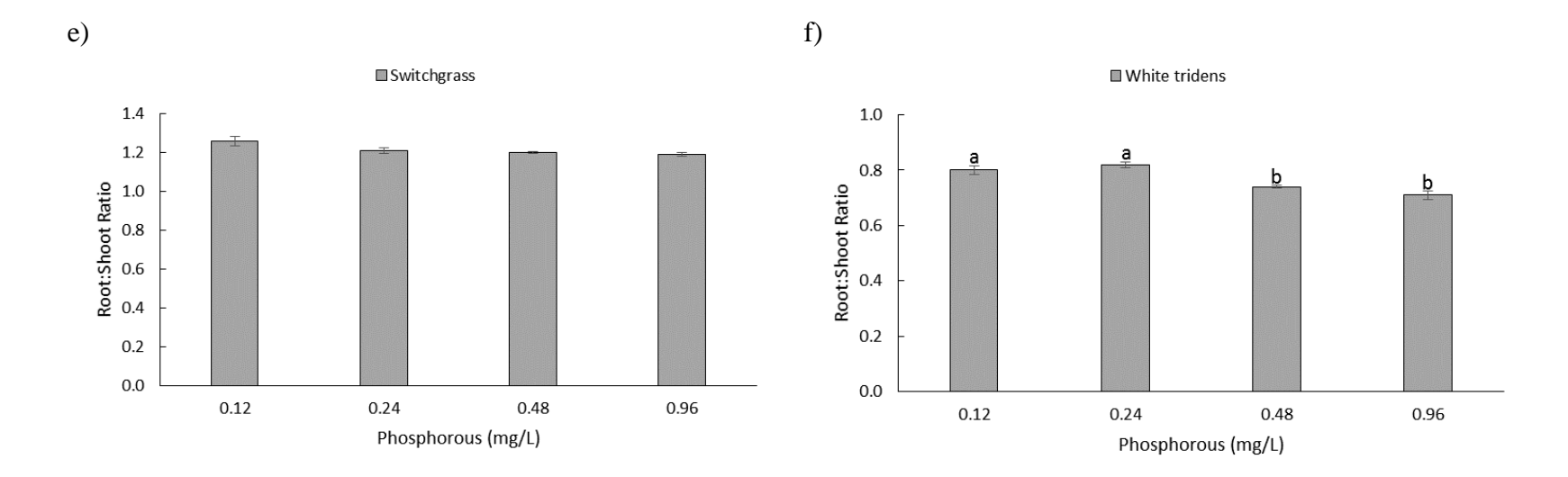
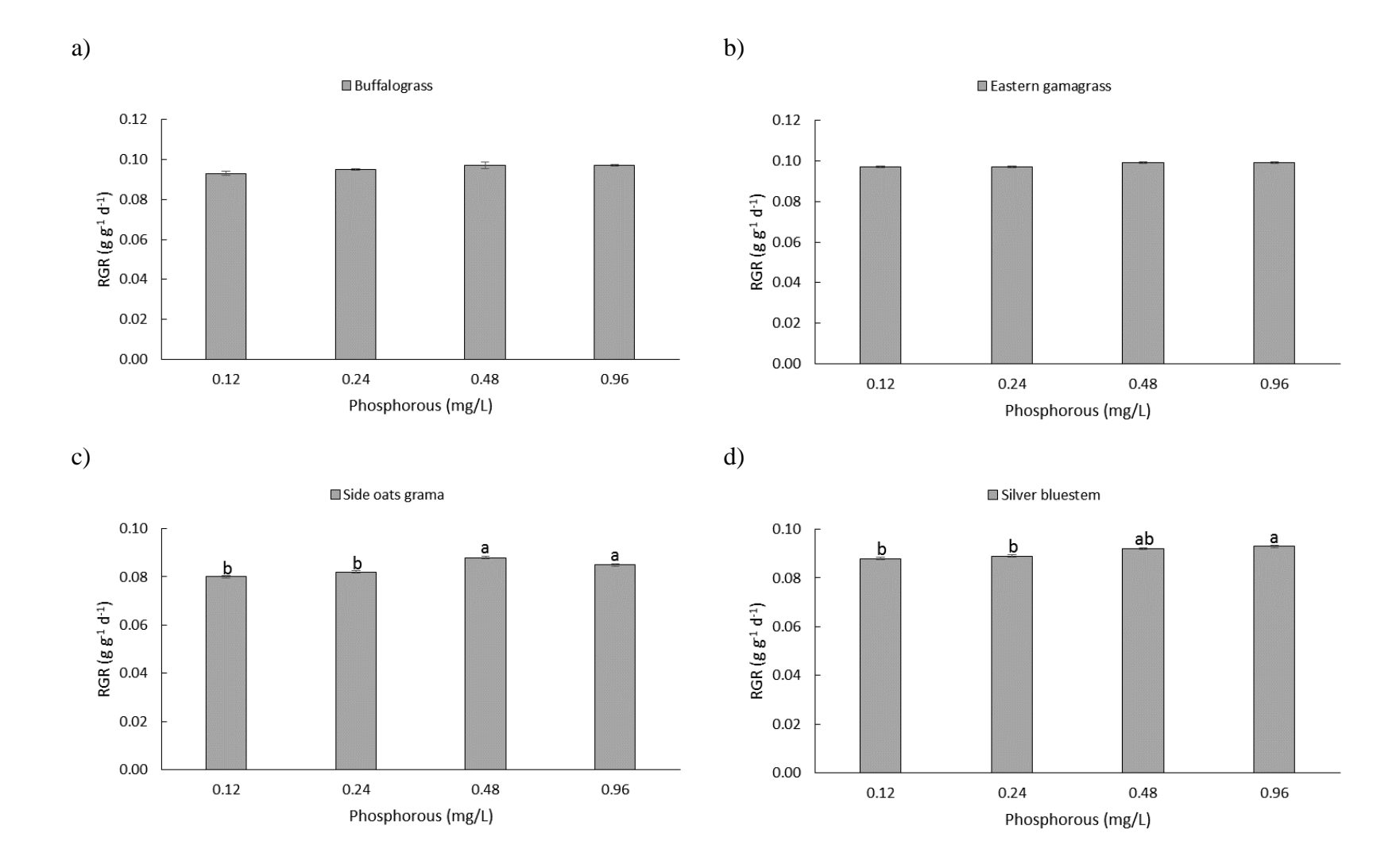


Figure 19. Root-to-shoot ratios for phosphorus at four increasing concentrations for a) buffalograss (H = 5.020, df = 3, P = 0.170), b) eastern gamagrass (F = 0.758, df = 3, P = 0.531), c) sideoats grama (F = 0.493, df = 3, P = 0.691), d) silver bluestem (F = 6.222, df = 3, P = 0.004), e) switchgrass (F = 0.763, df = 3, P = 0.528), and f) white tridens (F = 7.244, df = 3, P = 0.002) grown for 3 months under greenhouse conditions. Different letters indicate significant differences (P < 0.05) based on Tukey's mean separation test. Bars represent standard error.



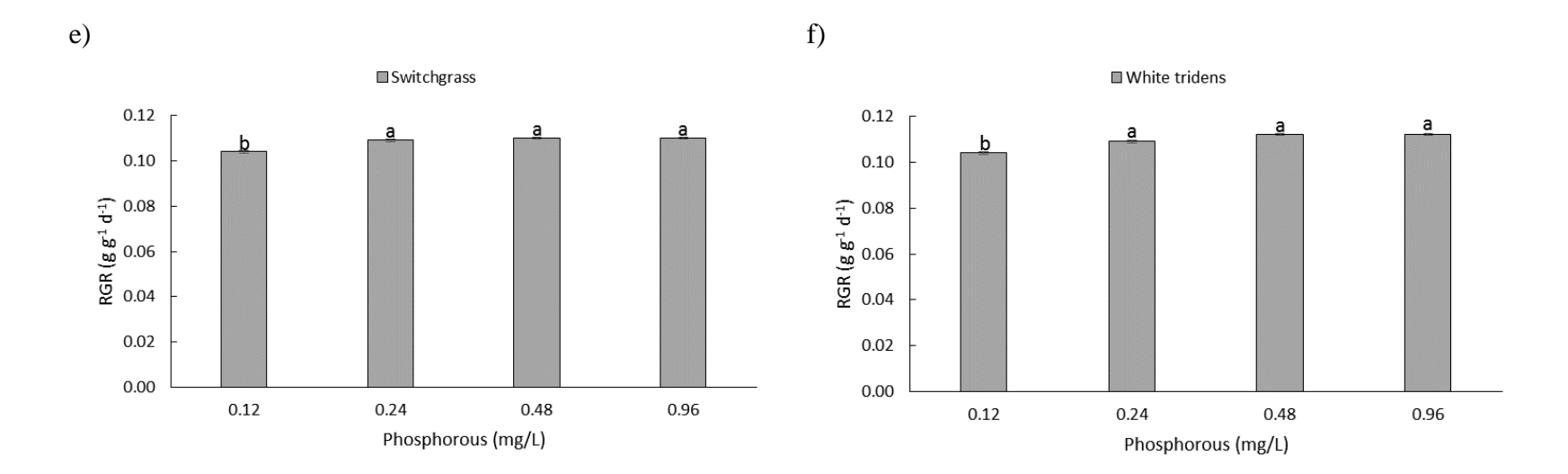
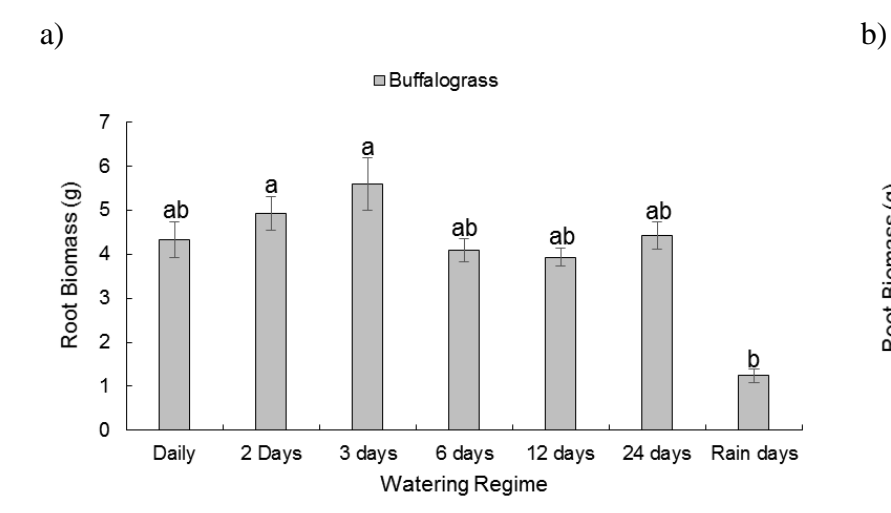
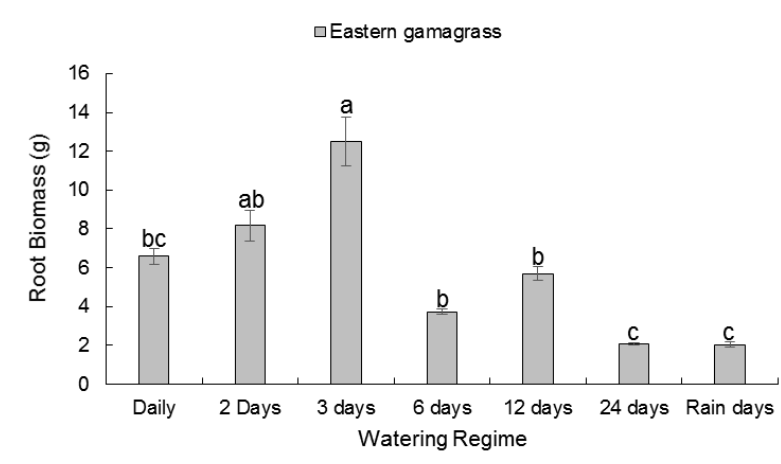
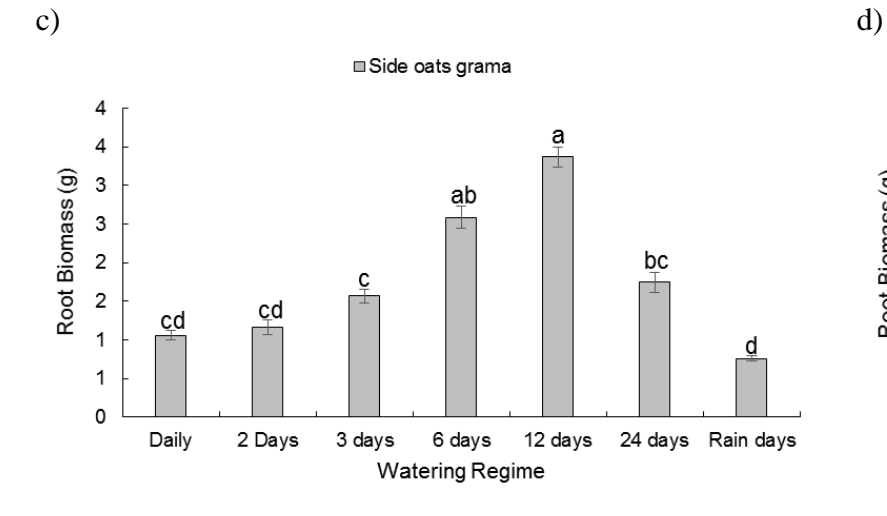
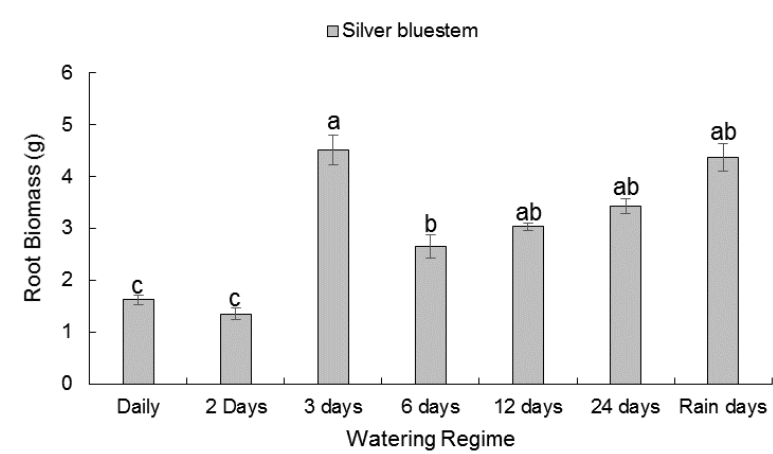


Figure 20. Relative growth rates (RGR; g g⁻¹ d⁻¹) for phosphorus at four increasing concentrations for a) buffalograss (H = 5.961, df = 3, P = 0.114), b) eastern gamagrass (H = 12.012, df = 3, P = 0.05), c) sideoats grama (F = 20.779, df = 3, P < 0.001), d) silver bluestem (F = 5.682, df = 3, P = 0.006), e) switchgrass (F = 20.936, df = 3, P < 0.001), and f) white tridens (F = 12.244, df = 3, P < 0.001) grown for 3 months under greenhouse conditions. Different letters indicate significant differences (P < 0.05) based on Tukey's mean separation test. Bars represent standard error.









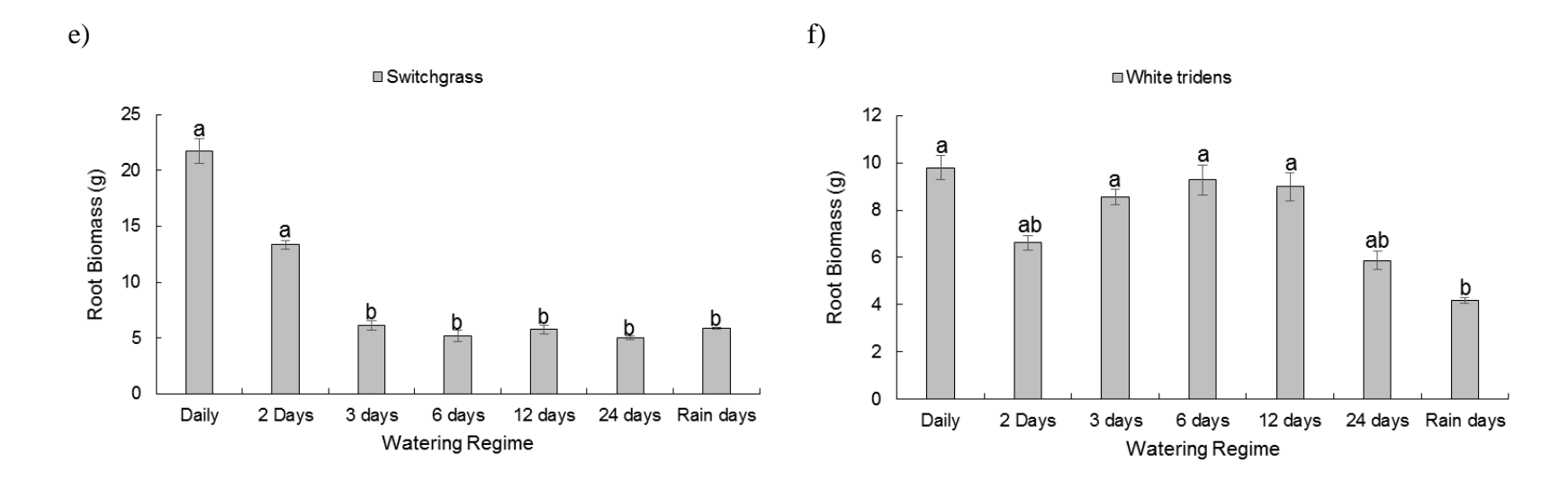
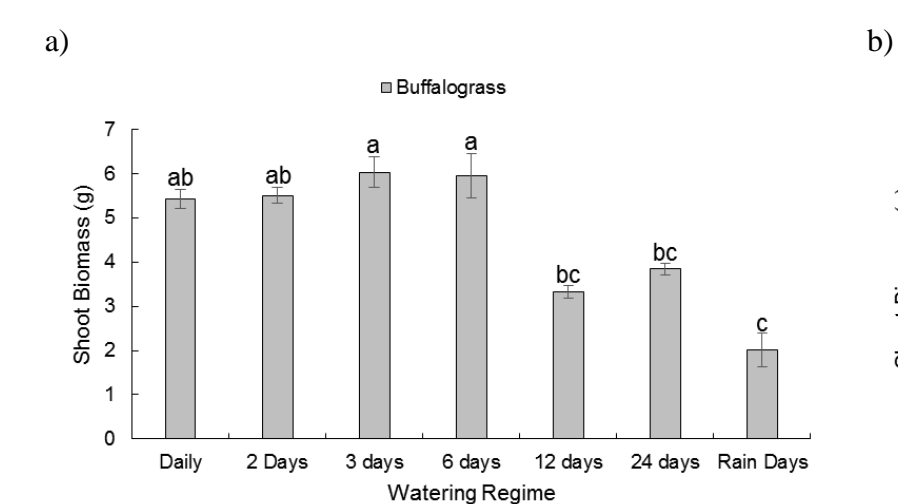
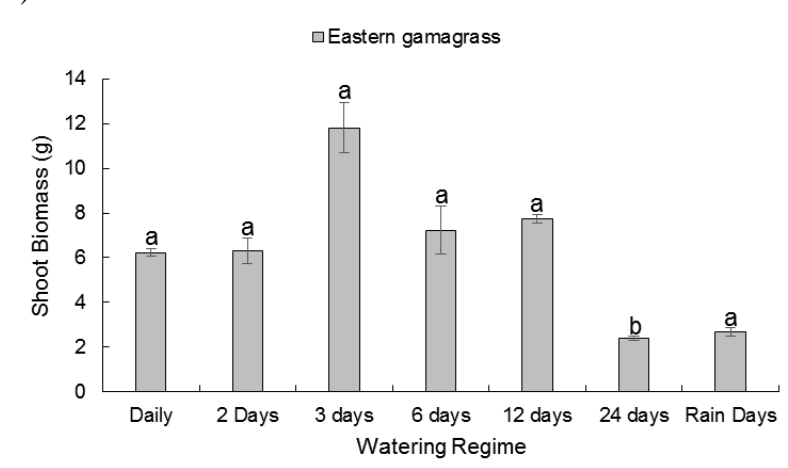
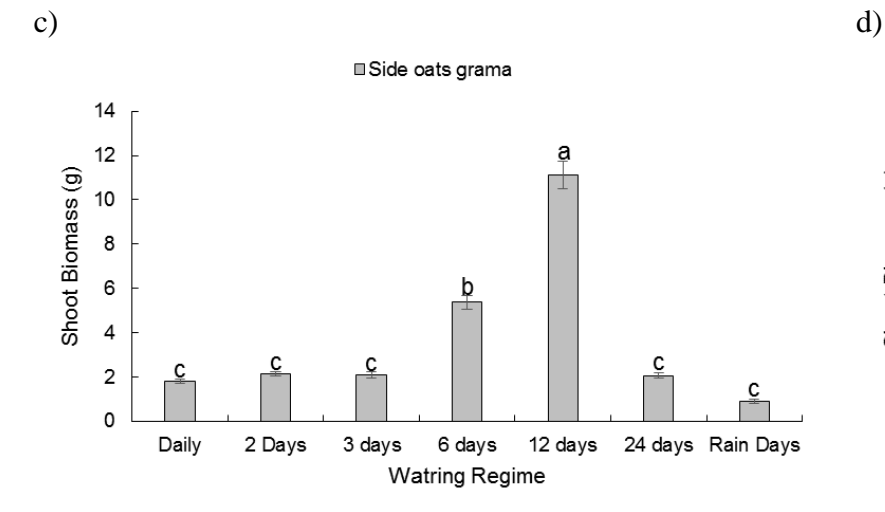
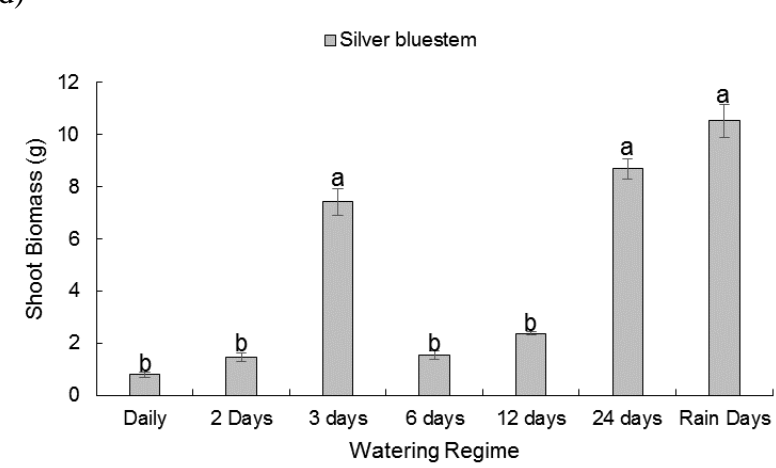


Figure 21. Root biomass in response to variable watering regimes (1-24 days and rain days) for a) buffalograss (F = 3.687, df = 6, P = 0.008), b) eastern gamagrass (F = 9.575, df = 6, P < 0.001), c) sideoats grama (F = 19.29, df = 6, P < 0.001), d) silver bluestem (F = 10.382, df = 6, P < 0.001), e) switchgrass (F = 26.328, df = 6, P < 0.001), and f) white tridens (F = 5.63, df = 6, P < 0.001) grown for 3 months under greenhouse conditions. Different letters indicate significant differences (P < 0.05) based on Tukey's mean separation test. Bars represent standard error.









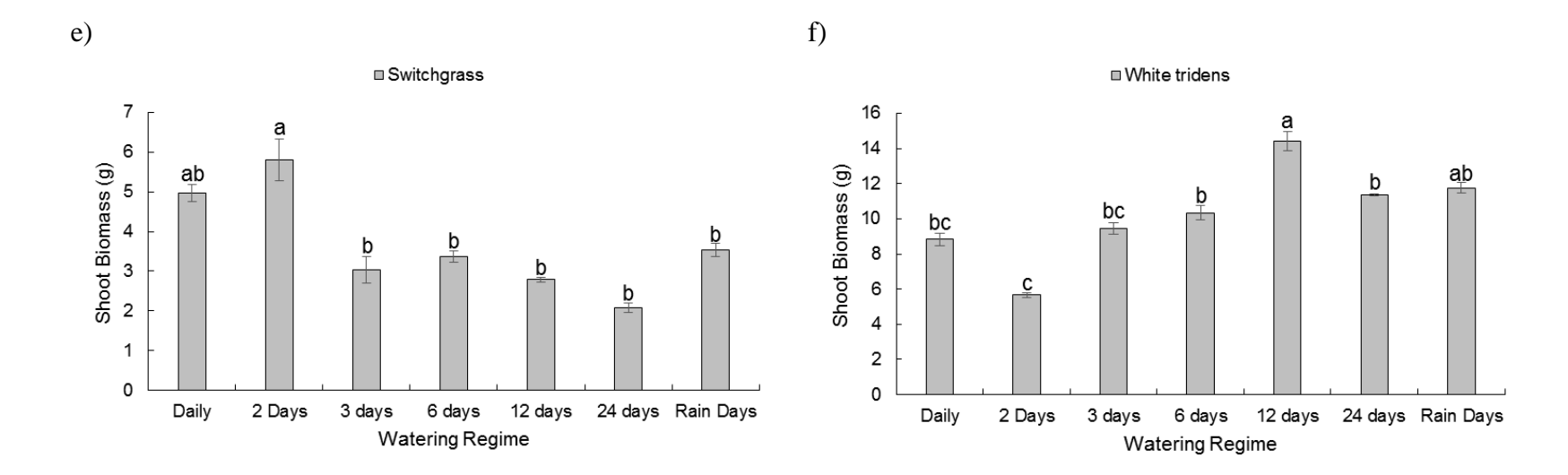
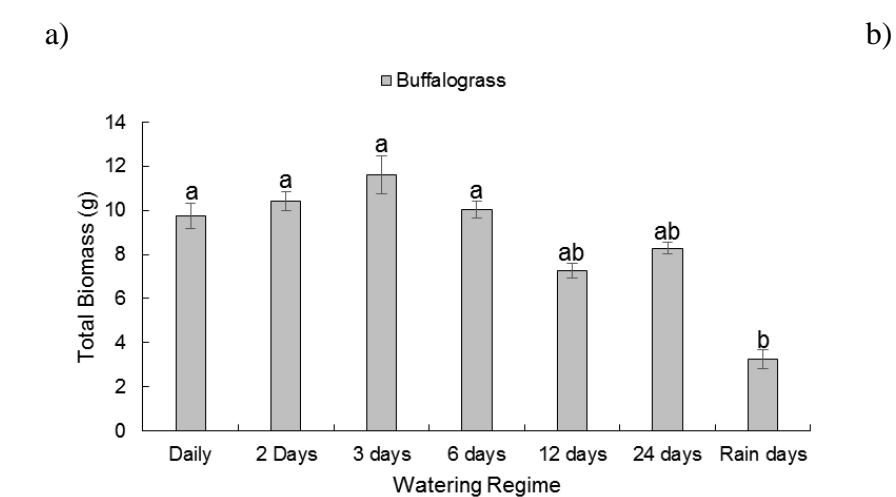
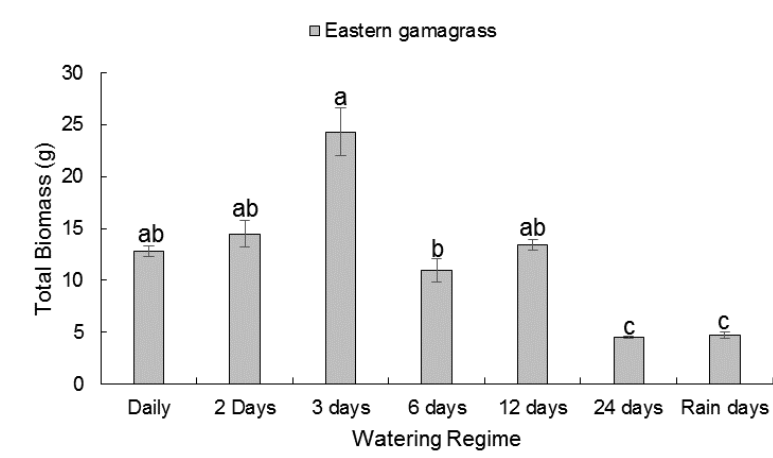
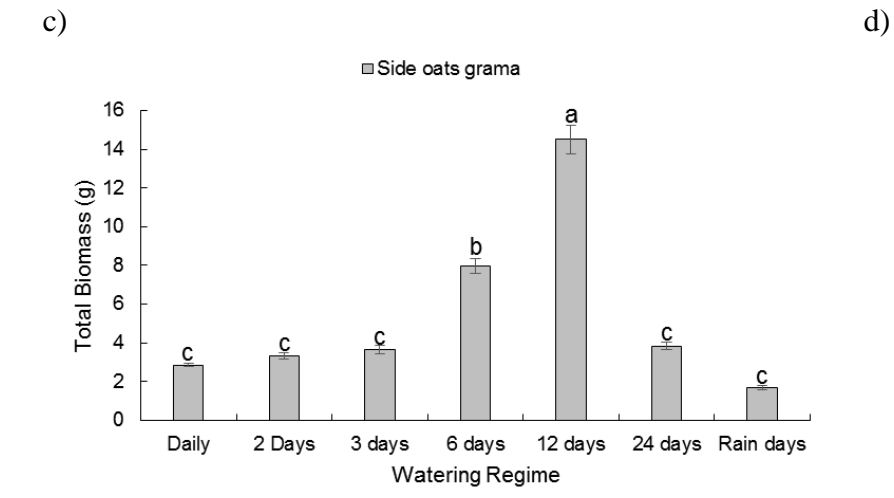
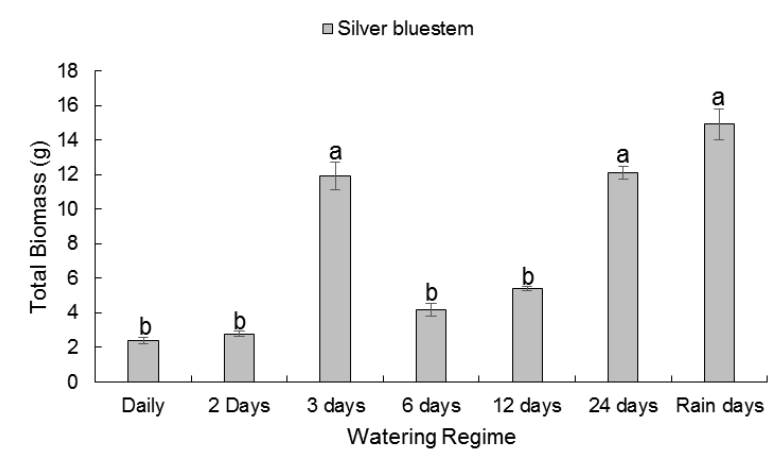


Figure 22. Shoot biomass in response to variable watering regimes (1-24 days and rain days) for a) buffalograss (F = 5.761, df = 6, P < 0.001), b) eastern gamagrass (F = 9.661, df = 6, P < 0.001), c) sideoats grama (F = 41.966, df = 6, P < 0.001), d) silver bluestem (F = 32.877, df = 6, P < 0.001), e) switchgrass (F = 6.107, df = 6, P < 0.001), and f) white tridens (F = 16.176, df = 6, P < 0.001) grown for 3 months under greenhouse conditions. Different letters indicate significant differences (P < 0.05) based on Tukey's mean separation test. Bars represent standard error.









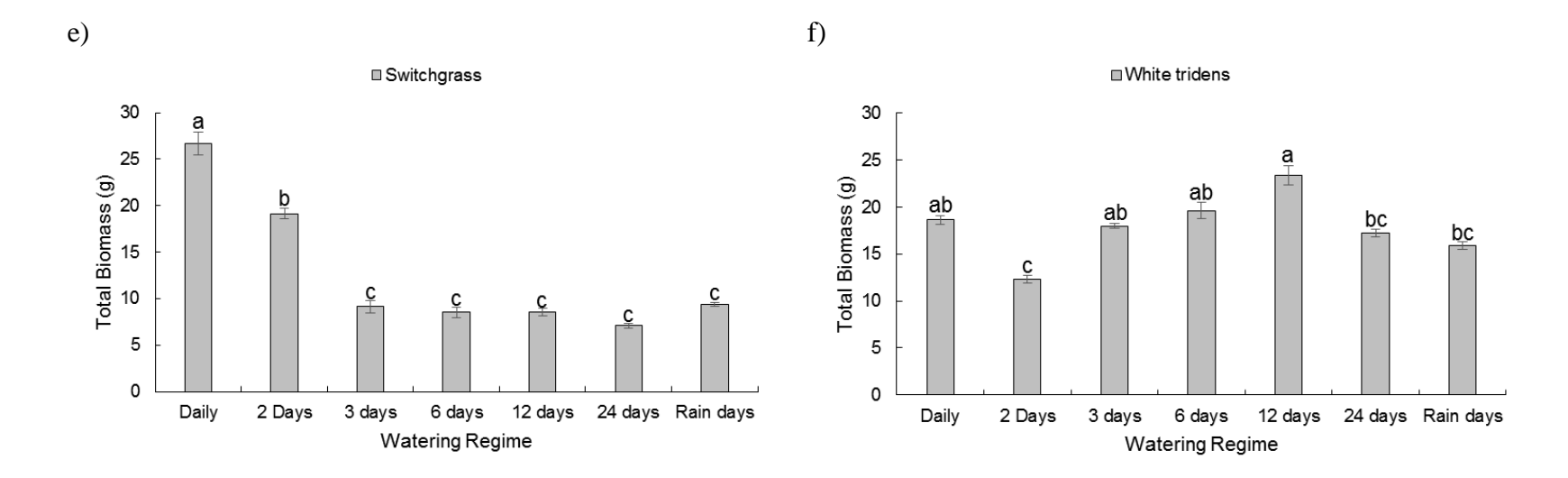
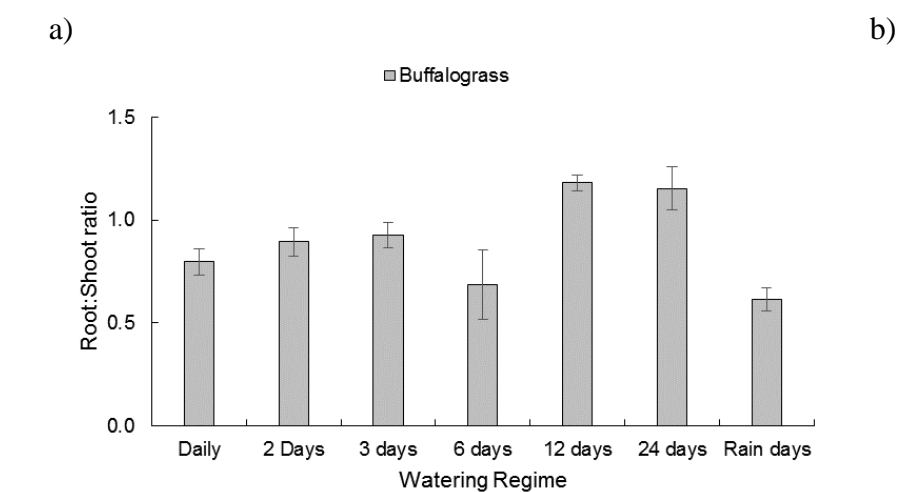
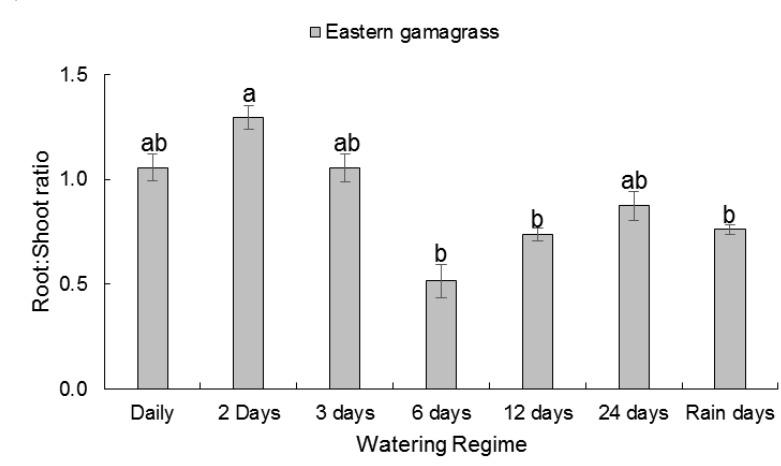
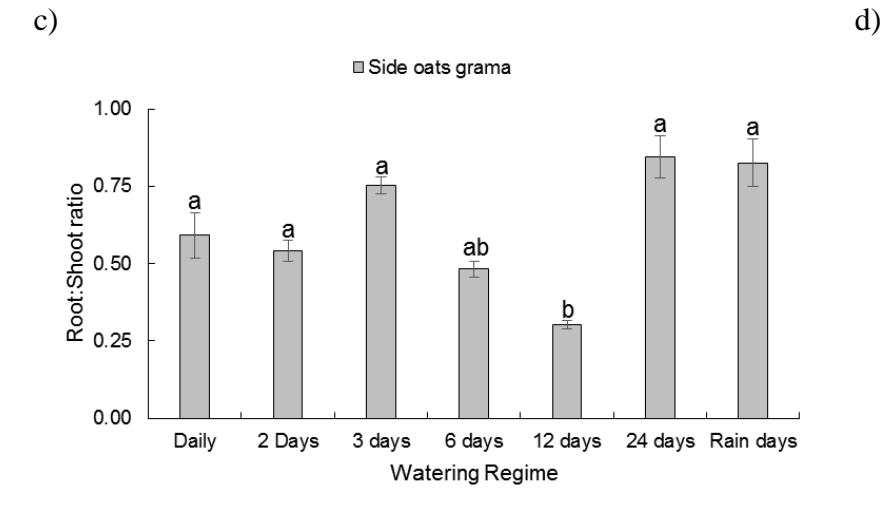
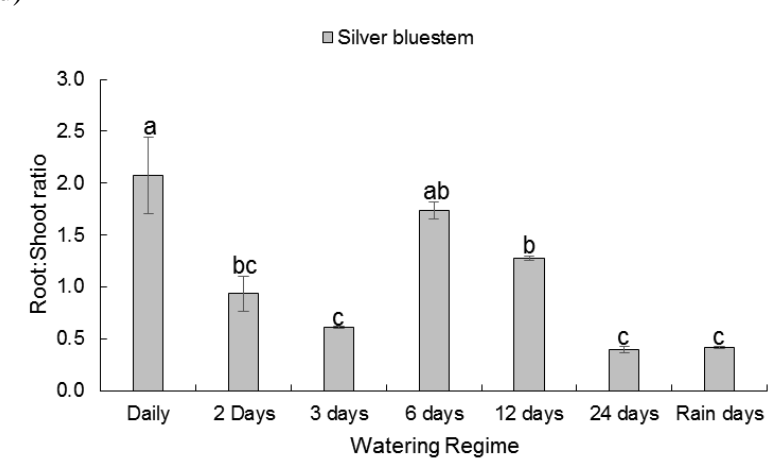


Figure 23. Total biomass (shoots + roots) in response to variable watering regimes (1-24 days and rain days) for a) buffalograss (F = 6.506, df = 6, P < 0.001), b) eastern gamagrass (F = 12.92, df = 6, P < 0.001), c) sideoats grama (F = 43.465, df = 6, P < 0.001), d) silver bluestem (F = 25.86, df = 6, P < 0.001), e) switchgrass (F = 34.117, df = 6, P < 0.001), and f) white tridens (F = 8.237, df = 6, P < 0.001) grown for 3 months under greenhouse conditions. Different letters indicate significant differences (P < 0.05) based on Tukey's mean separation test. Bars represent standard error.









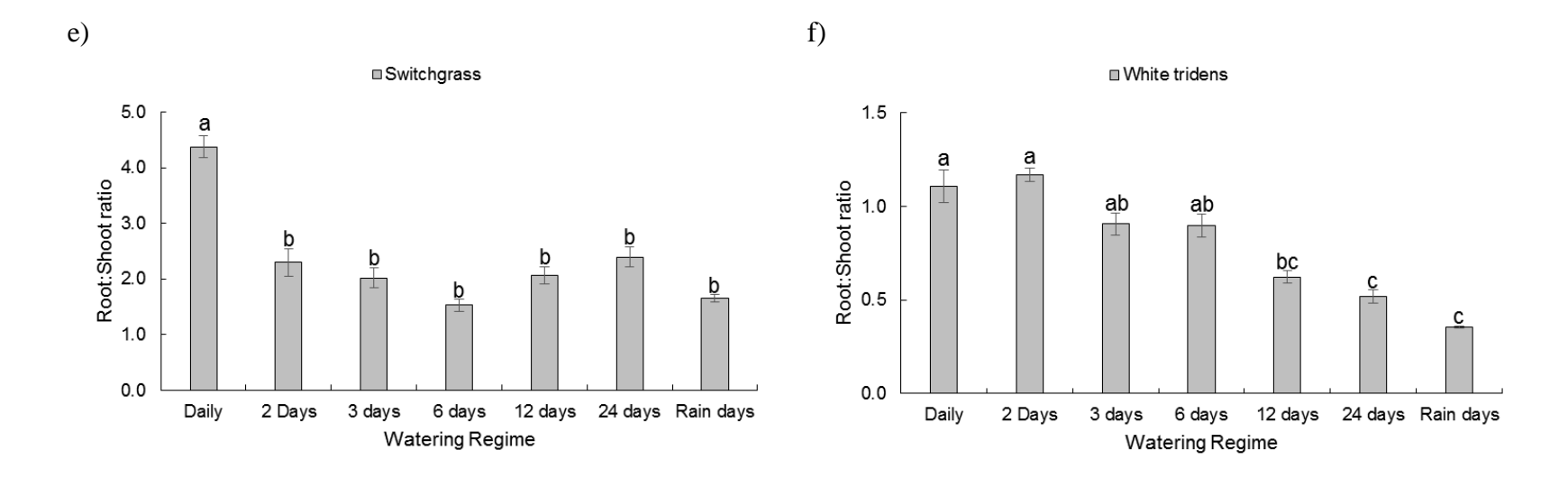
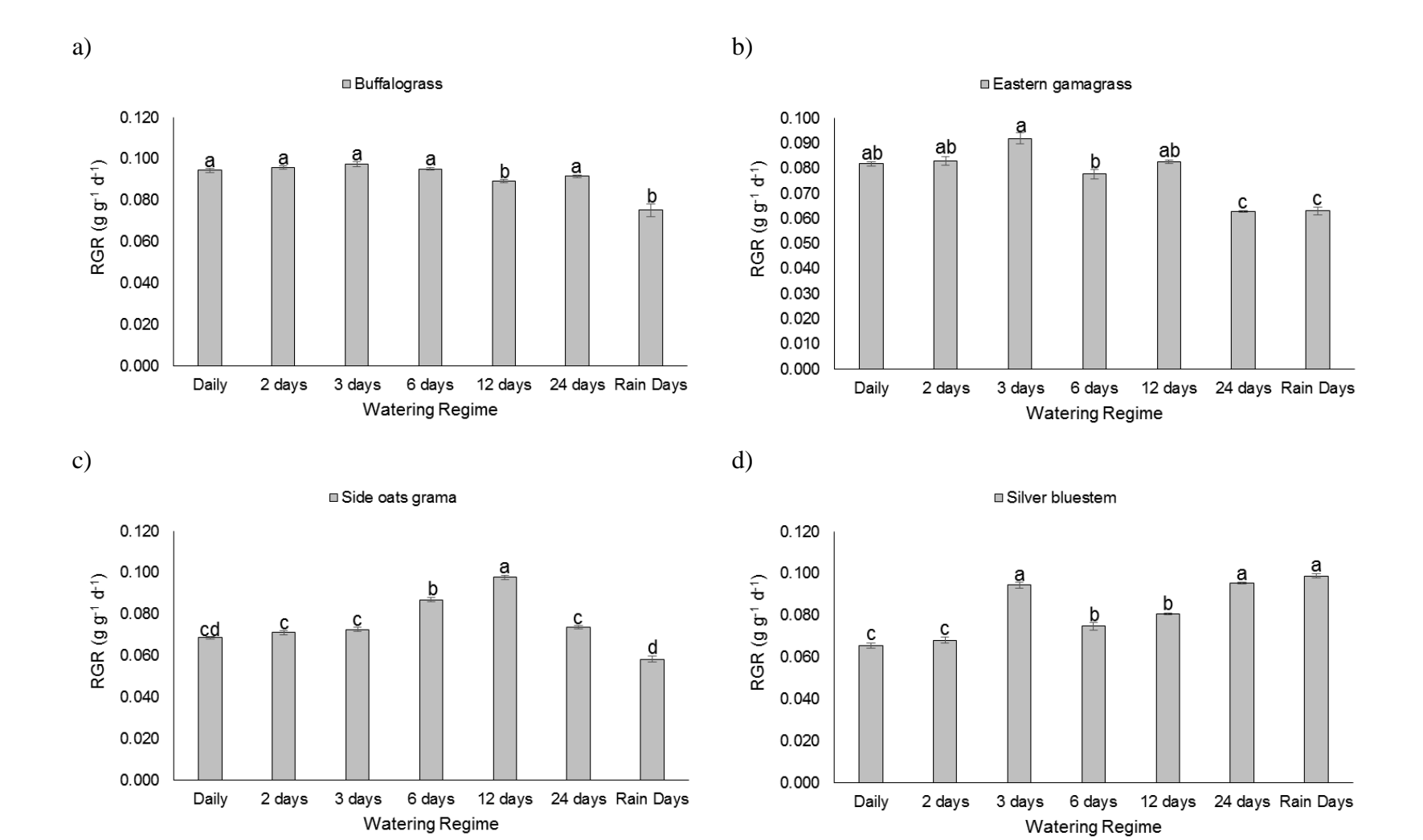


Figure 24. Root-to-shoot ratios in response to variable watering regimes (1-24 days and rain days) for a) buffalograss (F = 1.926, df = 6, P = 0.111), b) eastern gamagrass (F = 3.343, df = 6, P = 0.013), c) sideoats grama (F = 4.788, df = 6, P = 0.002), d) silver bluestem (F = 6.652, df = 6, P < 0.001), e) switchgrass (F = 7.748, df = 6, P < 0.001), and f) white tridens (F = 9.319, df = 6, P < 0.001) grown for 3 months under greenhouse conditions. Different letters indicate significant differences (P < 0.05) based on Tukey's mean separation test. Bars represent standard error.



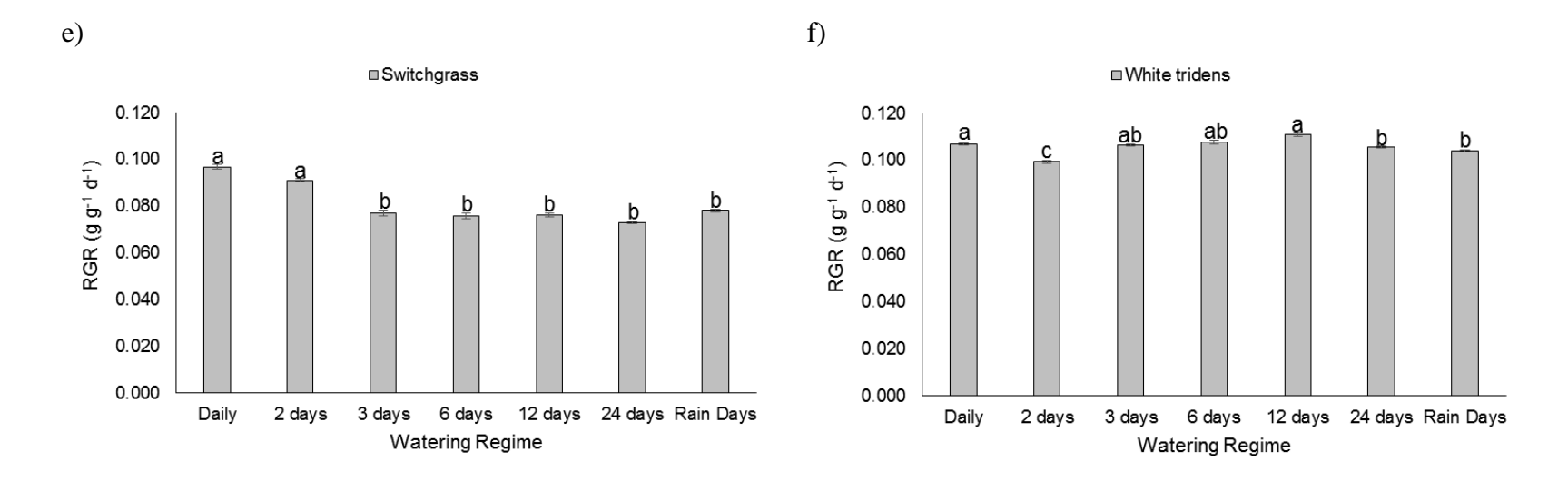
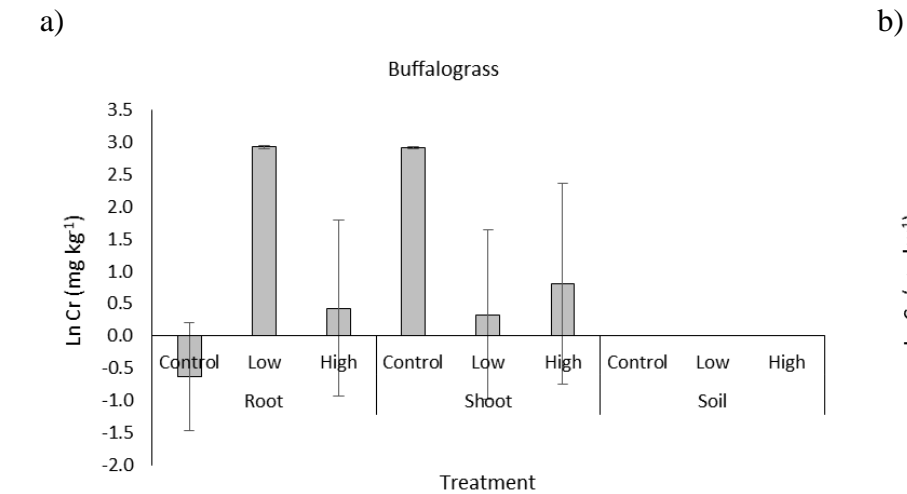
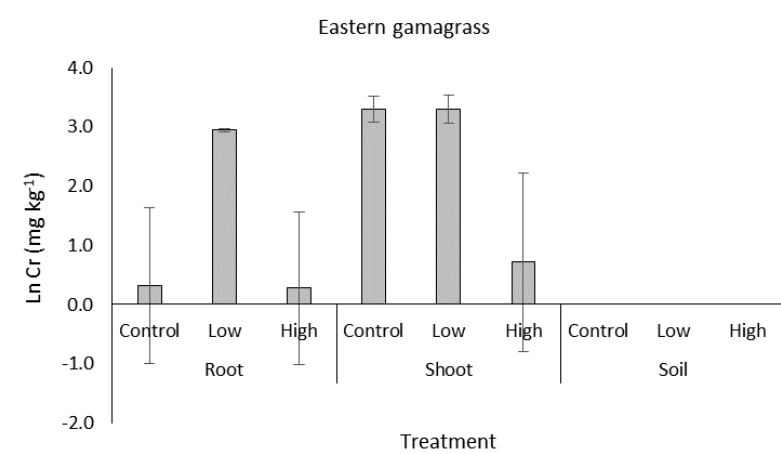
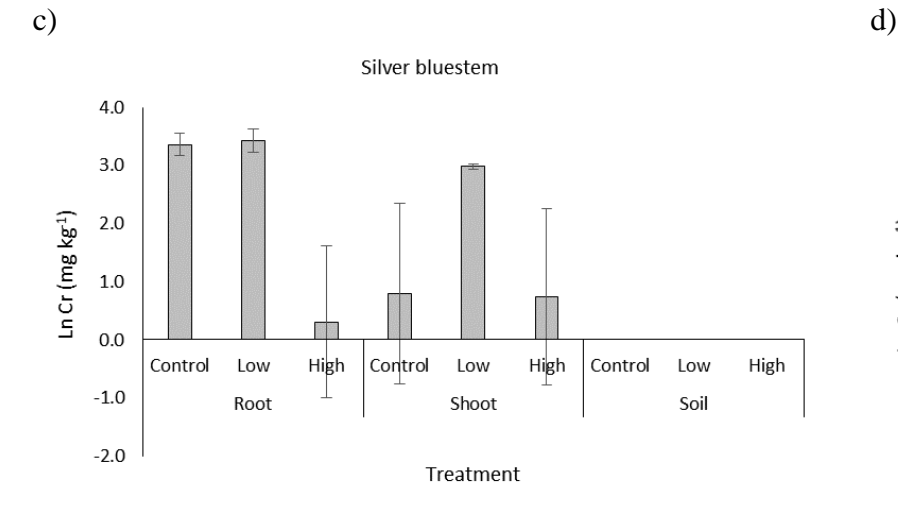
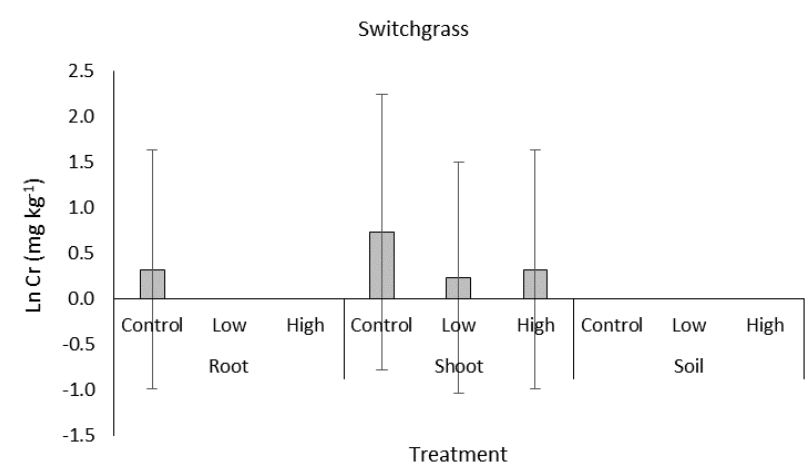


Figure 25. Relative growth rates (RGR; g g⁻¹ d⁻¹) in response to variable watering regimes (1-24 days and rain days) for a) buffalograss (F = 7.67, df = 6, P < 0.001), b) eastern gamagrass (F = 12.99, df = 6, P < 0.001), c) sideoats grama (F = 42.63, df = 6, P < 0.001), d) silver bluestem (F = 34.62, df = 6, P < 0.001), e) switchgrass (F = 25.89, df = 6, P < 0.001), and f) white tridens (F = 9.99, df = 6, P < 0.001) grown for 3 months under greenhouse conditions. Different letters indicate significant differences (P < 0.05) based on Tukey's mean separation test. Bars represent standard error.









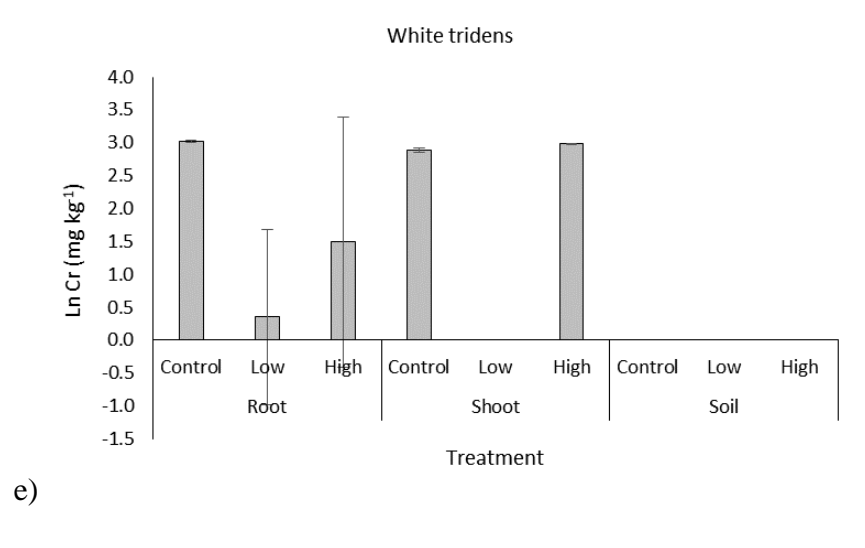
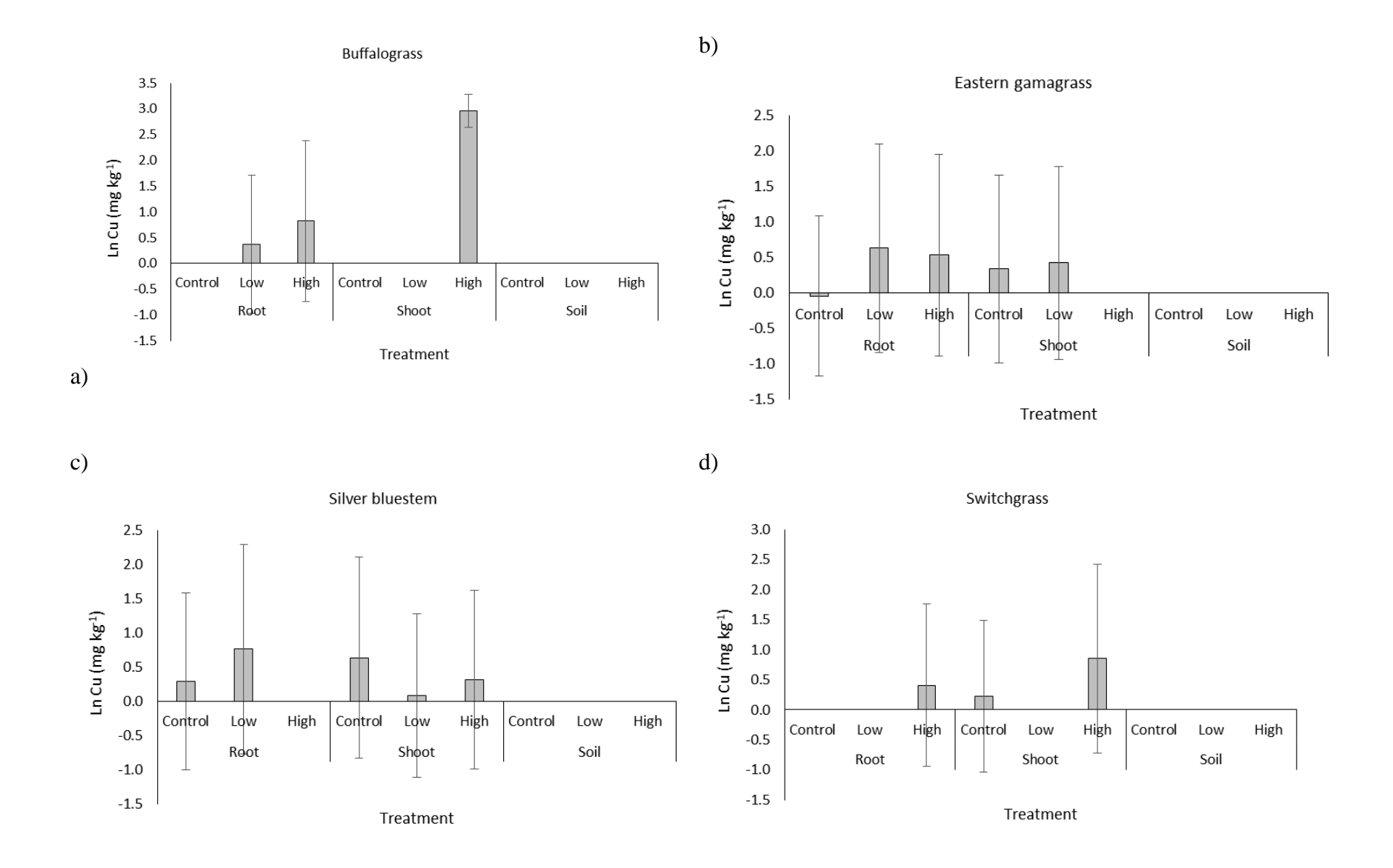


Figure 26. *Ex situ* metal concentrations (ln value) of chromium (Cr) in roots, shoots, and soils for controls (no metal added), low concentration (0.021 mg kg⁻¹), and high concentration (0.106 mg kg⁻¹) for a) buffalograss (H = 8.182, df = 8, P = 0.416), b) eastern gamagrass (H = 10.372, df = 0.240), c) silver bluestem (H = 9.651, df = 0.290), d) switchgrass (H = 6.114, df = 0.290), and e) white tridens (H = 11.571, df = 0.171). Data were ln transformed to improve the variance due to the small sample size (H = 0.182) of each treatment. Bars represent standard error.



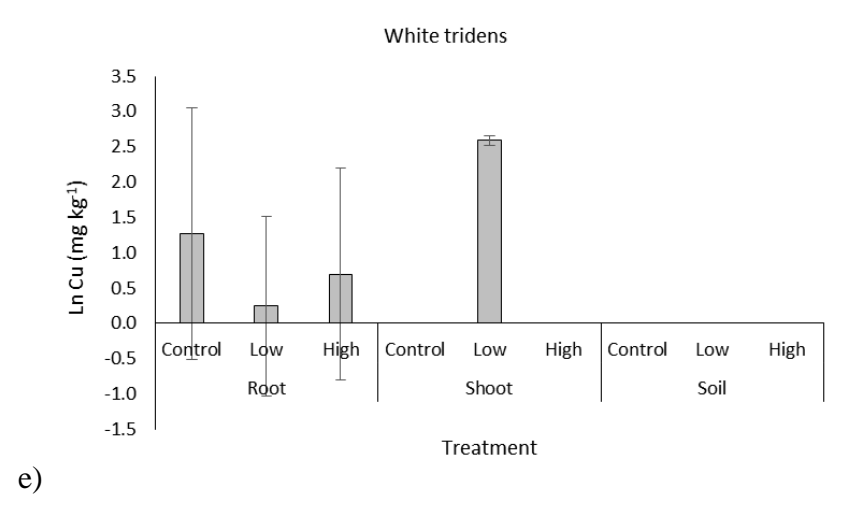
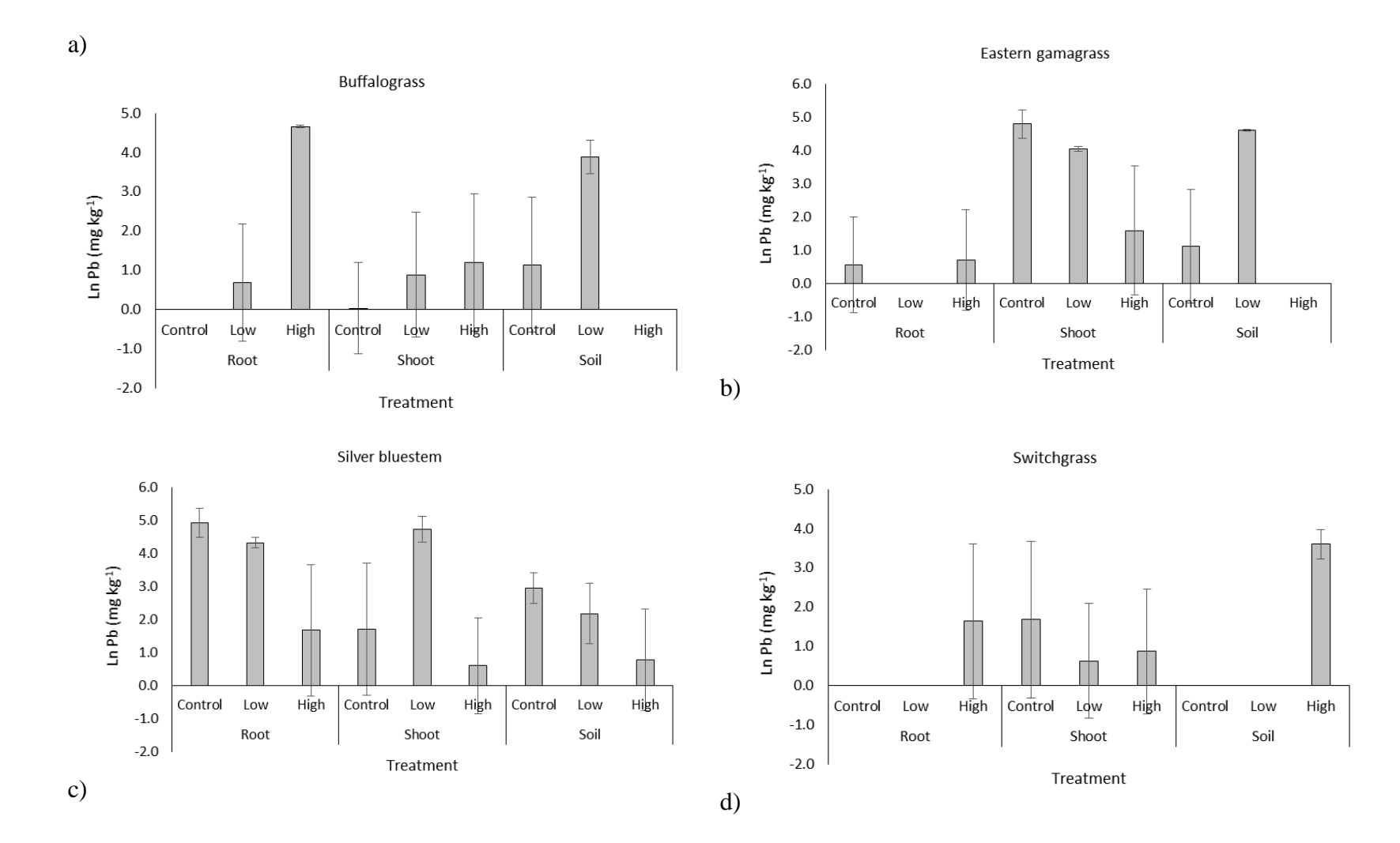


Figure 27. *Ex situ* metal concentrations (ln value) of copper (Cu) in roots, shoots, and soils for controls (no metal added), low concentration (0.101 mg kg⁻¹), and high concentration (0.504 mg kg⁻¹) for a) buffalograss (H = 10.832, df = 8, P = 0.211), b) eastern gamagrass (H = 5.339, df = 8, P = 0.721), c) silver bluestem (H = 5.339, df = 8,


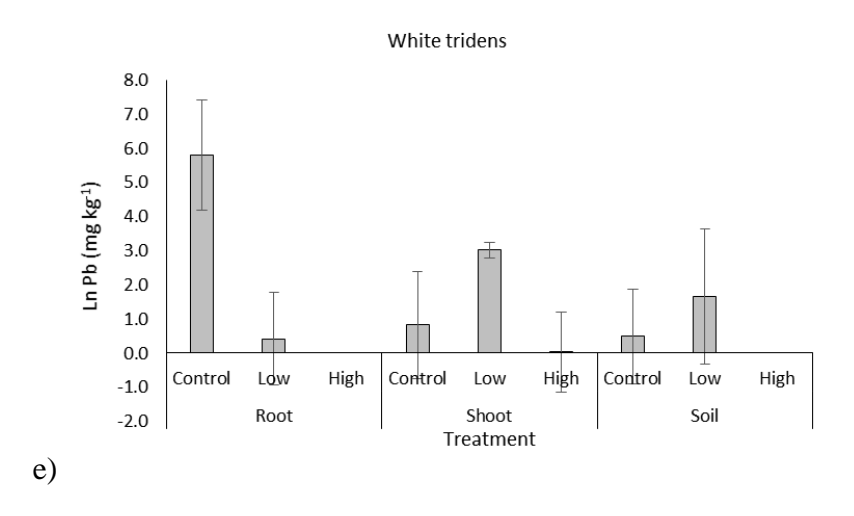


Figure 28. *Ex situ* metal concentrations (ln value) of lead (Pb) in roots, shoots, and soils for controls (no metal added), low concentration (0.052 mg kg⁻¹), and high concentration (0.262 mg kg⁻¹) for a) buffalograss (H = 9.031, df = 8, P = 0.340), b) eastern gamagrass (H = 10.507, df = 8, P = 0.231), c) silver bluestem (H = 7.392, df = 8, P = 0.495), d) switchgrass (H = 7.542, df = 8, P = 0.479), and e) white tridens (H = 7.187, df = 8, P = 0.517). Data were ln transformed to improve the high variance due to the small sample size (n = 2) of each treatment. Bars represent standard error.

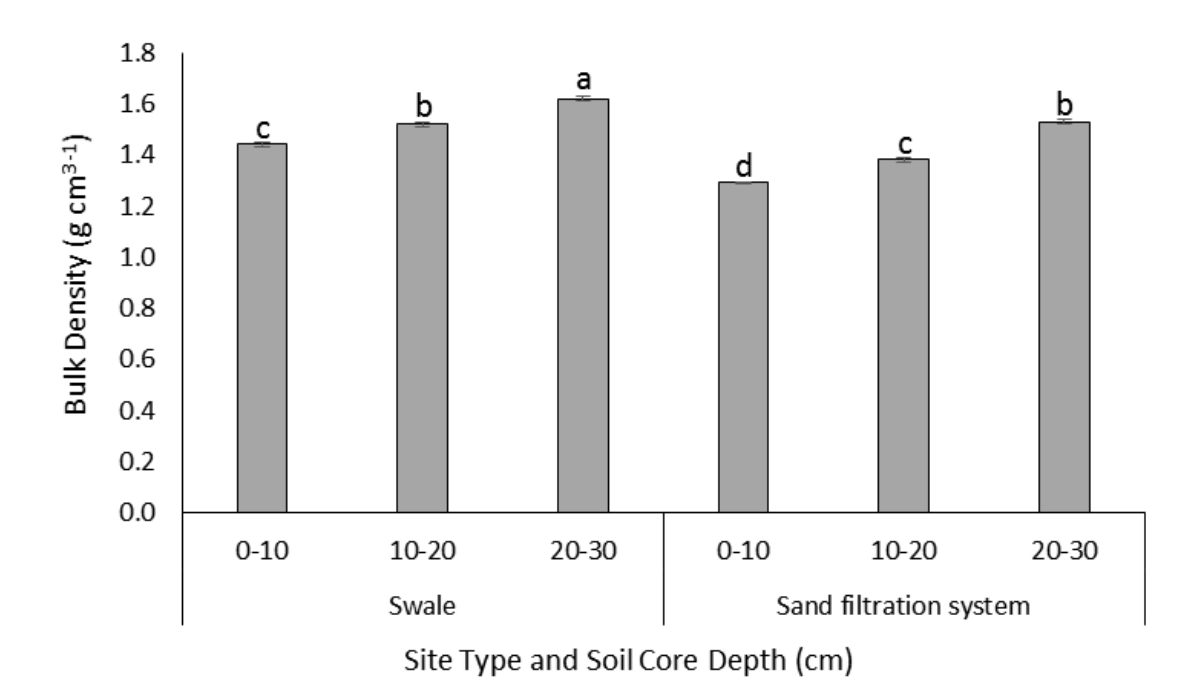


Figure 29. Soil bulk densities taken from soil cores at depths of 0-10, 10-20, and 20-30 cm in swales and sand filtration systems. Different letters indicate significant differences based on a one-way ANOVA (F = 52.22, df = 5, P < 0.001) and Tukey's mean separation test (P < 0.05). Bars represent standard error.

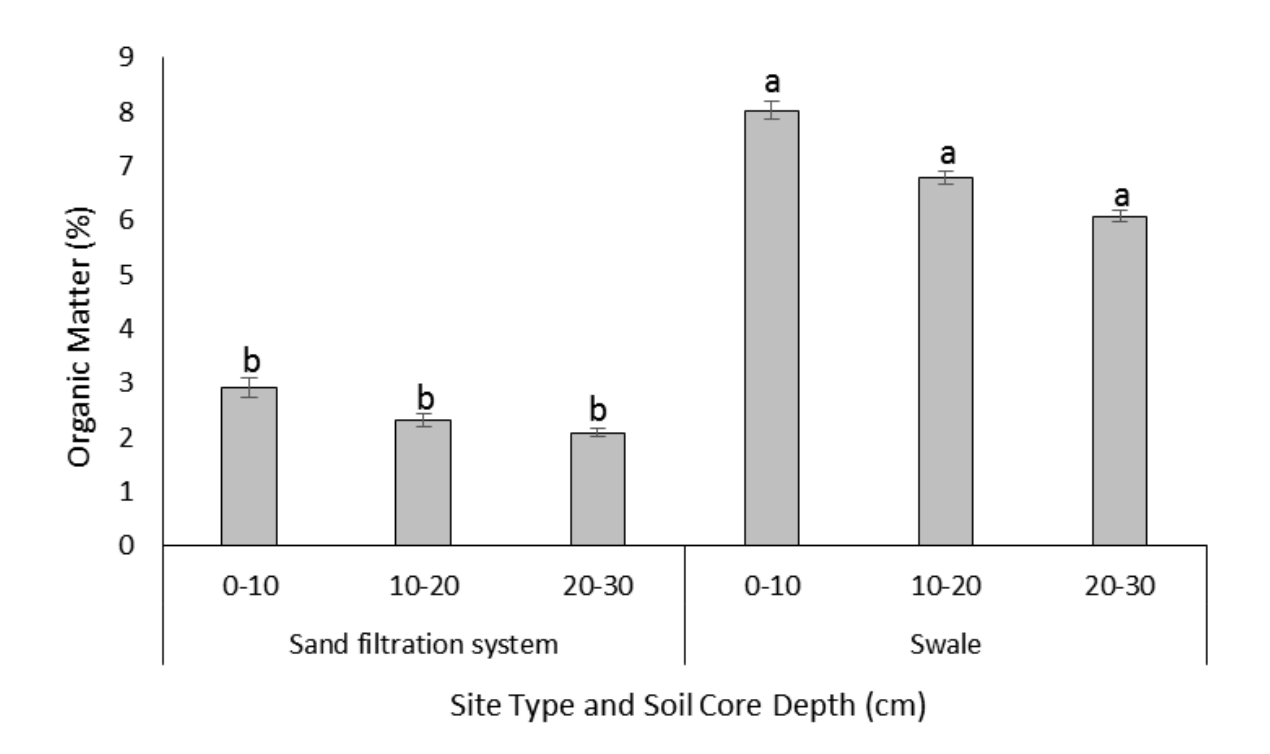


Figure 30. Soil organic matter (%) taken from soil cores at depths of 0-10, 10-20, and 20-30 cm in swales and sand filtration systems. Different letters indicate significant differences based on a Kruskal-Wallis non-parametric ANOVA (H = 312.58, df = 5, P < 0.001) and Tukey's mean separation test (P < 0.05). Bars represent standard error.

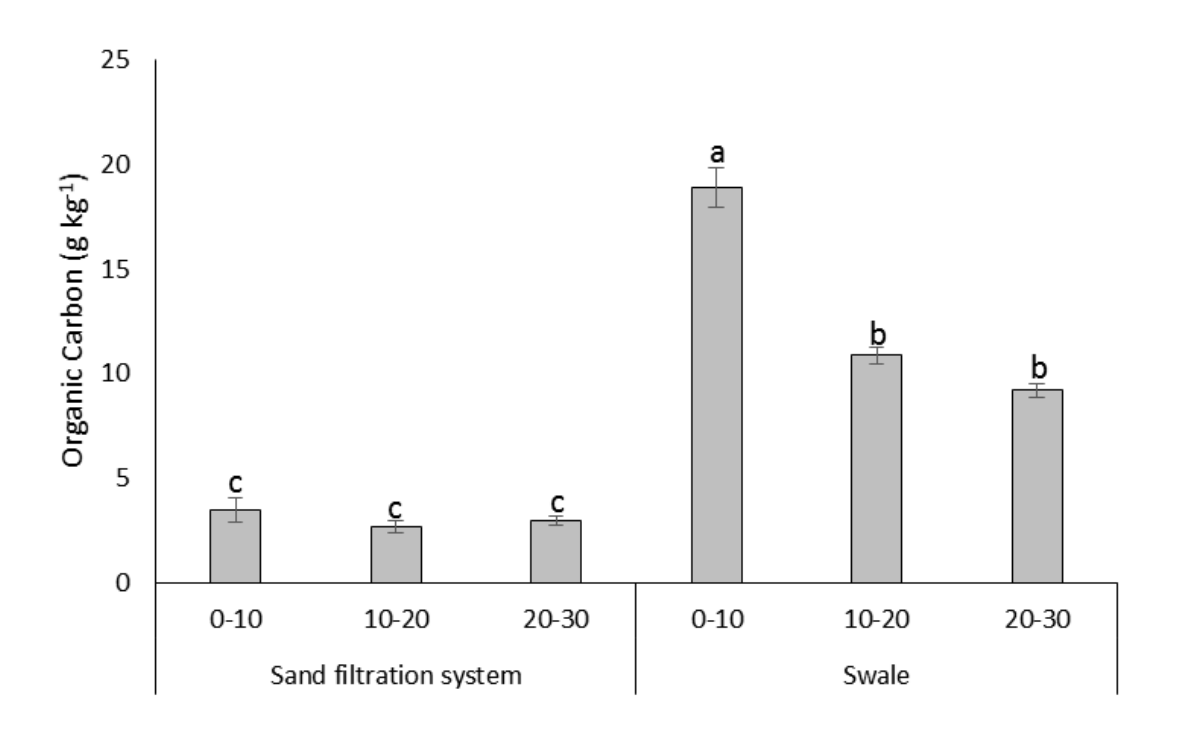


Figure 31. Soil organic carbon (g kg $^{-1}$) taken from soil cores at depths of 0-10, 10-20, and 20-30 cm in swales and sand filtration systems. Different letters indicated significant differences based on a one-way ANOVA (F = 49.62, df = 5, P < 0.001) and Tukey's mean separation test (P < 0.05). Bars represent standard error.

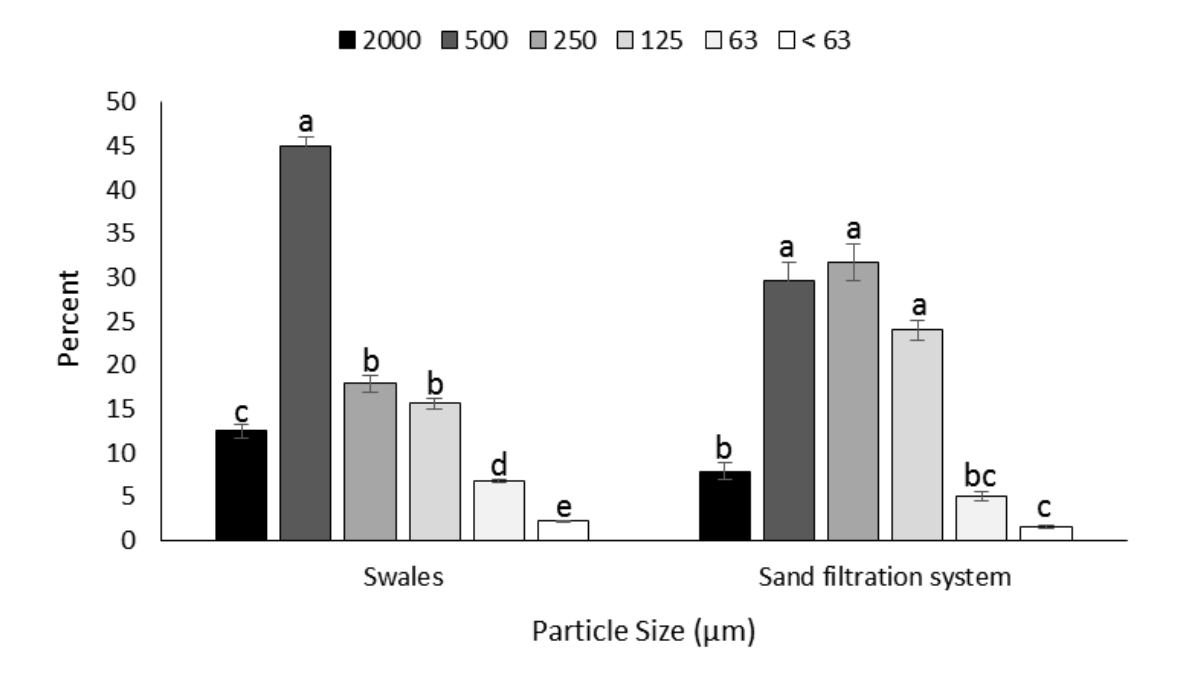
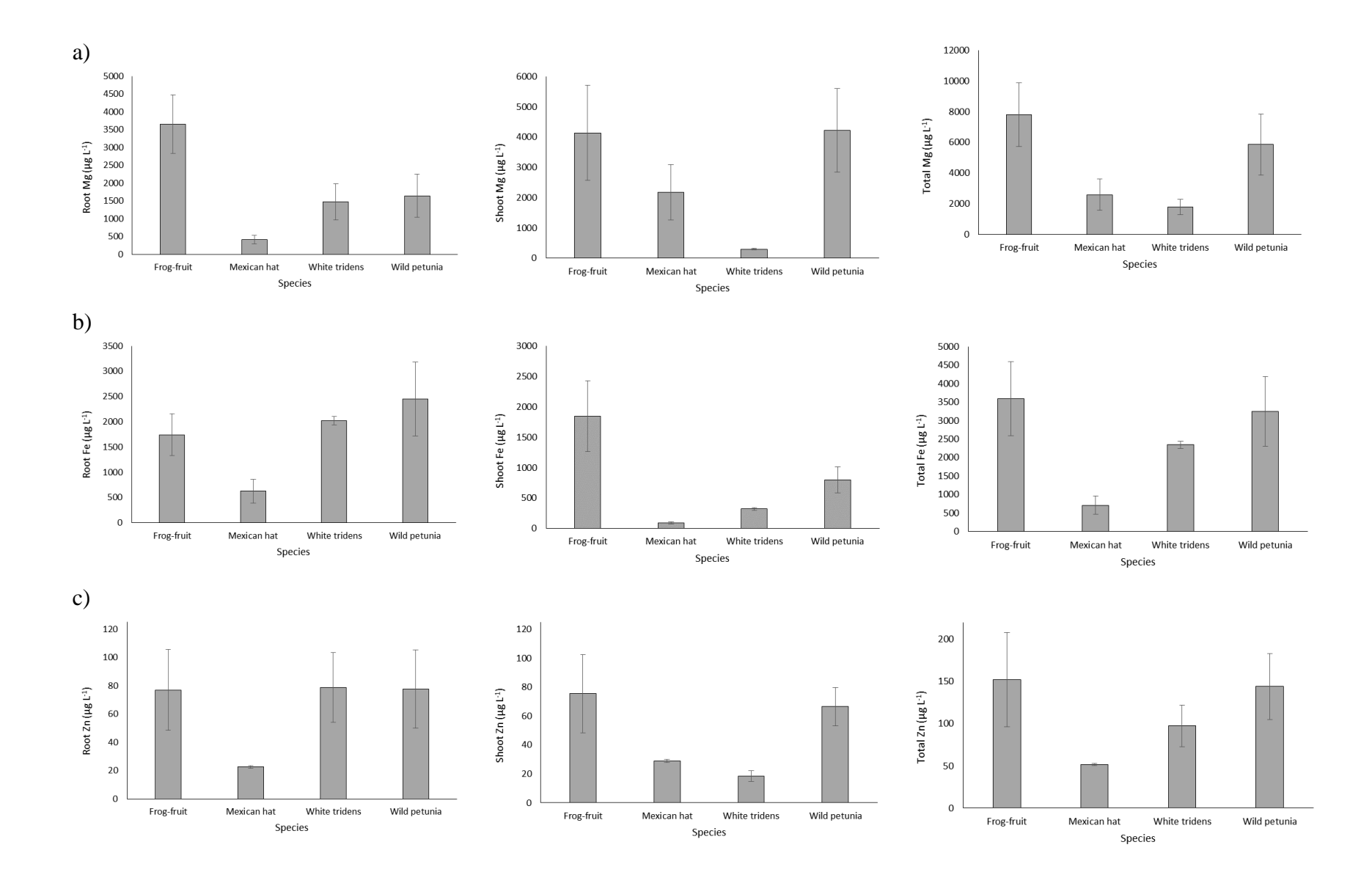
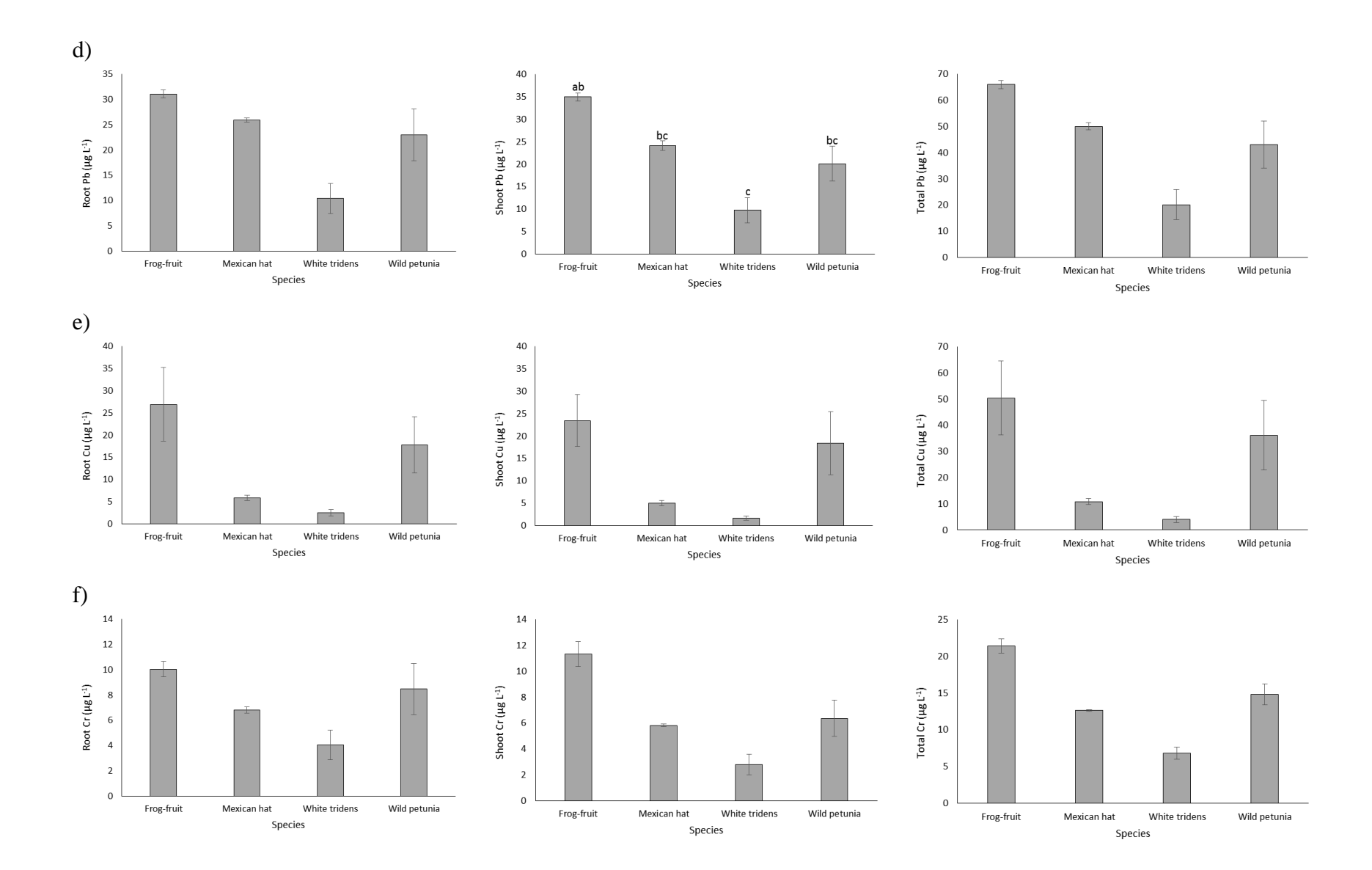


Figure 32. Percent sediment particle size (μ m) among sieve sizes ranging from < 63 to 2000 μ m form soil core in swales (H = 525.9, df = 5, P < 0.001) and sand filtration systems (H = 464.8, df = 5, P < 0.001). Letters represent significant differences at P < 0.05. Bars represent standard error.





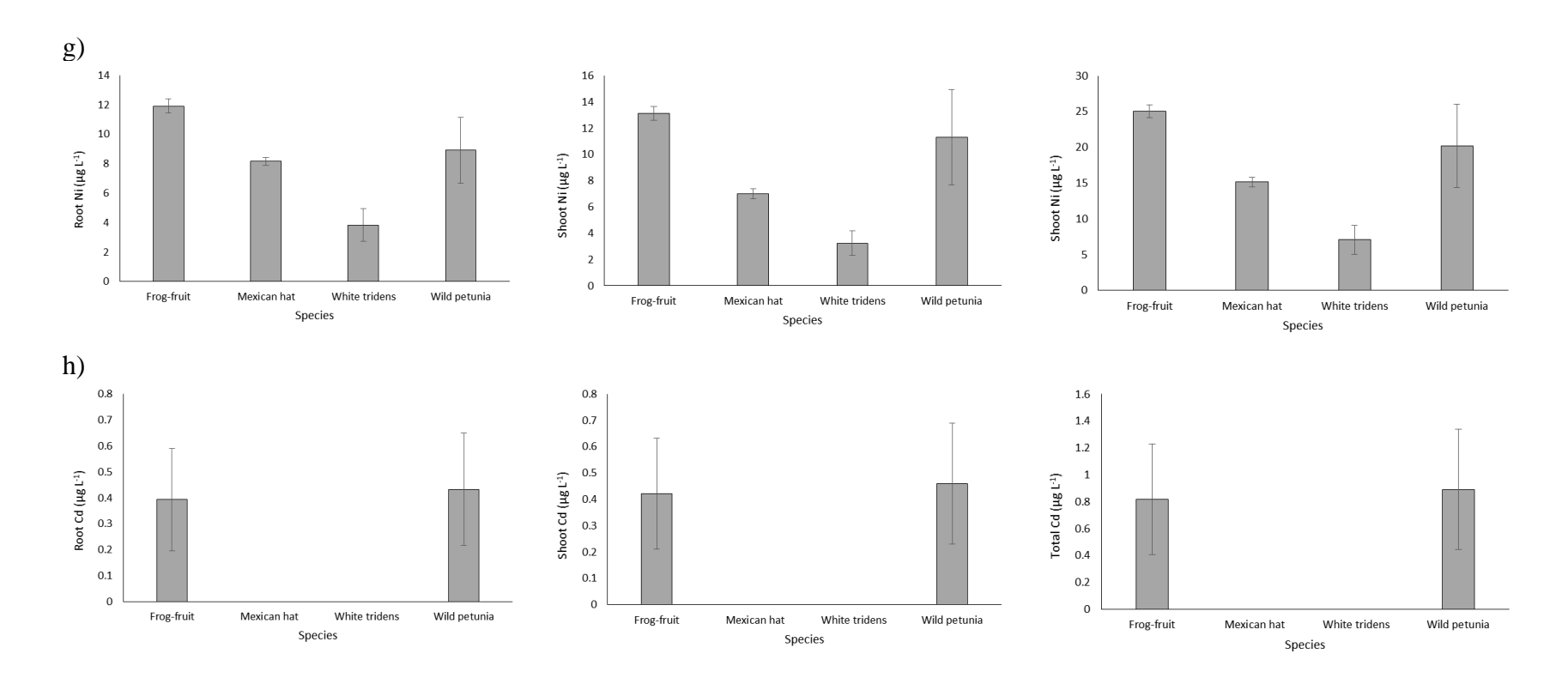


Figure 33. Concentrations of metal uptake in the roots, shoots, and total (left to right) for a) magnesium, b) iron, c) zinc, d) lead, e) copper, f) chromium, g) nickel, and h) cadmium for frog-fruit (*Phyla nodiflora*), Mexican hat (*Ratibida columnifera*), white tridens (*Tridens albescens*), and wild petunia (*Ruellia nudiflora*). The only significant difference was for lead detected in shoots (F = 4.11, df = 3, P = 0.035). All other statistical tests were not significant (P > 0.05). Lines represent standard error.

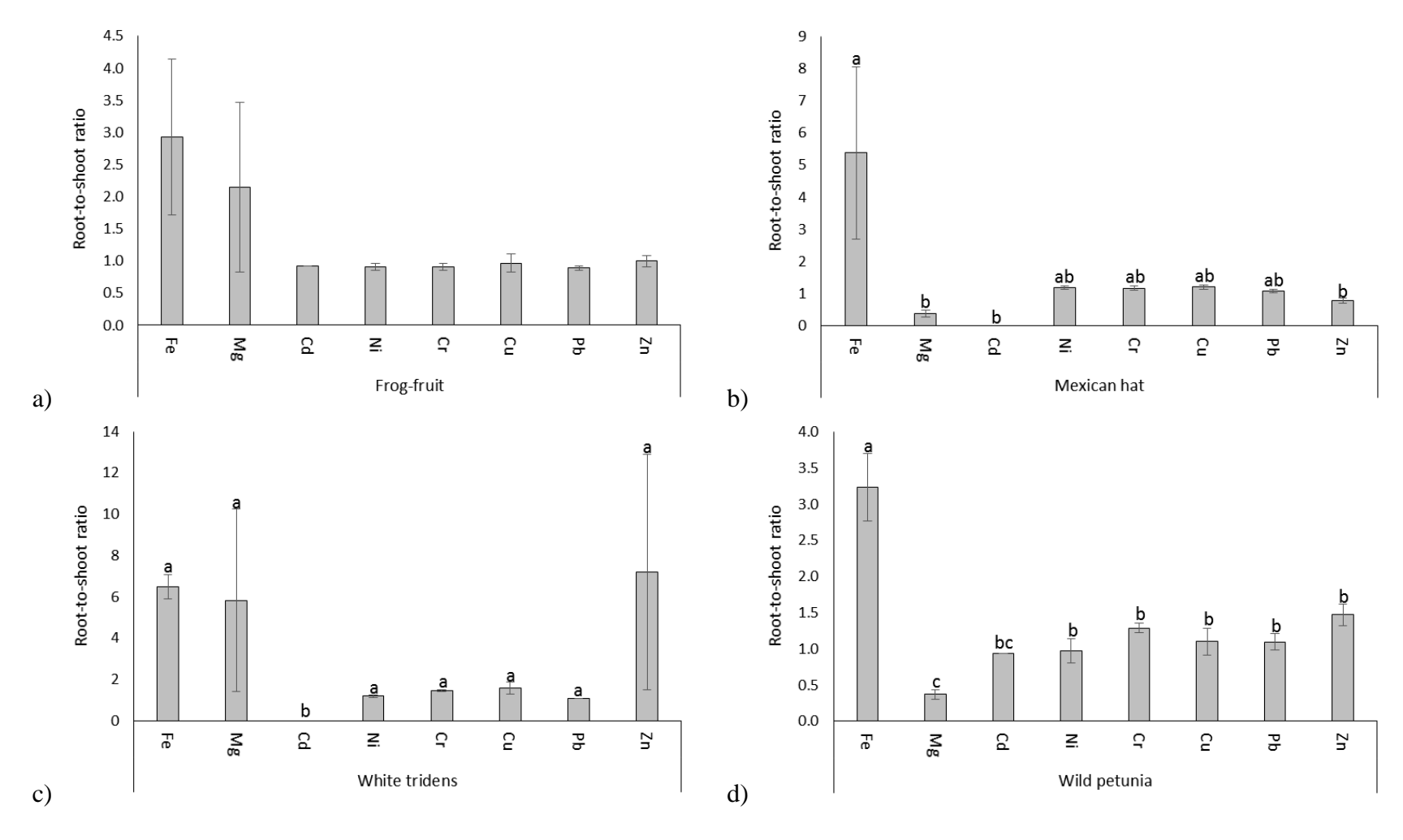
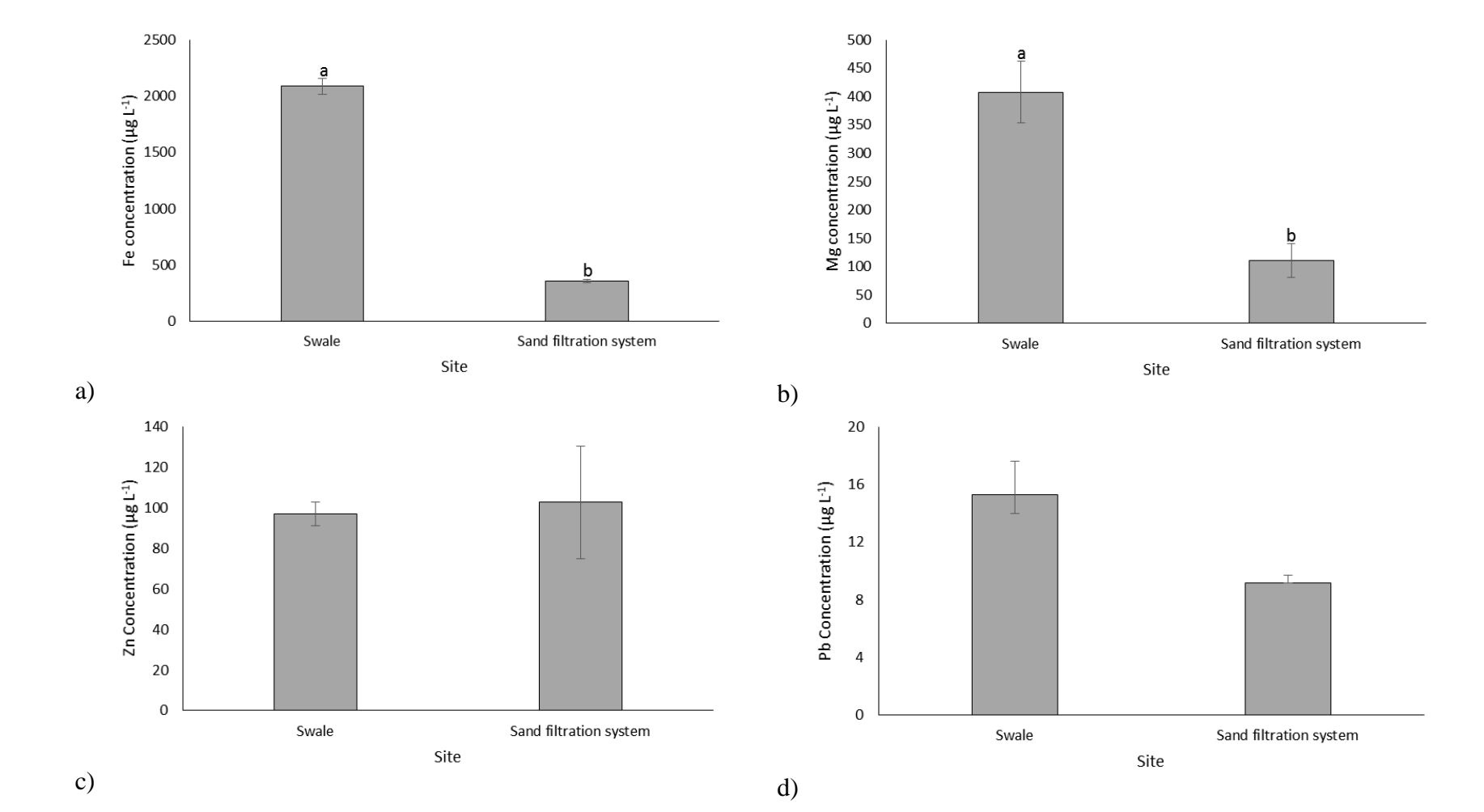


Figure 34. The root-to-shoot ratios of eight metals in a) frog-fruit (H = 1.897, df = 7, P = 0.965), b) Mexican hat (F = 19.118, df = 6, P < 0.001), c) white tridens (F = 7.576, df = 6, P = 0.002), and d) wild petunia (F = 22.322, df = 6, P < 0.001). Different letters indicate significant differences at P < 0.05. Lines represent standard error bars.



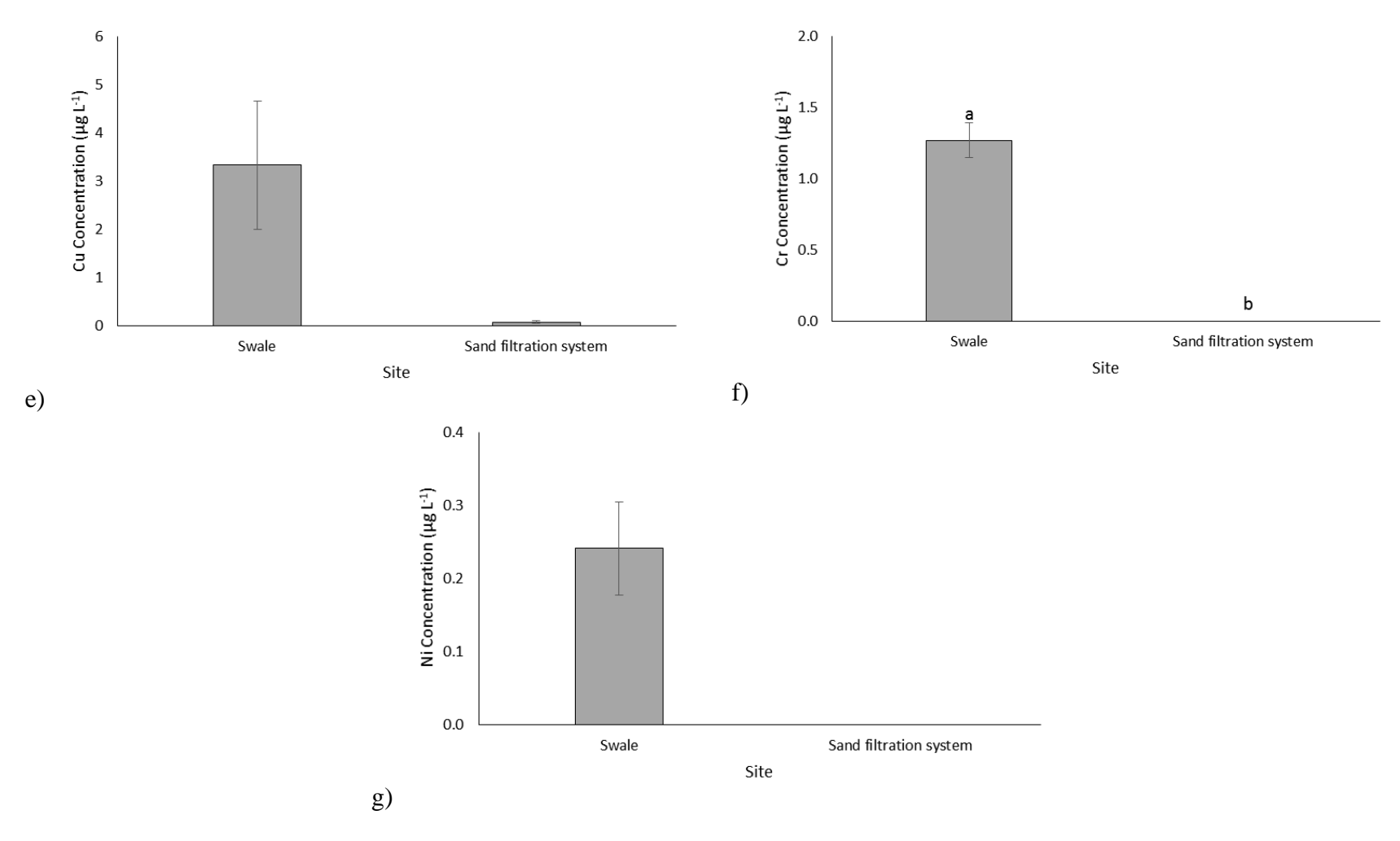
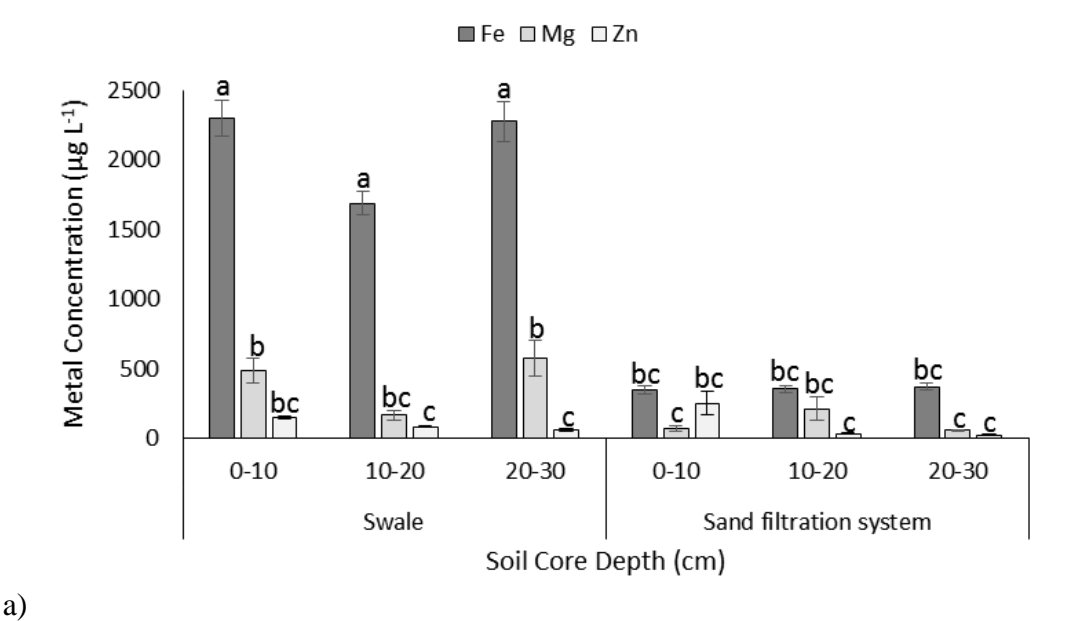


Figure 35. Mean metal concentration (μ g L⁻¹) in sand filtration systems and swale soils for a) Fe (t = 11.66, df = 106, P < 0.001), b) Mg (t = 2.42, df = 106, P = 0.017), c) Zn (t = -0.101, df = 106, P = 0.92), d) Pb (t = 1.29, df = 106, P = 0.199), e) Cu (t = 1.22, df = 106, P = 0.224), f) Cr (t = 5.18, df = 106, P < 0.001), and g) Ni (t = 1.88, df = 106, P = 0.062). Cadmium (Cd) was not detected in the soil samples from sand filtration systems or swales. Different letters represent significant differences at P < 0.05 and lines represent standard error.



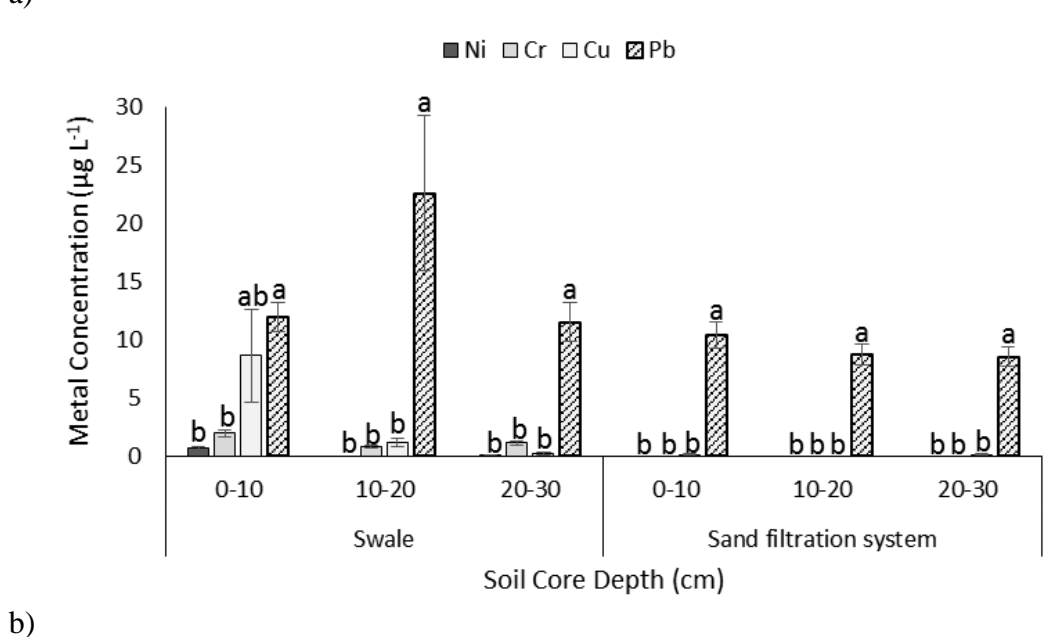


Figure 36. Soil metal concentrations ($\mu g \ L^{-1}$) in sand filtration systems and swale at depths of 0-10, 10-20, and 20-30 cm for concentrations a) $> 50 \ \mu g \ L^{-1}$ (H = 203.8, df = 17, P < 0.001) and b) $< 50 \ \mu g \ L^{-1}$ (H = 175.7, df = 23 degrees, P < 0.001). Different letters represent difference at P < 0.05 and lines represent standard error.

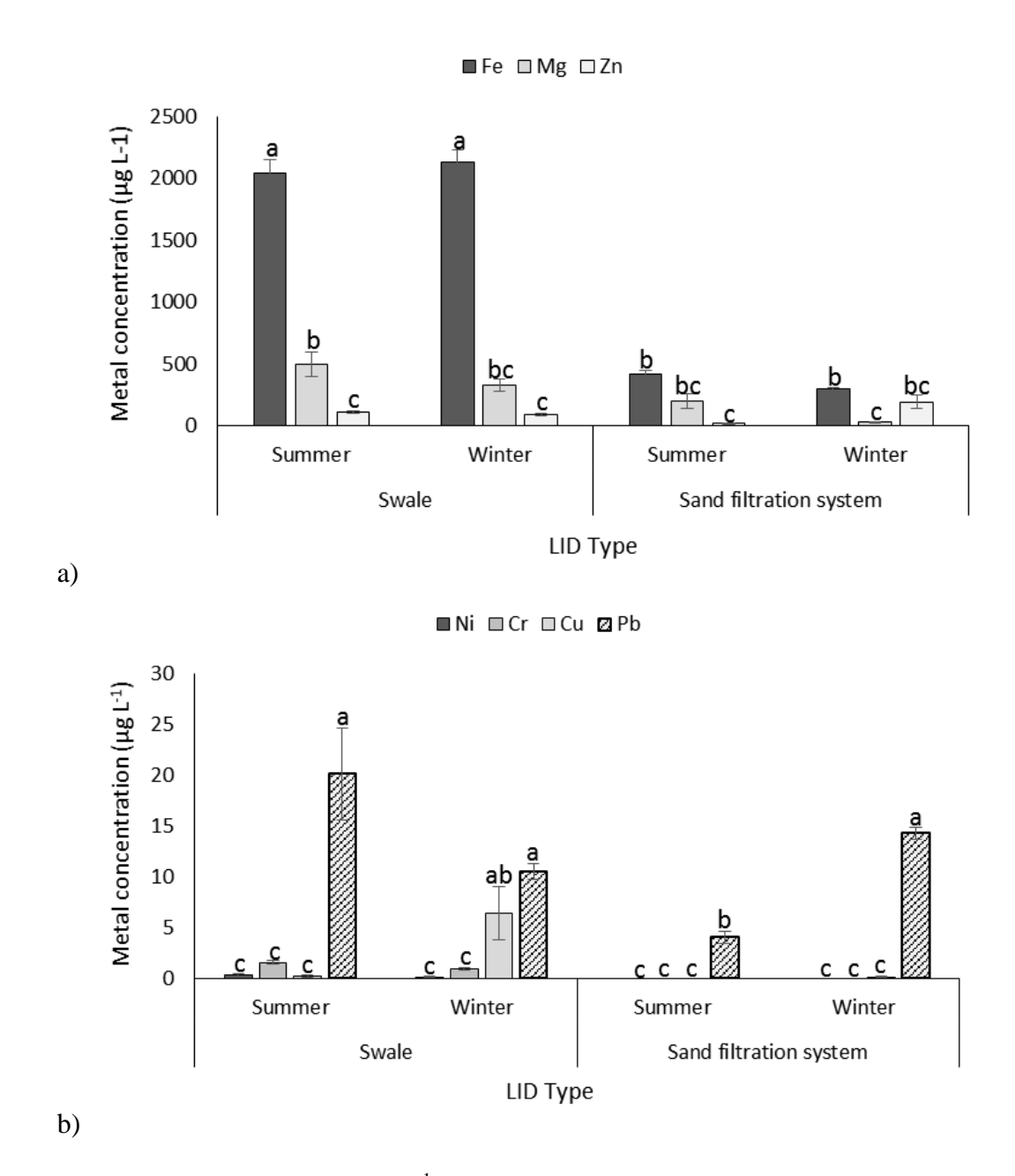
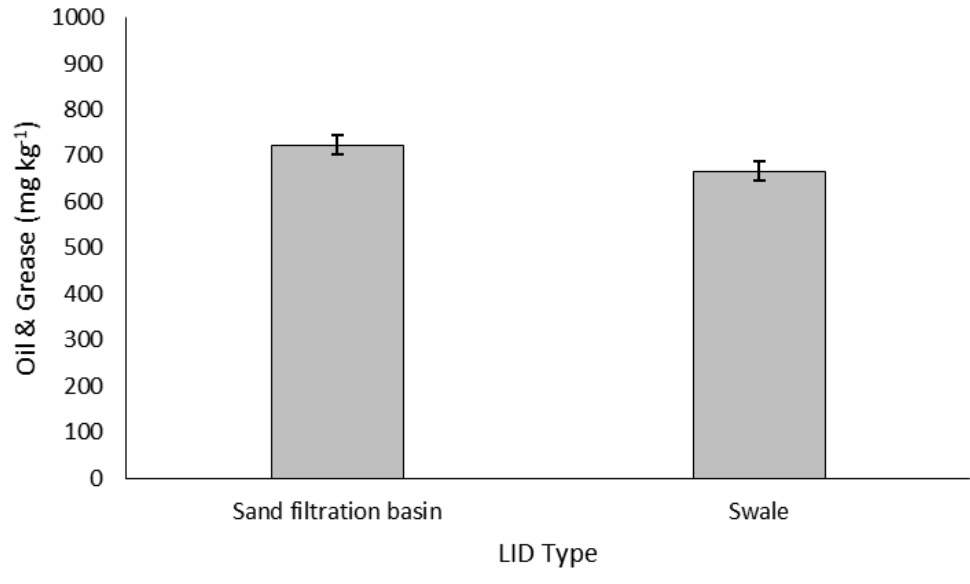


Figure 37. Concentrations ($\mu g \ L^{-1}$) of metals in sand filtration systems and swales by season (summer and winter) for a) concentrations $> 50 \ \mu g \ L^{-1}$ (H = 208.04, df = 11, P < 0.001) and b) concentrations $< 50 \ \mu g \ L^{-1}$ (H = 206.84, df = 15, P < 0.001). Different letters indicate significant differences at P < 0.05. Lines represent standard error.



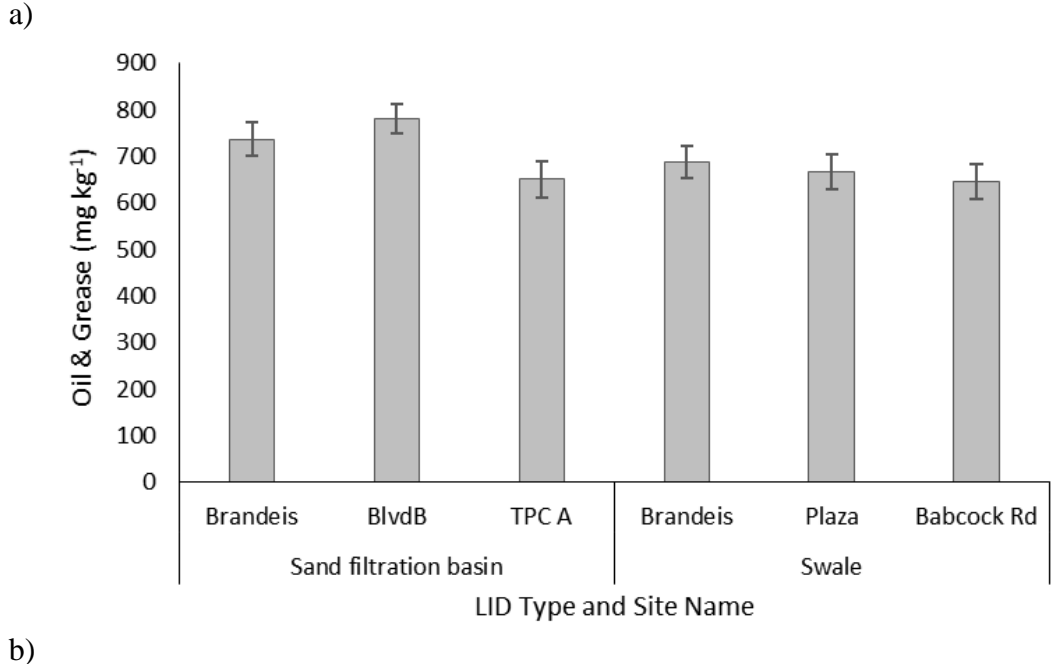
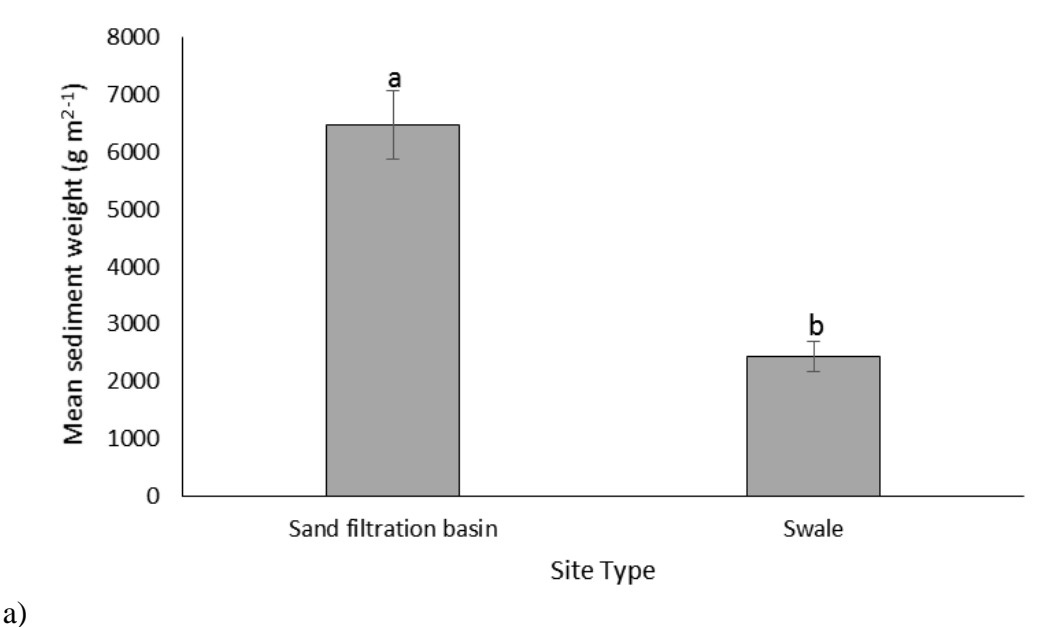


Figure 38. Oil and grease concentration (mg kg $^{-1}$) collected from runoff sediment for a) LID type (t stat = 0.945, df = 142, P = 0.34) and b) sample location (inlet, middle, and outlet) within LID type (F = 0.523, df = 5, P = 0.76). Bars represent standard error.



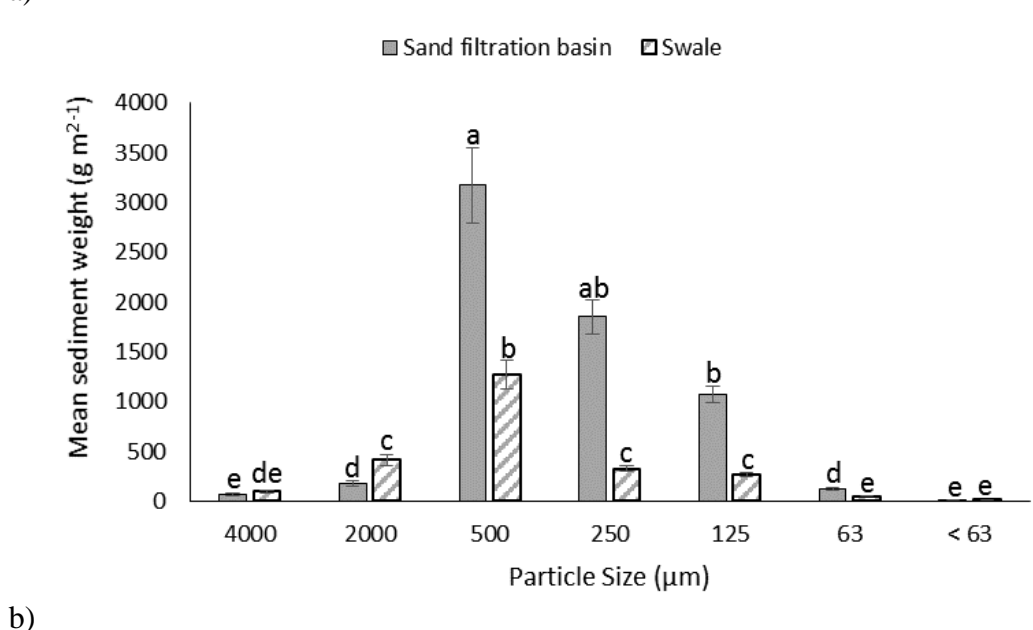


Figure 39. Mean a) total sediment weight (g m 2 - 1) by particle size collected from precipitation runoff in swales and sand filtration systems (t-value = 1.97, df = 142, P < 0.002) for oil and grease analysis, and b) weight of sediment (g m 2 - 1) by particle size collected from precipitation runoff in swales and sand filtration systems (H = 586.964, df = 13, P < 0.001) for oil and grease analysis. Different letters indicate significant differences at P < 0.05. Bars represent standard error.

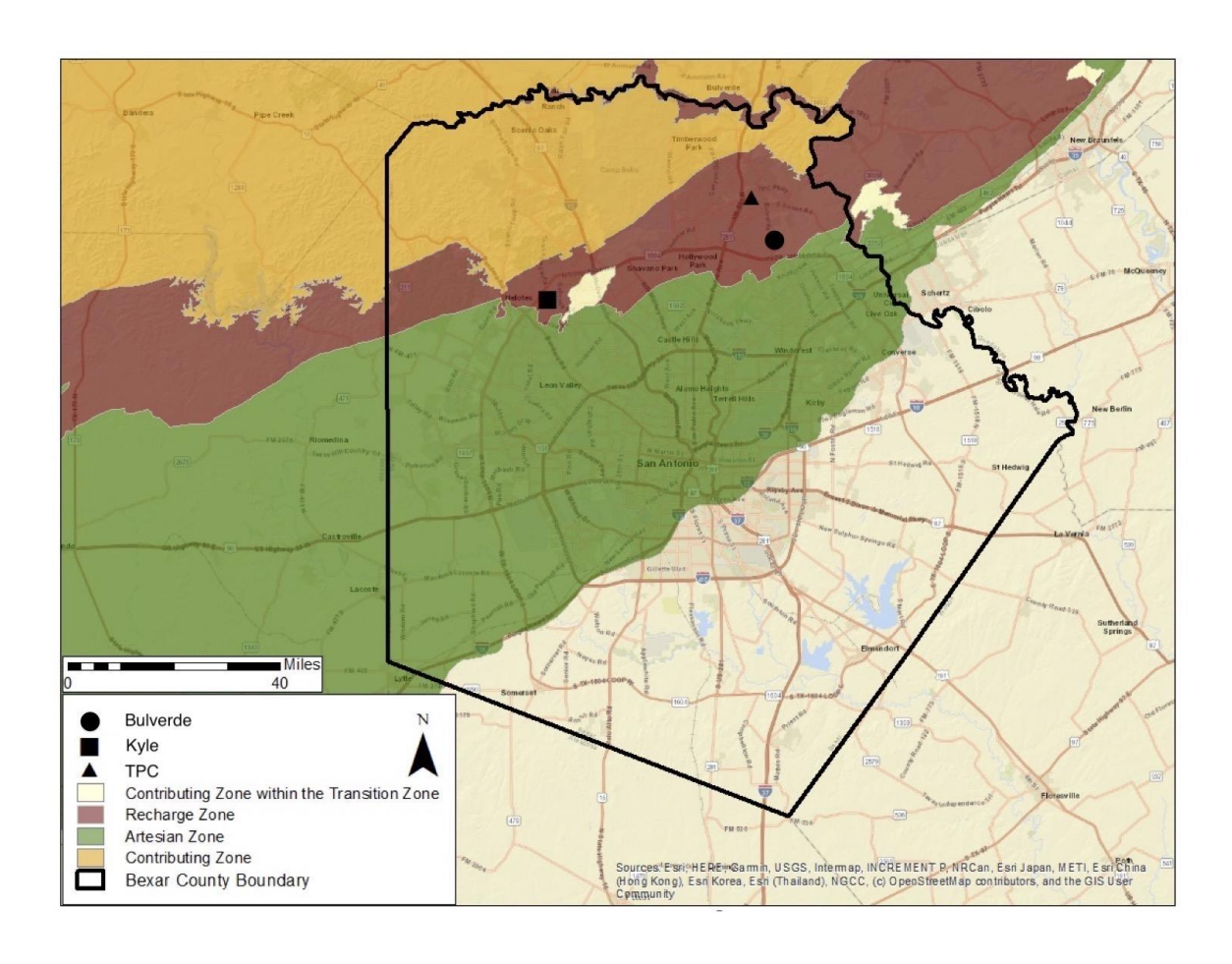


Figure 40. Study sites' location in Bexar County and the Edwards Aquifer zones.

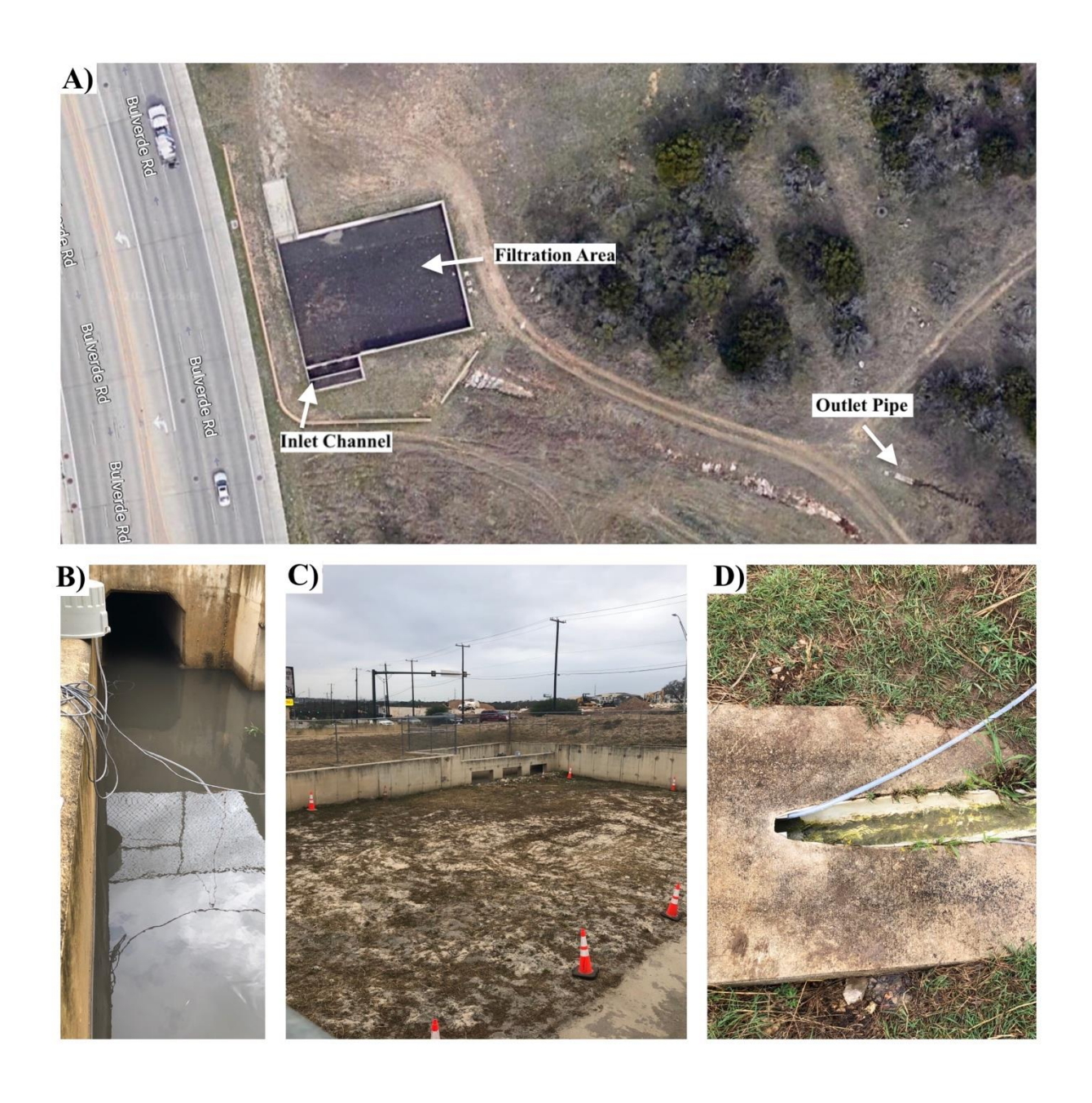


Figure 41. Bulverde Basin A) plan view image of Bulverde site with the inlet channel, filtration area and outlet pipe B) inlet channel C) basin filtration area D) Outlet pipe.

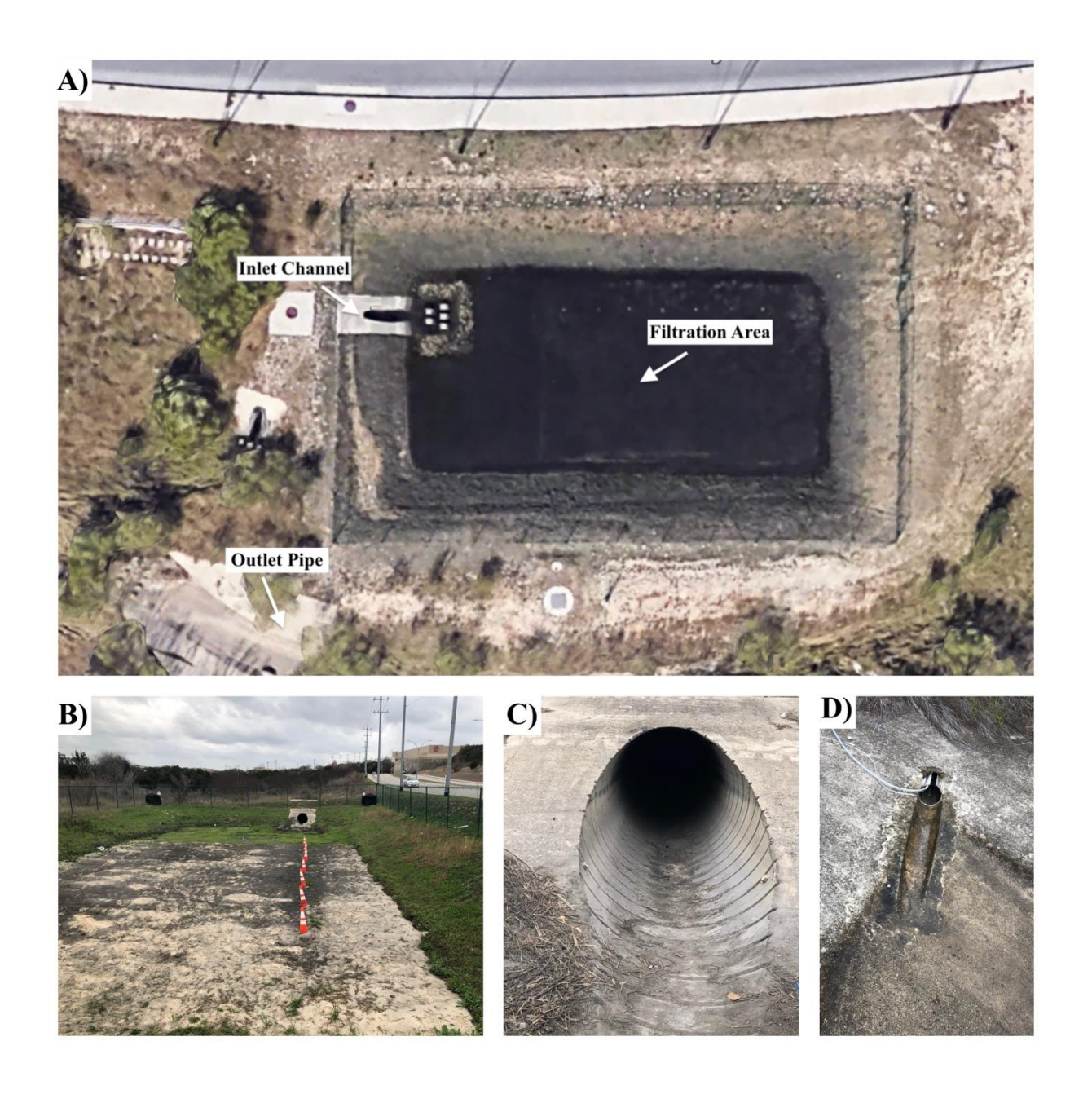


Figure 42. TPC Basin A) plan view image of TPC site with the inlet channel, filtration area and outlet pipe B) the view from the inside of the basin C) inlet channel D) Outlet pipe.

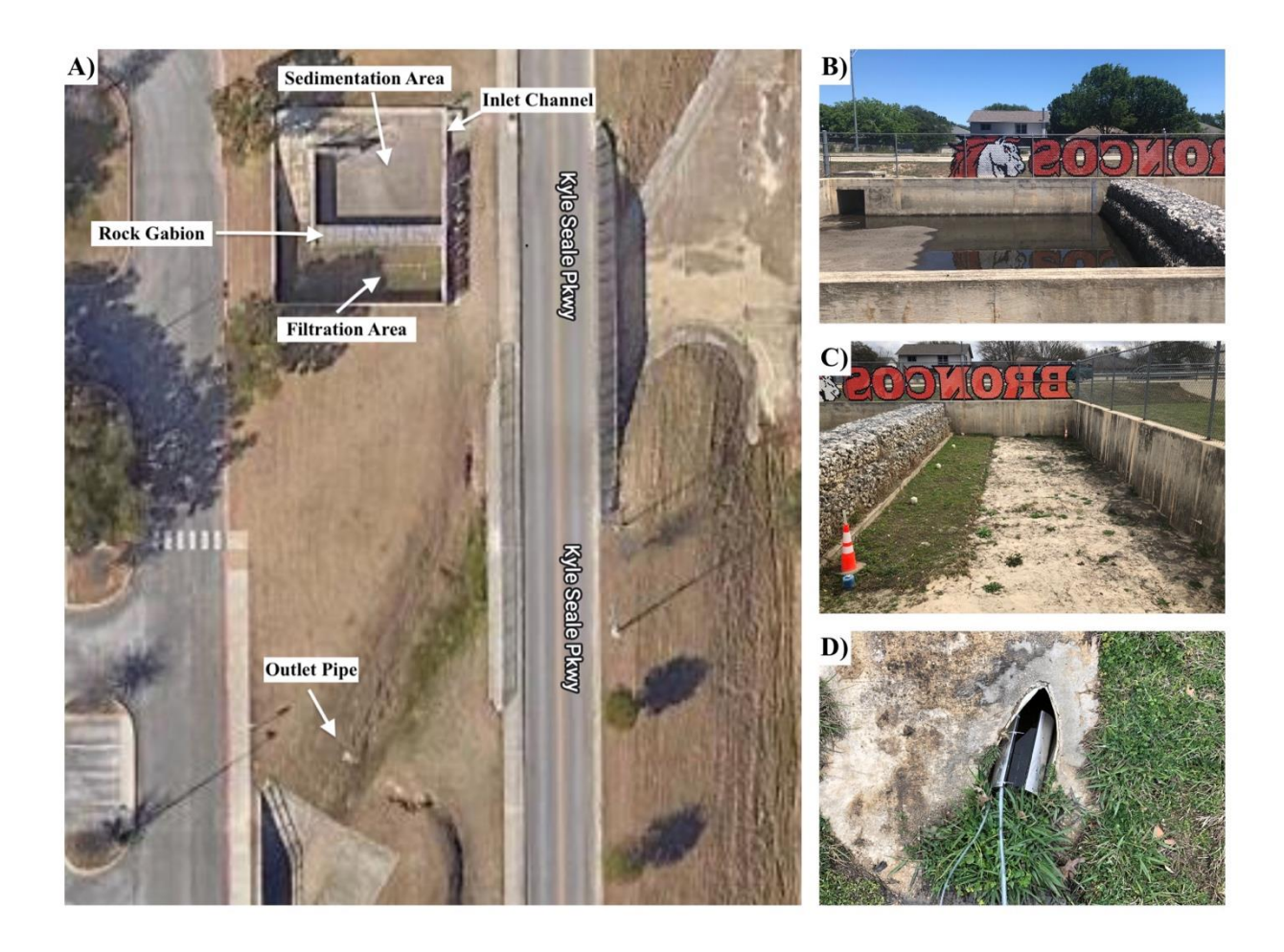


Figure 43. Kyle Basin A) plan view image of Kyle site with the inlet channel, sedimentation area, filtration area, rock gabion and outlet pipe B) sedimentation area and inlet channel C) filtration area and rock gabion D) Outlet pipe.

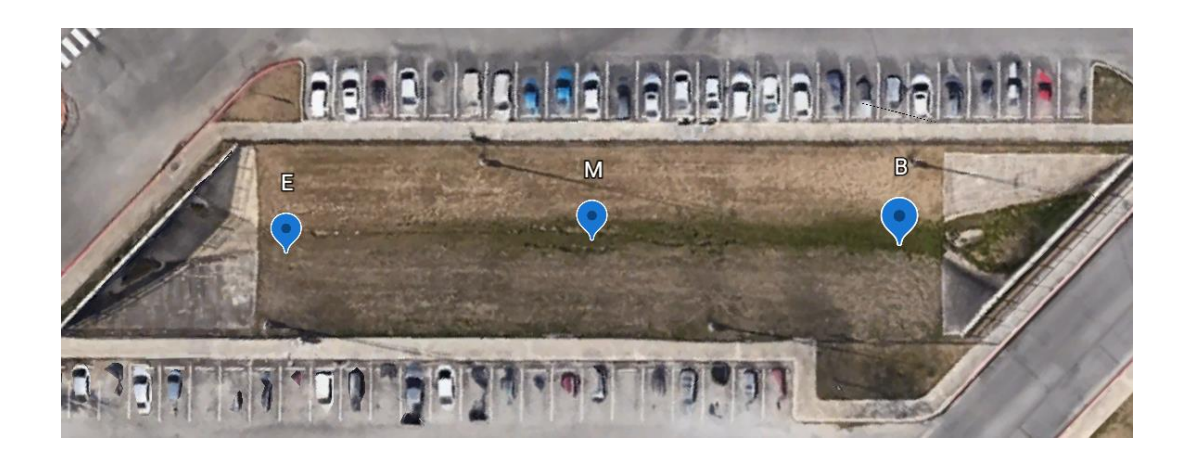


Figure 44. Kyle Seale swale.



Figure 45. The Plaza swale.



Figure 46. Roadrunner Way swale.

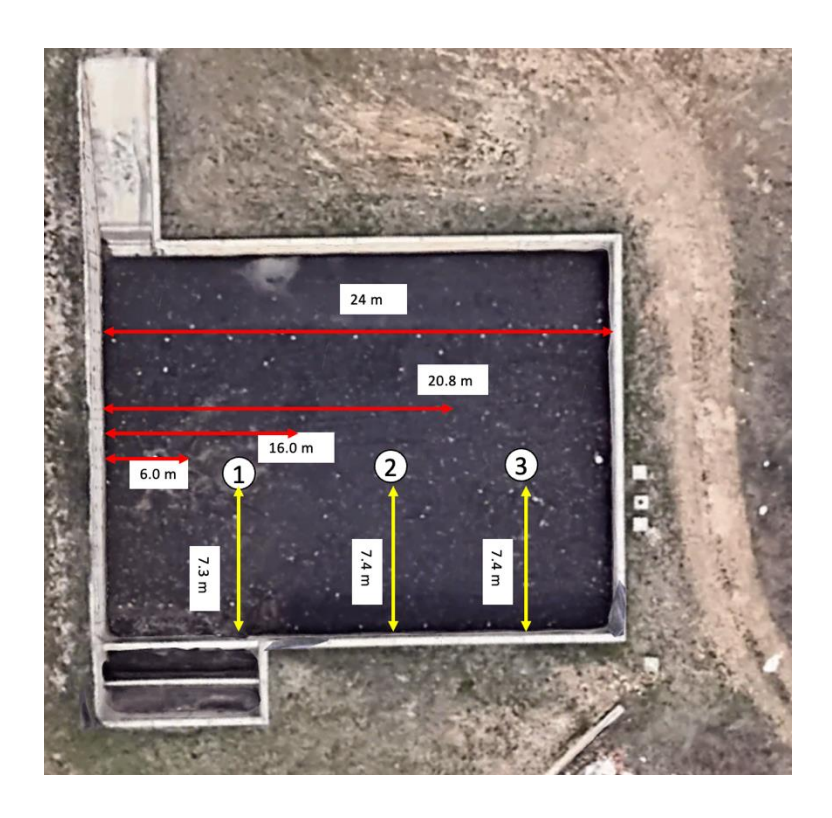


Figure 47. Bulverde Basin soil core locations.

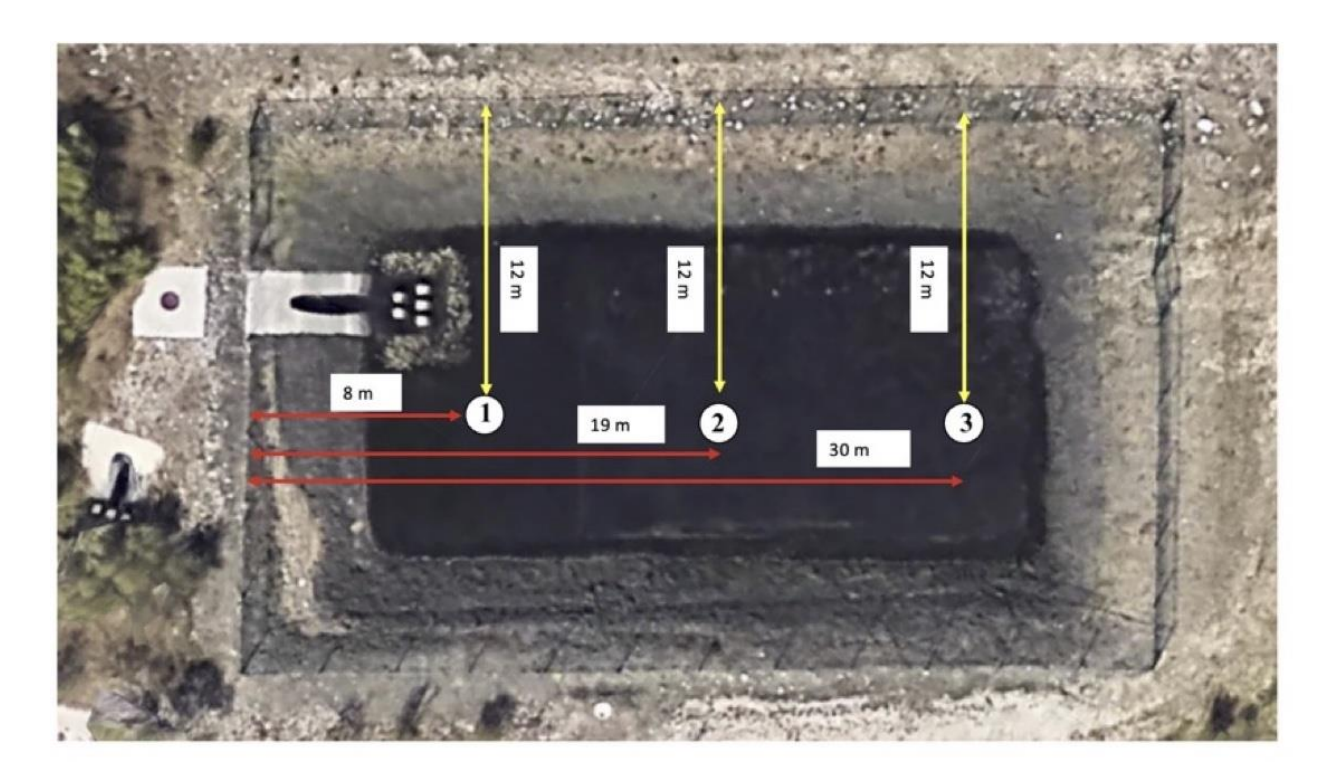


Figure 48. TPC basin soil core locations.



Figure 49. Kyle basin soil core locations.

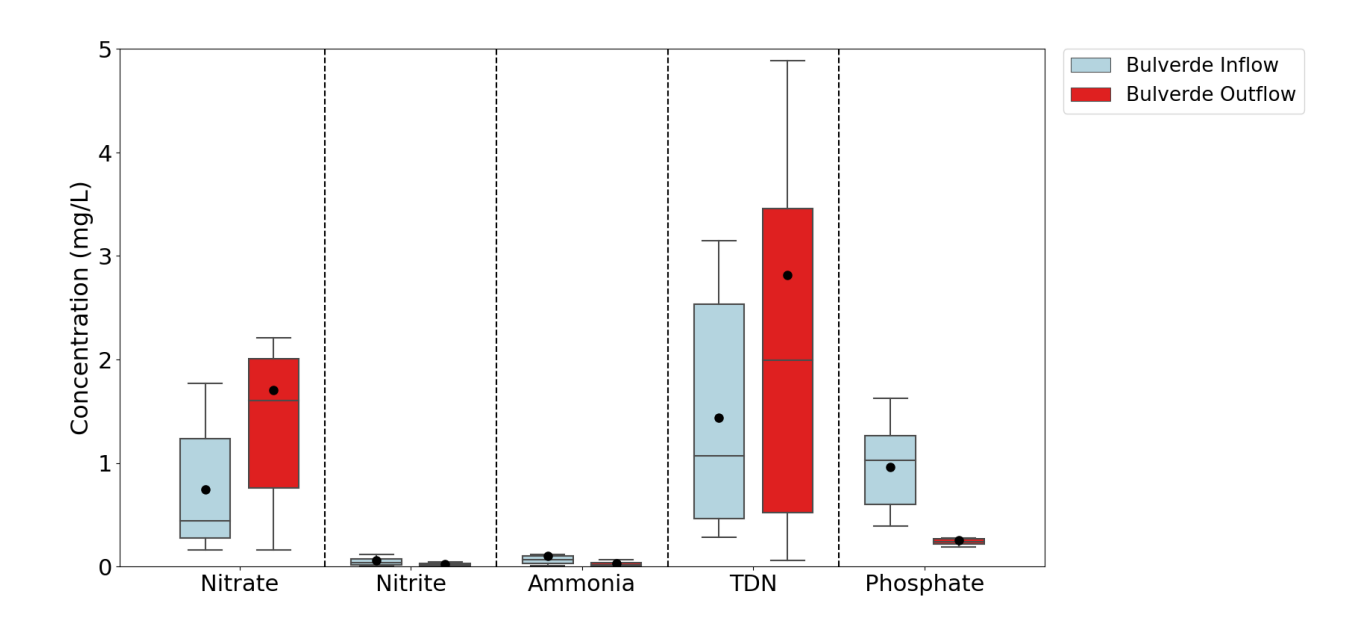


Figure 50. Bulverde nutrients box plot shows the sample median and range between all samples' first and third quartiles. (•) shows the mean.

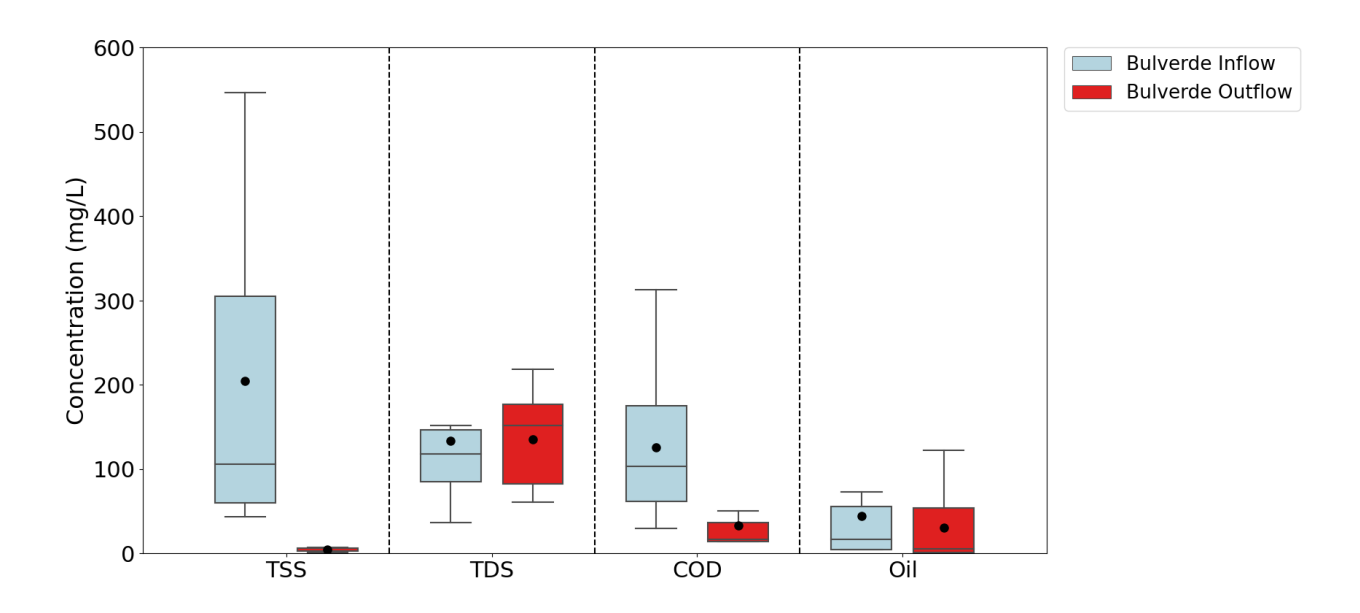


Figure 51. Bulverde solids, COD, and oil and grease box plot show the sample median and range between all samples' first and third quartiles. (•) shows the mean.

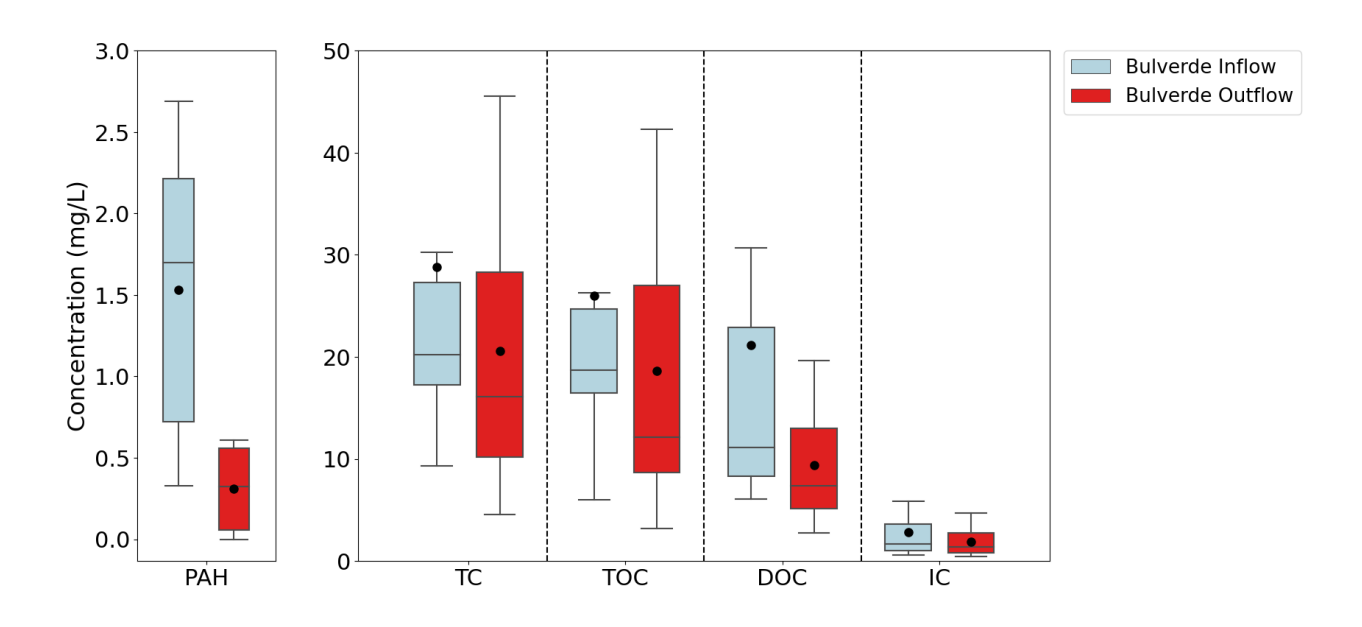


Figure 52. Bulverde PAHs and carbon species box plot shows the sample median and range between all samples' first and third quartiles. (•) shows the mean.

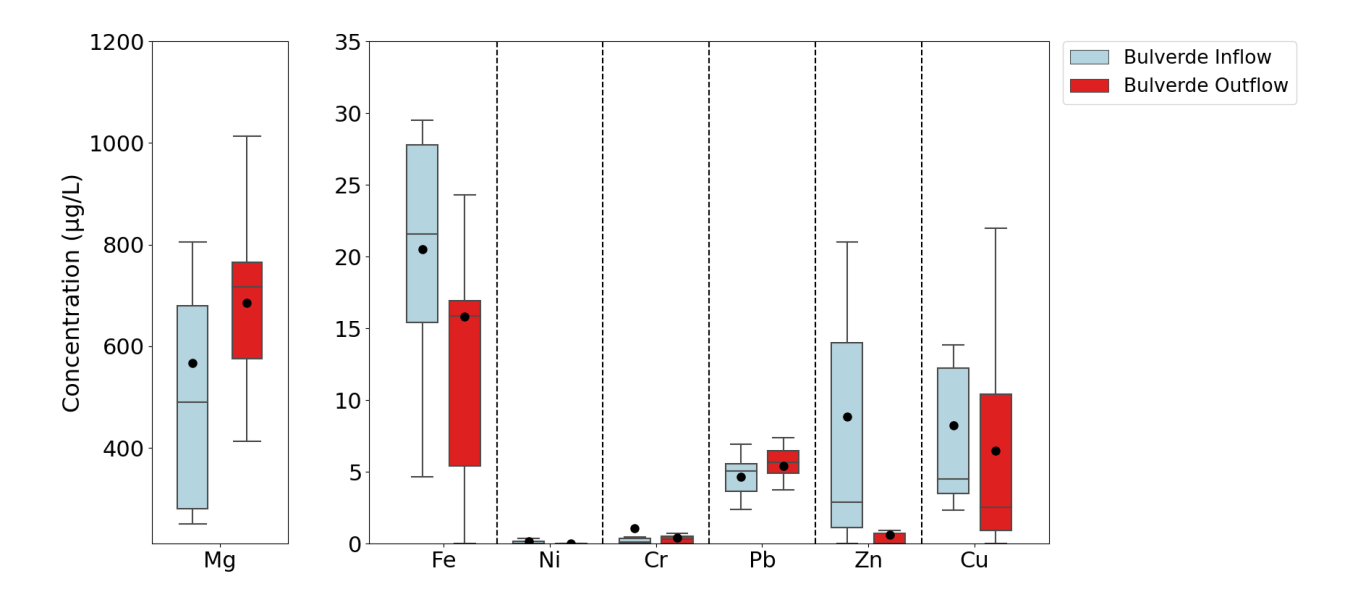


Figure 53. Bulverde heavy metals species box plot shows the sample median and range between all samples' first and third quartiles. (•) shows the mean.

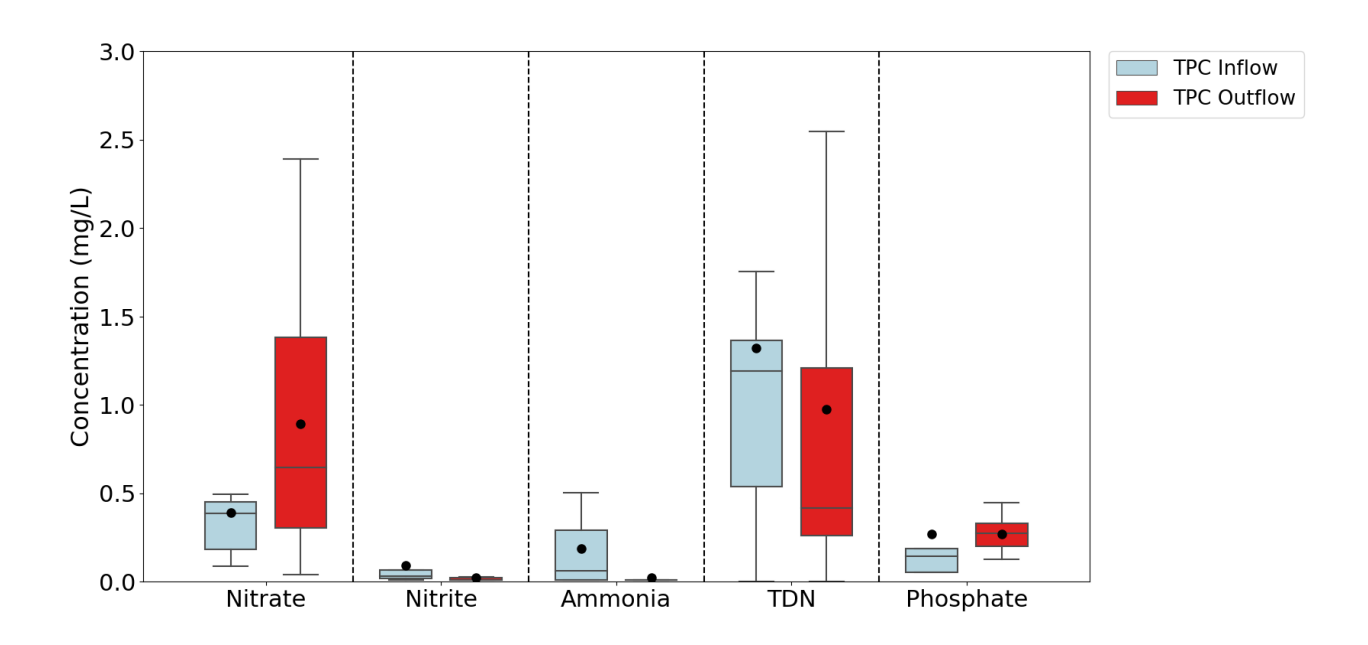


Figure 54. TPC nutrients box plot shows the sample median and range between all samples' first and third quartiles. (•) shows the mean.

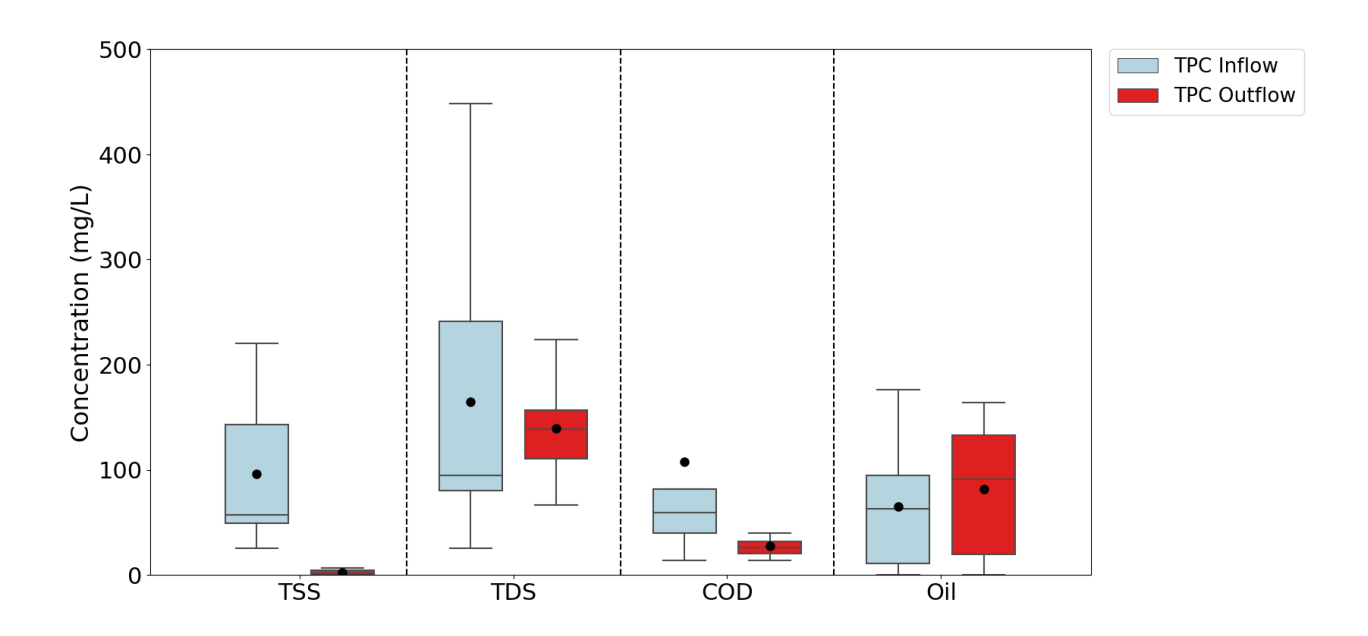


Figure 55. TPC solids, COD, and oil and grease box plot show the sample median and range between all samples' first and third quartiles. (•) shows the mean.

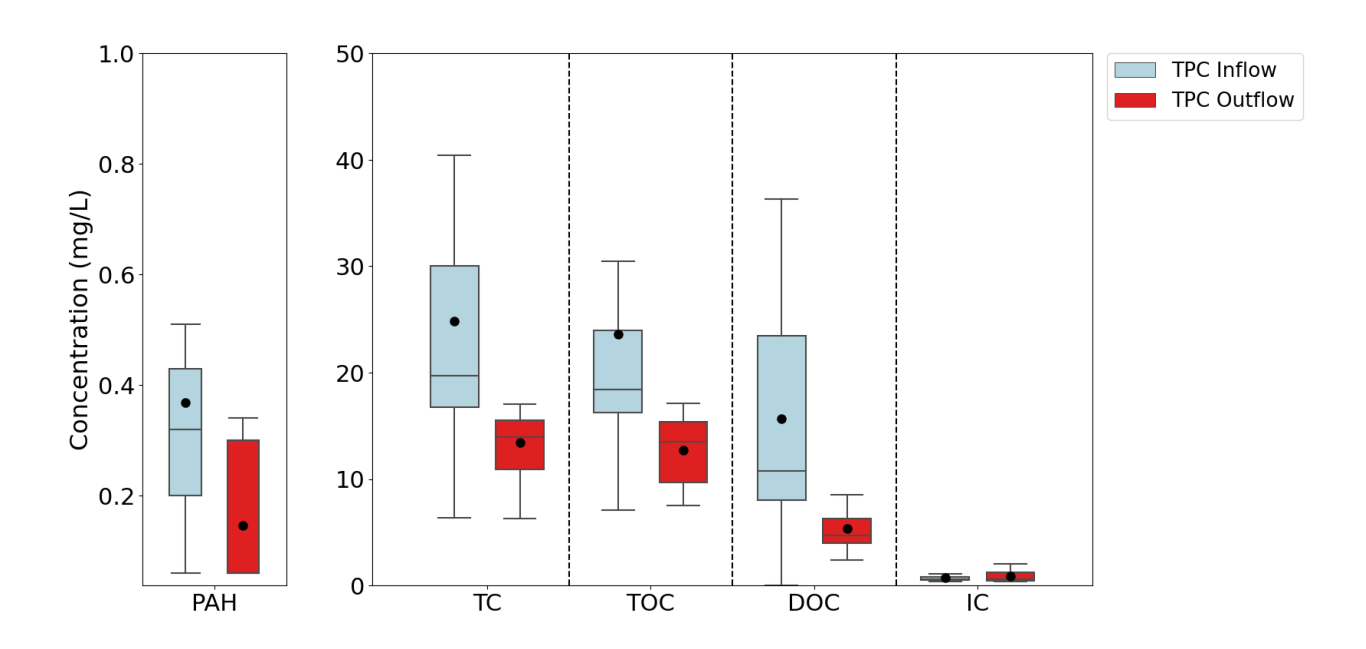


Figure 56. TPC PAHs, carbon species box plot shows the sample median and range between all samples' first and third quartiles. (•) shows the mean.

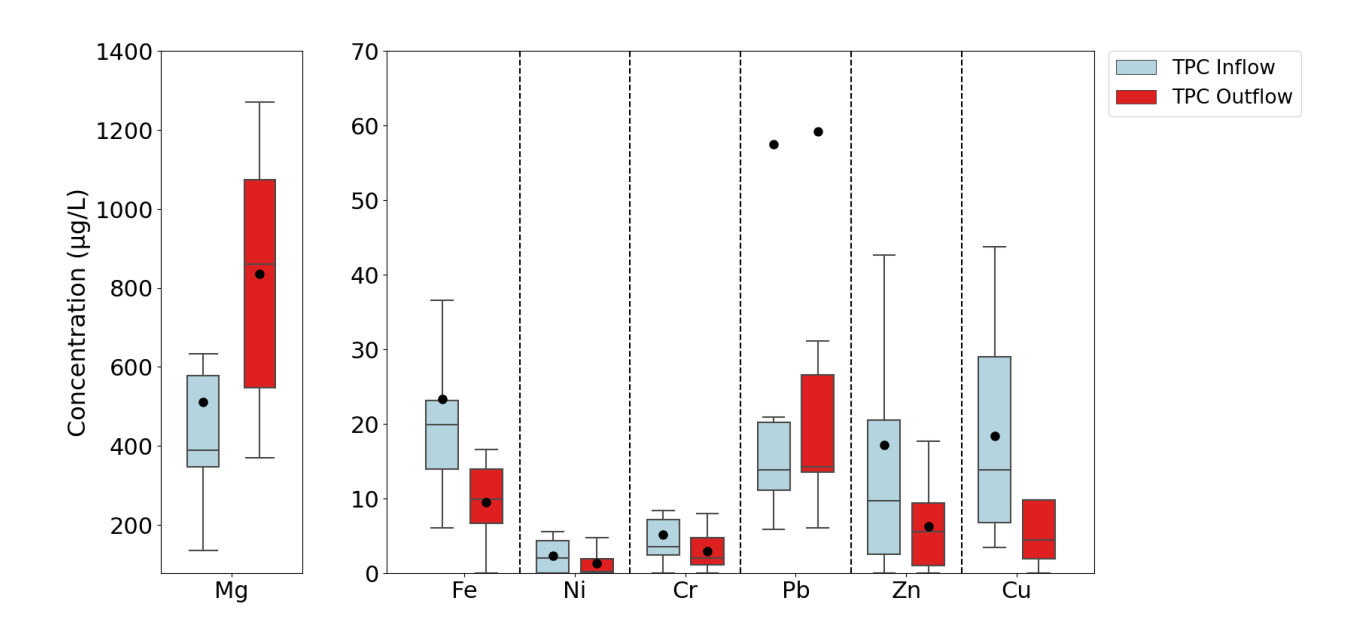


Figure 57. TPC heavy metals species box plot shows the sample median and range between all samples' first and third quartiles. (•) shows the mean.

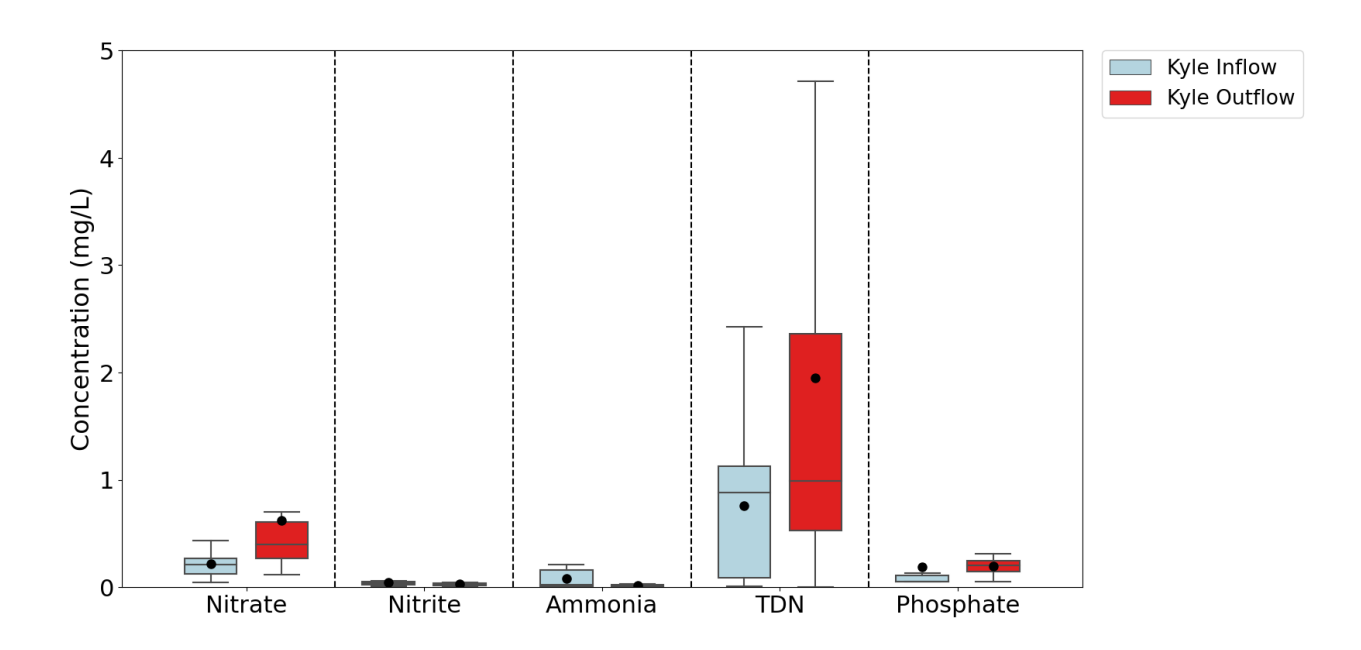


Figure 58. Kyle nutrients box plot shows the sample median and range between all samples' first and third quartiles. (•) shows the mean.

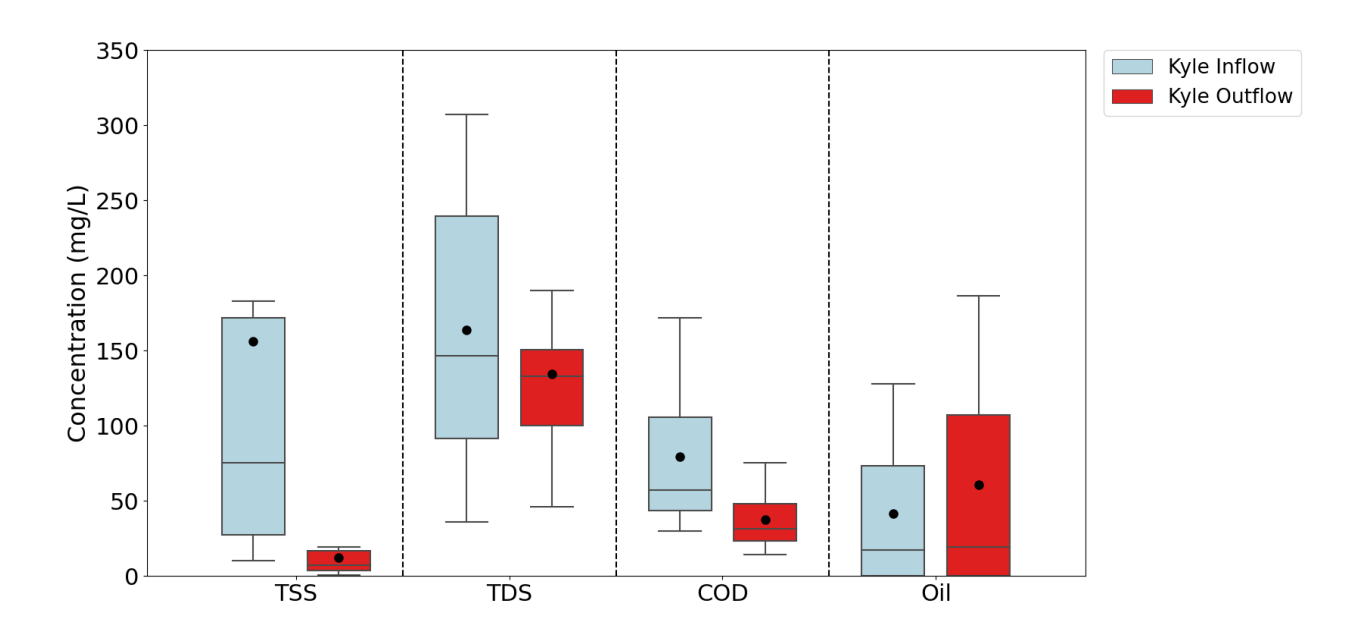


Figure 59. Kyle solids, COD, and oil and grease box plots show the sample median and range between all samples' first and third quartiles. (•) shows the mean.

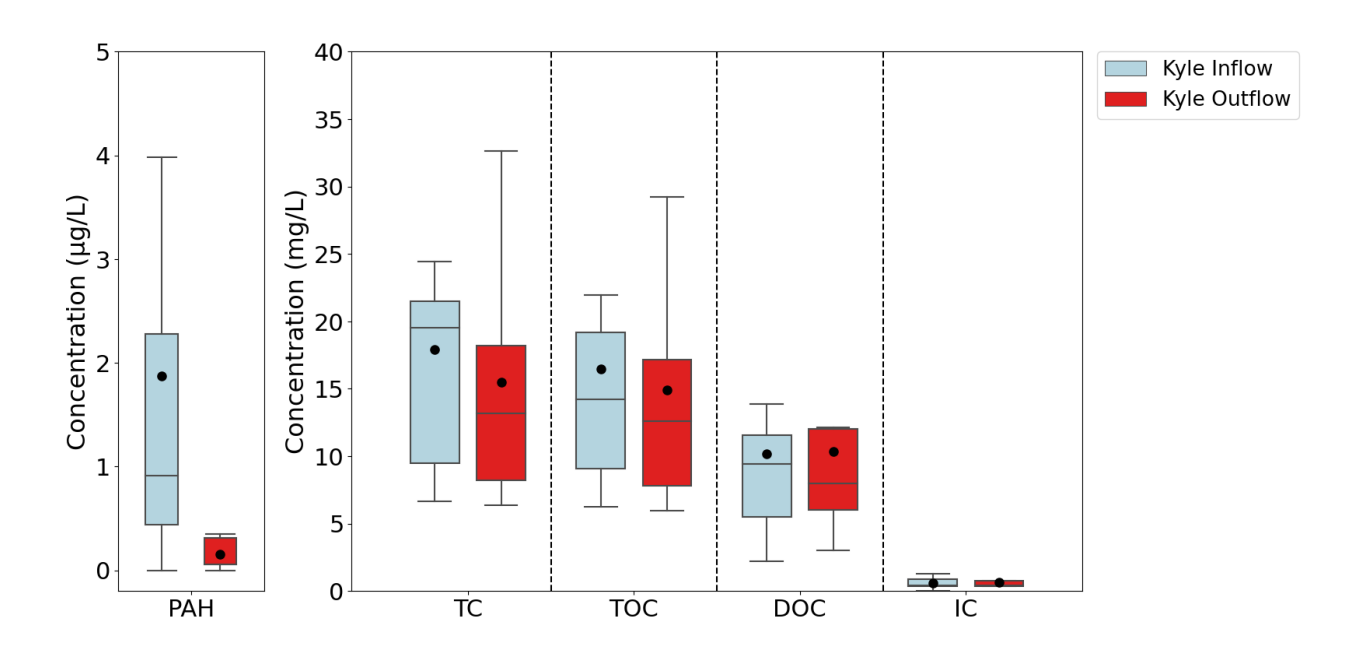


Figure 60. Kyle PAHs, carbon species box plot shows the sample median and range between all samples' first and third quartiles. (•) shows the mean.

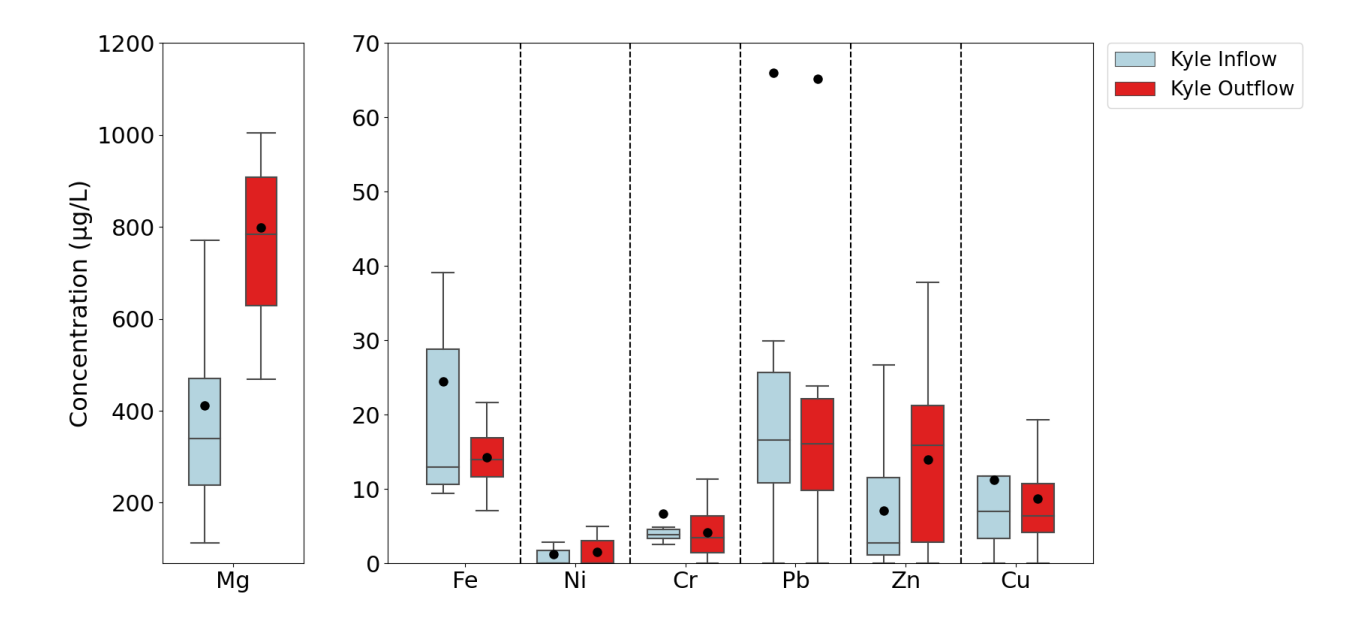


Figure 61. Kyle heavy metals species box plot shows the sample median and range between all samples' first and third quartiles. (•) shows the mean.

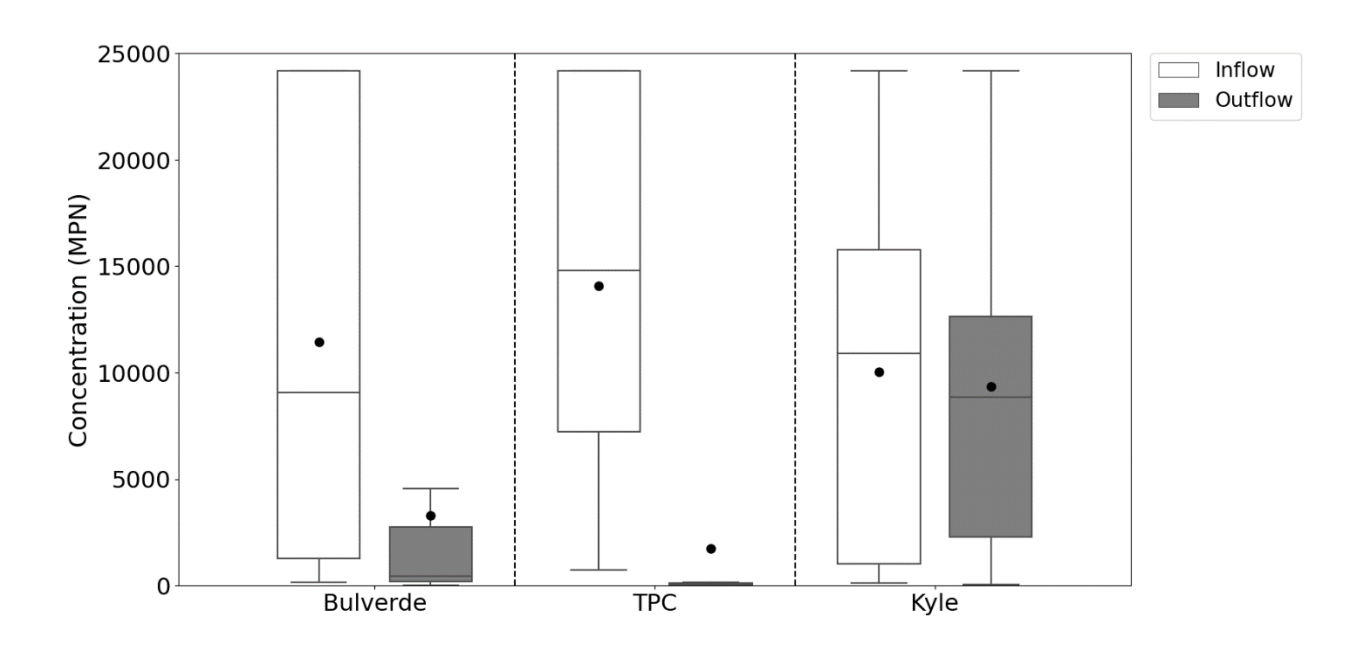


Figure 62. Fecal coliform box plot for all basins.

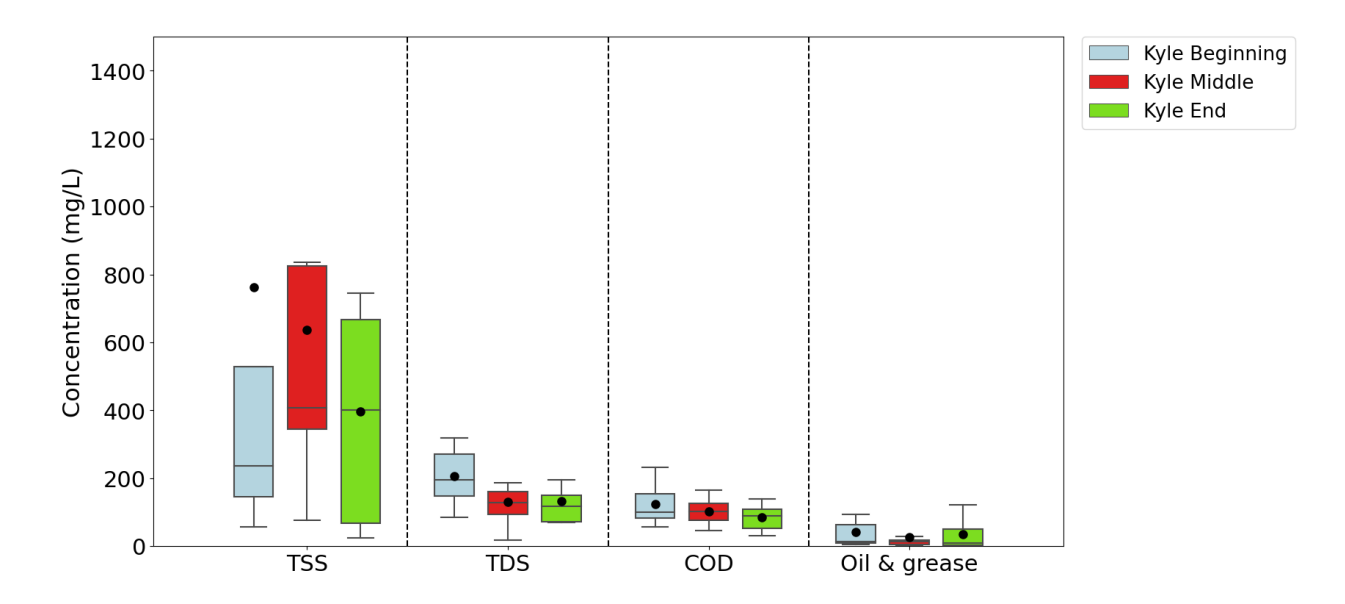


Figure 63. Kyle swale solids, COD, and Oil and grease box plots.

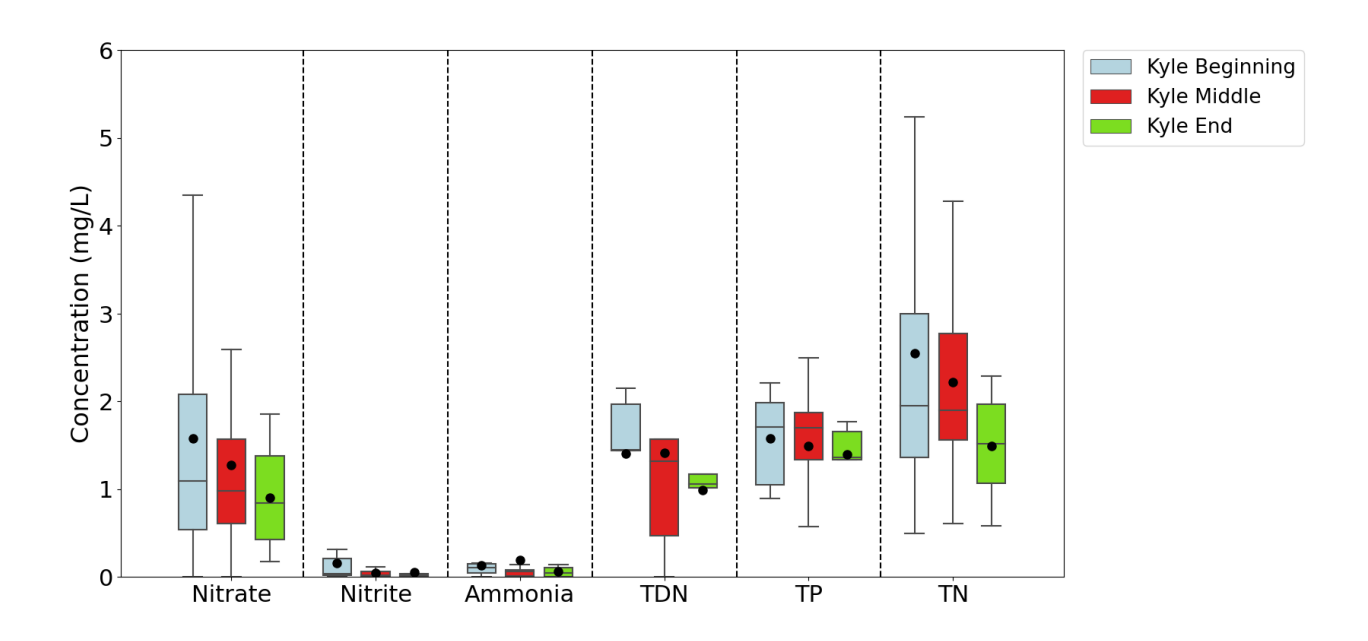


Figure 64. Kyle swale nutrients box plots.

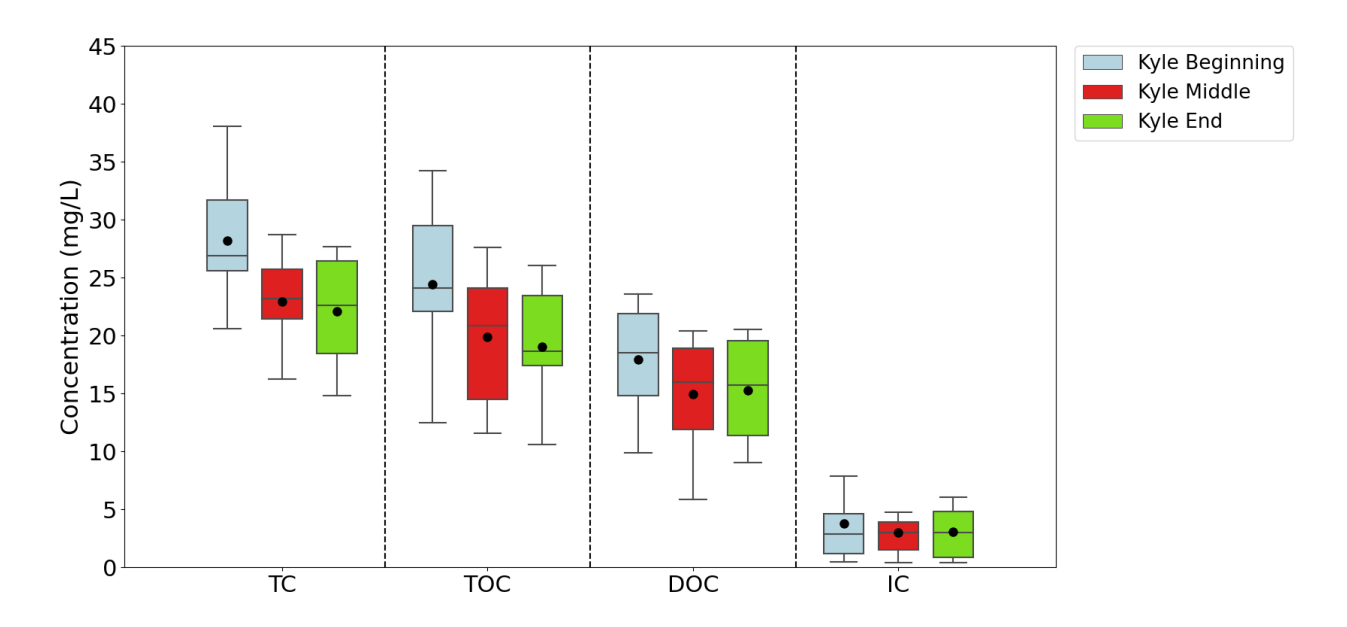


Figure 65. Kyle swale carbon species box plot shows the sample median and range between all samples' first and third quartiles. (•) shows the mean.

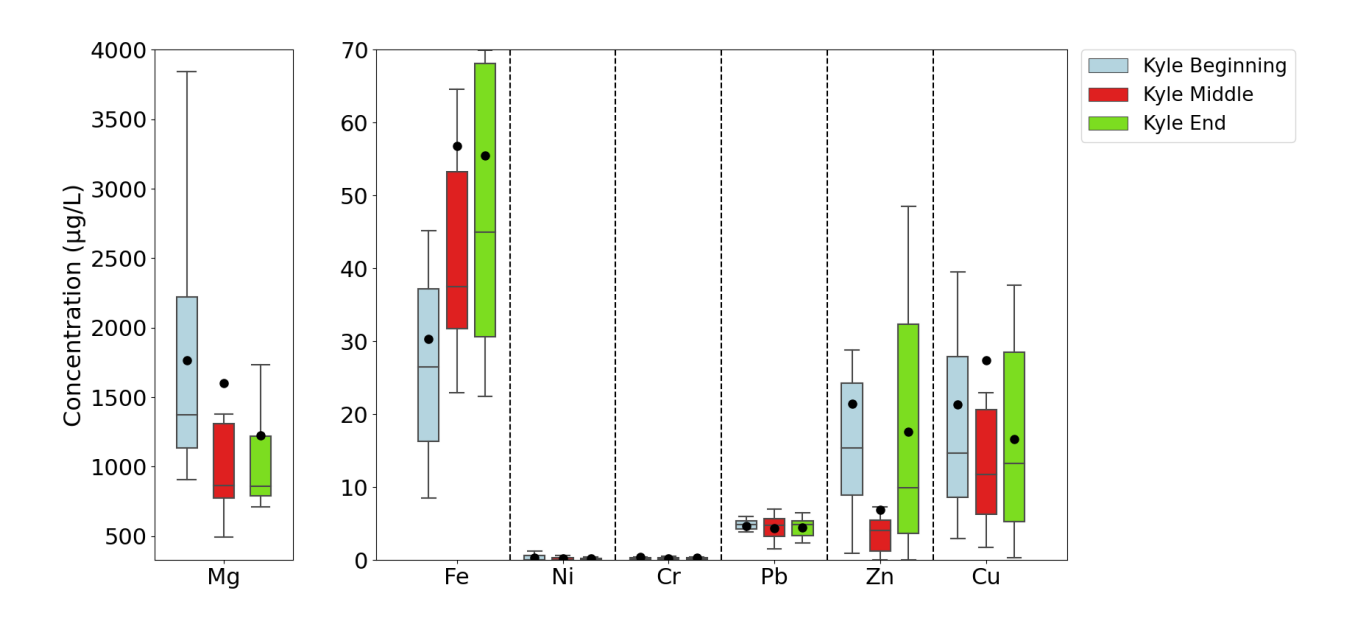


Figure 66. Kyle swale heavy metals species box plot shows the sample median and range between all samples' first and third quartiles. (•) shows the mean.

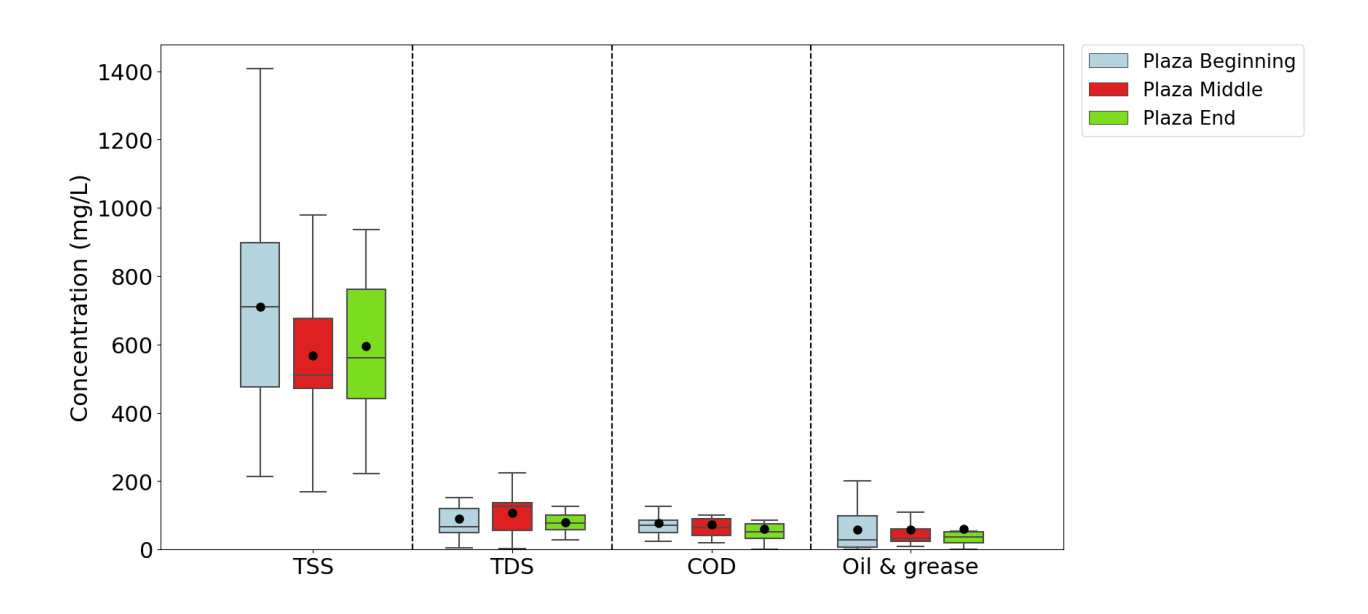


Figure 67. Plaza swale solids, COD, and oil and grease box plots.

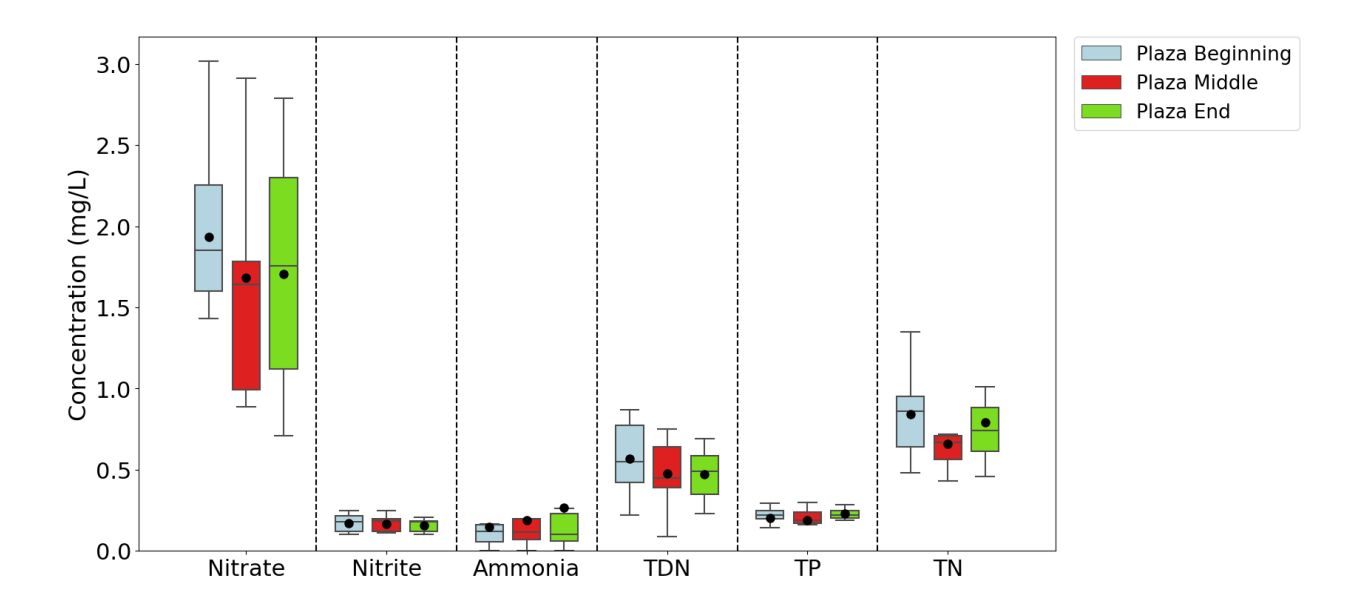


Figure 68. Plaza swale nutrients box plots.

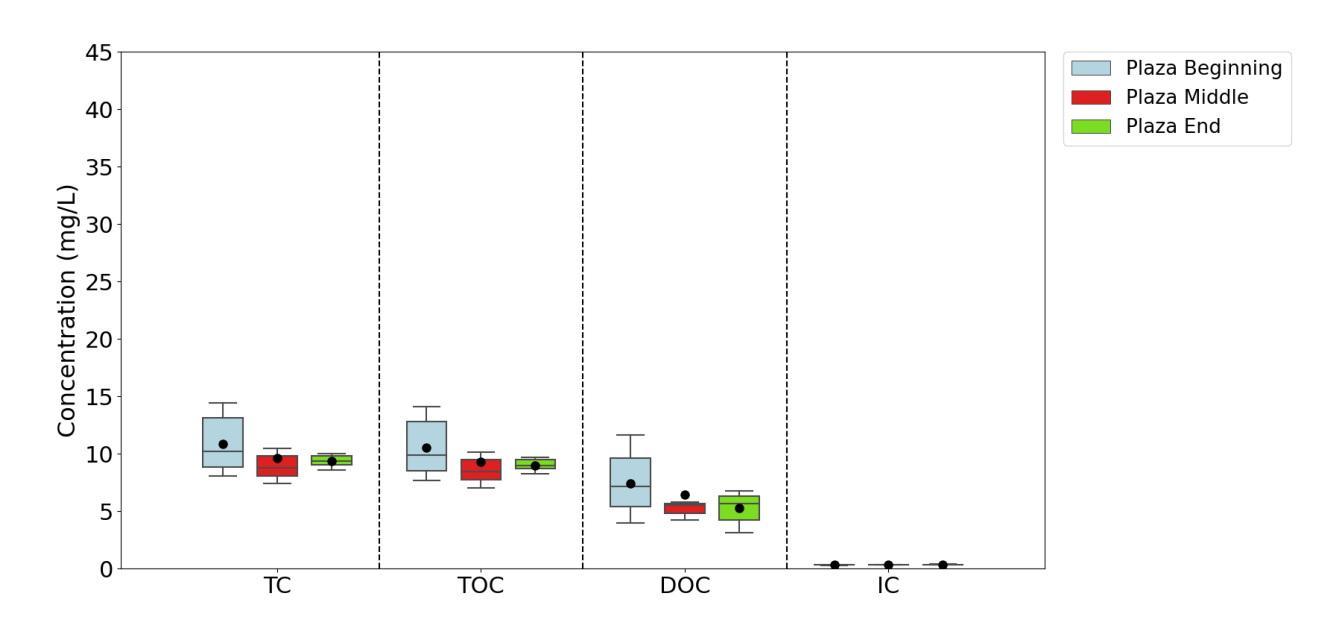


Figure 69. Plaza carbon species box plots.

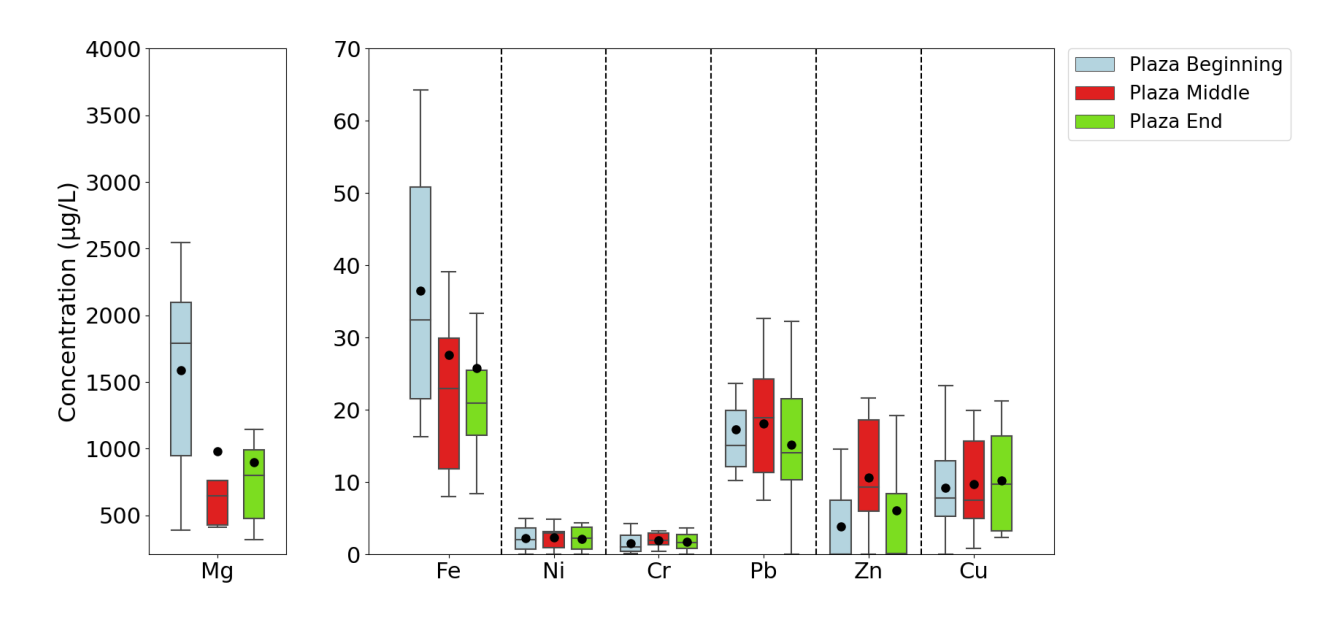


Figure 70. Heavy metals box plots.

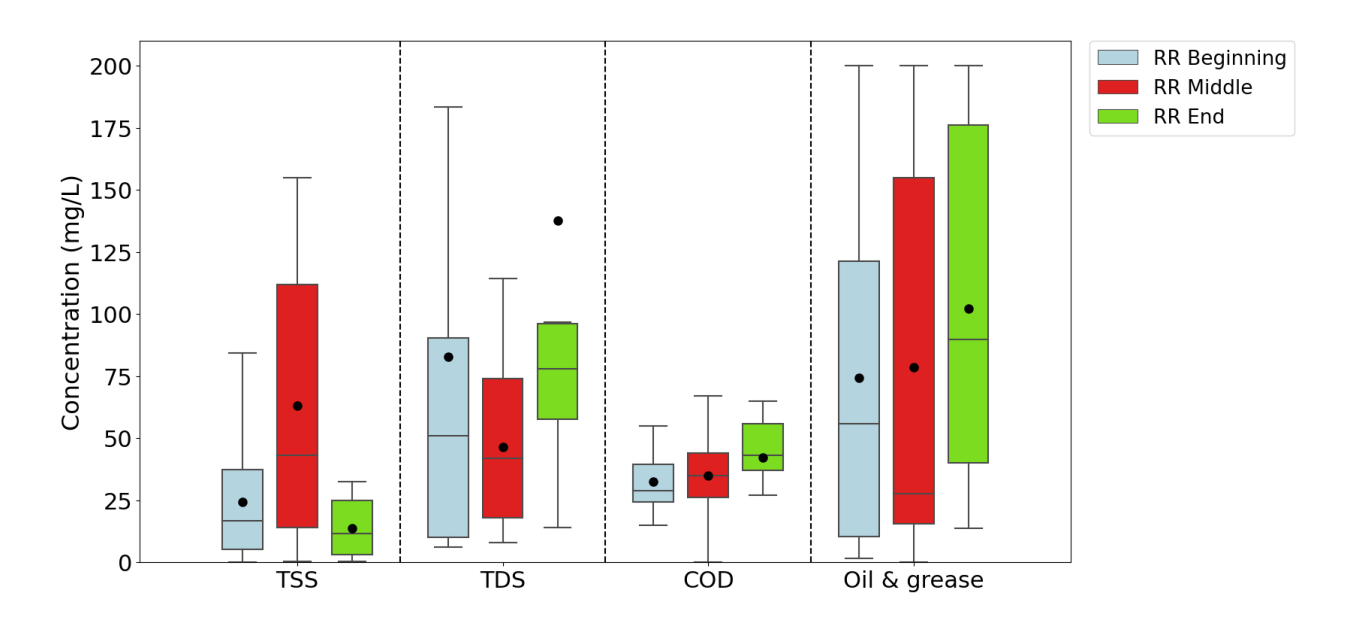


Figure 71. Roadrunner way swale solids, COD, and oil and grease box plots.

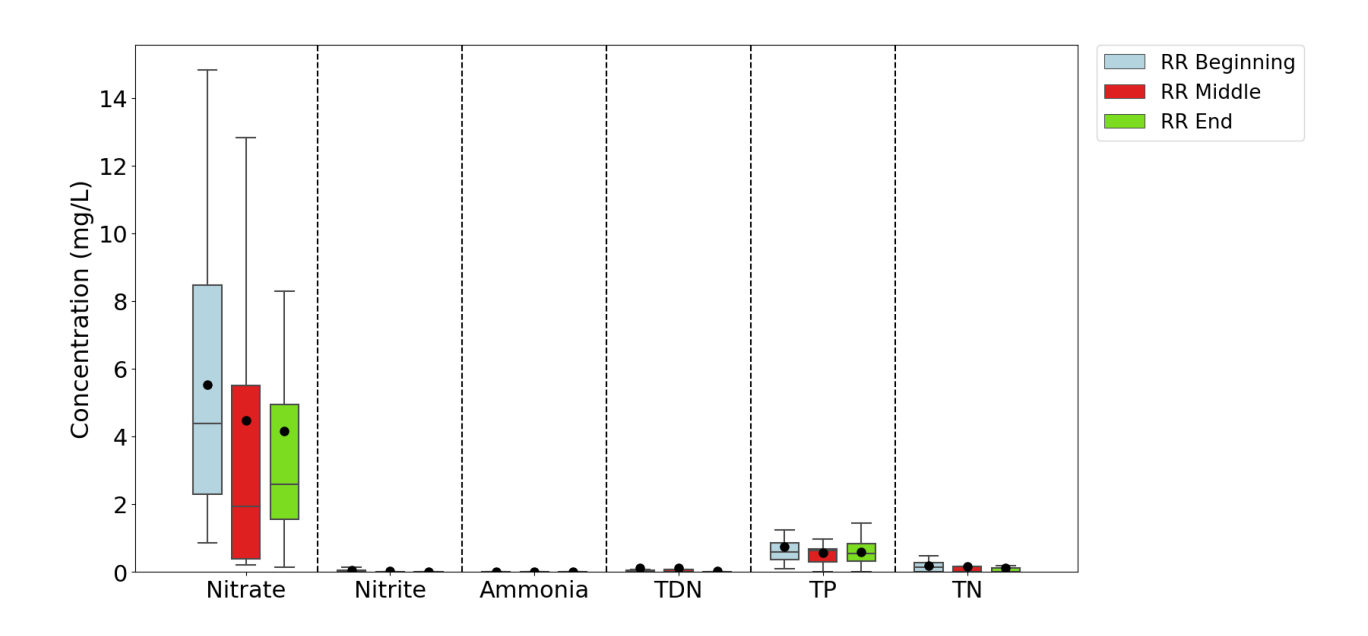


Figure 72. Roadrunner way swale nutrients box plots.

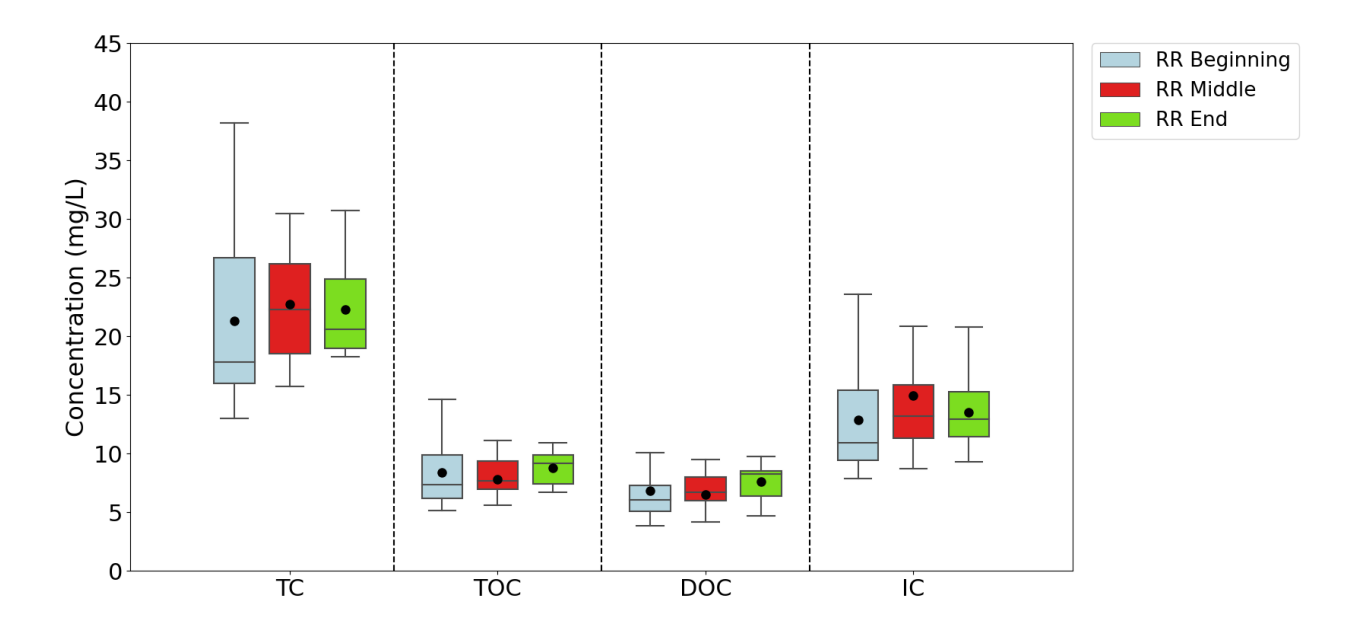


Figure 73. Roadrunner way swale carbon species box plots.

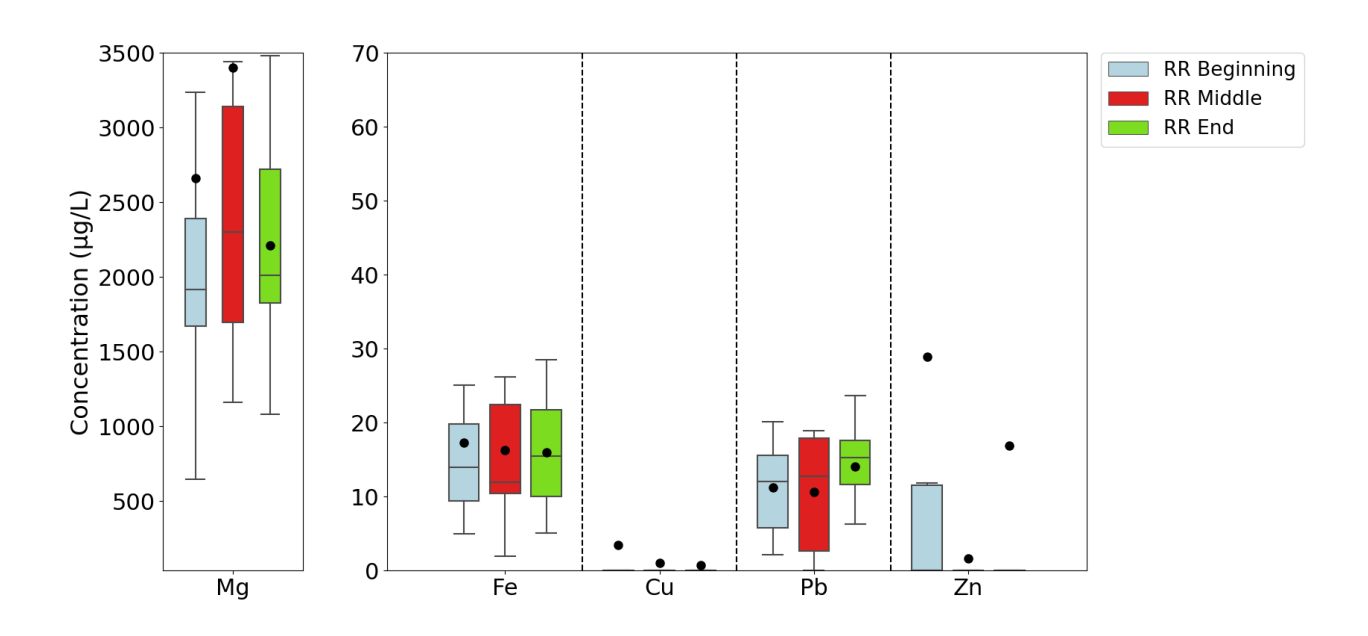


Figure 74. Heavy metals box plots.

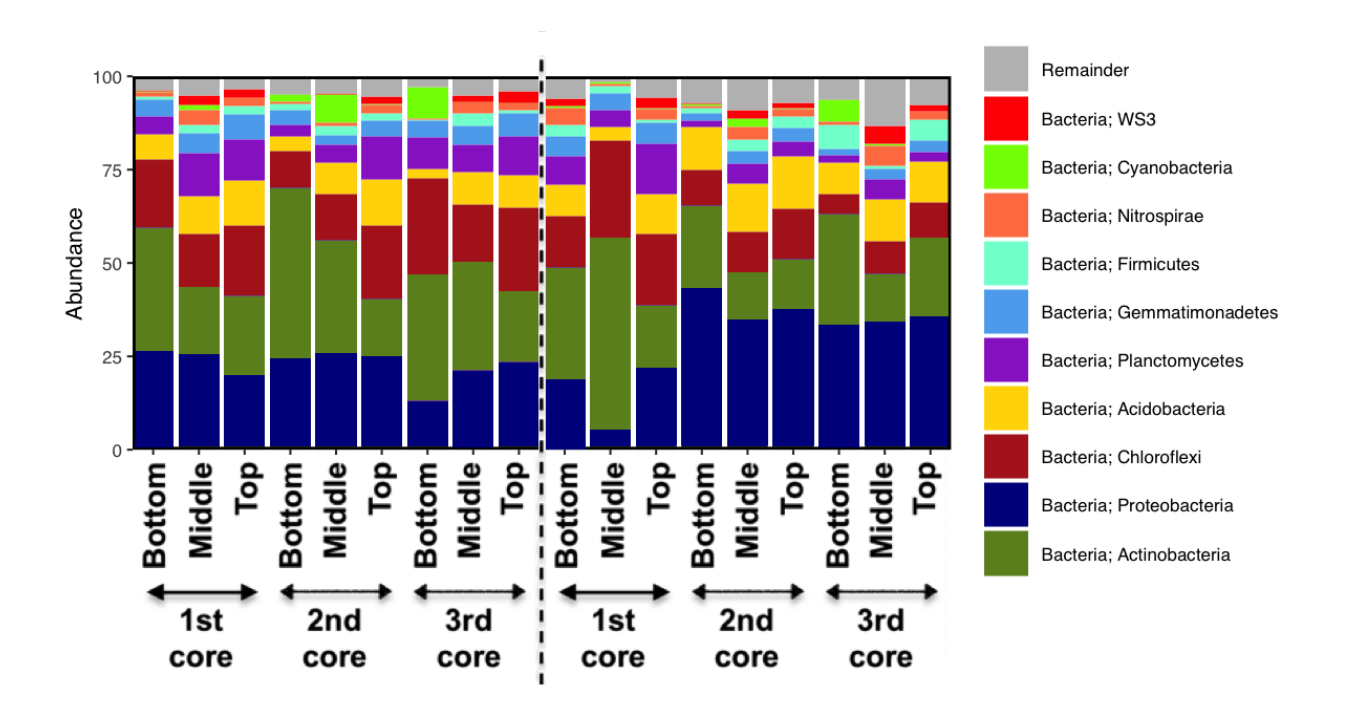


Figure 75. Bulverde basin relative abundance of the top 10 bacterial phyla in the different soil layers and seasons.

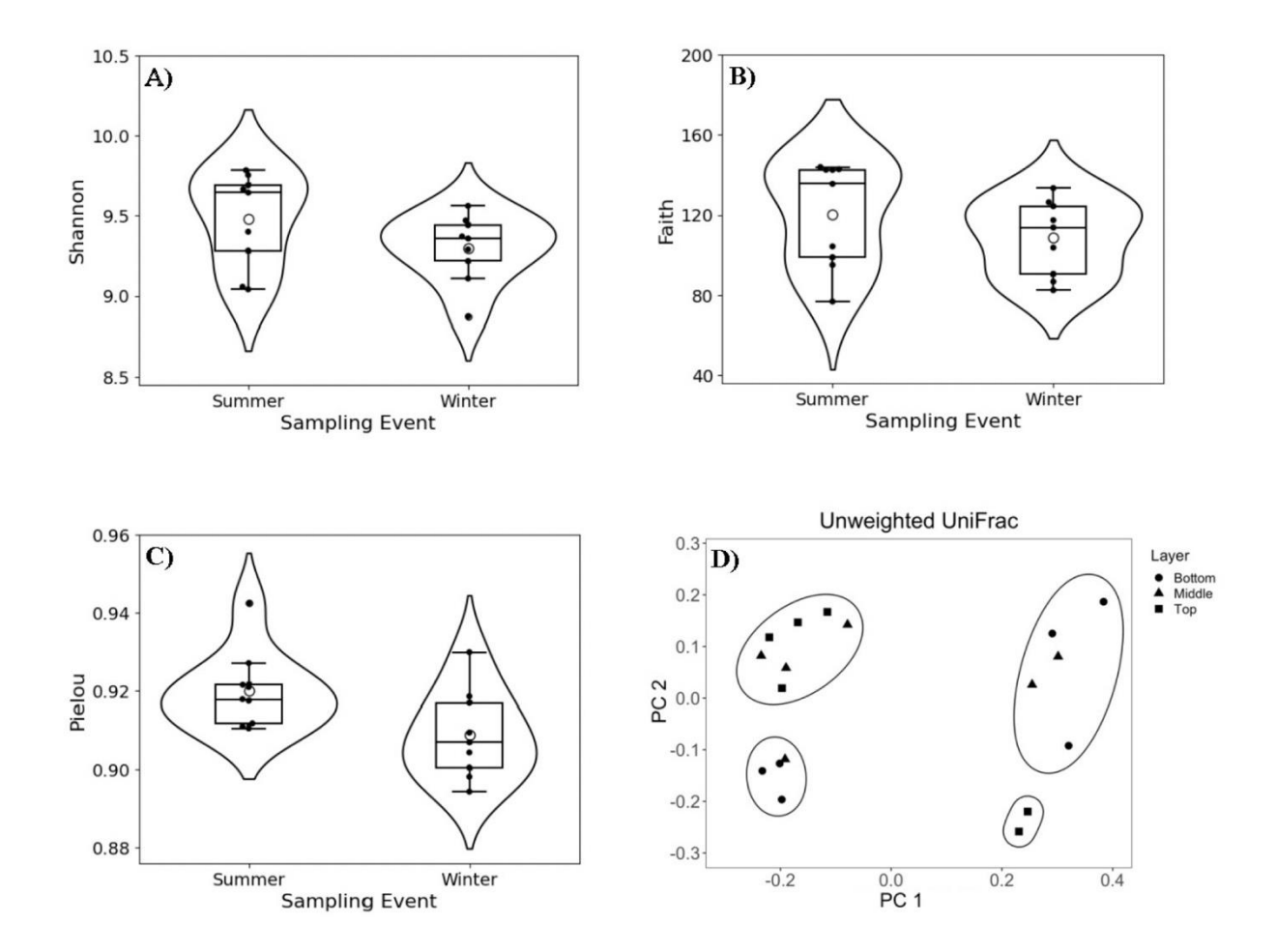


Figure 76. Bulverde basin Alpha and Beta diversity of soil samples. Violin plot illustrating A) Shannon alpha diversity in summer and winter samples, B) Faith's richness values in summer and winter samples, and C) Pielou's evenness values in summer and winter samples. D) Unweighted Unifrac beta diversity in different sampling layers.

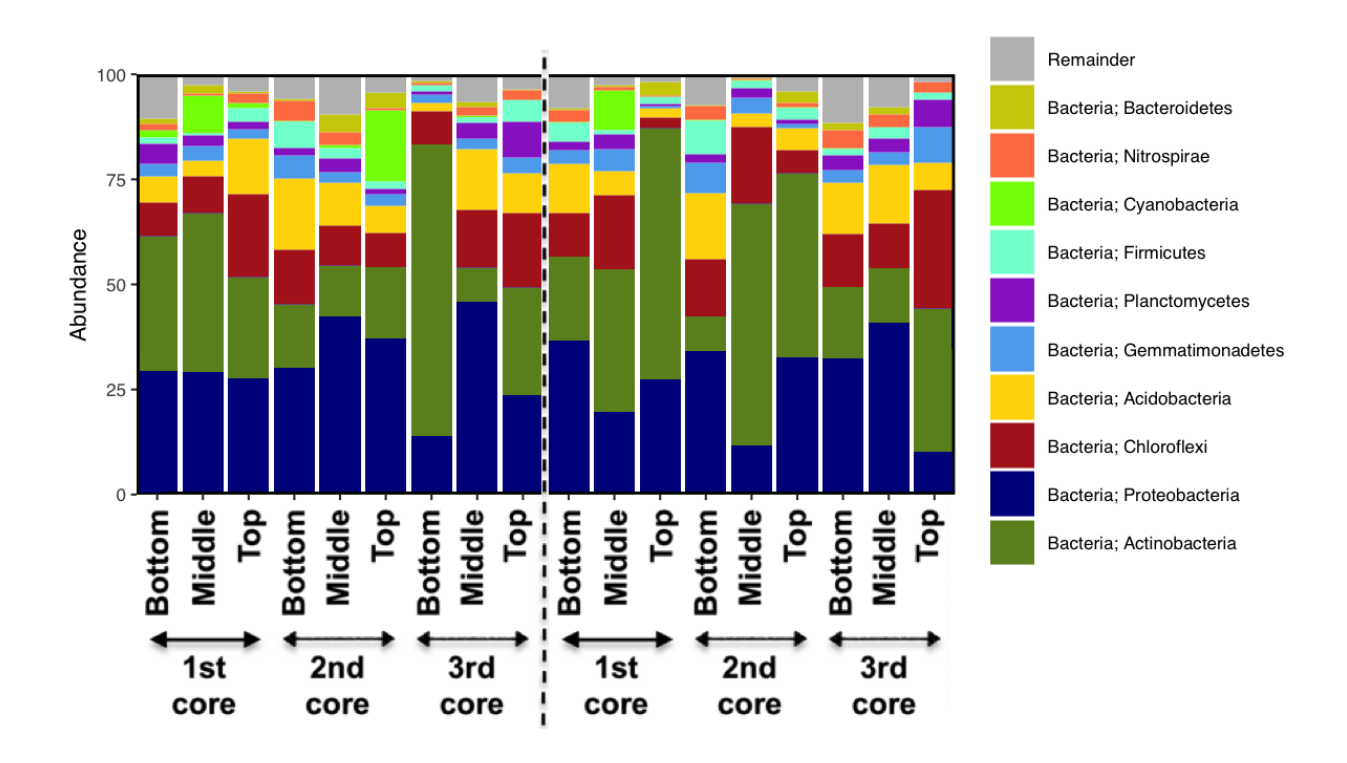


Figure 77. TPC basin relative abundance of the top 10 bacterial phyla in the different soil layers and seasons.

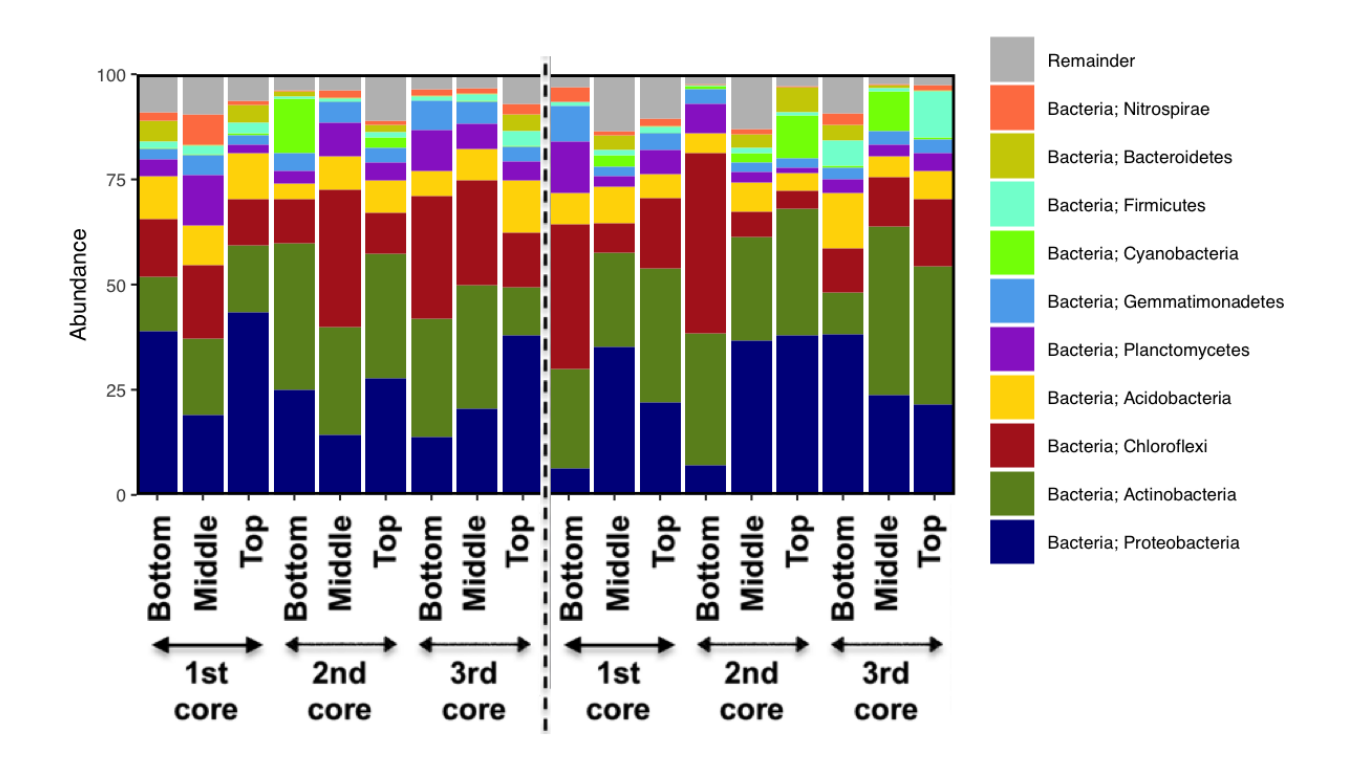


Figure 78. Kyle basin relative abundance of the top 10 bacterial phyla in the different soil layers and seasons.

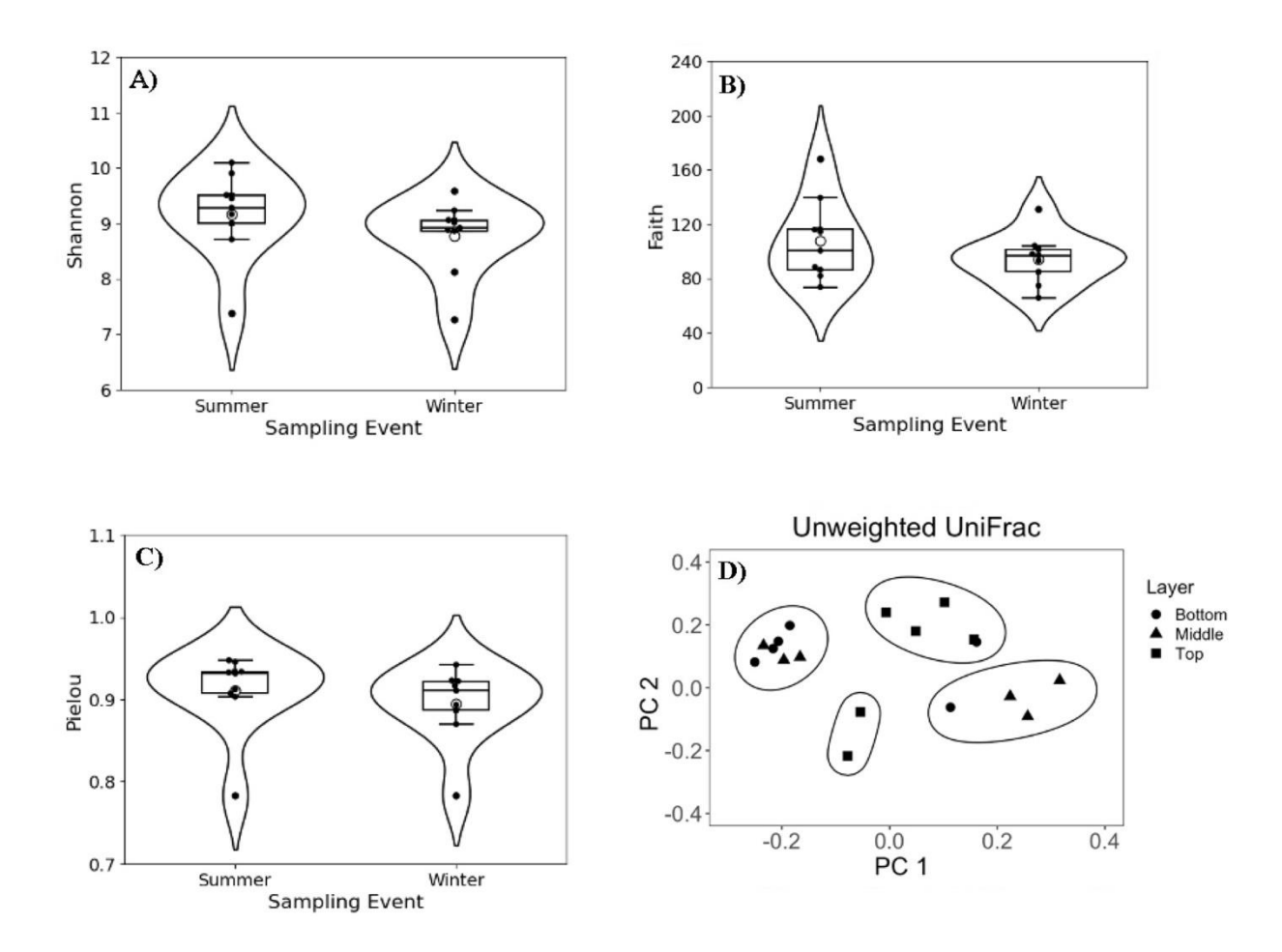


Figure 79. TPC basin Alpha and Beta diversity of soil samples. Violin plot illustrating A) Shannon alpha diversity in summer and winter samples, B) Faith's richness values in summer and winter samples, and C) Pielou's evenness values in summer and winter samples. D) Unweighted Unifrac beta diversity in different sampling layers.

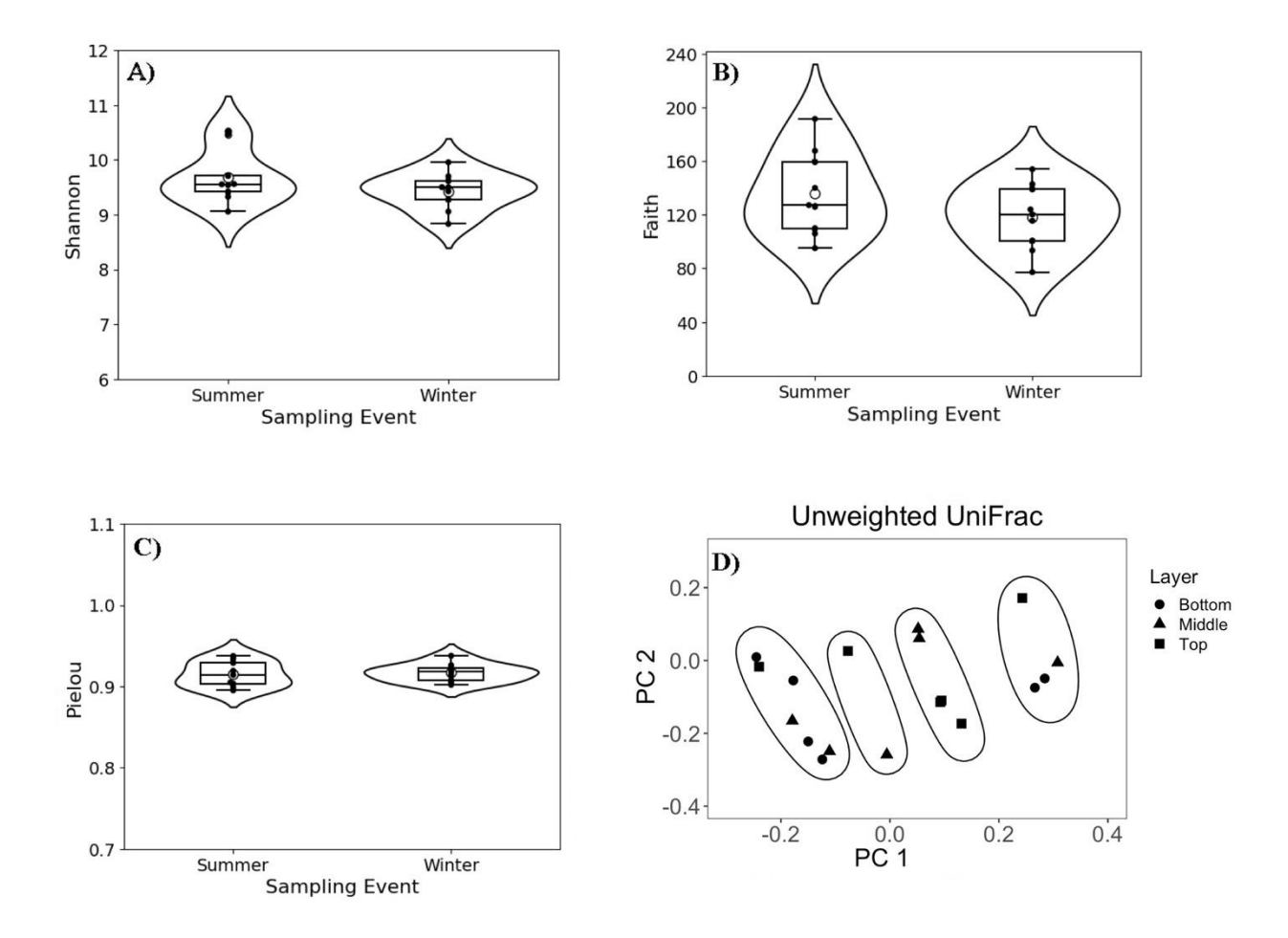
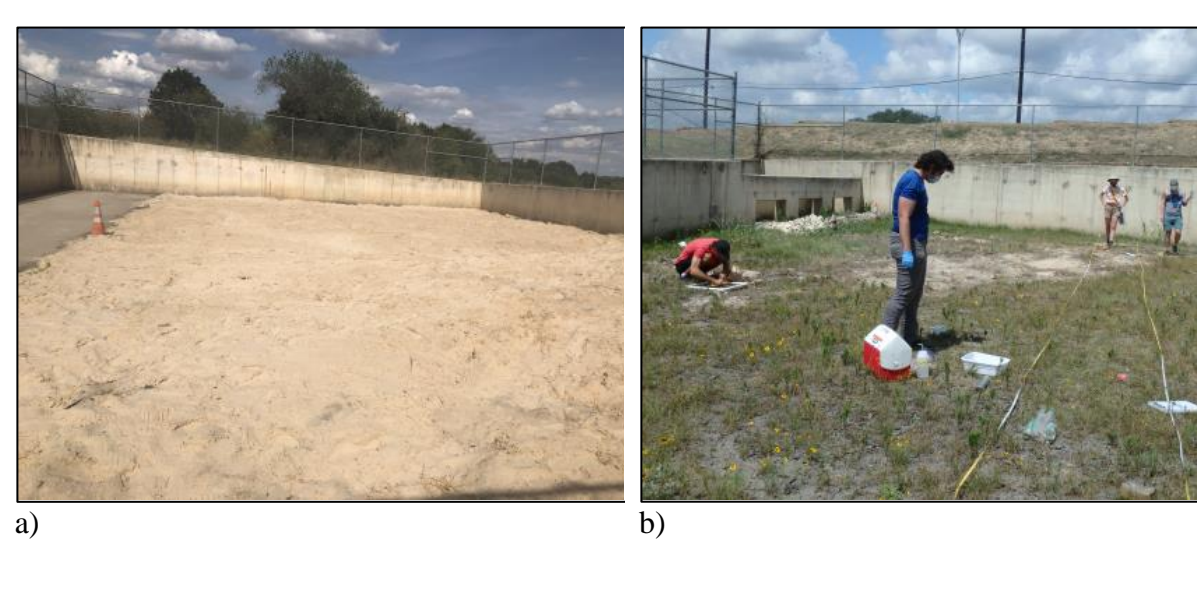


Figure 80. Kyle basin Alpha and Beta diversity of soil samples. Violin plot illustrating A) Shannon alpha diversity in summer and winter samples, B) Faith's richness values in summer and winter samples, and C) Pielou's evenness values in summer and winter samples. D) Unweighted Unifrac beta diversity in different sampling layers.

Appendix 1. Low Impact Sites (LID; sand filtration systems and swales), site name, and GPS locations.

LID Type	Site Name	GPS Coordinates
Sand filtration systems		
Primary	Bulverde Road – Basin B	29°36'24.7"N, 98°25'04.9"W
Primary	Brandeis H.S. / Kyle Seale Parkway	29°33'56.1"N, 98°38'40.0"W
Primary	TPC Parkway – Basin A	29°39'14.7"N, 98°26'28.0"W
Secondary	Bulverde Road – Basin D	29°37'17.4"N, 98°25'20.6"W
Secondary	Prue Road	29°32'30.7"N, 98°37'51.3"W
Secondary	TPC Parkway – Basin B	29°39'36.3"N, 98°26'10.3"W
Swale		
Primary	Babcock Road	29°36'45.9"N, 98°37'54.7"W
Primary	Brandeis High School / Kyle Seale	29°33'51.8"N, 98°38'42.4"W
Primary	The Plaza	29°34'45.9"N, 98°35'09.6"W
Secondary	Roadrunner Way Road	29°34'25.4"N, 98°37'43.2"W
Secondary	Savannah Oaks Apartment	29°34'47.9"N, 98°35'12.5"W
Secondary	The Rim	29°36'37.4"N 98°36'09.8"W

Appendix 2.1 - Photos of the Bulverde Road Basin B sand filtration system: a) replacement of the top 5 cm of sand, b) sampling vegetation at the early to mid-stage of succession following sand replacement, c) water retention approximately 10 hours following a rain event, and d) robust vegetation following no disturbance for 5 months.





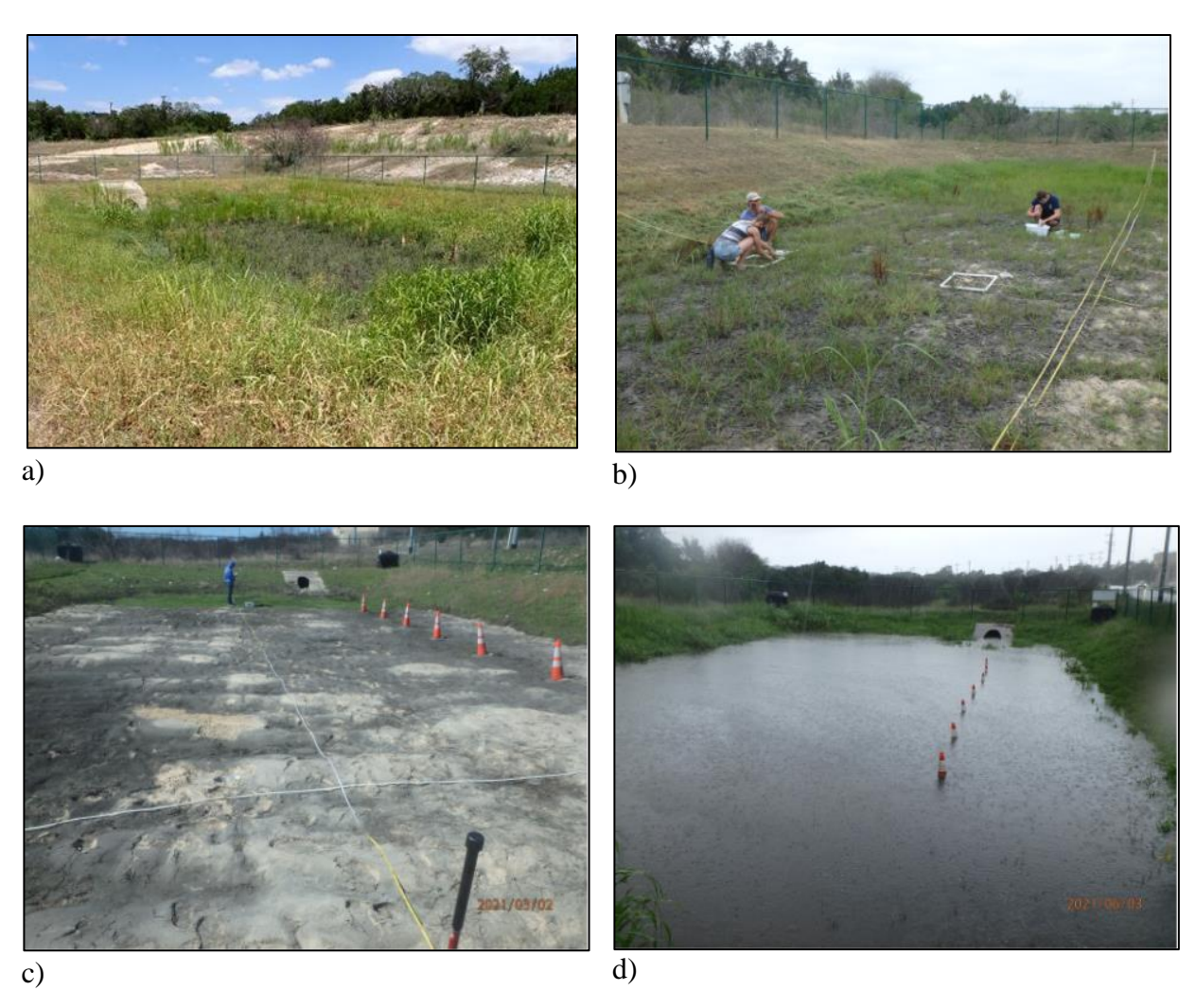


 \overline{d}

Appendix 2.2 - Photos of the Brandeis High School/Kyle Seale Parkway sand filtration system: a) early successional vegetation following disturbance, b) mid-successional vegetation following no disturbance, c) vegetation and soil sampling, and d) vegetation following mowing and approximately 5-6 months following sand replacement.



Appendix 2.3 - Photos of the TPC Parkway Basin A sand filtration system: a) robust vegetation cover following no disturbance in 5-6 months, b) early successional vegetation in the foreground and more robust vegetation in the background within a low depression at the inflow, c) sampling following sand replacement and a rain event where oil and grease can be observed on the soil surface, and d) inundation of the sand filtration system within 15 minutes following a rain event.



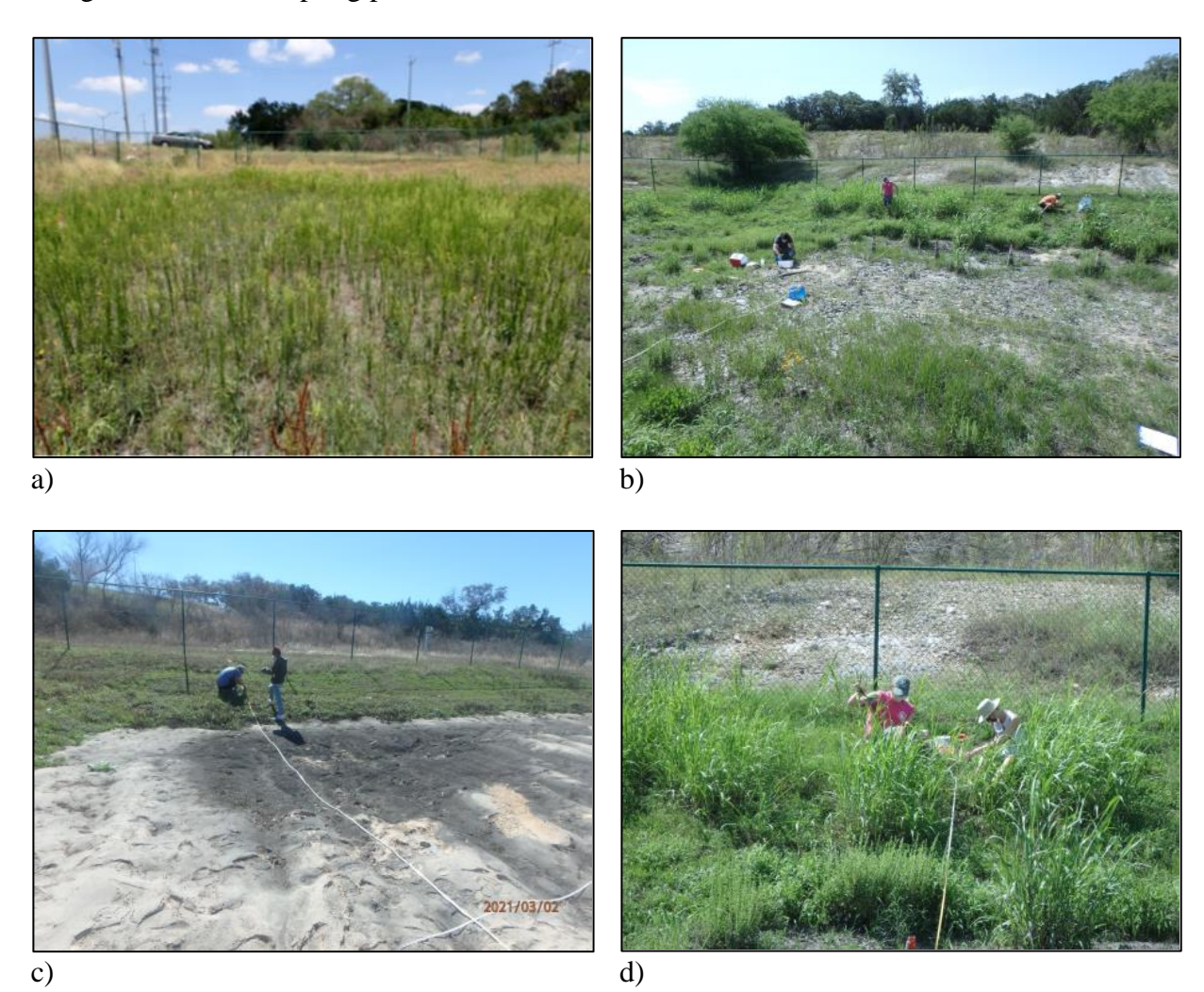
Appendix 2.4 - Photos of the Bulverde Road Basin D sand infiltration system: a) early successional vegetation, b) raking of the system to remove debris and trash washed in from runoff following a rain event, c) early successional vegetation following a rain event, d) silt, sediment, and trash accumulation at the outflow section of the system following a rain event.



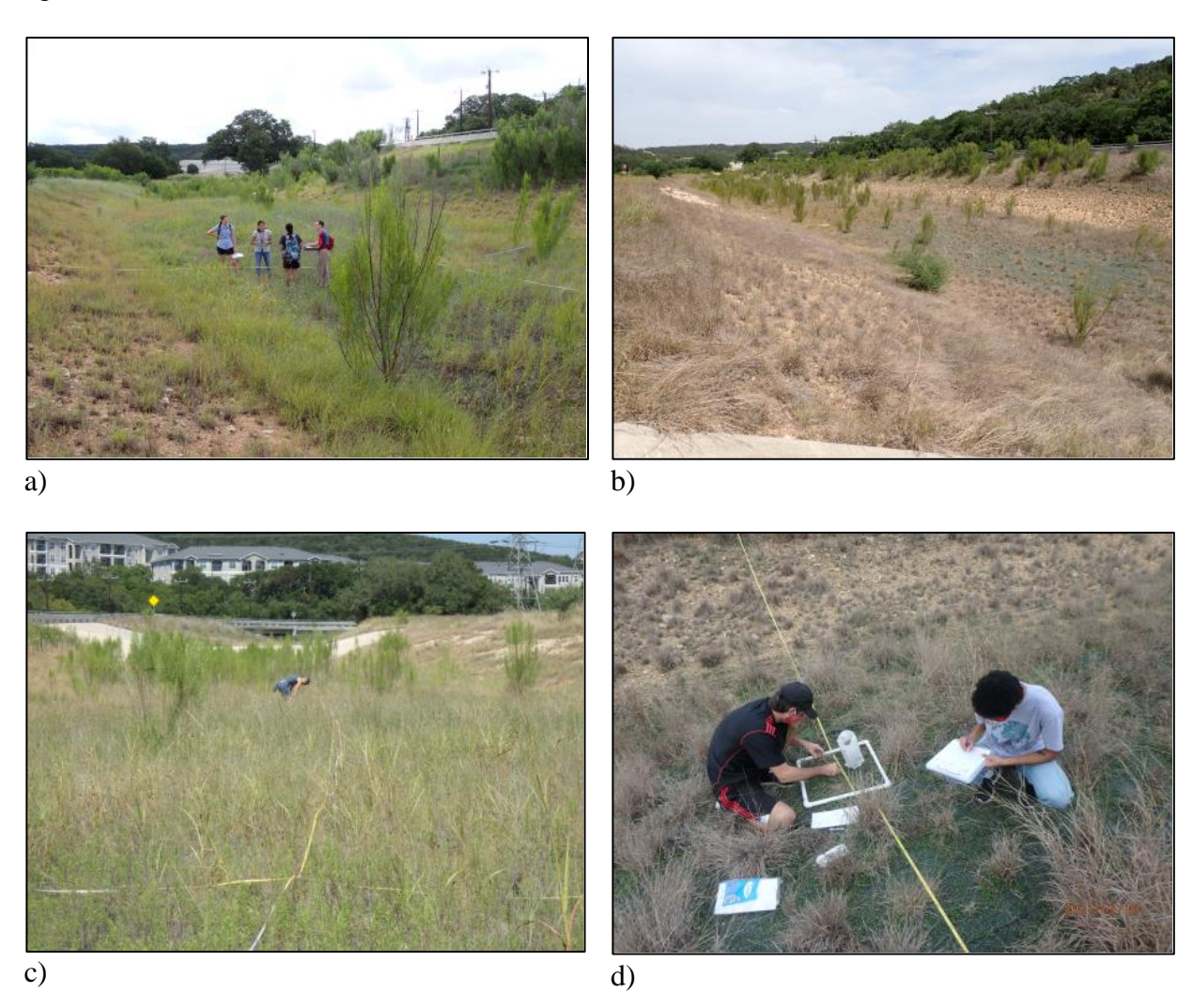
Appendix 2.5 - Photos of the Prue Road sand filtration system: a) sampling vegetation and soils, b) recently mowed, c) no maintenance for 2-3 months, and d) collection of soil sample.



Appendix 2.6 - Photos of the TPC Parkway Basin B sand filtration system: a) robust growth of horseweed (*Conyza canadensis*) exhibiting rapid growth following disturbance, b) variation in the plant cover along the length and width of the sand filtration basin, c), and d) robust grasses during the summer sampling period.



Appendix 2.7 - Photos of the Babcock Road swale: a) early summer, b) winter, c) sampling robust vegetation in the summer with high coverage of native grasses, and d) sampling dormant vegetation in the winter.



Appendix 2.8 - Photos of the Brandeis High School/Kyle Seale Parkway swale: a) mowed early summer, b) sampling vegetation mid-summer, c) sampling vegetation during the winter, and d) mid-summer.



Appendix 2.9 - Photos of The Plaza swale: a) vegetation sampling during a period of limited rainfall during the summer, b) summer sampling under normal rainfall, c) low depression in the upper basin from scouring holding water for an extended period, and d) sampling of vegetation during the winter with water accumulated in small depressions within the lower basin.



Appendix 2.10 - Photos of the Roadrunner Way Road swale: a) sampling vegetation under wet conditions following mowing 3-4 weeks prior, b) planting native graminoids, c) measuring out a line transect to randomly plant native grasses, and d) planting native graminoids.



Appendix 2.11 - Photos of the Savannah Oaks Apartment swale: a) robust vegetation in the swale during the summer, b) sampling vegetation in the swale during the summer, c) sampling vegetation in the early summer following mowing, and d) vegetation in the winter following mowing.



Appendix 2.12 - Photos of The Rim swale: a) overview of the swale looking south, b) collecting vegetation biomass samples from plots, c) recently mowed, and d) overview of the swale looking north. This swale was mowed often during the growing season for aesthetics due to its location adjacent to IH-10 and The Rim Mall.



Appendix 3. Common name, taxonomic name, USDA code, status (native or non-native), group (monocot or dicot), duration (annual, perennial, etc.), growth habit (forb/herb, graminoid, shrub, etc.), and wetland status (obligate, facultative wetland, facultative, etc.) of plants observed along line transects in sand filtration systems and swales from 2020-2021.

		USDA				Growth	Wetland
Common name	Taxonomic name	Code	Status	Group	Duration	Habit	Status
Common threeseed mercury	Acalypha rhomboidea Raf.	ACRH	Native	Dicot	Annual	Forb/Herb	FACU
Meadow garlic	Allium canadense L.	ALCA3	Native	Monocot	Perennial	Forb/Herb	FACU
Carelessweed	Amaranthus palmeri S. Watson	AMPA	Native	Dicot	Annual	Forb/Herb	FACU
Cuman ragweed	Ambrosia psilostachya DC.	AMPS	Native	Dicot	Ann/Per	Forb/Herb	FACU
Giant ragweed	Ambrosia trifida L.	AMTR	Native	Dicot	Annual	Forb/Herb	FAC
Broomweed	Amphiachyris dracunculoides (DC.) Nutt.	AMDR	Native	Dicot	Annual	Forb/Herb	Upland
Scarlet pimpernel	Anagallis arvensis L.	ANAR	Non-Nat	Dicot	Ann/Bi	Forb/Herb	FACU
Smallflowered milkvetch	Astragalus nuttallianus DC.	ASNU4	Native	Dicot	Ann/Per	Forb/Herb	Upland
Rooseveltweed	Baccharis neglecta Britton	BANE2	Native	Dicot	Perennial	Shrub	FAC
Yellow Bluestem	Bothriochloa ischaemum (L.) Keng	BOIS	Non-Nat	Monocot	Perennial	Graminoid	Upland
Silver beardgrass	Bothriochloa laguroides (DC.) Herter	BOLA2	Native	Monocot	Perennial	Graminoid	FACU
Sideoats Grama	Bouteloua curtipendula (Michx.) Torr.	BOCU	Native	Monocot	Perennial	Graminoid	Upland
Buffalograss	Bouteloua dactyloides (Nutt.) J.T. Columbus	BODA2	Native	Monocot	Perennial	Graminoid	FACU
Texas grama	Bouteloua rigidiseta (Steud.) Hitchc.	BORI	Native	Monocot	Perennial	Graminoid	Upland
Rescuegrass	Bromus catharticus Vahl	BRCA6	Non-Nat	Monocot	Ann/Per	Graminoid	Upland
Corn gromwell	Buglossoides arvensis (L.) I.M. Johnst.	BUAR3	Non-Nat	Dicot	Annual	Forb/herb	Upland
Straggler daisy	Calyptocarpus vialis Less.	CAVI2	Non-Nat	Dicot	Perennial	Forb/Herb	FAC
Shepherd's purse	Capsella bursa-pastoris (L.) Medik.	CABU2	Non-Nat	Dicot	Annual	Forb/Herb	FACU
Indian paintbrush	Castilleja indivisa Engelm.	CAIN13	Native	Dicot	Annual	Forb/Herb	FAC

Ferngrass	Catapodium rigidum (L.) C.E. Hubbard ex Dony	CARI2	Non-Nat	Monocot	Annual	Graminoid	FACU
American star-thistle	Centaurea americana Nutt.	CEAM2	Native	Dicot	Annual	Forb/Herb	Upland
Maltese star-thistle	Centaurea melitensis L.	CEME2	Non-Nat	Dicot	Ann/Bi	Forb/Herb	Upland
Lady Bird's centaury	Centaurium texense (Griseb.) Fernald	CETE2	Native	Dicot	Annual	Forb/Herb	Upland
Hairyfruit chervil	Chaerophyllum tainturieri Hook.	CHTA	Native	Dicot	Annual	Forb/Herb	FAC
Thymeleaf sand mat	Chamaesyce serpyllifolia (Pers.) Small ssp. Serpyllifolia	CHSES	Native	Dicot	Annual	Forb/Herb	Upland
Pitseed goosefoot	Chenopodium berlandieri Moq.	CHBC4	Native	Dicot	Annual	Forb/Herb	Upland
Texas thistle	Cirsium texanum Buckley	CITE2	Native	Dicot	Bi/Per	Forb/Herb	Upland
Sorrelvine	Cissus trifoliata (L.) L.	CITR2	Native	Dicot	Perennial	Vine	FACU
Drummond's clematis	Clematis drummondii Torr. & A. Gray	CLDR	Native	Dicot	Perennial	Vine	FACU
Whitemouth Dayflower	Commelina communis L.	COER	Native	Monocot	Perennial	Forb/Herb	FACU
Texas bindweed	Convolvulus equitans Benth.	COEQ	Native	Dicot	Ann/Per	Forb/Herb	FACU
Canadian horseweed	Conyza canadensis (L.) Cronquist	COCA5	Native	Dicot	Ann/Bi	Forb/Herb	Upland
Goldenmane tickseed	Coreopsis basalis (A. Dietr.) S.F. Blake	COBA2	Native	Dicot	Annual	Forb/Herb	FACU
Hogwort	Croton capitatus Michx.	CRCA6	Native	Dicot	Annual	Forb/Herb	Upland
Bush croton	Croton fruticulosus Engelm. ex Torr.	CRFR	Native	Dicot	Perennial	Forb/Herb	Upland
Bermudagrass	Cynodon dactylon (L.) Pers.	CYDA	Non-Nat	Monocot	Perennial	Graminoid	FACU
Fragrant flatsedge	Cyperus odoratus L.	CYOD	Native	Monocot	Ann/Per	Graminoid	FACW
Bentawn flatsedge	Cyperus reflexus Vahl	CYRE2	Native	Monocot	Perennial	Graminoid	FAC
Purple nutsedge	Cyperus rotundus L.	CYRO	Non-Nat	Monocot	Perennial	Graminoid	FAC
Tropical flatsedge	Cyperus surinamensis Rottb.	CYSU	Native	Monocot	Perennial	Graminoid	FACW
Illinois bundleflower	Desmanthus illinoensis (Michx.) MacMill. ex B.L. Rob. & Fernald	DEIL	Native	Dicot	Perennial	Forb/Herb	FAC
Tapered rosette grass	Dichanthelium acuminatum (Sw.) Gould & C.A. Clark	DIAC2	Native	Monocot	Perennial	Graminoid	FAC

Silky bluestem	Dichanthium sericeum (R. Br.) A. Camus	DISE5	Non-Nat	Monocot	Perennial	Graminoid	Upland
Carolina ponyfoot	Dichondra carolinensis Michx.	DICA3	Native	Dicot	Perennial	Forb/Herb	FAC
Virginia buttonweed	Diodia virginiana L.	DIVI3	Native	Dicot	Ann/Per	Forb/Herb	Obligate
Common spikerush	Eleocharis palustris (L.) Roem. & Schult.	ELPA3	Native	Monocot	Perennial	Graminoid	Obligate
Indian goosegrass	Eleusine indica (L.) Gaertn.	ELIN3	Non-Nat	Monocot	Annual	Graminoid	FACU
Mediterranean lovegrass	Eragrostis barrelieri Daveau	ERBA2	Non-Nat	Monocot	Annual	Graminoid	Upland
Mexican fireplant	Euphorbia heterophylla L.	EUHE4	Native	Dicot	Ann/Per	Forb/Herb	FACU
Snow on the mountain	Euphorbia marginata Pursh	EUMA8	Native	Dicot	Annual	Forb/Herb	FACU
Indian blanket	Gaillardia pulchella Foug.	GAPU	Native	Dicot	An/Bi/Pr	Forb/Herb	Upland
Stickywilly	Galium aparine L.	GAAP2	Native	Dicot	Annual	Forb/Herb	FACU
Southwest bedstraw	Galium virgatum Nutt.	GAVI	Native	Dicot	Annual	Forb/Herb	Upland
Carolina geranium	Geranium carolinianum L.	GECA5	Native	Dicot	Ann/Bi	Forb/Herb	Upland
Dakota mock vervain	<i>Glandularia bipinnatifida</i> (Nutt.) Nutt.	GLBI2	Native	Dicot	Ann/Per	Forb/Herb	Upland
Gumhead	Gymnosperma glutinosum (Spreng.) Less.	GYGL	Native	Dicot	Perennial	Forb/Herb	Upland
Baby's breath	Gypsophila spp.	GYPSO	Non-Nat	Dicot	An/Bi/Per	Forb/Herb	Upland
Drummond's false pennyroyal	Hedeoma drummondii Benth.	HEDR	Native	Dicot	An/Bi/Per	Forb/Herb	FACU
Longdisk sneezeweed	<i>Helenium quadridentatum</i> Labill.	HEQU	Native	Dicot	Annual	Forb/Herb	FAC
Common sunflower	Helianthus annuus L.	HEAN3	Native	Dicot	Annual	Forb/Herb	FACU
Fourspike heliotrope	Heliotropium procumbens Mill.	HEPR	Native	Dicot	Ann/Per	Forb/Herb	FACW
Texas burstwort	Hermannia texana A. Gray	HETE9	Native	Dicot	Perennial	Forb/Herb	Upland
Little barley	Hordeum pusillum Nutt.	HOPU	Native	Monocot	Annual	Graminoid	FAC
Carolina woolywhite	Hymenopappus scabiosaeus L'Hér.	HYSC	Native	Dicot	Biennial	Forb/Herb	Upland
Tievine	<i>Ipomoea cordatotriloba</i> Dennst. var. <i>cordatotriloba</i>	IPCOC2	Native	Dicot	Perennial	Vine	Upland
American water-willow	Justicia americana (L.) Vahl	JUAM	Native	Dicot	Perennial	Forb/Herb	Obligate
Canada lettuce	Lactuca canadensis L.	LACA	Native	Dicot	Ann/Bi	Forb/Herb	FACU
Prickly Lettuce	Lactuca serriola L.	LASE	Non-Nat	Dicot	Ann/Bi	Forb/Herb	FAC

Henbit deadnettle	Lamium amplexicaule L.	LAAM	Non-Nat	Dicot	Ann/Bi	Forb/Herb	Upland
West Indian shrubverbena	Lantana urticoides Hayek	LAUR2	Native	Dicot	Perennial	Shrub	FACU
Virginia pepperweed	Lepidium virginicum L.	LEVI3	Native	Dicot	An/Bi/Pr	Forb/Herb	FACU
Ozark grass	<i>Limnodea arkansana</i> (Nutt.) L.H. Dewey	LIAR	Native	Monocot	Annual	Graminoid	FAC
Yellowseed false pimpernel	Lindernia dubia (L.) Pennell	LIDU	Native	Dicot	Ann/Bi	Forb/Herb	FACW
Texas yellowstar	<i>Lindheimera texana</i> A. Gray & Engelm.	LITE3	Native	Dicot	Annual	Forb/Herb	Upland
Texas lupine	Lupinus texensis Hook.	LUTE	Native	Dicot	Annual	Forb/Herb	Upland
Algerita	<i>Mahonia trifoliolata</i> (Moric.) Fedde	MATR3	Native	Dicot	Perennial	Shrub	Upland
Common mallow	Malva neglecta Wallr.	MANE	Non-Nat	Dicot	An/Bi/Pr	Forb/Herb	Upland
Bigfoot waterclover	<i>Marsilea macropoda</i> Engelm. ex A. Braun	MAMA9	Native	Fern	Perennial	Forb/Herb	Obligate
Black medick	Medicago lupulina L.	MELU	Non-Nat	Dicot	Ann/Per	Forb/Herb	FACU
Burclover	Medicago polymorpha L.	MEPO3	Non-Nat	Dicot	Ann/Per	Forb/Herb	FACU
Alfalfa	Medicago sativa L.	MESA	Non-Nat	Dicot	Ann/Per	Forb/Herb	Upland
Annual yellow sweetclover	Melilotus indicus (L.) All.	MEIN2	Non-Nat	Dicot	Annual	Forb/Herb	FACU
Sweetclover	Melilotus officinalis (L.) Lam.	MEOF	Non-Nat	Dicot	An/Bi/Pr	Forb/Herb	FACU
Pyramidflower	Melochia pyramidata L.	MEPY	Native	Dicot	Ann/Per	Forb/Herb	FAC
Littleleaf sensitive-briar	Mimosa microphylla Dryand.	MIMI22	Native	Dicot	Perennial	Forb/Herb	FACU
Marvel of Peru	Mirabilis jalapa L.	MIJA	Non-Nat	Dicot	Perennial	Forb/Herb	Upland
Carolina bristlemallow	Modiola caroliniana (L.) G. Don	MOCA	Native	Dicot	An/Bi/Pr	Forb/Herb	FAC
Lemon beebalm	<i>Monarda citriodora</i> Cerv. ex Lag.	MOCI	Native	Dicot	An/Bi/Pr	Forb/Herb	Upland
Texas wintergrass	Nassella leucotricha (Trin. & Rupr.) Pohl	NALE3	Native	Monocot	Perennial	Graminoid	FACU
Yellow-puff	Neptunia lutea (Leavenworth) Benth.	NELU2	Native	Dicot	Perennial	Forb/Herb	FACU
Cutleaf evening primrose	Oenothera laciniata Hill	OELA	Native	Dicot	Ann/Per	Forb/Herb	FACU
Pinkladies	Oenothera speciosa Nutt.	OESP2	Native	Dicot	Perennial	Forb/Herb	Upland
Scarlet beeblossom	Oenothera suffrutescens (Ser.) W.L. Wagner & Hoch	OESU3	Native	Dicot	Perennial	Forb/Herb	Upland
Slender yellow woodsorrel	Oxalis dillenii Jacq.	OXDI2	Native	Dicot	Perennial	Forb/Herb	FACU

Drummond's woodsorrel	Oxalis drummondii A. Gray	OXDR	Native	Dicot	Perennial	Forb/Herb	FACU
Kleingrass	Panicum coloratum L.	PACO2	Non-Nat	Monocot	Perennial	Graminoid	FAC
Pennsylvania pellitory	Parietaria pensylvanica Muhl. ex Willd.	PAPE5	Native	Dicot	Annual	Forb/Herb	FAC
Santa Maria feverfew	Parthenium hysterophorus L.	PAHY	Non-Nat	Dicot	Annual	Forb/Herb	FAC
Western wheatgrass	<i>Pascopyrum smithii</i> (Rydb.) Á. Löve	PASM	Native	Monocot	Perennial	Graminoid	FACU
Dallisgrass	Paspalum dilatatum Poir.	PADI3	Non-Nat	Monocot	Perennial	Graminoid	FAC
Hairyseed paspalum	Paspalum pubiflorum Rupr. ex Fourn.	PAPU5	Native	Monocot	Perennial	Graminoid	FACW
Vasey's grass	Paspalum urvillei Steud.	PAUR2	Non-Nat	Monocot	Perennial	Graminoid	FACW
Carolina canarygrass	Phalaris caroliniana Walter	PHCA6	Native	Monocot	Annual	Graminoid	FACW
Turkey tangle fogfruit	Phyla nodiflora (L.) Greene	PHNO2	Native	Dicot	Perennial	Forb/Herb	FAC
Chamber bitter	Phyllanthus urinaria L.	PHUR	Non-Nat	Dicot	Annual	Forb/Herb	FAC
Starhair groundcherry	Physalis viscosa L.	PHVI17	Native	Dicot	Perennial	Forb/Herb	Upland
White rocklettuce	Pinaropappus roseus (Less.)	PIRO	Native	Dicot	Perennial	Forb/Herb	Upland
Sweetscent	Pluchea odorata (L.) Cass. var. odorata	PLODO	Native	Dicot	Ann/Per	Forb/Herb	FAC
Kentucky bluegrass	Poa pratensis L.	POPR	Non-Nat	Monocot	Perennial	Graminoid	FACU
Denseflower knotweed	Polygonum glabrum Willd.	POGL10	Native	Dicot	Ann/Per	Forb/Herb	Obligate
Little hogweed	Portulaca oleracea L.	POOL	Native	Dicot	Annual	Forb/Herb	FAC
Wingpod purslane	Portulaca umbraticola Kunth	POUM	Native	Dicot	Annual	Forb/Herb	FAC
Smallflower desert-chicory	<i>Pyrrhopappus pauciflorus</i> (D. Don) DC.	PYPA4	Native	Dicot	Ann/Per	Forb/Herb	Upland
Annual bastardcabbage	Rapistrum rugosum (L.) All.	RARU	Non-Nat	Dicot	Annual	Forb/Herb	Upland
Upright prairie coneflower	Ratibida columnifera (Nutt.) Wooton & Standl.	RACO3	Native	Dicot	Perennial	Forb/Herb	Upland
Buffpetal	Rhynchosida physocalyx (A. Gray) Fryxell	RHPH2	Native	Dicot	Perennial	Forb/Herb	Upland
Blackeyed Susan	Rudbeckia hirta L.	RUHI2	Native	Dicot	An/Bi/Pr	Forb/Herb	FACU
Britton's wild petunia	Ruellia caerulea Morong	RUCA19	Non-Nat	Dicot	Perennial	Forb/Herb	FAC
Violet wild petunia	Ruellia nudiflora (Engelm. & A. Gray) Urb.	RUNU	Native	Dicot	Perennial	Forb/Herb	Upland
Curly dock	Rumex crispus L.	RUCR	Non-Nat	Dicot	Perennial	Forb/Herb	FAC

Little bluestem	Schizachyrium scoparium (Michx.) Nash	SCSC	Native	Monocot	Perennial	Graminoid	FACU
Drummond's skullcap	Scutellaria drummondii Benth.	SCDR2	Native	Dicot	Annual	Forb/Herb	Upland
Catclaw acacia	Senegalia greggii (A. Gray) Britton & Rose	SEGR4	Native	Dicot	Perennial	Shrub	Upland
Southwestern bristlegrass	Setaria scheelei (Steud.) Hitchc.	SESC2	Native	Monocot	Perennial	Graminoid	FACU
Spreading fanpetals	Sida abutifolia Mill.	SIAB	Native	Dicot	Ann/Per	Forb/Herb	Upland
Prickly fanpetal	Sida spinosa L.	SISP	Native	Dicot	Ann/Per	Forb/Herb	Upland
Rosinweed	Silphium spp.		Native	Dicot	Perennial	Forb/Herb	Upland
Swordleaf blue-eyed grass	Sisyrinchium chilense Hook.	SICH2	Native	Monocot	Perennial	Forb/Herb	Upland
Saw greenbrier	Smilax bona-nox L.	SMBO2	Native	Monocot	Perennial	Vine	FACU
Silverleaf nightshade	Solanum elaeagnifolium Cav.	SOEL	Native	Dicot	Perennial	Forb/Herb	Upland
Buffalobur nightshade	Solanum rostratum Dunal	SORO	Native	Dicot	Annual	Forb/Herb	Upland
Spiny sowthistle	Sonchus asper (L.) Hill	SOAS	Non-Nat	Dicot	Annual	Forb/Herb	FAC
Common sowthistle	Sonchus oleraceus L.	SOOL	Non-Nat	Dicot	Annual	Forb/Herb	Upland
Mescal bean	Sophora secundiflora (Ortega) Lag. ex DC.	SOSE3	Native	Dicot	Perennial	Tree	Upland
Johnsongrass	Sorghum halepense (L.) Pers.	SOHA	Non-Nat	Monocot	Perennial	Graminoid	FACU
Bristly scaleseed	<i>Spermolepis echinata</i> (Nutt. ex DC.) A. Heller	SPEC2	Native	Dicot	Annual	Forb/Herb	FACU
Diamond-flowers	Stenaria nigricans (Lam.) Terrell	STNI6	Native	Dicot	Perennial	Forb/Herb	Upland
Common dandelion	Taraxacum officinale F.H. Wigg.	TAOF	Non-Nat	Dicot	Perennial	Forb/Herb	FACU
Stiff greenthread	Thelesperma filifolium (Hook.) A. Gray	THFI	Native	Dicot	Ann/Per	Forb/Herb	FACU
Spreading hedgeparsley	Torilis arvensis (Huds.) Link	TOAR	Non-Nat	Dicot	Annual	Forb/Herb	Upland
Betonyleaf noseburn	Tragia betonicifolia Nutt.	TRBE4	Native	Dicot	Perennial	Forb/Herb	FACU
White tridens	Tridens albescens (Vasey) Wooton & Standl.	TRAL2	Native	Monocot	Perennial	Graminoid	FAC
Clasping Venus' looking- glass	Triodanis perfoliata (L.) Nieuwl.	TRPE4	Native	Dicot	Annual	Forb/Herb	FAC
Cedar elm	Ulmus crassifolia Nutt.	ULCR	Native	Dicot	Perennial	Tree	FAC
Texas signalgrass	<i>Urochloa texana</i> (Buckley) R. Webster	URTE2	Native	Monocot	Annual	Graminoid	Upland
Heartleaf nettle	Urtica chamaedryoides Pursh	URCH3	Native	Dicot	Annual	Forb/Herb	FACU

Sweet acacia	Vachellia farnesiana (L.) Wight & Arn.	VAFA	Native	Dicot	Perennial	Tree	FACU
Common mullein	Verbascum thapsus L.	VETH	Non-Nat	Dicot	Biennial	Forb/Herb	Upland
Brazilian vervain	Verbena brasiliensis Vell.	VEBR2	Non-Nat	Dicot	Annual	Forb/Herb	FAC
Texas vervain	Verbena halei Small	VEHA	Native	Dicot	Perennial	Forb/Herb	FACU
Golden crownbeard	Verbesina encelioides (Cav.) Benth. & Hook. f. ex A. Gray	VEEN	Native	Dicot	Annual	Forb/Herb	FAC
Birdeye speedwell	Veronica persica Poir.	VEPE3	Non-Nat	Dicot	Annual	Forb/Herb	FAC
Louisiana vetch	Vicia ludoviciana Nutt.	VILU	Native	Dicot	Annual	Forb/Herb	Upland
Buckley's yucca	Yucca constricta Buckley	YUCO	Native	Monocot	Perennial	Forb/Herb	Upland
Unknown seedling	Unknown seedling						

Appendix 4. Native plant species suggested for planting in Low Impact Development Structures in Bexar County.

		USDA			Growth	Wetland
Common name	Taxonomic name	Symbol	Group	Duration	Habit	$Status^1$
Silver bluestem	Bothriochloa laguroides	BOLA2	Monocot	Perennial	Graminoid	FACU
Sideoats Grama	Bouteloua curtipendula	BOCU	Monocot	Perennial	Graminoid	Upland
Buffalograss	Bouteloua dactyloides	BODA2	Monocot	Perennial	Graminoid	FACU
Texas grama	Bouteloua rigidiseta	BORI	Monocot	Perennial	Graminoid	Upland
Indian paintbrush	Castilleja indivisa	CAIN13	Dicot	Annual	Forb/Herb	FAC
American star-thistle	Centaurea americana	CEAM2	Dicot	Annual	Forb/Herb	Upland
Lady Bird's centaury	Centaurium texense	CETE2	Dicot	Annual	Forb/Herb	Upland
Sorrelvine	Cissus trifoliata	CITR2	Dicot	Perennial	Vine	FACU
Drummond's clematis	Clematis drummondii	CLDR	Dicot	Perennial	Vine	FACU
Whitemouth Dayflower	Commelina communis	COER	Monocot	Perennial	Forb/Herb	FACU
Goldenmane tickseed	Coreopsis basalis	COBA2	Dicot	Annual	Forb/Herb	FACU
Bush croton	Croton fruticulosus	CRFR	Dicot	Perennial	Forb/Herb	Upland
Fragrant flatsedge	Cyperus odoratus	CYOD	Monocot	Ann/Per	Graminoid	FACW ¹
Bentawn flatsedge	Cyperus reflexus	CYRE2	Monocot	Perennial	Graminoid	FAC^1
Tropical flatsedge	Cyperus surinamensis	CYSU	Monocot	Perennial	Graminoid	$FACW^1$
Carolina ponyfoot	Dichondra carolinensis Michx.	DICA3	Dicot	Perennial	Forb/Herb	FAC^1
Common spikerush	Eleocharis palustris	ELPA3	Monocot	Perennial	Graminoid	Obligate ¹
Indian blanket	Gaillardia pulchella	GAPU	Dicot	An/Bi/Pr	Forb/Herb	Upland
Dakota mock vervain	Glandularia bipinnatifida	GLBI2	Dicot	Ann/Per	Forb/Herb	Upland
Longdisk sneezeweed	Helenium quadridentatum	HEQU	Dicot	Annual	Forb/Herb	FAC^1
Common sunflower	Helianthus annuus	HEAN3	Dicot	Annual	Forb/Herb	FACU
Little barley	Hordeum pusillum	HOPU	Monocot	Annual	Graminoid	FAC^1
Carolina woolywhite	Hymenopappus scabiosaeus	HYSC	Dicot	Biennial	Forb/Herb	Upland
Tievine	Ipomoea cordatotriloba	IPCOC2	Dicot	Perennial	Vine	Upland
American water-willow	Justicia americana	JUAM	Dicot	Perennial	Forb/Herb	Obligate ¹
Ozark grass	Limnodea arkansana	LIAR	Monocot	Annual	Graminoid	FAC^1
Texas yellowstar	Lindheimera texana	LITE3	Dicot	Annual	Forb/Herb	Upland
Texas lupine	Lupinus texensis	LUTE	Dicot	Annual	Forb/Herb	Upland

Algerita	Mahonia trifoliolata	MATR3	Dicot	Perennial	Shrub	Upland
Bigfoot waterclover	Marsilea macropoda	MAMA9	Fern	Perennial	Forb/Herb	Obligate ¹
Lemon beebalm	Monarda citriodora	MOCI	Dicot	An/Bi/Pr	Forb/Herb	Upland
Texas wintergrass	Nassella leucotricha	NALE3	Monocot	Perennial	Graminoid	FACU
Yellow-puff	Neptunia lutea	NELU2	Dicot	Perennial	Forb/Herb	FACU
Pinkladies	Oenothera speciosa	OESP2	Dicot	Perennial	Forb/Herb	Upland
Scarlet beeblossom	Oenothera suffrutescens	OESU3	Dicot	Perennial	Forb/Herb	Upland
Slender yellow woodsorrel	Oxalis dillenii	OXDI2	Dicot	Perennial	Forb/Herb	FACU
Drummond's woodsorrel	Oxalis drummondii	OXDR	Dicot	Perennial	Forb/Herb	FACU
Western wheatgrass	Pascopyrum smithii	PASM	Monocot	Perennial	Graminoid	FACU
Carolina canarygrass	Phalaris caroliniana	PHCA6	Monocot	Annual	Graminoid	$FACW^1$
Turkey tangle fogfruit	Phyla nodiflora	PHNO2	Dicot	Perennial	Forb/Herb	FAC
Sweetscent	Pluchea odorata	PLODO	Dicot	Ann/Per	Forb/Herb	FAC^1
Denseflower knotweed	Polygonum glabrum	POGL10	Dicot	Ann/Per	Forb/Herb	Obligate ¹
Upright prairie coneflower	Ratibida columnifera	RACO3	Dicot	Perennial	Forb/Herb	Upland
Blackeyed Susan	Rudbeckia hirta	RUHI2	Dicot	An/Bi/Pr	Forb/Herb	FACU
Violet wild petunia	Ruellia nudiflora	RUNU	Dicot	Perennial	Forb/Herb	Upland
Little bluestem	Schizachyrium scoparium	SCSC	Monocot	Perennial	Graminoid	FACU
Southwestern bristlegrass	Setaria scheelei	SESC2	Monocot	Perennial	Graminoid	FACU
Swordleaf blue-eyed grass	Sisyrinchium chilense	SICH2	Monocot	Perennial	Forb/Herb	Upland
Saw greenbrier	Smilax bona-nox	SMBO2	Monocot	Perennial	Vine	FACU
Silverleaf nightshade	Solanum elaeagnifolium	SOEL	Dicot	Perennial	Forb/Herb	Upland
Buffalobur nightshade	Solanum rostratum	SORO	Dicot	Annual	Forb/Herb	Upland
Stiff greenthread	Thelesperma filifolium	THFI	Dicot	Ann/Per	Forb/Herb	FACU
White tridens	Tridens albescens	TRAL2	Monocot	Perennial	Graminoid	FAC
Texas signalgrass	Urochloa texana	URTE2	Monocot	Annual	Graminoid	Upland
Golden crownbeard	Verbesina encelioides	VEEN	Dicot	Annual	Forb/Herb	FAC
Louisiana vetch	Vicia ludoviciana	VILU	Dicot	Annual	Forb/Herb	Upland

 $^{^{\}rm 1}$ - Recommended for LID structures that have longer hydroperiods and higher soil moisture.